



Pilkington Library

Author/Filing Title RATCLIFFE

Vol. No. Class Mark T

**Please note that fines are charged on ALL
overdue items.**

FOR REFERENCE ONLY		
---------------------------	--	--

0402589912



Trapped Modes In The Presence Of Thin Obstacles

Keith Ratcliffe

A DOCTORAL THESIS.

SUBMITTED IN PARTIAL FULFILMENT OF THE REQUIREMENTS


FOR THE AWARD OF

DOCTOR OF PHILOSOPHY OF LOUGHBOROUGH UNIVERSITY

JANUARY 2002.

Supervisor: C.M. Linton, PhD. Loughborough University

© K RATCLIFFE 2002

 Loughborough University Physical Library
Date Sept 02
Class
Acc No. 040258991

Abstract

In this thesis we use various techniques to investigate the occurrence of trapped modes in the presence of thin obstacles. Physically trapped modes are oscillations of finite energy in a fluid which is unbounded in at least one direction. These oscillations mainly occur locally to some structure and decay to zero at large distances away from it. Trapped modes are important as they have been found to exist in a wide range of physical situations.

We consider a number of problems in two and three dimensions including waveguides containing bodies and arrays of identical structures. A modified residue calculus technique, a variational technique and a method based on the truncation of matched eigenfunction expansions are used to solve the problems, with numerous results presented.

Keywords

trapped modes
embedded trapped modes
Rayleigh-Bloch waves
acoustic resonances
thin obstacles
Helmholtz equation
waveguides
modified residue calculus
variational techniques
matched eigenfunction expansions

Acknowledgements

Firstly, I would like to thank my supervisor, Dr. Chris Linton for his guidance and enthusiasm for the project throughout the last three years and in particular for always being willing to offer help and advice at a moments notice.

I thank the Engineering and Physical Sciences Research Council whose financial support through award reference 98316228 is gratefully acknowledged.

Thanks must also go to Dr. Keith Watling for maintaining the excellent computing facilities and the administrative staff of the department, for always being exceedingly helpful.

I would like to take this opportunity to thank my fellow research students, in particular: Jon, Paul and Dave for their help, advice and humour.

I would like to thank all my friends (in Loughborough and back home), especially my Mum and Dad. This couldn't have been completed without your help, encouragement and support. Finally I give special thanks to Vic for her support and smiles.

In memory of Rufus Littlehales 1918–2001...

Contents

1	Introduction	1
I	Two-Dimensional Waveguides	5
2	Two-dimensional laterally coupled waveguides	6
2.1	Introduction to the problem	6
2.2	Background	7
2.3	Formulation	10
2.4	Trapped modes below the first cut-off	15
2.5	Trapped modes below the second cut-off	38
2.6	Trapped modes below the third cut-off	47
2.7	Summary	47
3	Two-dimensional waveguides containing a plate on the centreline	49
3.1	Introduction to the problem	49
3.2	Background	50
3.3	Formulation	52
3.4	Trapped modes below the first cut-off	55
3.5	Trapped modes below the second cut-off	64
3.6	Summary	69
4	Two-dimensional waveguides containing an off-centre plate	71
4.1	Introduction to the problem	71
4.2	Background	72
4.3	Formulation	73
4.4	Trapped modes below the first cut-off	75

4.5	Trapped modes below the second cut-off	86
4.6	Trapped modes below the third cut-off	94
4.7	Summary	101
5	Two-dimensional array of parallel plates containing finite gaps	103
5.1	Introduction to the problem	103
5.2	Background	104
5.3	Formulation	106
5.4	Rayleigh-Bloch waves below the first cut-off	108
5.5	Rayleigh-Bloch waves below the second cut-off	116
5.6	Rayleigh-Bloch waves below the third cut-off	121
5.7	Summary	126
II	Three-Dimensional Waveguides	127
6	Three-dimensional laterally coupled cylindrical waveguides	128
6.1	Introduction to the problem	128
6.2	Background	128
6.3	Formulation	130
6.4	Trapped modes below the first cut-off	135
6.5	Summary	142
7	Three-dimensional laterally coupled planar waveguides	144
7.1	Introduction to the problem	144
7.2	Background	145
7.3	Formulation	146
7.4	Trapped modes below the first cut-off	150
7.5	Summary	158
8	Annular waveguide.	160
8.1	Introduction to the problem.	160
8.2	Formulation	161
8.3	Results	170
8.4	Summary	183

9 Conclusion	184
A Integral of product of Bessel functions	186
B Zeros of cross-products of Bessel functions	194
Bibliography	196

Chapter 1

Introduction

Free oscillations are widely observed phenomena in the physical world. A familiar example is the simple pendulum which will continue to oscillate for a long time after being set in motion. A ‘trapped mode’ is a free oscillation of finite energy within a fluid which is unbounded in at least one direction. Trapped-mode oscillations are mostly confined to the vicinity of a structure and rapidly decay to zero at large distances away from that structure. Physically trapped modes are important because they are associated with resonances in forced initial-value problems. A forced motion at a frequency near a trapped-mode frequency can set up large fluid oscillations which may cause considerable damage to a structure, even though the oscillations are limited by the action of nonlinearity and viscosity.

The classical example of a trapped mode, which has been observed in the ocean, is the simple exponential solution based on linear water wave theory and derived by Stokes (1846). This so-called edge wave is trapped above a sloping beach, propagates along the shoreline, and decays to zero away from the shore. Little interest was shown in the solution for over a hundred years, but recently other examples of these trapped modes have been found to exist in a wide range of physical situations. A review of some of the recent developments in the theory of trapped modes in water waves is presented by Evans and Kuznetsov (1997).

The occurrence of trapped modes in the air, where they are known as acoustic resonances, was brought to the forefront by a series of papers by Parker (1966) and (1967). A discussion of the importance of acoustic resonances and how they have been observed in a wide range of engineering situations was given in a review paper by Parker and Stoneman (1989). These situations include flow-induced vibration of cooler tubes, the

vibration of blades in axial-flow compressors and other turbo-machines, and noise and vibration from support spokes and corner vanes in pipe or duct systems. An extensive list of references on the subject is also provided.

In this thesis we consider a number of different theoretical problems concerning trapped modes in the vicinity of thin obstacles and approach each problem from an acoustical viewpoint. The field equation for small time-harmonic acoustic perturbations is the Helmholtz equation, which is derived by separating the time factor $\exp(-i\omega t)$ from the three-dimensional wave equation

$$\frac{\partial^2 \Phi}{\partial t^2} = c_s^2 (\nabla^2 \Phi), \quad (1.0.1)$$

where ω is the frequency of oscillation and c_s is the speed of sound. If we look for a solution to (1.0.1) in the form $\Phi(x, y, z, t) = \Re[\phi(x, y, z) \exp(-i\omega t)]$ we obtain

$$(\nabla^2 + k^2)\phi = 0, \quad k = \omega/c_s, \quad (1.0.2)$$

where the complex-valued function ϕ is the time-independent acoustic potential.

Although we use an acoustic interpretation of each problem the model has physical relevance in other fields, as it can be shown that the Helmholtz equation (1.0.2) arises in a number of different areas of technology such as quantum mechanics and electromagnetism as well as in water-wave theory. A review of some of the different applications of the Helmholtz equation is given by Liboff (1999).

The boundary conditions used on the surfaces of bodies in this work are either Neumann conditions (the so-called sound-hard acoustic condition)

$$\frac{\partial \phi}{\partial \underline{n}} = 0, \quad (1.0.3)$$

where \underline{n} is the unit normal to the surface directed into the fluid, or Dirichlet (sound-soft) conditions

$$\phi = 0. \quad (1.0.4)$$

In the acoustic field the Neumann condition is interpreted physically as a rigid boundary on which the normal velocity of the fluid is zero and the Dirichlet condition is a ‘pressure release’ boundary, where the pressure of the fluid is zero.

In this thesis various sets of integers are often used. To keep the notation consistent we define the set of integers by \mathbb{Z} , the set of non-negative integers by \mathbb{N}_0 and the set of positive integers by \mathbb{N} .

Overview of thesis

The thesis is thus organized as follows:

We divide the thesis into two parts, with part I consisting of the two-dimensional problems considered in chapters 2–5 and part II consisting of the three-dimensional problems considered in chapters 6–8.

- **Chapter 2**

We consider a two-dimensional waveguide consisting of a pair of parallel-plate waveguides coupled laterally by a finite length hole in the common boundary. The pair of waveguides are assumed to have different widths and trapped modes are sought in various frequency bands.

- **Chapter 3**

In this chapter we consider the same waveguide as in the previous chapter and assume that the pair of waveguides are of equal width. The problem is equivalent to a parallel-plate waveguide containing a finite length thin plate placed on the centreline and parallel to the guide walls. The symmetry properties of the guide allow us to provide a simpler formulation to that of the previous chapter.

- **Chapter 4**

We move the plate off the centreline of the waveguide and seek trapped modes in a parallel-plate waveguide containing a finite length thin plate placed off the centreline and parallel to the guide walls. The work in this chapter forms part of the publication Linton et al. (2002).

- **Chapter 5**

We consider a two-dimensional array of equally spaced infinite length parallel plates each containing an identical finite length gap and arranged so that the line of symmetry passes through the mid-point of each gap. The trapped modes sought in this chapter differ from the trapped modes in previous chapter as the modes here travel through the gaps of the array. The trapped modes are known as Rayleigh-Bloch waves and are similar to Stokes' edge waves mentioned earlier.

- **Chapter 6**

We seek trapped modes in a three-dimensional waveguide formed by rotating the waveguide considered in chapter 2 about one of the outer waveguide walls. The waveguide consists of two concentric circular cylindrical waveguides coupled laterally by a finite length gap along the axis of the inner cylinder.

- **Chapter 7**

We consider the waveguide formed by rotating the waveguide considered in chapter 2 about its line of symmetry. The waveguide consists of a pair of different width planar layers coupled laterally by a circular hole in the common boundary. The case when the planar layers are of equal width is also considered, i.e. the waveguide formed by rotating the waveguide in chapter 3 about the line of symmetry perpendicular to the walls. When the layers are equal width the problem is equivalent to a disc on the centreline of a planar waveguide. We finally consider the case of a number of discs placed on the centreline of a planar waveguide.

- **Chapter 8**

We consider a cylindrical waveguide with an annular cross-section containing a number of identical finite length thin radial plates equally spaced around the guide. The problem extends work done by Linton and McIver (1998b), who considered the case of a circular cylindrical waveguide containing a number of radial fins.

- **Chapter 9**

We present conclusions from the work in this thesis.

Part I

Two-Dimensional Waveguides

Chapter 2

Two-dimensional laterally coupled waveguides

2.1 Introduction to the problem

In this chapter we seek trapped modes in a two-dimensional laterally coupled waveguide. The waveguide considered here consists geometrically of a pair of two-dimensional parallel plate waveguides coupled laterally through a finite width window in the common boundary. The problem has been approached from an acoustical point of view, although it is shown in section 2.2 that the model also has physical relevance in quantum mechanics as the field equation and boundary conditions can be shown to be the same in both situations. The geometry of the problem is defined by two non-dimensional parameters, these being the width of the window in the common boundary compared to the width of the whole guide and the height of the window compared to the width of the full coupled guide ($2a/d$ and b/d , respectively, in figure 2.1).

This chapter is presented in the following manner. After a brief discussion in section 2.2 of previous work done on problems involving two-dimensional laterally coupled waveguides we formulate the problem in section 2.3, and show that there exists a cut-off frequency below which waves cannot propagate to infinity within the guide.

In section 2.4 various techniques are used to investigate the existence of trapped modes below this first cut-off. The first method used in section 2.4.1 is the modified residue calculus technique. The method firstly produces an approximate solution for the trapped-mode frequencies which is highly accurate for all but very small window widths. This approximation provides a very useful insight into how to solve the full problem in

a numerically efficient way. The full problem is then solved and numerical results presented, together with a comparison between the approximate and full solutions. When looking below the cut-off trapped modes can be found by either fixing the width of the window or the height of the window and varying the other parameter. The results show that trapped modes occur for any size window width or height. The modified residue calculus method does not provide a rigorous proof of the existence of trapped modes, but can be used to prove the existence of trapped modes for a sufficiently long window. Such a proof, however, is not presented in this chapter. In section 2.4.2 we use a variational argument to prove the existence of trapped modes for a sufficiently wide window and also provide estimates to the trapped-mode frequencies. It is shown that the upper bound of these estimates provides a very good approximation to the actual computed trapped-mode frequencies.

Trapped-modes are sought above the first cut-off and below the second cut-off in section 2.5. Between the two cut-offs the problem permits two wave-like modes in the window region and one mode which can propagate down the guide. A modified residue calculus technique is used and the method allows the amplitude of the propagating mode to be set to zero. The trapped mode frequencies are shown to correspond to the intersection of two lines (coming from the two wave-like modes in the model). When looking for trapped modes above the first cut-off the number of parameters we can fix is reduced by one. The only parameter we are able to fix is the height of the window and trapped modes occur only for specific window widths.

In section 2.6 existence of trapped modes between the second and third cut-offs is discussed. Trapped modes above the second cut-off correspond to the intersection of three sets of lines, but for this particular problem no solutions appear to exist. A summary of the results obtained in the chapter is presented in section 2.7.

2.2 Background

Some basic mathematical results

It is useful to state some mathematical results that will be used later.

The work here briefly describes the relationship between trapped modes and eigenfunctions of the Laplace operator in unbounded domains (in this case the unbounded domain being the waveguide).

We are trying to find values of λ for which there is a non-trivial solution $\phi(x, y)$ to the boundary-value problem

$$-\nabla^2\phi = \lambda\phi, \tag{2.2.1}$$

subject to some appropriate boundary conditions. The problem is a spectral problem in which λ is the spectral parameter and the spectrum is a sub-set of the semi-interval $[0, \infty)$, see, for example Jones (1953).

If a non-trivial potential ϕ can be found which satisfies (2.2.1) and the boundary conditions (including a condition requiring exponential decay at infinity), then the value λ corresponding to the potential ϕ is an eigenvalue of the problem. In terms of spectral theory of operators the eigenvalues λ make up the point spectrum of the problem.

If a value of λ is found that it produces a non-trivial potential ϕ that satisfies (2.2.1) and the boundary conditions, grows as $x \rightarrow \pm\infty$ not faster than polynomially (i.e. not as $\exp|x|$) and is non-zero as $x \rightarrow \pm\infty$ then in spectral terms we say that the value λ belongs to the continuous spectrum of the problem. The potentials corresponding to values of λ belonging to the continuous spectrum do not correspond to trapped modes as they do not satisfy the decay condition.

Another term commonly mentioned in spectral terminology is the essential spectrum. The essential spectrum consists of the continuous spectrum including any eigenvalues embedded in the continuous spectrum.

The spectral terminology can be directly related to the theory of trapped modes. The eigenvalues of the full problem are related to the trapped-mode frequencies, and the corresponding potentials (eigenfunctions) are trapped modes. Potentials relating to the values of λ in the continuous spectrum are known as propagating modes.

Most of the work on quantum waveguides described below uses this spectral terminology, but a comparison can be made with the associated trapped mode problem in acoustics.

Motivation behind the problem

The recent rapid development in nanoelectronics has brought about a remarkable progress in semiconductor physics. The most spectacular progress has been concerned with fabrication techniques of microscopic structures of pure semiconductor material. When dealing with these small structures the term mesoscopic physics is often used. More

details of the key features found in these systems and a guide to the physical literature can be found in the review paper by Duclos and Exner (1995).

These microstructures tend to have certain common properties: (a) small size (typically tens to hundreds of nanometres ($1nm = 10^{-9}m$)); (b) high purity (the electron free path can be a few micrometres or even larger); (c) crystalline structure; (d) the wavefunctions are usually suppressed at the boundaries between different semiconductor materials. The description of an electron moving in mesoscopic systems is governed by the many-body Schrödinger equation describing its interaction with the lattice atoms including many impurities. Combining the properties (a)–(d) allows us to simulate the electron motion inside the microstructure as a free (spinless) particle living in the corresponding spatial region with the Dirichlet condition on its boundary; an interaction term must only be added if the whole structure is placed into an external field.

The waveguides for these problems, often referred to as quantum waveguides, have a direct relation to classical acoustic and electromagnetic waveguides. The basic equations for these cases, the Schrödinger and wave equation are different but for stationary problems involving free electrons or particles, both reduce to the Helmholtz equation in the appropriate region. A free electron is considered as it has no potential energy and so the potential term in the time-independent Schrödinger equation is set to zero.

A lot of previous work on quantum waveguides or quantum wires, as the two-dimensional quantum channels are sometimes known, involves the study of bound-states, which are isolated (resonant) eigenvalues below the threshold of the continuous spectrum. Work in this area is both experimental, see for example Carini et al. (1992) and theoretical, see Duclos and Exner (1995). These problems are important from a physical point of view as these eigenvalues and resonances have great influence on electron transport in mesoscopic systems.

One area of recent study is laterally coupled quantum waveguides. These guides consist of two straight parallel waveguides containing a window in the common boundary. Experimental observations of a waveguide with a similar configuration are found in Hirayama et al. (1992) and Hirayama et al. (1993) who considered two parallel in-plane-gated wires coupled by a ballistic window. A numerical model, based on classical rebound effect in a straight wire for the experimental specification described in Hirayama et al. (1992), was provided in Takagaki and Ploog (1994).

Kunze (1993) found analytic expressions for the transmissivity along a wire coupled

either to infinite space or to another wire via a small hole. The work shows that there are energies at which resonances or quasibound states in the wire become possible. These quasibound states cause a sharp downward dip in the conductance plots for the wire.

Work by Exner et al. (1996) explores the bound states and scattering in quantum waveguides again coupled laterally through a boundary window. A modification of the variational technique presented in Evans, Levitin, and Vassiliev (1994) is used to show that the system always has at least one bound state for any window width. A variational technique similar to that used in this chapter also provides estimates to the trapped-mode frequencies. The problem is solved using a mode-matching technique which shows the corresponding wave functions and how the bound-state energies depend on the parameters of the problem. The work also presents a discussion on how the first eigenvalue emerges from below the continuous spectrum as the window opens. Work by Bulla et al. (1997) showed that if the window was small enough so that only one simple eigenvalue below the essential spectrum was present, this eigenvalue could be bounded from below. The work by Exner and Vugalter (1996) extended this paper by using a variational method to show that for a sufficiently small window a two-sided asymptotic estimate for the gap between the essential spectrum and this eigenvalue could be obtained.

The case of a coupled waveguide containing a finite number N of windows in the common boundary was considered in Exner and Vugalter (1997). It was shown that if the windows are small enough there is just one isolated eigenvalue. Upper and lower bounds of the gap between this eigenvalue and the continuous spectrum are found using a variational approach.

2.3 Formulation

The problem consists of a pair of two-dimensional waveguides of widths b and c ($=d-b$), and for convenience we assume that b is greater than $d/2$, coupled laterally through a window of width $2a$ in the common boundary. The case when $b = d/2$ is considered separately in chapter 3. Cartesian axes are chosen so that the x -axis coincides with the lower boundary of the waveguide and the y -axis is chosen so that the waveguide is symmetric about the line $x = 0$, as shown in figure 2.1. The geometry of the problem allows any solution to be expressed as the sum of solutions which are either symmetric or

antisymmetric about $x = 0$. Initially we shall seek a solution which is even (symmetric) about $x = 0$, by considering the region $x > 0$ and seeking a function $\phi(x, y)$ which satisfies

$$\frac{\partial \phi}{\partial x} = 0 \text{ on } x = 0, \quad 0 < y < d. \quad (2.3.1)$$

The function $\phi(x, y)$ must also satisfy the Helmholtz equation within the waveguide

$$(\nabla^2 + k^2)\phi = 0, \quad 0 < y < d \text{ except on } y = b, \quad |x| > a. \quad (2.3.2)$$

In the acoustic context $k = \omega/c_s$ where ω is the frequency of oscillation and c_s is the speed of sound. In the related quantum problem $k^2 = 2mE/\hbar^2$, where m is the mass of the electron, E is the total energy of the electron and \hbar is Plank's constant divided by 2π . The function ϕ satisfies Dirichlet boundary conditions on the waveguide walls,

$$\phi = 0 \text{ on } y = 0, \quad x > 0, \quad (2.3.3)$$

$$\phi = 0 \text{ on } y = b, \quad x > a, \quad (2.3.4)$$

$$\phi = 0 \text{ on } y = d, \quad x > 0, \quad (2.3.5)$$

and a radiation condition specifying that no waves propagate out to infinity,

$$\phi \rightarrow 0 \text{ as } x \rightarrow \infty. \quad (2.3.6)$$

Condition (2.3.6) comes from the idea that trapped modes possess finite energy, i.e.

$$\int_{\Omega} |\nabla \phi|^2 d\Omega < \infty, \quad (2.3.7)$$

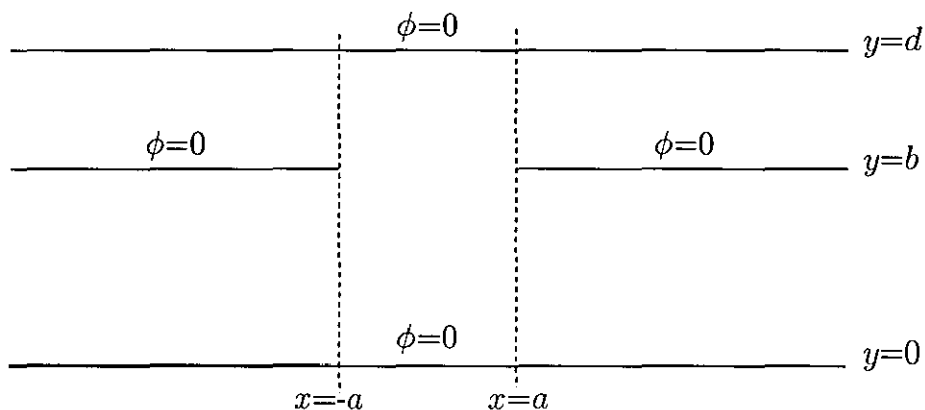


Figure 2.1: Definition sketch.

where Ω is the entire fluid domain. For this particular problem it can be shown using Green's theorem that the radiation condition (2.3.6) is equivalent to (2.3.7). We finally assume ϕ is non-singular and that

$$\nabla\phi = O(r^{-\frac{1}{2}}) \text{ as } r \equiv \{(x-a)^2 + (y-b)^2\}^{\frac{1}{2}} \rightarrow 0, \quad (2.3.8)$$

anticipating singular behaviour in the velocity field at the edge. This condition can be derived from a conformal map of an ideal fluid around the end of a plate.

It is useful to split the domain into three regions. Region *I* is $b < y < d$, $x > a$, region *II* is $0 < y < b$, $x > a$, and region *III* is $0 < y < d$, $0 < x < a$, as shown in figure 2.2. We can represent the function ϕ by a function ϕ_i ($i = 1, 2, 3$) in each region, with the following continuity conditions applied at the boundaries between the regions:

$$\phi_i = \phi_3, \quad \frac{\partial\phi_i}{\partial x} = \frac{\partial\phi_3}{\partial x}, \quad \text{on } L_i, \quad i = 1, 2, \quad (2.3.9)$$

where L_1 is $x = a, b < y < d$, L_2 is $x = a, 0 < y < b$ and we write L_3 for $L_1 \cup L_2$. The physical interpretation of these continuity conditions are that the horizontal pressure and velocity are continuous across $x = a$.

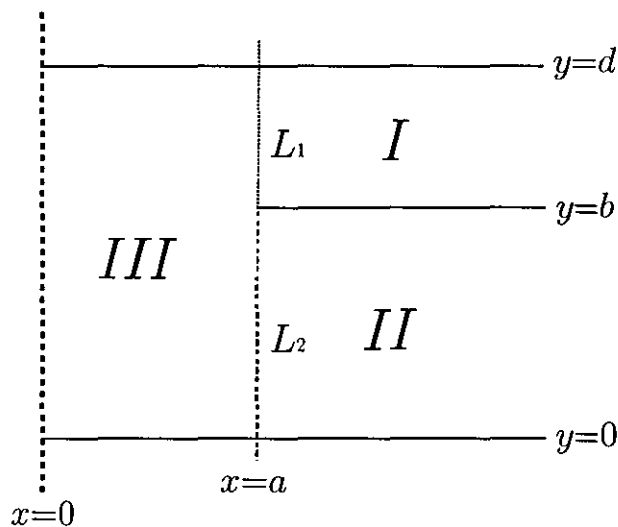


Figure 2.2: A schematic representation of the regions *I*, *II* and *III* along with the lines L_1 and L_2 .

If we let $\phi_i = U_i(x)V_i(y)$ for $i = 1, 2, 3$, and substitute into (2.3.2), we have after a slight rearrangement

$$\frac{U_i''(x)}{U_i(x)} = -\frac{V_i''(y)}{V_i(y)} - k^2. \quad (2.3.10)$$

As in each region the function on the left-hand side of (2.3.10) is a function of x only and the right-hand side is a function of y only, both sides must equal the same constant.

If we let the constant in region I equal α^2 , say, with $\alpha > 0$ we have

$$U_1''(x) - \alpha^2 U_1(x) = 0, \quad (2.3.11)$$

which has general solution

$$U_1(x) = A_1 e^{\alpha x} + B_1 e^{-\alpha x}. \quad (2.3.12)$$

The boundary condition (2.3.6) requires $U_1(x) \rightarrow 0$ as $x \rightarrow \infty$, and so (2.3.12) becomes,

$$U_1(x) = B_1 e^{-\alpha x}. \quad (2.3.13)$$

By setting the constant in region II equal to β^2 , with $\beta > 0$, a similar argument leads to

$$U_2(x) = B_2 e^{-\beta x}. \quad (2.3.14)$$

Setting the constant for region III equal to γ^2 , with $\gamma > 0$, the general solution (2.3.12) can be rewritten

$$U_3(x) = A_3 \sinh \gamma x + B_3 \cosh \gamma x. \quad (2.3.15)$$

Substituting the boundary condition (2.3.1) into (2.3.15), we have

$$U_3(x) = B_3 \cosh \gamma x. \quad (2.3.16)$$

Substituting (2.3.11) back into (2.3.10), we obtain

$$\frac{V_1''(y)}{V_1(y)} = -(\alpha^2 + k^2). \quad (2.3.17)$$

If we let $\alpha^2 + k^2 = \nu^2$, the general solution to (2.3.17) can be written

$$V_1(y) = A_1 \cos \nu y + B_1 \sin \nu y. \quad (2.3.18)$$

Applying the boundary conditions (2.3.4) and (2.3.5) we have

$$A_1 \cos \nu b + B_1 \sin \nu b = 0, \quad (2.3.19)$$

$$A_1 \cos \nu d + B_1 \sin \nu d = 0. \quad (2.3.20)$$

Eliminating A_1 between the two equations we leave

$$B_1 \sin \nu c = 0. \quad (2.3.21)$$

As we are not interested in the trivial solution, $B_1 \neq 0$, and so

$$\nu c = n\pi, \quad n \in \mathbb{N}. \quad (2.3.22)$$

Similar processes for regions *II* and *III* give the solutions

$$V_2(y) = B_2 \sin \mu y, \quad (2.3.23)$$

where $\beta^2 + k^2 = \mu^2$, and

$$\mu = \frac{n\pi}{b}, \quad n \in \mathbb{N}, \quad (2.3.24)$$

and

$$V_3(y) = B_3 \sin \lambda y, \quad (2.3.25)$$

where $\gamma^2 + k^2 = \lambda^2$, and

$$\lambda = \frac{(n+1)\pi}{d}, \quad n \in \mathbb{N}_0. \quad (2.3.26)$$

We introduce the complete orthonormal sets

$$\Psi_n^{(1)}(y) = 2^{1/2} \sin \nu_n(d-y), \quad \nu_n = n\pi/c, \quad n \in \mathbb{N}, \quad (2.3.27)$$

$$\Psi_n^{(2)}(y) = 2^{1/2} \sin \mu_n(b-y), \quad \mu_n = n\pi/b, \quad n \in \mathbb{N}, \quad (2.3.28)$$

$$\Psi_n^{(3)}(y) = 2^{1/2} \sin \lambda_n(d-y), \quad \lambda_n = (n+1)\pi/d, \quad n \in \mathbb{N}_0, \quad (2.3.29)$$

which satisfy

$$\frac{1}{|L_i|} \int_{L_i} \Psi_n^{(i)}(y) \Psi_m^{(i)}(y) dy = \delta_{mn}, \quad i = 1, 2, 3, \quad (2.3.30)$$

where δ_{mn} is the Kronecker delta. This is done so that any function defined in any of the regions can be represented by a series based on the appropriate set of orthonormal functions (see, for example Hobson (1926), Chapter 10).

The eigenfunction expansions for the three regions can be written

$$\phi_1(x, y) = \sum_{n=1}^{\infty} U_n^{(1)} \frac{e^{-\alpha_n(x-a)} \Psi_n^{(1)}(y)}{-\alpha_n}, \quad \alpha_n = (\nu_n^2 - k^2)^{1/2}, \quad (2.3.31)$$

$$\phi_2(x, y) = \sum_{n=1}^{\infty} U_n^{(2)} \frac{e^{-\beta_n(x-a)} \Psi_n^{(2)}(y)}{-\beta_n}, \quad \beta_n = (\mu_n^2 - k^2)^{1/2}, \quad (2.3.32)$$

$$\phi_3(x, y) = \sum_{n=0}^{\infty} U_n^{(3)} \frac{\cosh \gamma_n x \Psi_n^{(3)}(y)}{\gamma_n \sinh \gamma_n a}, \quad \gamma_n = (\lambda_n^2 - k^2)^{1/2}, \quad (2.3.33)$$

where $U_n^{(i)}$, $i = 1, 2, 3$, are unknown complex constants and various factors have been introduced for convenience. As we assumed $b > d/2$, we find that if we restrict the frequency to

$$kb < \pi, \quad (2.3.34)$$

the values α_n and β_n , $n \in \mathbb{N}$ will all be real and positive. As these terms appear in the eigenfunction expansions as coefficients of negative exponentials, the restriction of frequency produces exponential decay down the guide in both regions and therefore no propagating modes. We define $kb = \pi$ as the first cut-off of the two-dimensional laterally coupled waveguide.

We now proceed by considering the case of trapped modes whose frequencies are below the first cut-off.

2.4 Trapped modes below the first cut-off

The cut-off $kb < \pi$ is chosen so that α_n and β_n given by (2.3.31) and (2.3.32) are all real and positive for $n \in \mathbb{N}$. This frequency restriction also produces real and positive values for γ_n , $n \in \mathbb{N}$ in (2.3.33). The only wave-like mode that can possibly appear in the whole problem is the mode corresponding to γ_0 . If we restrict the frequency so that $kd > \pi$, γ_0 will be purely imaginary and the corresponding mode will be oscillatory in region *III*. We thus anticipate a necessary condition for the existence of trapped modes to be

$$\pi < kd < \frac{d\pi}{b}, \quad (2.4.1)$$

as by definition if a mode is found in this frequency range it is a trapped mode. This is typical of trapped mode phenomena, see for example, Evans (1992).

The first method we shall use to investigate trapped modes is the modified residue calculus technique.

2.4.1 Modified residue calculus method

We now apply the continuity conditions (2.3.9). Matching $\phi_i = \phi_3$ on L_i , $i = 1, 2$, we have

$$\sum_{n=0}^{\infty} U_n^{(3)} \frac{\coth \gamma_n a}{\gamma_n} \Psi_n^{(3)}(y) = \begin{cases} \sum_{n=1}^{\infty} U_n^{(1)} \frac{\Psi_n^{(1)}(y)}{-\alpha_n}, & y \in L_1, \\ \sum_{n=1}^{\infty} U_n^{(2)} \frac{\Psi_n^{(2)}(y)}{-\beta_n}, & y \in L_2. \end{cases} \quad (2.4.2)$$

Matching $\partial\phi_i/\partial x = \partial\phi_3/\partial x$ on $L_i, i = 1, 2$, we arrive at

$$\sum_{n=0}^{\infty} U_n^{(3)} \Psi_n^{(3)}(y) = \begin{cases} \sum_{n=1}^{\infty} U_n^{(1)} \Psi_n^{(1)}(y), & y \in L_1, \\ \sum_{n=1}^{\infty} U_n^{(2)} \Psi_n^{(2)}(y), & y \in L_2. \end{cases} \quad (2.4.3)$$

We can convert (2.4.2) and (2.4.3) into an infinite system of linear algebraic equations by multiplying each by $\Psi_m^{(3)}, m \in \mathbb{N}_0$, and integrating over L_3 . From (2.4.3) we find

$$\int_{L_3} \sum_{n=0}^{\infty} U_n^{(3)} \Psi_n^{(3)}(y) \Psi_m^{(3)}(y) dy = \int_{L_1} \sum_{n=1}^{\infty} U_n^{(1)} \Psi_n^{(1)}(y) \Psi_m^{(3)}(y) dy + \int_{L_2} \sum_{n=1}^{\infty} U_n^{(2)} \Psi_n^{(2)}(y) \Psi_m^{(3)}(y) dy, \quad m \in \mathbb{N}_0. \quad (2.4.4)$$

Reversing the order of summation and integration we can simplify this to

$$U_m^{(3)} = \sum_{n=1}^{\infty} U_n^{(1)} d_{nm} + \sum_{n=1}^{\infty} U_n^{(2)} e_{nm}, \quad m \in \mathbb{N}_0, \quad (2.4.5)$$

where we have defined

$$d_{nm} = \frac{1}{d} \int_{L_1} \Psi_n^{(1)}(y) \Psi_m^{(3)}(y) dy, \quad m \in \mathbb{N}_0, n \in \mathbb{N}, \quad (2.4.6)$$

$$e_{nm} = \frac{1}{d} \int_{L_2} \Psi_n^{(2)}(y) \Psi_m^{(3)}(y) dy, \quad m \in \mathbb{N}_0, n \in \mathbb{N}. \quad (2.4.7)$$

Similarly from (2.4.2) we obtain

$$U_m^{(3)} \frac{\coth \gamma_m a}{\gamma_m} = \sum_{n=1}^{\infty} \frac{U_n^{(1)}}{-\alpha_n} d_{nm} + \sum_{n=1}^{\infty} \frac{U_n^{(2)}}{-\beta_n} e_{nm}, \quad m \in \mathbb{N}_0. \quad (2.4.8)$$

Evaluating the integral d_{nm} , we have

$$\begin{aligned} d_{nm} &= \frac{1}{d} \int_b^d 2 \sin \nu_n(d-y) \sin \lambda_m(d-y) dy, \\ &= \frac{1}{d} \left[\frac{\sin(\nu_n + \lambda_m)(d-y)}{\nu_n + \lambda_m} - \frac{\sin(\nu_n - \lambda_m)(d-y)}{\nu_n - \lambda_m} \right]_b^d, \quad \text{provided } \nu_n \neq \lambda_m, \\ &= \frac{1}{d(\nu_n^2 - \lambda_m^2)} \left[(\nu_n + \lambda_m) (\sin \nu_n c \cos \lambda_m c - \cos \nu_n c \sin \lambda_m c) - \right. \\ &\quad \left. (\nu_n - \lambda_m) (\sin \nu_n c \cos \lambda_m c + \cos \nu_n c \sin \lambda_m c) \right]. \end{aligned} \quad (2.4.9)$$

Note that since n is an integer, $\sin \nu_n c = 0$ and $\cos \nu_n c = (-1)^n$. Using the relationships $\nu_n^2 - \alpha_n^2 = k^2$, and $\lambda_n^2 - \gamma_n^2 = k^2$, in (2.4.9) we find, (provided $\gamma_m \neq \alpha_n$)

$$d_{nm} = \frac{2\nu_n(-1)^n \sin \lambda_m c}{d(\gamma_m^2 - \alpha_n^2)}. \quad (2.4.10)$$

If we evaluate the integral (2.4.7), we find

$$\begin{aligned} e_{nm} &= \frac{1}{d} \int_0^b 2 \sin \mu_n (b-y) \sin \lambda_m (d-y) dy, \\ &= \frac{1}{d(\lambda_m^2 - \mu_n^2)} \left[-(\lambda_m + \mu_n) (\sin(\mu_n b - \lambda_m d) - \sin(-\lambda_m c)) \right. \\ &\quad \left. - (\lambda_m - \mu_n) (\sin(\lambda_m c) - \sin(\mu_n b + \lambda_m d)) \right], \end{aligned} \quad (2.4.11)$$

provided $\lambda_m \neq \mu_n$. Now $\sin(\mu_n b \pm \lambda_m d) = \sin(\pi(n \pm m)) = 0$, as n and m are integers, and therefore provided $\gamma_m \neq \beta_n$

$$e_{nm} = \frac{2\mu_n \sin \lambda_m c}{d(\gamma_m^2 - \beta_n^2)}. \quad (2.4.12)$$

We will assume that b/d (and hence also c/d) is irrational so that $\nu_n \neq \lambda_m$, in (2.4.9) and $\lambda_m \neq \mu_n$ in (2.4.11), for any m and n , although Evans, Linton, and Ursell (1993), Appendix D, show how continuity arguments can be used so that for the final trapped-mode condition this restriction may be removed.

Eliminating $U_m^{(3)}$ from (2.4.5) and (2.4.8) we obtain

$$\left(\sum_{n=1}^{\infty} U_n^{(1)} d_{nm} + \sum_{n=1}^{\infty} U_n^{(2)} e_{nm} \right) \frac{\coth \gamma_m a}{\gamma_m} = \sum_{n=1}^{\infty} \frac{U_n^{(1)}}{-\alpha_n} d_{nm} + \sum_{n=1}^{\infty} \frac{U_n^{(2)}}{-\beta_n} e_{nm}, \quad (2.4.13)$$

which can be rewritten

$$\sum_{n=1}^{\infty} U_n^{(1)} d_{nm} \left(\gamma_m^{-1} \coth \gamma_m a + \alpha_n^{-1} \right) + \sum_{n=1}^{\infty} U_n^{(2)} e_{nm} \left(\gamma_m^{-1} \coth \gamma_m a + \beta_n^{-1} \right) = 0, \quad m \in \mathbb{N}_0. \quad (2.4.14)$$

We could have eliminated either $U_n^{(1)}$ or $U_n^{(2)}$ from (2.4.5) and (2.4.8) by multiplying (2.4.2) and (2.4.3) by either $\Psi_m^{(1)}$ or $\Psi_m^{(2)}$, $m \in \mathbb{N}$, but in order to use residue calculus theory, we require (2.4.14) to be in the form shown.

Substituting (2.4.10) and (2.4.12) into (2.4.14), with slight rearrangement we have

$$\begin{aligned} \sum_{n=1}^{\infty} \frac{U_n^{(1)} (-1)^n \nu_n}{\alpha_n} \left(\frac{(\alpha_n + \gamma_m) + (\alpha_n - \gamma_m) e^{-2\gamma_m a}}{(\alpha_n + \gamma_m)(\alpha_n - \gamma_m)} \right) \\ - \sum_{n=1}^{\infty} \frac{U_n^{(2)} \mu_n}{\beta_n} \left(\frac{(\beta_n + \gamma_m) + (\beta_n - \gamma_m) e^{-2\gamma_m a}}{(\beta_n + \gamma_m)(\beta_n - \gamma_m)} \right) = 0, \quad m \in \mathbb{N}_0. \end{aligned} \quad (2.4.15)$$

We can simplify (2.4.15) as

$$\begin{aligned} \sum_{n=1}^{\infty} U_n \left(\frac{1}{\alpha_n - \gamma_m} + \frac{\zeta_m}{\alpha_n + \gamma_m} \right) - \\ \sum_{n=1}^{\infty} V_n \left(\frac{1}{\beta_n - \gamma_m} + \frac{\zeta_m}{\beta_n + \gamma_m} \right) = 0, \quad m \in \mathbb{N}_0, \end{aligned} \quad (2.4.16)$$

where we have defined

$$U_n = \frac{U_n^{(1)}(-1)^n \nu_n}{\alpha_n}, \quad V_n = \frac{U_n^{(2)} \mu_n}{\beta_n}, \quad \text{and } \zeta_m = e^{-2\gamma_m a}. \quad (2.4.17)$$

So far we have only used the boundary conditions (2.3.1)–(2.3.6) and not the condition (2.3.8), which anticipates the singular behaviour near the edge. Condition (2.3.8) enables us to derive a unique solution to the problem. By combining all the conditions (2.3.3)–(2.3.8), we can produce a valid solution to the complete problem under consideration.

To show how the edge condition (2.3.8) influences the asymptotic behaviour of the coefficients $U_n^{(1)}$, $U_n^{(2)}$ and $U_n^{(3)}$ in (2.3.31)–(2.3.33) we consider the derivatives of $\phi_1(x, y)$:

$$\frac{\partial \phi_1}{\partial x} = \sum_{n=1}^{\infty} U_n^{(1)} 2^{\frac{1}{2}} e^{-\alpha_n(x-a)} \sin \nu_n(d-y), \quad |x| > a, \quad (2.4.18)$$

$$\frac{\partial \phi_1}{\partial y} = \sum_{n=1}^{\infty} U_n^{(1)} 2^{\frac{1}{2}} \frac{\nu_n}{\alpha_n} e^{-\alpha_n(x-a)} \cos \nu_n(d-y), \quad |x| > a. \quad (2.4.19)$$

As $n \rightarrow \infty$ we have from (2.3.31) that $\alpha_n = n\pi/c + O(n^{-1})$. If we assume that $U_n^{(1)} = O(n^\tau)$ as $n \rightarrow \infty$, where τ is to be determined, then as $x \rightarrow a+$ when $y = b$ we see from (2.4.18) and (2.4.19) that

$$|\nabla \phi_1| = O(h(x)), \quad \text{as } x \rightarrow a+, \quad (2.4.20)$$

where

$$h(x) = \sum_{n=1}^{\infty} n^\tau e^{-n(x-a)}. \quad (2.4.21)$$

Making use of Mellin transforms, see Martin (1995), we can show that

$$h(x) = O(x^{-1-\tau}) \quad \text{as } x \rightarrow a+. \quad (2.4.22)$$

Using the edge condition (2.3.8), we find that

$$\tau = -\frac{1}{2}, \quad (2.4.23)$$

and hence

$$U_n^{(1)} = O(n^{-\frac{1}{2}}) \quad \text{as } n \rightarrow \infty. \quad (2.4.24)$$

We can also show, using a similar method, that

$$U_n^{(2)}, U_n^{(3)} = O(n^{-\frac{1}{2}}) \quad \text{as } n \rightarrow \infty. \quad (2.4.25)$$

Since both $U_n^{(1)}, U_n^{(2)} = O(n^{-\frac{1}{2}})$ as $n \rightarrow \infty$, we see from (2.4.17) that the solutions U_n and V_n must also satisfy

$$U_n, V_n = O(n^{-\frac{1}{2}}) \text{ as } n \rightarrow \infty. \quad (2.4.26)$$

In the next section we derive an approximate solution to (2.4.16) for large a , taking into account the asymptotic behaviour required from (2.4.26).

Approximate solution for large a

We now note that since $\gamma_m, m \in \mathbb{N}$, is real, the terms $\zeta_m, m \in \mathbb{N}$, appearing in (2.4.16) decay rapidly to zero as $a/d \rightarrow \infty$. A good approximation for large a is therefore to set $\zeta_m = 0$ for $m \in \mathbb{N}$. The idea for this type of approximation goes back to Hurd (1954) who was studying the propagation of surface waves along a grating of parallel plates. The equivalence of this approximation to the wide-spacing approximation, which has been used previously in water-wave diffraction problems, see for example Evans (1990), was shown for a different but related problem by Linton and Evans (1993). This wide-spacing approximation, which is derived using physical arguments, requires the window to be sufficiently wide so that the edges of the window do not effect each other.

Using this approximation in (2.4.16) we find

$$\sum_{n=1}^{\infty} \left(\frac{U_n}{\alpha_n - \gamma_m} - \frac{V_n}{\beta_n - \gamma_m} \right) = -\delta_{m0} \zeta_0 \sum_{n=1}^{\infty} \left(\frac{U_n}{\alpha_n + \gamma_0} - \frac{V_n}{\beta_n + \gamma_0} \right), \quad m \in \mathbb{N}_0, \quad (2.4.27)$$

with U_n and V_n having the behaviour shown in (2.4.26).

We shall now solve (2.4.27) using a method originally described in Whitehead (1951) and Berz (1951) and since used by many authors. A full description of the method is given by Mittra and Lee (1971).

Consider the integrals

$$I_m = \lim_{N \rightarrow \infty} \frac{1}{2\pi i} \int_{C_N} \frac{f(z)}{z - \gamma_m} dz, \quad J_m = \lim_{N \rightarrow \infty} \frac{1}{2\pi i} \int_{C_N} \frac{f(z)}{z + \gamma_m} dz, \quad m \in \mathbb{N}_0, \quad (2.4.28)$$

where C_N is a sequence of contours (to be determined) on which $z \rightarrow \infty$ as $N \rightarrow \infty$ and $f(z)$ is a meromorphic function which has the following properties:

- P1. $f(z)$ has simple poles at $z = \alpha_n$ and $z = \beta_n, n \in \mathbb{N}$;
- P2. $f(z)$ has simple zeros at $z = \gamma_n, n \in \mathbb{N}$, but not at $z = \gamma_0$;
- P3. $f(z) = O(z^{-\frac{1}{2}})$ as $|z| \rightarrow \infty$ on C_N as $N \rightarrow \infty$.

Condition P3 is required so that $I_m = 0$ and $J_m = 0$. As we will see later, condition P3 leads to the correct behaviour required by the edge condition (2.4.26).

Applying Cauchy's residue theorem to I_m and J_m we find

$$\sum_{n=1}^{\infty} \frac{R(f : \alpha_n)}{\alpha_n - \gamma_m} + \sum_{n=1}^{\infty} \frac{R(f : \beta_n)}{\beta_n - \gamma_m} + \delta_{m0} f(\gamma_0) = 0, \quad (2.4.29)$$

$$\sum_{n=1}^{\infty} \frac{R(f : \alpha_n)}{\alpha_n + \gamma_m} + \sum_{n=1}^{\infty} \frac{R(f : \beta_n)}{\beta_n + \gamma_m} + f(-\gamma_m) = 0, \quad (2.4.30)$$

where $R(f : z_0)$ represents the residue of $f(z)$ at $z = z_0$, and $m \in \mathbb{N}_0$, in each case. Due to the linear nature of the problem we can normalise $f(z)$ by setting

$$f(\gamma_0) = 1. \quad (2.4.31)$$

Comparing (2.4.29) and (2.4.30) with (2.4.27) we find

$$U_n = R(f : \alpha_n), \quad n \in \mathbb{N}, \quad (2.4.32)$$

and

$$V_n = -R(f : \beta_n), \quad n \in \mathbb{N}, \quad (2.4.33)$$

provided from (2.4.30) with $m = 0$, we have

$$f(-\gamma_0) \zeta_0 = -1. \quad (2.4.34)$$

The result given in (2.4.34) is the condition for trapped modes, provided we can determine a suitable $f(z)$.

Construction of $f(z)$

We would like to choose a function of the form

$$f(z) = h_1 g(z), \quad (2.4.35)$$

where

$$g(z) = \prod_{n=1}^{\infty} \frac{(1 - z/\gamma_n)}{(1 - z/\alpha_n)(1 - z/\beta_n)}, \quad (2.4.36)$$

as $g(z)$ has the correct zeros and poles to satisfy P1 and P2. The constant h_1 has to be chosen to satisfy the normalization condition given by (2.4.31).

To derive the correct solution the function $f(z)$ must have the asymptotics shown in P3, and hence we must examine the behaviour of $g(z)$ for large z . With this in mind we write

$$g(z) = \prod_{n=1}^{\infty} \frac{1 - z/\nu_n}{1 - z/\alpha_n} \prod_{n=1}^{\infty} \frac{1 - z/\mu_n}{1 - z/\beta_n} \prod_{n=1}^{\infty} \frac{1 - z/\gamma_n}{1 - z/\lambda_n} \prod_{n=1}^{\infty} \frac{(1 - z/\lambda_n)}{(1 - z/\mu_n)(1 - z/\nu_n)}. \quad (2.4.37)$$

The first infinite product can be expanded as

$$\prod_{n=1}^{\infty} \frac{1 - z/\nu_n}{1 - z/\alpha_n} = \prod_{n=1}^{\infty} \frac{\alpha_n}{\nu_n} \prod_{n=1}^{\infty} \frac{1 - \nu_n/z}{1 - \alpha_n/z} = \prod_{n=1}^{\infty} \left(1 - \frac{k^2}{\nu_n^2}\right)^{\frac{1}{2}} \prod_{n=1}^{\infty} \left(1 + \frac{\alpha_n - \nu_n}{z - \alpha_n}\right). \quad (2.4.38)$$

Using Gradshteyn and Ryzhik (1980), eqn 1.431(1), we simplify this to

$$\prod_{n=1}^{\infty} \frac{1 - z/\nu_n}{1 - z/\alpha_n} = \left(\frac{\sin kc}{kc}\right)^{\frac{1}{2}} \prod_{n=1}^{\infty} \left(1 - \frac{k^2}{(z - \alpha_n)(\alpha_n + \nu_n)}\right). \quad (2.4.39)$$

In a similar way, we have

$$\prod_{n=1}^{\infty} \frac{1 - z/\mu_n}{1 - z/\beta_n} = \left(\frac{\sin kb}{kb}\right)^{\frac{1}{2}} \prod_{n=1}^{\infty} \left(1 - \frac{k^2}{(z - \beta_n)(\beta_n + \mu_n)}\right), \quad (2.4.40)$$

and

$$\prod_{n=1}^{\infty} \frac{1 - z/\gamma_n}{1 - z/\lambda_n} = \left[\left(1 - \frac{(kd)^2}{\pi^2}\right)^{-1} \left(\frac{\sin kd}{kd}\right)\right]^{-\frac{1}{2}} \prod_{n=1}^{\infty} \left(1 + \frac{k^2}{(z - \lambda_n)(\lambda_n + \gamma_n)}\right). \quad (2.4.41)$$

All the infinite products in (2.4.39)–(2.4.41) can be shown to converge uniformly as $z \rightarrow \infty$ provided z does not take certain values. We use the fact that the infinite product $\prod_{n=1}^{\infty} [1 + u_n(z)]$ is uniformly convergent on any compact set D if the series $\sum_{n=1}^{\infty} |u_n(z)|$ is uniformly convergent on D , (see Gradshteyn and Ryzhik (1980), eqn 0.255). As all the terms α_n , β_n and γ_n are of the form $An + O(n^{-1})$ as $n \rightarrow \infty$ where A is a constant independent of n , a comparison of the products with $\sum_{n=1}^{\infty} n^{-2}$, shows that they are uniformly convergent on any compact set excluding $z = \alpha_n$, $z = \beta_n$ and $z = \lambda_n$, respectively. Provided $z \rightarrow \infty$ through a sequence of values which avoids these points we have

$$g(z) \sim \left[\left(1 - \frac{(kd)^2}{\pi^2}\right) \left(\frac{d \sin kb \sin kc}{kbc \sin kd}\right)\right]^{\frac{1}{2}} \prod_{n=1}^{\infty} \frac{(1 - z/\lambda_n)}{(1 - z/\mu_n)(1 - z/\nu_n)}. \quad (2.4.42)$$

We now use the result from Gradshteyn and Ryzhik (1980), eqn 8.325(2),

$$\prod_{n=1}^{\infty} \left(1 - \frac{z}{n+b}\right) e^{z/n} = \frac{e^{\gamma z} \Gamma(1+b)}{\Gamma(1+b-z)}, \quad (2.4.43)$$

where $\Gamma(\cdot)$ is the Gamma function and $\gamma \approx 0.5772$ is Euler's constant. It follows from (2.4.43) that

$$\begin{aligned} \prod_{n=1}^{\infty} \frac{(1 - z/\lambda_n)}{(1 - z/\mu_n)(1 - z/\nu_n)} &= \frac{\prod_{n=1}^{\infty} (1 - zd/(n+1)\pi) e^{zd/n\pi}}{\prod_{n=1}^{\infty} (1 - zb/(n\pi)) e^{zb/n\pi} (1 - zc/(n\pi)) e^{zc/n\pi}}, \\ &= \frac{e^{\gamma zd/\pi} \Gamma(2)}{\Gamma(2 - zd/\pi)} \times \frac{\Gamma(1 - zb/\pi)}{e^{\gamma zb/\pi} \Gamma(1)} \times \frac{\Gamma(1 - zc/\pi)}{e^{\gamma zc/\pi} \Gamma(1)}. \end{aligned} \quad (2.4.44)$$

From Abramowitz and Stegun (1972), eqn 6.139, we have

$$\Gamma(az + b) \sim \sqrt{2\pi} e^{-az} (az)^{az+b-\frac{1}{2}} \text{ as } |z| \rightarrow \infty, \quad z \neq -|z|, \quad a > 0. \quad (2.4.45)$$

Using (2.4.45) with (2.4.44) we see, after some simplification, that as $z \rightarrow \infty, z \neq |z|$,

$$\begin{aligned} \prod_{n=1}^{\infty} \frac{(1 - z/\lambda_n)}{(1 - z/\mu_n)(1 - z/\nu_n)} &\sim \left(\frac{2bc\pi^2}{-zd^3} \right)^{\frac{1}{2}} b^{-bz/\pi} c^{-cz/\pi} d^{dz/\pi}, \\ &= \left(\frac{2bc\pi^2}{-zd^3} \right)^{\frac{1}{2}} \exp \left\{ \frac{z}{\pi} (b \ln(d/b) + c \ln(d/c)) \right\}. \end{aligned} \quad (2.4.46)$$

From (2.4.42) we therefore find that

$$g(z) \sim \left[\left(1 - \frac{(kd)^2}{\pi^2} \right) \left(\frac{2\pi^2 \sin kb \sin kc}{(-z)kd^2 \sin kd} \right) \right]^{\frac{1}{2}} \exp \left\{ \frac{z}{\pi} (b \ln(d/b) + c \ln(d/c)) \right\}, \quad (2.4.47)$$

as $z \rightarrow \infty, z \neq |z|$ and so the function $f(z)$ given by (2.4.35) does not have the necessary asymptotic form.

For the case when z is real and positive we use the reflection property of the Gamma function

$$\Gamma(w)\Gamma(-w) = \frac{-\pi}{w \sin w\pi}. \quad (2.4.48)$$

Substituting this into (2.4.44), and using (2.4.45) we find the asymptotic behaviour to be

$$\begin{aligned} g(z) &\sim \left[\left(1 - \frac{(kd)^2}{\pi^2} \right) \left(\frac{(bc)^2 \sin kb \sin kc}{2kd^4 \sin kd} \right) \right]^{\frac{1}{2}} \\ &\quad \times \frac{\sin zd}{\sin zb \sin zc} z^{-\frac{1}{2}} \exp \left\{ \frac{z}{\pi} (b \ln(d/b) + c \ln(d/c)) \right\}, \end{aligned} \quad (2.4.49)$$

as $z \rightarrow \infty, z \neq -|z|$, through any sequence of values which avoids the points $z = n\pi/b$ and $z = n\pi/c, n \in \mathbb{N}$. If we take C_N to be a sequence of circles with centre at the origin and radius R_N which avoids the points $z = \alpha_n, z = \beta_n, z = \lambda_n, z = n\pi/b$ and $z = n\pi/c, n \in \mathbb{N}$, instead of (2.4.36), we can consider the function

$$g(z) = \exp \left\{ \frac{-z}{\pi} (b \ln(d/b) + c \ln(d/c)) \right\} \prod_{n=1}^{\infty} \frac{(1 - z/\gamma_n)}{(1 - z/\alpha_n)(1 - z/\beta_n)}, \quad (2.4.50)$$

which is $O(z^{-\frac{1}{2}})$ as $|z| \rightarrow \infty$ on C_N as $N \rightarrow \infty$. If we now choose

$$h_1 = \exp \left\{ \frac{\gamma_0}{\pi} (b \ln(d/b) + c \ln(d/c)) \right\} \prod_{n=1}^{\infty} \frac{(1 - \gamma_0/\alpha_n)(1 - \gamma_0/\beta_n)}{(1 - \gamma_0/\gamma_n)} \quad (2.4.51)$$

then $f(z) = h_1 g(z)$ has all the required properties to satisfy (2.4.31).

To ensure that the edge condition (2.3.8) is satisfied the solutions U_n and V_n must satisfy (2.4.26). Earlier we have shown that $U_m = R(f : \alpha_m)$ and $V_m = R(f : \beta_m)$ and so

$$U_m = -\alpha_m h_1 \exp \left\{ \frac{-\alpha_m}{\pi} (b \ln(d/b) + c \ln(d/c)) \right\} \times \prod_{n=1}^{\infty} \frac{(1 - \alpha_m/\gamma_n)}{(1 - \alpha_m/\beta_n)} \prod_{\substack{n=1 \\ n \neq m}}^{\infty} \frac{1}{(1 - \alpha_m/\alpha_n)}. \quad (2.4.52)$$

Using the same idea as in (2.4.37) we can expand this to

$$U_m = -\alpha_m \left(1 - \frac{\alpha_m c}{m\pi}\right) h_1 \exp \left\{ \frac{-\alpha_m}{\pi} (b \ln(d/b) + c \ln(d/c)) \right\} \times \prod_{n=1}^{\infty} \frac{(1 - \alpha_m b/n\pi)(1 - \alpha_m/\gamma_n)}{(1 - \alpha_m/\beta_n)(1 - \alpha_m d/(n+1)\pi)} \prod_{\substack{n=1 \\ n \neq m}}^{\infty} \frac{(1 - \alpha_m c/n\pi)}{(1 - \alpha_m/\alpha_n)} \times \prod_{n=1}^{\infty} \frac{(1 - \alpha_m/\lambda_n)}{(1 - \alpha_m/\mu_n)(1 - \alpha_m/\nu_n)}. \quad (2.4.53)$$

The first two infinite products can be rearranged in the form shown in (2.4.39)–(2.4.41) and are therefore $O(1)$ as $m \rightarrow \infty$. Using (2.4.49) on the last infinite product in (2.4.53) we have

$$\begin{aligned} & \exp \left\{ \frac{-\alpha_m}{\pi} (b \ln(d/b) + c \ln(d/c)) \right\} \prod_{n=1}^{\infty} \frac{(1 - \alpha_m/\lambda_n)}{(1 - \alpha_m/\mu_n)(1 - \alpha_m/\nu_n)} \\ & \sim \frac{C \sin \alpha_m d \alpha_m^{-\frac{1}{2}}}{\sin \alpha_m b \sin \alpha_m c}, \\ & \sim \frac{C \sin \alpha_m d}{\sin \alpha_m b} \operatorname{cosec} \left(m\pi - \frac{(kc)^2}{2m\pi} + O(m^{-2}) \right) \left(\frac{m\pi}{c} \right)^{-\frac{1}{2}} \left(1 + O(m^{-2}) \right), \\ & \sim \frac{2C\pi^{1/2} \sin \alpha_m d}{k^2 c^{3/2} \sin \alpha_m b} m^{\frac{1}{2}} \left(1 + O(m^{-1}) \right), \end{aligned} \quad (2.4.54)$$

as $m \rightarrow \infty$, where,

$$C = \left[\left(1 - \frac{(kd)^2}{\pi^2} \right) \left(\frac{(bc)^2 \sin kb \sin kc}{2kd^4 \sin kd} \right) \right]^{\frac{1}{2}} \quad (2.4.55)$$

and since,

$$\alpha_m \sim \frac{m\pi}{c} + \frac{k^2 c}{2m\pi} + O(m^{-2}). \quad (2.4.56)$$

As $m \rightarrow \infty$ we also have

$$\left(1 - \frac{\alpha_m c}{m\pi}\right) \sim \frac{1}{2} \left(\frac{kc}{m\pi}\right)^2 + O(m^{-3}). \quad (2.4.57)$$

Combining (2.4.53)–(2.4.57) we can see that U_n is $O(n^{-\frac{1}{2}})$ as $n \rightarrow \infty$. By changing the α_m terms to β_m terms in (2.4.53)–(2.4.57) we find that V_n is also $O(n^{-\frac{1}{2}})$ as $n \rightarrow \infty$. The chosen function $f(z)$ therefore has the required asymptotics to take account of the expected singularity in the velocity field near the plate edge.

Trapped mode condition

The only condition now left to satisfy is (2.4.34). If we let $\gamma_0 = -i\gamma'$, where $\gamma' = \left(k^2 - \left(\frac{\pi}{d}\right)^2\right)^{\frac{1}{2}}$, this condition reduces to

$$f(i\gamma') = -e^{-2i\gamma'a}. \quad (2.4.58)$$

Using (2.4.35), (2.4.50) and (2.4.51) we find

$$f(i\gamma') = \exp\left\{\frac{-2i\gamma'}{\pi}(b \ln(d/b) + c \ln(d/c))\right\} \times \prod_{n=1}^{\infty} \frac{(1 + i\gamma'/\alpha_n)(1 + i\gamma'/\beta_n)(1 - i\gamma'/\gamma_n)}{(1 - i\gamma'/\alpha_n)(1 - i\gamma'/\beta_n)(1 + i\gamma'/\gamma_n)}, \quad (2.4.59)$$

which clearly has magnitude one, since the top line of the product is the complex conjugate of the bottom line. If we use the definition

$$\tan^{-1}(z) = \frac{1}{2i} \ln\left(\frac{1 + iz}{1 - iz}\right), \quad (2.4.60)$$

we see that

$$\exp\left(2i \sum_{n=1}^{\infty} \tan^{-1}(z/z_n)\right) = \prod_{n=1}^{\infty} \left(\frac{1 + iz/z_n}{1 - iz/z_n}\right), \quad (2.4.61)$$

and hence (2.4.59) can be reduced to

$$f(i\gamma') = \exp\left(-2i(\gamma'\Theta + \chi)\right), \quad (2.4.62)$$

where

$$\chi = \sum_{n=1}^{\infty} \left(\tan^{-1}\left(\frac{\gamma'}{\gamma_n}\right) - \tan^{-1}\left(\frac{\gamma'}{\alpha_n}\right) - \tan^{-1}\left(\frac{\gamma'}{\beta_n}\right)\right), \quad (2.4.63)$$

and

$$\Theta = \frac{1}{\pi}(b \ln(d/b) + c \ln(d/c)). \quad (2.4.64)$$

The condition for the existence of trapped modes, (2.4.58), becomes

$$e^{2i\gamma'(a-\Theta)} = -e^{2i\chi} \quad (2.4.65)$$

which can be simplified to

$$\gamma'(a - \Theta) = \chi + \left(n - \frac{1}{2}\right)\pi, \quad n \text{ an integer.} \quad (2.4.66)$$

Antisymmetry about $x = 0$

For the case of antisymmetry about $x = 0$, the condition (2.3.1) is replaced by

$$\phi = 0 \text{ on } x = 0, \quad 0 < y < d, \quad (2.4.67)$$

and hence the cosh and sinh terms in (2.3.33) are replaced by sinh and cosh respectively.

Equation (2.4.16) becomes

$$\sum_{n=1}^{\infty} U_n \left(\frac{1}{\alpha_n - \gamma_m} - \frac{\zeta_m}{\alpha_n + \gamma_m} \right) - \sum_{n=1}^{\infty} V_n \left(\frac{1}{\beta_n - \gamma_m} - \frac{\zeta_m}{\beta_n + \gamma_m} \right) = 0, \quad m \in \mathbb{N}_0, \quad (2.4.68)$$

and (2.4.58) becomes

$$f(i\gamma') = e^{-2i\gamma'a}, \quad (2.4.69)$$

with exactly the same function f as before. The condition for the existence of trapped modes antisymmetric about $x = 0$, equivalent to (2.4.66), is therefore

$$\gamma'(a - \Theta) = \chi + n\pi, \quad n \text{ an integer,} \quad (2.4.70)$$

where Θ and χ are defined as before.

Full solution using the modified residue calculus method

The idea behind this method is due to VanBlaricum Jr and Mittra (1969) and Itoh and Mittra (1969) and is described briefly by Jones (1979), §2.12.

We form a solution to (2.4.16) by considering the integrals

$$I_m = \lim_{N \rightarrow \infty} \frac{1}{2\pi i} \int_{C_N} f(z) \left(\frac{1}{z - \gamma_m} + \frac{\zeta_m}{z + \gamma_m} \right) dz, \quad m \in \mathbb{N}_0, \quad (2.4.71)$$

where C_N is a sequence of contours (to be determined) on which $z \rightarrow \infty$ as $N \rightarrow \infty$ and $f(z)$ is a meromorphic function which has the following properties:

P1. $f(z)$ has simple poles at $z = \alpha_n$ and $z = \beta_n$, $n \in \mathbb{N}$;

P2. $f(z) = O(z^{-\frac{1}{2}})$ as $|z| \rightarrow \infty$ on C_N as $N \rightarrow \infty$.

To construct a function for the full solution using modified residue calculus theory we use the same ideas as previously and let

$$f(z) = g(z)h(z), \quad (2.4.72)$$

where $g(z)$ is given by (2.4.50) and

$$h(z) = 1 + \sum_{n=1}^{\infty} \frac{A_n}{z - \gamma_n}, \quad (2.4.73)$$

for some constants A_n .

The reasoning behind this choice for $h(z)$ is as follows. Unlike the approximate method described previously, we no longer require $f(z)$ to vanish at $z = \gamma_n$ ($n \in \mathbb{N}$). We do anticipate however, that as $a \rightarrow \infty$, $h(z) \rightarrow 1$, since the exponential terms ζ_n will decay rapidly to zero, i.e. we also expect the constants A_m to tend to zero rapidly as $a \rightarrow \infty$. The function $h(z)$ replaces the normalization constant h_1 and is chosen so that the zeros of $g(z)$ at γ_n are cancelled by the poles of $h(z)$ at these points.

If we choose the same curves as in the approximate method we have,

$$f(z) = O(z^{-\frac{1}{2}}) \text{ as } |z| \rightarrow \infty \text{ on } C_N \text{ as } N \rightarrow \infty, \quad (2.4.74)$$

and so P2 is satisfied. We can apply Cauchy's residue theorem to (2.4.71) to obtain

$$\begin{aligned} \sum_{n=1}^{\infty} R(f : \alpha_n) \left(\frac{1}{\alpha_n - \gamma_m} + \frac{\zeta_m}{\alpha_n + \gamma_m} \right) + \sum_{n=1}^{\infty} R(f : \beta_n) \left(\frac{1}{\beta_n - \gamma_m} + \frac{\zeta_m}{\beta_n + \gamma_m} \right) \\ + f(\gamma_m) + \zeta_m f(-\gamma_m) = 0, \quad m \in \mathbb{N}_0. \end{aligned} \quad (2.4.75)$$

Comparing (2.4.75) with (2.4.16) we find that $U_n = R(f : \alpha_n)$, $V_n = -R(f : \beta_n)$, $n \in \mathbb{N}$, provided

$$f(\gamma_m) + \zeta_m f(-\gamma_m) = 0, \quad m \in \mathbb{N}_0. \quad (2.4.76)$$

To find the coefficients A_m appearing in (2.4.73), we have for $m \in \mathbb{N}$

$$\begin{aligned} f(\gamma_m) = - \exp \left\{ - \frac{\gamma_m}{\pi} (b \ln(d/b) + c \ln(d/c)) \right\} \left(\frac{A_m}{\gamma_m (1 - \gamma_m/\alpha_m) (1 - \gamma_m/\beta_m)} \right) \\ \times \prod_{\substack{n=1 \\ n \neq m}}^{\infty} \frac{1 - \gamma_m/\gamma_n}{(1 - \gamma_m/\alpha_n) (1 - \gamma_m/\beta_n)}, \end{aligned} \quad (2.4.77)$$

and

$$f(-\gamma_m) = \left(1 - \sum_{n=1}^{\infty} \frac{A_n}{\gamma_m + \gamma_n}\right) \exp \left\{ \frac{\gamma_m}{\pi} (b \ln(d/b) + c \ln(d/c)) \right\} \\ \times \left(\frac{2}{(1 + \gamma_m/\alpha_m)(1 + \gamma_m/\beta_m)} \right) \prod_{\substack{n=1 \\ n \neq m}}^{\infty} \frac{1 + \gamma_m/\gamma_n}{(1 + \gamma_m/\alpha_n)(1 + \gamma_m/\beta_n)}. \quad (2.4.78)$$

Substituting (2.4.77) and (2.4.78) into (2.4.76), we obtain

$$A_m + B_m \sum_{n=1}^{\infty} \frac{A_n}{\gamma_m + \gamma_n} = B_m, \quad m \in \mathbb{N}, \quad (2.4.79)$$

where

$$B_m = \left(\frac{2\gamma_m(\alpha_m - \gamma_m)(\beta_m - \gamma_m)}{(\alpha_m + \gamma_m)(\beta_m + \gamma_m)} \right) \exp \left\{ \frac{2\gamma_m}{\pi} (b \ln(d/b) + c \ln(d/c) - a\pi) \right\} \\ \times \prod_{\substack{n=1 \\ n \neq m}}^{\infty} \frac{(1 + \gamma_m/\gamma_n)(1 - \gamma_m/\alpha_n)(1 - \gamma_m/\beta_n)}{(1 + \gamma_m/\alpha_n)(1 + \gamma_m/\beta_n)(1 - \gamma_m/\gamma_n)}. \quad (2.4.80)$$

The infinite system of equations (2.4.79) has very nice properties as it is firstly real and the presence of the factor ζ_m in B_m enables one to see that as $a \rightarrow \infty$, the coefficients A_m decay exponentially to zero. This condition was expected and discussed earlier. Moreover, the terms B_m decay exponentially as $m \rightarrow \infty$ and so the system can be solved very efficiently via a numerical truncation approach.

Infinite systems of the form shown in (2.4.79) occur regularly in this thesis. Writing (2.4.79) in the most general form we have

$$A_m + \sum_{n=1}^{\infty} C_{mn} A_n = B_m, \quad m \in \mathbb{N}. \quad (2.4.81)$$

A sufficient condition that the infinite system (2.4.81) has a unique solution A_n with $\sum_{n=1}^{\infty} A_n^2 < \infty$ is that

$$\sum_{n=1}^{\infty} B_n^2 < \infty, \quad (2.4.82)$$

and

$$\sum_{m=1}^{\infty} \sum_{n=1}^{\infty} C_{mn}^2 < 1, \quad (2.4.83)$$

are both satisfied, see for example, Hutson and Pym (1980), §3.6. It can be shown, using methods described in Evans (1992), Appendix B, and Evans et al. (1993), Appendix C, that these conditions are satisfied provided a/d is sufficiently large.

Trapped mode condition

We now return to the one condition still to be satisfied, namely (2.4.76) with $m = 0$. If we let $\gamma_0 = -i\gamma'$, where $\gamma' = \left(k^2 - \left(\frac{\pi}{d}\right)^2\right)^{\frac{1}{2}}$, this condition reduces to

$$e^{2i\gamma'a} = -\frac{f(-i\gamma')}{f(i\gamma')}. \quad (2.4.84)$$

From (2.4.50) we have

$$\frac{g(-i\gamma')}{g(i\gamma')} = \exp\{2i\gamma'\Theta\} \prod_{n=1}^{\infty} \frac{(1 + i\gamma'_m/\gamma_n)(1 - i\gamma'_m/\alpha_n)(1 - i\gamma'_m/\beta_n)}{(1 + i\gamma'_m/\alpha_n)(1 + i\gamma'_m/\beta_n)(1 - i\gamma'_m/\gamma_n)}. \quad (2.4.85)$$

Substituting (2.4.61) into (2.4.85) we obtain

$$\frac{g(-i\gamma')}{g(i\gamma')} = e^{2i(\chi + \gamma'\Theta)}, \quad (2.4.86)$$

where χ and Θ are given by (2.4.63) and (2.4.64). We finally have

$$\frac{h(-i\gamma')}{h(i\gamma')} = \frac{1 - \sum_{n=1}^{\infty} A_n/(\gamma_n + i\gamma')}{1 - \sum_{n=1}^{\infty} A_n/(\gamma_n - i\gamma')} = e^{2i\sigma}, \quad (2.4.87)$$

where, since A_m and γ_n are real for $n \in \mathbb{N}$,

$$\sigma = \arg(h(-i\gamma')) = \arg\left(1 - \sum_{n=1}^{\infty} \frac{A_n}{\gamma_n + i\gamma'}\right). \quad (2.4.88)$$

The condition for the existence of trapped modes, (2.4.84), reduces to

$$e^{2i\gamma'(a-\Theta)} = -e^{2i\chi}e^{2i\sigma} \quad (2.4.89)$$

which is simplified as

$$\gamma'(a - \Theta) = \chi + \sigma + \left(n - \frac{1}{2}\right)\pi, \quad n \text{ an integer}, \quad (2.4.90)$$

where χ , Θ and σ are given by (2.4.63), (2.4.64) and (2.4.88) respectively. We see that this condition differs from the approximate condition (2.4.66) by the addition of the term σ . The σ term is dependent on a/d and as $a/d \rightarrow \infty$ in (2.4.88), we see that $\sigma \rightarrow \arg(1) = 0$.

Condition (2.4.90) is in a form which will occur many times in this thesis. It is possible to prove the existence of a solution to (2.4.90) for sufficiently large a/d . Sufficiently large a/d is required as this guarantees a unique solution to (2.4.79) and we can also provide a bound for σ . As we can also provide a bound for χ it follows that

for $kd \in (\pi, d\pi/b)$, with a sufficiently large value of a/d the right-hand side of (2.4.90) lies between the two values $(n - \frac{1}{2})\pi + \epsilon_1$ and $(n - \frac{1}{2})\pi + \epsilon_2$, where $\epsilon_1 < \epsilon_2$. As kd varies between π and $d\pi/b$ for fixed b/d , the left-hand side of (2.4.90) varies continuously between 0 and $C(a/d - \Theta/d)$, where C is strictly positive. We let $n = N$ so that $(N - \frac{1}{2})\pi + \epsilon_1 \geq 0$, and then the right-hand side of (2.4.90) lies between two non-negative values. To provide a solution to (2.4.90) we choose a/d sufficiently large so that $C(a/d - \Theta/d) \geq (N - \frac{1}{2})\pi + \epsilon_2$. With this choice of a/d we can see that there will be a value of kd in the range $(\pi, d\pi/b)$ for which (2.4.90) is satisfied.

Antisymmetry about $x = 0$

For the case of antisymmetry about $x = 0$, (2.4.76) becomes

$$f(\gamma_m) - \zeta_m f(-\gamma_m) = 0, \quad m \in \mathbb{N}_0, \quad (2.4.91)$$

with the infinite system of equations equivalent to (2.4.79) being

$$-A_m + B_m \sum_{n=1}^{\infty} \frac{A_n}{\gamma_m + \gamma_n} = B_m \quad m \in \mathbb{N}, \quad (2.4.92)$$

where B_m is given by (2.4.80). The condition for antisymmetric modes, equivalent to (2.4.90), is thus

$$\gamma'(a - \Theta) = \chi + \sigma' + n\pi, \quad n \text{ an integer}, \quad (2.4.93)$$

where σ' is the argument of $h(-i\gamma')$ with the constants A_n given by the solution of (2.4.92).

Results

The systems of equations (2.4.79) and (2.4.92) need to be solved by truncation and due to the exponential convergence of the B_m terms only a small truncation parameter is used. In the following results a truncation parameter $N = 5$ is used.

Figure 2.3 shows a comparison between the trapped-mode wavenumbers, kd/π , computed from the approximate solution and the full solution when $b/d = 0.6$. The solid lines correspond to modes symmetric and antisymmetric about $x = 0$ for the full modified residue calculus method, and the dashed lines correspond to modes symmetric and antisymmetric about $x = 0$, computed from the approximate method. The two modes

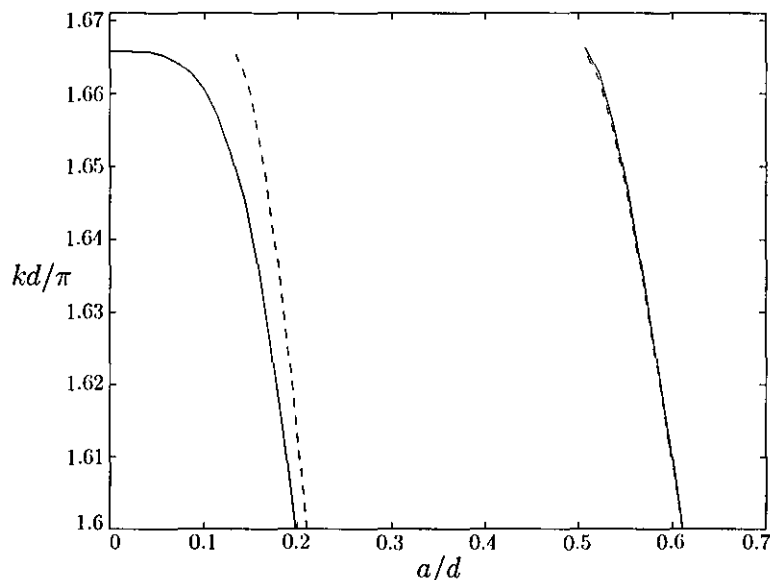


Figure 2.3: A comparison of the trapped-mode wavenumbers, kd/π , for modes symmetric and antisymmetric about $x = 0$ for the approximate solution, (dashed), and the full solution, (solid), plotted against a/d when $b/d = 0.6$.

on the left-side of figure 2.3 are symmetric about $x = 0$ and the other two are antisymmetric about $x = 0$. For all but the smallest values of a/d , the results computed from the full and approximate methods are indistinguishable. Only when a/d is less than about 0.5 do the full solution and the approximate solution produce significantly different results.

In figure 2.4 a typical set of trapped-mode wavenumbers, kd/π , computed from the full solutions (2.4.90) and (2.4.93), are plotted against a/d , for $b/d = 0.75$. The solid lines correspond to modes symmetric about $x = 0$ and the dashed lines correspond to modes antisymmetric about $x = 0$. We see that as a/d increases the number of modes present also increases, and the modes appear alternatively symmetric and antisymmetric from the cut-off $kd = d\pi/b = 4\pi/3$, and decrease towards $kd = \pi$.

The variation of trapped-mode wavenumbers, kd/π , plotted against b/d when $a/d = 3$ is shown in figure 2.5. The solid lines represent modes symmetric about $x = 0$, the dashed lines modes antisymmetric about $x = 0$ and the dotted line represents the upper cut-off $kb = \pi$. It is clear that as b/d increases from 0.5, the number of modes present decreases and the frequency of each of the modes decreases slightly. The plot shows that modes are present for any value of b/d in the interval (0.5, 1).

It is apparent from figure 2.5 that trapped modes exist in this frequency range when

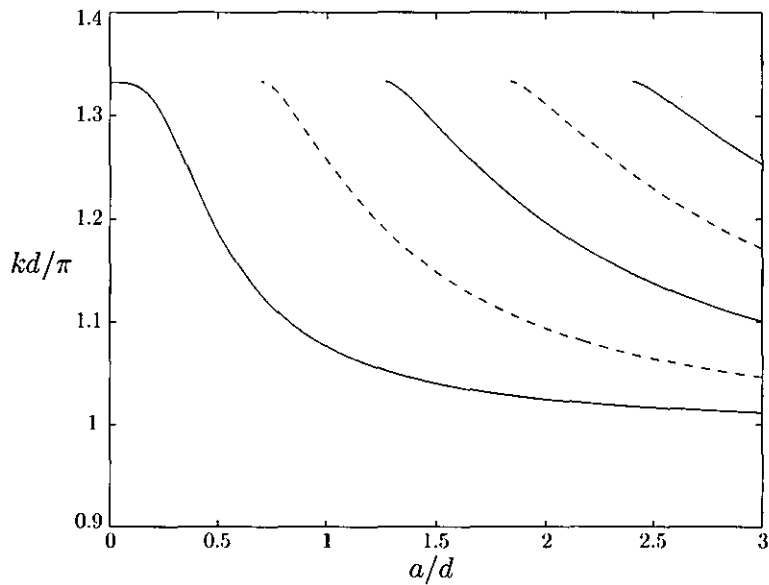


Figure 2.4: A comparison of the trapped-mode wavenumbers, kd/π , for modes symmetric (—) and antisymmetric (---) about $x = 0$ plotted against a/d when $b/d = 0.75$.

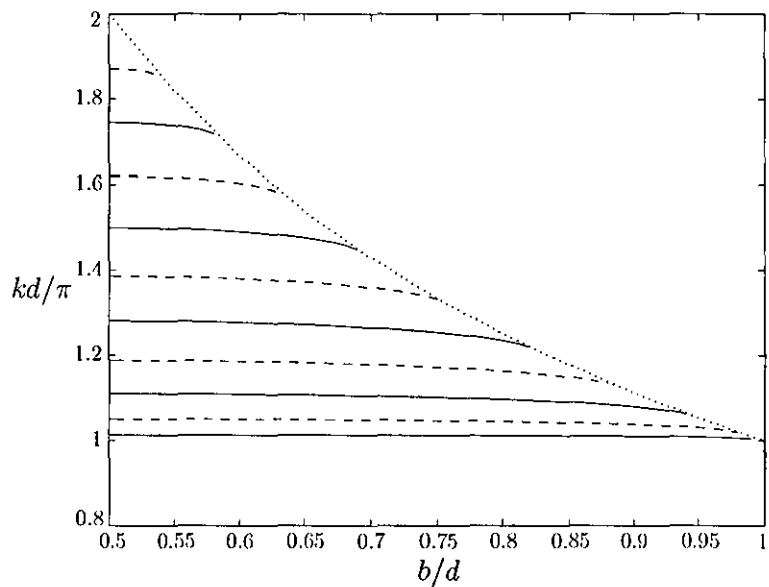


Figure 2.5: A comparison of the trapped-mode wavenumbers, kd/π , for modes symmetric (—) and antisymmetric (---) about $x = 0$ plotted against b/d when $a/d = 3$.

$b/d = 1/2$. This will be confirmed using a simplification of the theory due to symmetry in chapter 3.

Conclusion

The solution of the problem described in section 2.4.1 provides an elegant method for establishing the existence and computation of trapped-mode frequencies in a two-dimensional laterally coupled waveguide containing a window in the common boundary. The computation of the trapped modes is fairly straightforward as the system of equations that arises can be truncated with a low truncation parameter and ignored altogether when a/d is greater than one. Trapped modes either symmetric or antisymmetric about the line of symmetry of the guide have been shown to exist.

In solving the problem, an analytical approximation for a large window width was initially derived using residue calculus theory. The approximation provides an idea into how to solve the full problem efficiently. The computed results show that this approximation is very accurate for most window width sizes, even when the window is fairly small.

The full problem was solved using the modified residue calculus technique, which is an extension of the approximate solution. The full solution differs from the approximate solution only by the addition of one extra term in the trapped-mode condition. This extra term comes from the solution of a rapidly convergent infinite system.

The results computed show that the number of modes present depends on the values of a/d and b/d . As a/d increases the number of modes present increases, whereas as b/d increases the number of modes present decreases.

2.4.2 Variational methods

Introduction

The background given in section 2.2 discusses work involving quantum waveguides. In this section we review previous work done from a trapped-mode viewpoint in classical continuum mechanics.

Early work on differential operators on unbounded domains was done by Jones (1953), who gave a number of results concerning the spectrum of the Laplace operator and the existence of eigenvalues defined on certain types of semi-infinite domain. Later in his paper, the author relates the work to trapped modes (or the so-called ‘trapping modes’ occurring in Ursell (1951)).

When the resurgence of interest into trapped modes occurred forty years later, Evans,

Levitin, and Vassiliev (1994) used a variational formulation to prove the existence of at least one trapped mode in an acoustic waveguide containing an obstacle symmetric about the centreline of the guide parallel to the walls. Neumann conditions were placed on both the waveguide walls and the obstacle. The symmetry of the waveguide plays a key role in the proof as modes can be sought antisymmetric about the centreline, thus introducing a positive cut-off. Modes whose frequencies are below this cut-off cannot propagate to infinity allowing a standard variational argument to be used.

Further rigorous operator theory results concerning the existence or non-existence of trapped modes in waveguides can be found in Davies and Parnovski (1998), and the existence of edge resonances in an elastic strip are found in Roitberg, Vassiliev, and Weidl (1998). Both cases use the symmetry of the obstacle about the centreline of the guide to enable a cut-off to be introduced below which the modes can be found.

In the paper by Davies and Parnovski (1998), the authors also prove the existence of a trapped mode for the case of a two-dimensional or three dimensional cylinder containing a thin obstacle parallel to the axis of the cylinder. Similar situations are also discussed in Groves (1998) and Linton and McIver (1998a). The case of the thin obstacle differs from previous examples as a cut-off cannot be introduced by considering simple symmetry arguments. The main idea in the proof is to show that there is a more general way to introduce a cut-off by decomposing the space of L^2 functions into a set of generalised plane waves, one of which is not affected by the presence of the obstacle.

Work by Aslanyan, Parnovski, and Vassiliev (2000) uses a variational technique to deal with the situation when an obstacle symmetric about the centreline of the guide is moved away from the centreline. In this case the real eigenvalues found previously become complex resonances.

The trapped modes occurring in two-dimensional waveguides containing long obstacles symmetric about the centreline are considered in Khallaf, Parnovski, and Vassiliev (2000). In their paper the authors provide analytical estimates for the trapped mode frequencies and also prove that the number of trapped modes occurring is asymptotically proportional to the obstacle's length.

More recently Linton et al. (2002) and Linton and McIver (2002) have used a variational principle to prove the existence of trapped modes for waveguides containing certain off-centre bodies and for waveguides containing periodic structures.

In this section we shall use the method of Khallaf et al. (2000) to provide estimates

for the trapped mode frequencies and prove the existence of a single trapped mode occurring below the cut-off $kb = \pi$ in a two-dimensional laterally coupled waveguide for a sufficiently large window. The main difference between this problem and the one considered in Khallaf et al. (2000) is that the laterally coupled guide is not symmetric about the centreline of the waveguide.

Estimates of trapped-mode frequencies

We consider a two-dimensional laterally coupled waveguide. The waveguide can be thought of as an unbounded domain $\tilde{\Omega}$ defined as

$$\tilde{\Omega} = \{(-\infty, \infty) \times (0, d)\} \setminus \{(-\infty, -a] \times [b] \cup [a, \infty) \times [b]\},$$

where $a > 0$ and $\frac{1}{2} < b/d < 1$.

We are trying to find estimates for values of λ for which there is a non-trivial solution $\phi(x, y)$ to the boundary-value problem

$$-\nabla^2 \phi = \lambda \phi \quad \text{in } \tilde{\Omega}, \quad (2.4.94)$$

subject to the boundary conditions (2.3.3)–(2.3.6).

For the case of the laterally coupled waveguide, we have seen that if we restrict the frequency so that $k < \pi/b$ there are no modes that can propagate to infinity in either region *I* or *II*. The continuous spectrum for this problem is the semi-interval $[\pi^2/b^2, \infty)$, as k^2 is equivalent to λ .

To find the eigenvalues located below the continuous spectrum, i.e. in the region $[0, \pi^2/b^2)$, we can use the standard variational approach, see for example Evans et al. (1994) or Linton and McIver (1998a).

We consider the Rayleigh quotient defined by

$$Q(\phi) = \frac{\iint_{\tilde{\Omega}} |\nabla \phi|^2 \, dx \, dy}{\iint_{\tilde{\Omega}} |\phi|^2 \, dx \, dy}, \quad (2.4.95)$$

for all functions $\phi \in \mathcal{H}_0^1(\tilde{\Omega}) \setminus \{0\}$, where $\mathcal{H}_0^1(\tilde{\Omega})$ is the Sobolev space consisting of all functions in $L^2(\tilde{\Omega})$ which also have square-integrable first partial derivatives which satisfy $\phi = 0$ on $y = 0$, $y = d$ and $y = b$ ($|x| > a$). We also define

$$\lambda_{(1)} = \inf_{\phi \in \mathcal{H}_0^1} Q(\phi). \quad (2.4.96)$$

The value $\lambda_{(1)}$ is the lowest point of the spectrum of the problem (2.2.1) and (2.3.3)–(2.3.6). Due to the positive nature of both integrand in (2.4.95) it is easy to see that $\lambda_{(1)} > 0$. If the value $\lambda_{(1)} < \pi^2/b^2$, then $\lambda_{(1)}$ is the first eigenvalue of the problem and the function ϕ_1 from which $\lambda_{(1)}$ is found is the associated eigenfunction (trapped mode).

We now use ideas which can be found in, for example, Stakgold (1970), section 3.5. We define the inner product over the space of functions as,

$$\langle v, w \rangle = \iint_{\tilde{\Omega}} vw \, dx \, dy. \quad (2.4.97)$$

Let $\lambda_{(2)}$ be defined as

$$\lambda_{(2)} = \inf_{\substack{\phi \in \mathcal{K}_0^1 \\ \phi \perp \phi_1}} Q(\phi). \quad (2.4.98)$$

If $\lambda_2 < \pi^2/b^2$ then λ_2 is the second eigenvalue of the problem. This method can be repeated until we have

$$\lambda_{(n+1)} = \inf_{\substack{\phi \in \mathcal{K}_0^1 \\ \phi \perp \phi_i}} Q(\phi) = \pi^2/b^2, \quad i = 1, 2, \dots, n. \quad (2.4.99)$$

It can be easily seen that the spectrum $(0, \pi^2/b^2)$ for the problem (2.4.94) and (2.3.3)–(2.3.6) will contain exactly n eigenvalues.

One symmetry of the problem that we can take advantage of is the symmetry about the y -axis. We can place a Neumann condition or a Dirichlet condition on this axis and the continuous spectrum of the problem will remain unchanged. As was shown before, by placing either condition on the line $x = 0$ we can seek modes either symmetric or antisymmetric about the y -axis. We label the eigenvalues below the continuous spectrum as either $\lambda_{(j),s}$ for symmetric eigenvalues or $\lambda_{(j),a}$ for antisymmetric eigenvalues. The appropriate problem will now have either n_s or n_a eigenvalues below the continuous spectrum.

We only need now to consider the region Ω defined as

$$\Omega = \{(x, y) \in \tilde{\Omega} | x > 0\}, \quad (2.4.100)$$

and we shall initially only consider the case of a Neumann condition placed on $x = 0$. The space of functions is different for the two problems as trial functions have to satisfy Dirichlet conditions but not Neumann ones. The changes resulting from replacing this condition by a Dirichlet condition will be discussed later. We split the domain Ω into

the regions *I*, *II* and *III* defined previously and consider the eigenvalues associated with each region separately. For the following work we need to introduce some new notation.

We denote the j -th eigenvalue (arranged in order of increasing size) occurring in region i with a Dirichlet (or Neumann) condition on $x = a$, $0 < y < d$ as $\lambda_{(j)}^{i,D}$, (or $\lambda_{(j)}^{i,N}$). We also define a counting function $N^{i,D}(\lambda)$, (or $N^{i,N}(\lambda)$), as the number of eigenvalues less than λ in region i , with a Dirichlet (or Neumann) condition on $x = a$, $0 < y < d$.

The method behind the estimates concerns the idea of Dirichlet-Neumann bracketing along the line $x = a$, $0 < y < d$ (see, for example Courant and Hilbert (1989) VI §2.5) and is a consequence of the variational principle outlined above. If $\lambda < \pi^2/b^2$ we have

$$N^{I,D}(\lambda) + N^{II,D}(\lambda) + N^{III,D}(\lambda) \leq N_s(\lambda) \leq N^{I,N}(\lambda) + N^{II,N}(\lambda) + N^{III,N}(\lambda), \quad (2.4.101)$$

where $N_s(\lambda)$ is the total number of eigenvalues below λ with a symmetric condition placed on $x = 0$. Note that $N_s(\pi^2/b^2) = n_s$.

If a Dirichlet condition is placed on the ‘artificial’ boundary $x = a$, $0 < y < d$, the eigenfunctions in region *III* will take the form

$$\phi_{nm}^{III}(x, y) = \cos \frac{(n - 1/2)\pi x}{a} \sin \frac{m\pi y}{d}, \quad (2.4.102)$$

where m and n are non-negative integers, and hence

$$\{\lambda_{(j)}^{III,D}\}_{j=1}^{\infty} = \left\{ \frac{(n - 1/2)^2 \pi^2}{a^2} + \frac{(m\pi)^2}{d^2} \right\}_{n,m=1}^{\infty}. \quad (2.4.103)$$

Similarly replacing the Dirichlet condition on $x = a$ by a Neumann condition the eigenvalues become

$$\{\lambda_{(j)}^{III,N}\}_{j=1}^{\infty} = \left\{ \frac{(n - 1)^2 \pi^2}{a^2} + \frac{(m\pi)^2}{d^2} \right\}_{n,m=1}^{\infty}. \quad (2.4.104)$$

It is straightforward to show that there are no eigenvalues in regions *I* or *II* and so (2.4.101) becomes

$$N^{III,D}(\lambda) \leq N_s(\lambda) \leq N^{III,N}(\lambda), \quad (2.4.105)$$

provided $\lambda < \pi^2/b^2$. If we take $m > 1$ in (2.4.103) and (2.4.104) then the right-hand sides of both expressions will be greater than π^2/b^2 , so we assume that $m = 1$ in both cases. From (2.4.105) the following inequalities hold for all j , (for which $\lambda_{(j),s} < \pi^2/b^2$),

$$\lambda_{(j)}^{III,N} \leq \lambda_{(j),s} \leq \lambda_{(j)}^{III,D}, \quad (2.4.106)$$

(see Behnke, Mertins, Plum, and Wieners (2000), Lemma 4.1., for a proof of this.) Using (2.4.103) and (2.4.104) we simplify (2.4.106) to

$$\frac{\pi^2}{a^2}(j-1)^2 + \frac{\pi^2}{d^2} \leq \lambda_{(j),s} \leq \frac{\pi^2}{a^2}(j-1/2)^2 + \frac{\pi^2}{d^2}. \quad (2.4.107)$$

If the Neumann condition on $x = 0$ is replaced with a Dirichlet condition, the eigenfunction expansions and eigenvalues can be recalculated and (2.4.107) becomes

$$\frac{\pi^2}{a^2}(j-1/2)^2 + \frac{\pi^2}{d^2} \leq \lambda_{(j),a} \leq \frac{\pi^2}{a^2}j^2 + \frac{\pi^2}{d^2}. \quad (2.4.108)$$

The result of superimposing these intervals onto figure 2.4 is shown in figure 2.6. Al-

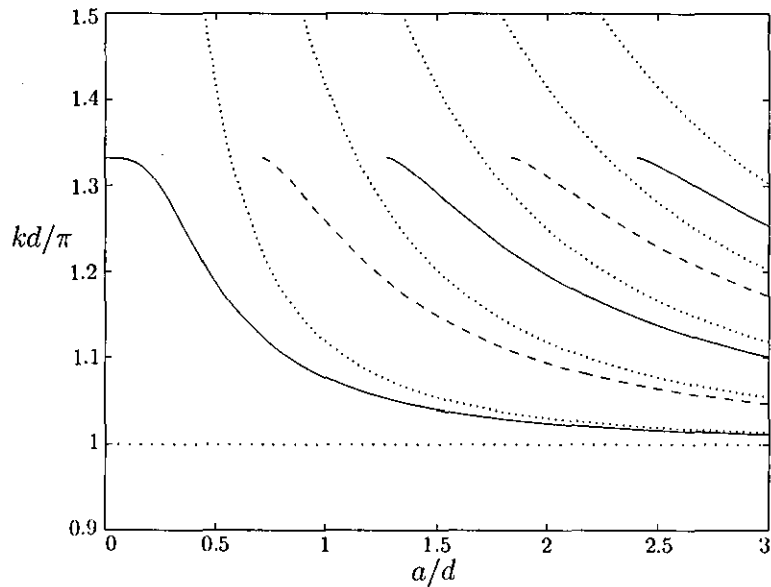


Figure 2.6: A comparison between the trapped-mode wavenumbers, kd/π , for modes symmetric and antisymmetric about $x = 0$ for the full solution, (solid and dashed), and the estimated intervals (dotted), plotted against a/d when $b/d = 0.75$.

though each mode appears between two estimates, it can be seen that as a/d increases along each curve, the estimate coming from the upper bound gives a better approximation to the frequency of the trapped mode.

Each interval of (2.4.107) and (2.4.108) whose right-end value is less than π^2/b^2 contains precisely one eigenvalue. This allows us to prove the existence of j trapped modes provided the value of the right-hand end of (2.4.107) or (2.4.108) is less than π^2/b^2 .

Proof of existence of a trapped mode

To prove the existence of a single symmetric trapped mode we put $j = 1$ into (2.4.107) to produce the following inequality

$$\frac{\pi^2}{4a^2} + \frac{\pi^2}{d^2} < \frac{\pi^2}{b^2}. \quad (2.4.109)$$

Rearranging this we find that a single symmetric trapped mode exists provided

$$a/d > [(2d/b)^2 - 4]^{-\frac{1}{2}}. \quad (2.4.110)$$

The similar condition for a single antisymmetric trapped mode is that

$$a/d > [(d/b)^2 - 1]^{-\frac{1}{2}}. \quad (2.4.111)$$

As b/d is increased from one half the required value of a/d increases from $1/\sqrt{12}$ for the symmetric case, and $1/\sqrt{3}$ for the antisymmetric case. As $b/d \rightarrow 1$ the required value of $a/d \rightarrow \infty$ in both cases. Similar results were found by Exner et al. (1996).

2.5 Trapped modes below the second cut-off

In this section we seek trapped modes for the laterally coupled waveguide whose frequencies are above the cut-off given by (2.3.34), i.e. trapped modes with frequencies $kb > \pi$. The modes found in section 2.4 were restricted in such a way that no propagating modes appeared in the region $x > a$ and only one wave-like mode appeared in the region $x < a$. The modes in this section will have frequencies above the cut-off for wave propagation down the guide. In the terminology of spectral theory this means that the eigenvalue associated with the trapped mode is embedded in the continuous spectrum of the relevant operator.

There is little previous work on trapped modes embedded in the continuous spectrum. Original numerical evidence for the existence of an isolated trapped mode embedded in the continuous spectrum was given by Evans and Porter (1998) for the case of a rigid circular cylinder placed on the centre-plane of the channel. Both Neumann and Dirichlet boundary conditions were considered on the channel walls. The trapped mode was shown to occur at a single precise cylinder radius and at a single frequency in each case.

More recently McIver et al. (2001) showed that this trapped mode was not isolated, but part of a continuous branch of modes which exist for ellipses with varying aspect

ratio. The ellipses are defined by two geometrical parameters a and b , say, where $(x/a)^2 + (y/b)^2 = 1$, and embedded trapped modes were found to exist for families of ellipses given by $a = a(b)$, with the corresponding wavenumber being of the form $k = k(b)$.

The branch structure of embedded trapped modes that exist for a class of obstacles with two planes of symmetry in two-dimensional waveguides, with Neumann conditions placed on both the waveguide walls and the obstacle, was shown in McIver, Linton, and Zhang (2002). The authors showed that branches of trapped modes exist as different length flat plates located on the centreline of a parallel-plate waveguide are transformed into either rectangular blocks or ellipses.

Trapped modes whose frequencies are embedded in the continuous spectrum for off-centre structures in guides were described in Linton et al. (2002). A Neumann condition was placed on the obstacle's boundary and either Neumann or Dirichlet boundary conditions placed on the waveguide walls. The authors used a variety of techniques to investigate the occurrence of trapped modes in various frequency bands. The techniques included slender body theory developed in Evans and McIver (1991), variational techniques and modified residue calculus methods like those used earlier in this thesis.

Both problems contain a number of cut-offs which are dependent upon the number of propagating modes occurring in an empty guide and not on the geometry of the obstacle. The authors defined the N th cut-off of both problems as the frequency below which $N - 1$ modes propagate in the empty Dirichlet guide and N modes propagate in the empty Neumann guide.

The authors stated that trapped modes may occur below the N th cut-off if the number of parameters that define the geometry of the obstacle is equal to the number of propagating modes plus two. In other words, below the first cut-off trapped modes may occur in the Dirichlet problem if the obstacle geometry is specified by two parameters, and in the Neumann problem if the geometry is specified by three parameters. Extra parameters are needed to satisfy side-conditions which force the amplitudes of any propagating modes to zero. The exception to the rule comes when the obstacle is a thin plate aligned parallel to the guide walls. The case of the thin plate can be solved using the modified residue calculus technique, which is useful as additional conditions ensuring that the amplitudes of propagating waves are zero are not necessary because the solution automatically ensures that no modes propagate to infinity. The authors showed

that trapped modes exist below the third cut-off for a Neumann guide containing a thin plate aligned parallel to the guide walls and not too far off the centreline.

Although the case of a thin plate is not considered in this chapter, the laterally coupled waveguide has a similar geometry to the waveguide containing an off-centre plate. Both problems are defined by two parameters, namely the off-set and width of the thin plate/window and so we may expect to find trapped modes below similar cut-offs.

Other papers concerning embedded trapped modes will be discussed in later chapters when the content is more relevant to the problem under discussion.

In the next section we use a modified residue calculus method to show the existence of trapped modes above the first cut-off and below the second cut-off for wave propagation down the guide.

2.5.1 Formulation

We set up the problem with similar eigenfunction expansions to those in section 2.3. The second cut-off is defined as the frequency below which only one mode can propagate in the region $x > a$, i.e. one mode in region *I* and none in region *II* or vice versa. We wish to restrict the frequency in such a way that two modes also propagate in the inner region. The reasoning for this restriction is discussed later when the function used in the modified residue calculus method is constructed. Two modes appear in the inner region when $kd > 2\pi$. The upper cut-off that allows only one mode in the outer region is dependent on the value of b/d . If $kd > 2\pi$, one mode will always appear in region *II*, but if $1/2 < b/d < 2/3$, another mode will appear in region *I* when $kc > \pi$, and if $2/3 < b/d < 1$, another mode will appear in region *II* when $kb > 2\pi$. We therefore restrict the frequency in such a way that

$$2\pi < kd < \frac{d\pi}{c}, \quad \text{when } 1/2 < b/d \leq 2/3, \quad (2.5.1)$$

$$2\pi < kd < \frac{2d\pi}{b}, \quad \text{when } 2/3 \leq b/d < 1. \quad (2.5.2)$$

The eigenfunction expansions for the three regions are

$$\phi_1(x, y) = \sum_{n=1}^{\infty} U_n^{(1)} \frac{e^{-\alpha_n(x-a)} \Psi_n^{(1)}(y)}{-\alpha_n}, \quad \alpha_n = (\nu_n^2 - k^2)^{1/2}, \quad (2.5.3)$$

$$\phi_2(x, y) = \sum_{n=2}^{\infty} U_n^{(2)} \frac{e^{-\beta_n(x-a)} \Psi_n^{(2)}(y)}{-\beta_n}, \quad \beta_n = (\mu_n^2 - k^2)^{1/2}, \quad (2.5.4)$$

$$\phi_3(x, y) = \sum_{n=0}^{\infty} U_n^{(3)} \frac{\cosh \gamma_n x \Psi_n^{(3)}(y)}{\gamma_n \sinh \gamma_n a}, \quad \gamma_n = (\lambda_n^2 - k^2)^{1/2}, \quad (2.5.5)$$

where $\Psi_n^{(1)}(y)$, $\Psi_n^{(2)}(y)$ and $\Psi_n^{(3)}(y)$ are given by (2.3.27)–(2.3.29).

These expansions are the same as (2.3.31)–(2.3.33) except that the sum in region *II* starts from $n = 2$, as we set the amplitude of the mode corresponding to β_1 equal to zero. With the restriction of frequency given by (2.5.1) and (2.5.2) we find that γ_0 and γ_1 (and β_1) are purely imaginary whereas α_1 , α_n , β_n and γ_n , $n \geq 2$ are all real and positive.

2.5.2 Modified residue calculus method

We now formulate a solution using the modified residue calculus technique.

Following (2.4.2) to (2.4.17) we can match $\phi_i = \phi_3$ and their derivatives along L_i , $i = 1, 2$, convert the results into an infinite system of equations and eliminate $U_m^{(3)}$ to arrive at

$$\sum_{n=1}^{\infty} U_n \left(\frac{1}{\alpha_n - \gamma_m} + \frac{\zeta_m}{\alpha_n + \gamma_m} \right) - \sum_{n=2}^{\infty} V_n \left(\frac{1}{\beta_n - \gamma_m} + \frac{\zeta_m}{\beta_n + \gamma_m} \right) = 0, \quad m \in \mathbb{N}_0, \quad (2.5.6)$$

where U_n , V_n and ζ_m are defined by (2.4.17). Notice that the only difference between (2.5.6) and (2.4.16) is that the summation for V_n starts from $n = 2$ instead of $n = 1$. The condition (2.4.26) describing the behaviour of U_n and V_n for large n remains the same. We now consider the integrals, (as in (2.4.28)),

$$I_m = \lim_{N \rightarrow \infty} \frac{1}{2\pi i} \int_{C_N} f(z) \left(\frac{1}{z - \gamma_m} + \frac{\zeta_m}{z + \gamma_m} \right) dz, \quad m \in \mathbb{N}_0, \quad (2.5.7)$$

where C_N is a sequence of contours on which $z \rightarrow \infty$ as $N \rightarrow \infty$ and $f(z)$ is a meromorphic function which has the following properties:

P1. $f(z)$ has simple poles at $z = \alpha_n$, $n \in \mathbb{N}$, and $z = \beta_n$, $n \geq 2$;

P2. $f(z) = O(z^{-\frac{1}{2}})$ as $|z| \rightarrow \infty$ on C_N as $N \rightarrow \infty$.

Construction of $f(z)$

We choose

$$f(z) = \exp(-z\Theta)g(z)h(z), \quad (2.5.8)$$

where Θ is given by (2.4.64) and

$$g(z) = \frac{1}{1-z/\alpha_1} \prod_{n=2}^{\infty} \frac{1-z/\gamma_n}{(1-z/\alpha_n)(1-z/\beta_n)}, \quad h(z) = 1 + \sum_{n=2}^{\infty} \frac{A_n}{z-\gamma_n}. \quad (2.5.9)$$

If we replace α_{n-1} by $\tilde{\alpha}_n$ in (2.5.9) we have

$$g(z) = \prod_{n=2}^{\infty} \frac{1-z/\gamma_n}{(1-z/\tilde{\alpha}_n)(1-z/\beta_n)}, \quad h(z) = 1 + \sum_{n=2}^{\infty} \frac{A_n}{z-\gamma_n}. \quad (2.5.10)$$

The function $g(z)$ is chosen to have the correct poles to satisfy P1. The function $h(z)$ is chosen so that the zeros of $g(z)$ at $z = \gamma_n$, $n \geq 2$ are cancelled by the poles of $h(z)$ at these points. Notice that the frequency constraints (2.5.1) and (2.5.2) lead to a function $g(z)$ which is the same order, as $z \rightarrow \infty$, as that given in (2.4.36) since one factor has been removed from both the numerator and the denominator. The function given by (2.5.8) therefore satisfies P2.

Applying Cauchy's residue theorem to (2.5.7) we obtain

$$\begin{aligned} \sum_{n=1}^{\infty} R(f : \alpha_n) \left(\frac{1}{\alpha_n - \gamma_m} + \frac{\zeta_m}{\alpha_n + \gamma_m} \right) + \sum_{n=2}^{\infty} R(f : \beta_n) \left(\frac{1}{\beta_n - \gamma_m} + \frac{\zeta_m}{\beta_n + \gamma_m} \right) \\ + f(\gamma_m) + \zeta_m f(-\gamma_m) = 0, \quad m \in \mathbb{N}_0. \end{aligned} \quad (2.5.11)$$

A comparison with (2.5.6) shows our solution is given by $U_n = R(f : \tilde{\alpha}_n)$ and $V_n = -R(f : \beta_n)$ provided

$$f(\gamma_m) + \zeta_m f(-\gamma_m) = 0, \quad m \in \mathbb{N}_0. \quad (2.5.12)$$

The coefficients A_n , $n = 2, 3, \dots$, can be found from an infinite system of equations. For $n \geq 2$, we have

$$\begin{aligned} f(\gamma_m) = -\exp \left\{ -\frac{\gamma_m}{\pi} (b \ln(d/b) + c \ln(d/c)) \right\} \left(\frac{A_m}{\gamma_m (1 - \gamma_m/\tilde{\alpha}_m)(1 - \gamma_m/\beta_m)} \right) \\ \times \prod_{\substack{n=2 \\ n \neq m}}^{\infty} \frac{1 - \gamma_m/\gamma_n}{(1 - \gamma_m/\tilde{\alpha}_n)(1 - \gamma_m/\beta_n)}, \end{aligned} \quad (2.5.13)$$

and

$$\begin{aligned} f(-\gamma_m) = \left(1 - \sum_{n=2}^{\infty} \frac{A_n}{\gamma_m + \gamma_n} \right) \exp \left\{ \frac{\gamma_m}{\pi} (b \ln(d/b) + c \ln(d/c)) \right\} \\ \times \left(\frac{2}{(1 + \gamma_m/\tilde{\alpha}_m)(1 + \gamma_m/\beta_m)} \right) \prod_{\substack{n=2 \\ n \neq m}}^{\infty} \frac{1 + \gamma_m/\gamma_n}{(1 + \gamma_m/\tilde{\alpha}_n)(1 + \gamma_m/\beta_n)}. \end{aligned} \quad (2.5.14)$$

Substituting (2.5.13) and (2.5.14) into (2.5.12) we obtain

$$A_m + B_m \sum_{n=2}^{\infty} \frac{A_n}{\gamma_m + \gamma_n} = B_m, \quad m = 2, 3, \dots, \quad (2.5.15)$$

where

$$B_m = \frac{2\gamma_m \exp(-2\gamma_m a)(\beta_m - \gamma_m)(\tilde{\alpha}_m - \gamma_m)}{(\beta_m + \gamma_m)(\tilde{\alpha}_m + \gamma_m)} \times \prod_{\substack{n=2 \\ n \neq m}}^{\infty} \frac{(1 - \gamma_m/\tilde{\alpha}_n)(1 - \gamma_m/\beta_n)(1 + \gamma_m/\gamma_n)}{(1 + \gamma_m/\tilde{\alpha}_n)(1 + \gamma_m/\beta_n)(1 - \gamma_m/\gamma_n)}. \quad (2.5.16)$$

Because of the presence of the rapidly decaying factor ζ_m in equation (2.5.16) for B_m , the system of equations (2.5.15) converges very quickly provided a/d is not too small and provides a very efficient method for computing the unknowns A_m .

Trapped mode condition

Unlike in the non-embedded case we now have two conditions to be satisfied simultaneously, whereas before we only had one. These conditions are (2.5.12) with $m = 0$ and $m = 1$. Letting $\gamma_0 = -i\gamma'_0$, where $\gamma'_0 = (k^2 - \lambda_0^2)^{\frac{1}{2}} = (k^2 - (\pi/d)^2)^{\frac{1}{2}}$, and $\gamma_1 = -i\gamma'_1$, where $\gamma'_1 = (k^2 - \lambda_1^2)^{\frac{1}{2}} = (k^2 - (2\pi/d)^2)^{\frac{1}{2}}$, we reduce these conditions to

$$e^{2i\gamma'_j a} = -\frac{f(-i\gamma'_j)}{f(i\gamma'_j)}, \quad j = 0, 1. \quad (2.5.17)$$

Following the method in section 2.4.1 we find the condition for trapped modes is that

$$\gamma'_j(a - \Theta) = \chi_j + \sigma_j + \left(n_j - \frac{1}{2}\right)\pi, \quad j = 0, 1, \quad (2.5.18)$$

are both satisfied simultaneously, where

$$\chi_j = \sum_{n=2}^{\infty} \left(\tan^{-1} \left(\frac{\gamma'_j}{\gamma_n} \right) - \tan^{-1} \left(\frac{\gamma'_j}{\tilde{\alpha}_n} \right) - \tan^{-1} \left(\frac{\gamma'_j}{\beta_n} \right) \right), \quad (2.5.19)$$

$$\sigma_j = \arg \left(h(-i\gamma'_j) \right) = \arg \left(1 - \sum_{n=2}^{\infty} \frac{A_n}{\gamma_n + i\gamma'_j} \right), \quad (2.5.20)$$

Θ is defined by (2.4.64) and n_0 and n_1 are an arbitrary pair of integers.

For the case of antisymmetry about $x = 0$, the conditions change to

$$\gamma'_j(a - \Theta) = \chi_j + \sigma'_j + n_j\pi, \quad j = 0, 1, \quad (2.5.21)$$

where σ'_j is the argument of $h(-i\gamma'_j)$ with the A_n coefficients coming from

$$-A_m + B_m \sum_{n=2}^{\infty} \frac{A_n}{\gamma_m + \gamma_n} = B_m, \quad m = 2, 3, \dots \quad (2.5.22)$$

Results

For the numerical results in this section, the system of equations (2.5.15) and (2.5.22) are truncated with a truncation parameter of $N = 5$.

In figure 2.7 a typical set of trapped-mode wavenumbers, kd/π , are plotted against a/d when $b/d = 0.6$, for which the relevant frequency range is $2 < kd/\pi < 2.5$. The modes symmetric about $x = 0$ are represented by a cross and the modes antisymmetric about $x = 0$ are shown by a circle. A detailed plot including five of these wavenumbers is shown in figure 2.8. Figure 2.8 also shows the solid lines corresponding to solutions of (2.5.18) and dashed lines corresponding to solutions of (2.5.21) for $j = 0, 1$, labelled with the corresponding n_0 and n_1 values. For each j , the trapped-mode wavenumbers correspond to the intersections of two lines. As a/d increases the number of trapped modes present in a small a/d interval also increases, a feature which was also apparent for modes below the first cut-off.

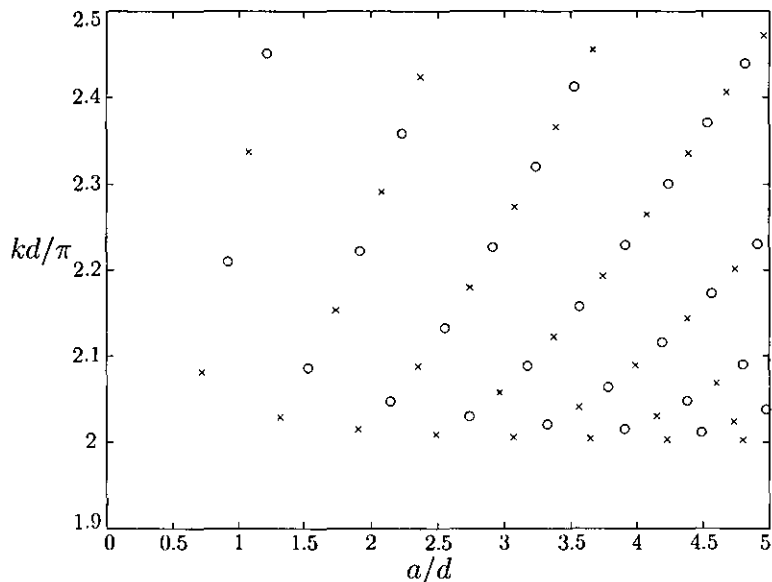


Figure 2.7: Trapped-mode wavenumbers for modes symmetric (\times) and antisymmetric (\circ) about $x = 0$ plotted against a/d , when $b/d = 0.6$.

The trapped modes symmetric about $x = 0$ obtained by keeping the integers n_0 and n_1 , in (2.5.18), constant and varying either kd/π in (a) or a/d in (b) against b/d are

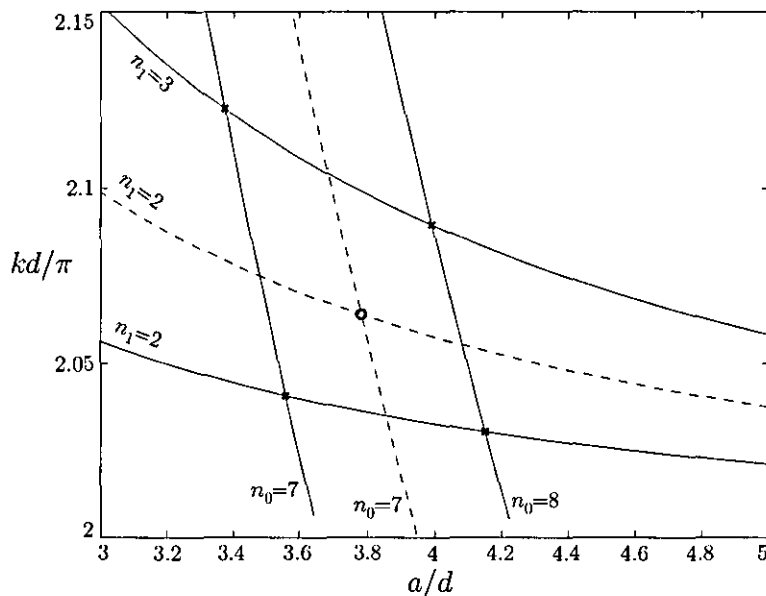


Figure 2.8: A detailed view of part of figure 2.7 showing the curves corresponding to the solutions of (2.5.18) and (2.5.21) for $j = 0, 1$, labelled with the corresponding n_0 and n_1 values. The solid curves correspond to modes symmetric about $x = 0$ and the dashed to modes antisymmetric about $x = 0$. The embedded trapped modes are denoted by \times (symmetric) and \circ (antisymmetric).

shown in figure 2.9. The vertical dotted line corresponds to the value $b/d = 2/3$, and the other two dotted lines correspond to the upper cut-offs given by (2.5.1) and (2.5.2). Only a selection of results for which $a/d < 2$ are given in figure 2.9. It can be seen from figure 2.9(a) that the higher wavenumbers appear when (n_0, n_1) take the form $(N, N - 1)$ with N large and the lower wavenumbers are when (n_0, n_1) take the form $(N, 1)$ with N large. Figure 2.9(b) shows that the lower values of a/d appear when (n_0, n_1) take the form $(N, N - 1)$ with N small and as n_0 increases a/d increases.

Figure 2.9(b) suggests, as below the first cut-off, that solutions may exist above the first cut-off when $b/d = 0.5$. This is not the case however as it can be seen in figure 2.9(a) that when $b/d = 0.5$ the possible frequency range decreases to zero. Trapped modes are found above the first cut-off, however, when $b/d = 0.5$ in chapter 3. The method uses symmetry properties to simplify the problem and the modes are found in a different frequency range.

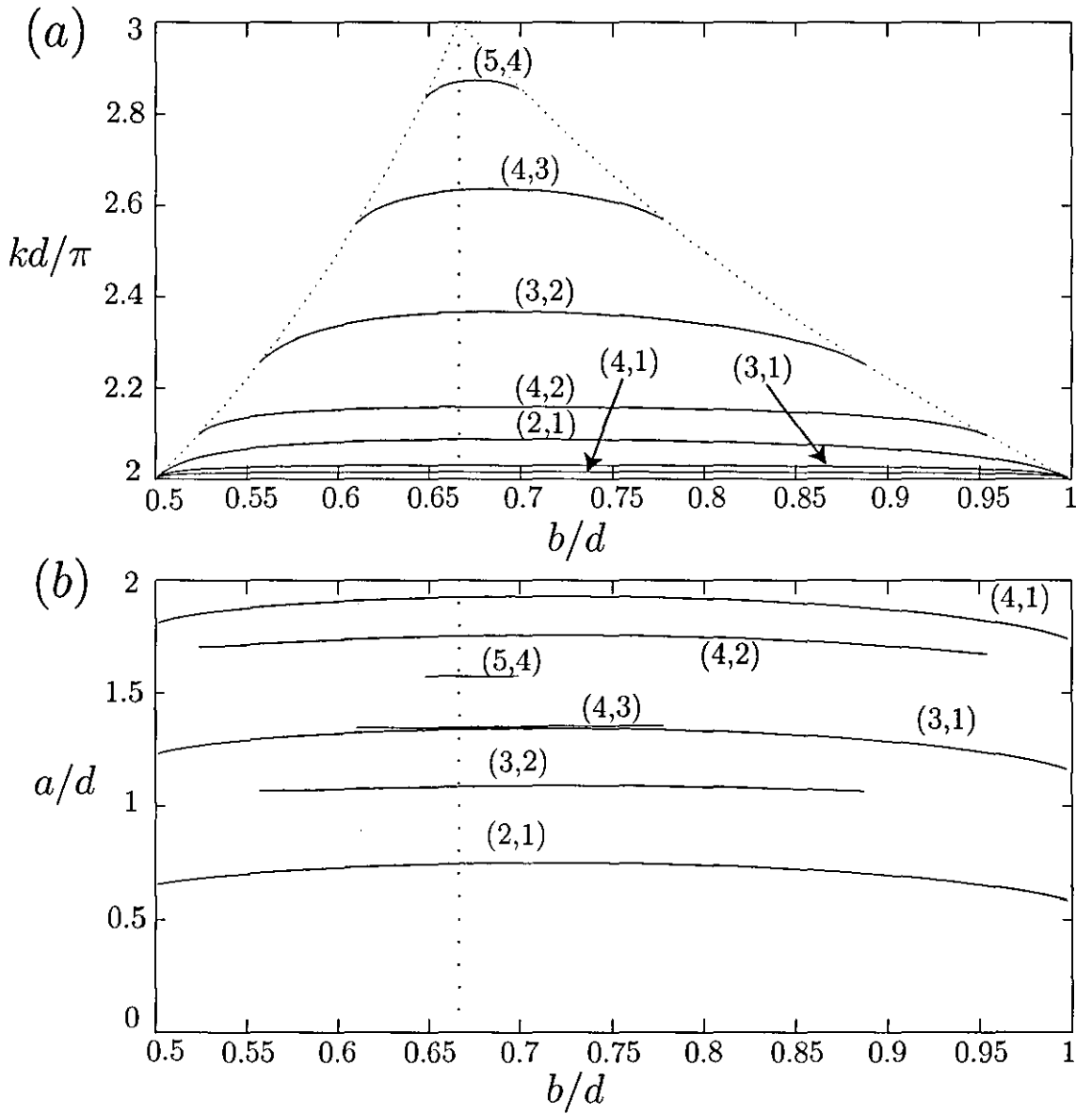


Figure 2.9: Variation of (a) kd/π and (b) a/d with b/d for modes symmetric about $x = 0$. The curves are labelled with the values of (n_0, n_1) used to generate them.

Conclusion

In this section we have used a modified residue calculus method to compute trapped modes frequencies between the first and second cut-offs for wave propagation down the guide. The trapped modes found are either symmetric or antisymmetric about the line of symmetry of the waveguide. The main difference when looking for modes above the first cut-off is that two conditions need to be solved simultaneously, compared to just the one condition when looking below the first cut-off. The modes correspond to the intersection of two lines in (a, k) parameter space and appear for any value of b/d in the

range $(0.5, 1)$, but for only specific values of a/d . The results provided show that there are no embedded trapped modes when the window size is below a certain value.

2.6 Trapped modes below the third cut-off

In the paper by Linton et al. (2002) trapped modes were found between the second and third cut-offs for wave propagation down the guide for the case of a Neumann waveguide containing an off-centre Neumann plate aligned parallel to the walls. The problem in this chapter has a similar geometry to the off-centre plate, so we may also expect to find trapped modes between the second and third cut-offs.

The problem can be set up as in section 2.5 with three wave-like modes appearing in the region $x < a$ and two propagating modes in the region $x > a$. Following the work in section 2.5 we find that trapped modes exist provided three conditions are satisfied simultaneously. However, these three conditions are found to be inconsistent and hence no trapped modes can be found in this frequency band.

2.7 Summary

In this chapter we have investigated the trapped modes that can occur in a two-dimensional laterally coupled waveguide. From a physical point of view, the trapped modes have a direct relevance to the bound-state eigenvalues occurring in quantum waveguides or quantum wires. The problem has been split into different sections depending upon the frequency of the trapped mode.

Initially we introduced a cut-off in the frequency below which modes cannot propagate to infinity. When seeking trapped modes below this cut-off a number of techniques were used. The first of which was the modified residue calculus method. The modified residue calculus technique provided a useful method to enable computation of trapped-mode frequencies. A number of results were provided that showed that the trapped modes occurred alternatively symmetric and antisymmetric about the line of symmetry of the guide, and that more modes appeared as the window got larger or as it moved towards the centre of the guide.

Using a variational principle we were able to provide estimates to these frequencies in the form of an inequality and prove the existence of a trapped mode for a sufficiently

large window width. As the size of the window in the common boundary was increased it was seen that a trapped-mode frequency would tend towards the upper bound of this inequality.

For modes whose frequencies were above this cut-off we were able to use a similar modified residue calculus technique to compute trapped-modes frequencies. From a spectral point of view, when looking above the cut-off we were seeking trapped modes whose frequencies were embedded in the continuous spectrum of the operator. The difference between the two sets of results came from the fact that there were two conditions to solve for the case above the cut-off compared to only one below the cut-off. The geometry of the problem can be described in terms of the two parameters a/d and b/d . When looking below the cut-off we can fix either a/d or b/d and vary the other to get solutions. For the case above the cut-off we can only fix was b/d and the solutions appear for only specific values of the parameter a/d .

An investigation was also made into trapped modes whose frequencies were above the second cut-off for wave propagation down the guide. Trapped modes were not found for any off-set or width of the window.

Chapter 3

Two-dimensional waveguides containing a plate on the centreline

3.1 Introduction to the problem

One of the assumptions made in chapter 2 was that the value of $b/d > 1/2$. If $2b = d$ the waveguide is symmetric about the mid-line parallel to the walls and this can be used to simplify the analysis. To seek trapped modes in a guide with such a geometry we decompose the problem into one symmetric about the mid-line and one antisymmetric about this line and consider just one guide. The latter case is that of a parallel-plate waveguide with Dirichlet conditions on both walls, a guide that does not contain trapped modes. On the other hand, the symmetric problem is equivalent to a two-dimensional waveguide with Dirichlet boundary conditions on the walls containing a thin plate on the centreline on which a Neumann condition is applied. In this chapter we seek trapped modes in such a guide.

The chapter is divided as follows. In section 3.2 we discuss previous work done on waveguides containing obstacles which are symmetric about the mid-line of the waveguide. The problem is formulated in section 3.3 and a cut-off corresponding to the lowest point of the continuous spectrum is introduced. The geometry of the problem is now only described by one non-dimensional parameter, this being the length of the plate compared to the width of the waveguide. The chapter is then split into two main sections as we seek modes whose frequencies are located below the continuous spectrum in section 3.4 and embedded in the continuous spectrum in section 3.5.

In section 3.4.1 a modified residue calculus method is used to prove the existence

of trapped modes in a waveguide containing a sufficiently long plate and compute the frequencies. A variational principle is used in section 3.4.2 to provide estimates for the trapped-mode frequencies and prove the existence of a single trapped mode for a sufficiently long plate. In both subsections the trapped modes are antisymmetric about the line forming the extension of the plate, either symmetric or antisymmetric about the line through the middle of and perpendicular to the plate and can be found for any value of the geometrical parameter corresponding to the plate length.

A modified residue calculus method is used to prove the existence of and compute the frequencies of trapped modes between the first and second cut-offs in section 3.5. The modes considered here have the same symmetric properties as those whose frequencies are below the cut-off but only occur for specific values of the plate length. This is consistent with what is found in chapter 2 as above the first cut-off trapped modes are only found for specific values of the window width.

A summary of the results obtained in the chapter is given in section 3.6.

3.2 Background

The previous work concerning trapped modes in two-dimensional parallel-plate waveguides containing obstacles that are symmetric about the centreline between the waveguide walls is extensive. The symmetry of the geometry can be used to restrict attention to modes which are antisymmetric about the line of symmetry parallel to the waveguide walls, enabling a cut-off to be introduced below which modes cannot propagate to infinity. If any non-trivial solutions to the problem are found with frequency below this cut-off then by definition they are trapped modes.

One of the first class of obstacles to be studied was a flat plate placed parallel to the waveguide walls, a situation of great practical importance in an engineering context. Detailed work on the excitation and consequences of modes trapped around a single flat plate in a rectangular flow passage can be found in Parker and Stoneman (1989), §2. Earlier work concerning the existence of trapped modes around a thin plate was presented by Parker in a series of papers both experimental (1966) and theoretical (1967).

In the first of these papers the author presented a detailed experimental study of acoustic resonances in waveguides of constant cross-section in which single plates, round

rods and a number of equally spaced flat plates spanning the guide were placed with their planes parallel to the airflow. The author showed that fairly large pressure amplitudes can be generated at resonance frequencies which are related to the geometry of the guide and not to the natural frequency of mechanical vibration. These resonances were local to the plates, excited by the vortex shedding from the trailing edges of the plates as air rapidly flows across them and quickly decayed down the guide.

In the later theoretical paper Parker studied trapped modes by numerically solving the wave equation using relaxation techniques and obtained a good agreement between the theory and previous experimental frequencies at which the resonances occurred. These resonances were dependent upon the length of the plates and the distance between the plates.

The resurgence of interest in trapped modes in the 1990's resulted in a number of papers containing work on symmetric obstacles. Much of the work concerns a water-wave interpretation of the problem whereas the ideas in this chapter come from the analogous acoustic problem. Using the terminology introduced in section 2.5 we can classify many of the problems considered as either a Neumann or Dirichlet problem. (The problems are defined due to the conditions appearing on the waveguide walls. The obstacle within the waveguide always has Neumann conditions on the boundary.)

The trapped modes arising from Neumann and Dirichlet problems are known as Neumann or Dirichlet modes for rigid structures. The Neumann and Dirichlet modes for rigid structures are of great importance from a physical viewpoint. An example was given by Maniar and Newman (1997) who showed numerically how large forces on cylinders in the middle of a large, finite array of cylinders occur near the wavenumbers of the corresponding Neumann and Dirichlet trapped modes found around a single cylinder in a channel.

Early work which fully exploits the symmetry of problem was done by Evans and Linton (1991) who provided numerical evidence for the determination of Neumann-mode frequencies for the case of a parallel-plate waveguide containing a symmetrically-placed rectangular block. A Dirichlet condition was placed on the centreline of the waveguide and the trapped modes found were antisymmetric about this line. The Neumann modes found are either symmetric or antisymmetric about the line of symmetry perpendicular to the waveguide walls. The case when the block is reduced to a flat plate on the centreline is also discussed.

Evans (1992) used the residue calculus method of Mittra and Lee (1971) to prove the existence of Neumann modes for the problem of a sufficiently long flat plate placed on the centreline. A Dirichlet condition is placed on the line which is an extension of the plate and the modes found are either symmetric or antisymmetric about a line perpendicular to the plate through its midpoint. The case when the boundary conditions are replaced by mixed boundary conditions on the plate and its extension are also discussed.

Using a boundary integral equation technique Linton and Evans (1992) were able to compute trapped-mode frequencies for the Neumann problem consisting of an obstacle, symmetric about the centreline of the guide, placed on the centreline of a two-dimensional parallel-plate waveguide. The integral equation method used in this example is useful as it allows general obstacle geometries to be considered.

Evans and Linton (1994) used a residue calculus technique to provide simple transcendental equations which can be used to find the frequencies of the Neumann and Dirichlet modes found by Parker (1966). Although the formulas given were approximate the authors showed that they were also very accurate.

Many of the problems discussed in section 2.4.2 concerning various variational techniques had symmetry built into the problem to allow a cut-off to arise. Some of these papers considered the case of a plate on the centreline of the waveguide and calculated the resulting trapped modes frequencies, but no general existence proof was given until the paper by Evans, Levitin, and Vassiliev (1994). In the paper the authors proved using a variational argument the existence of a Neumann mode in a two-dimensional parallel-plate waveguide containing an obstacle which was symmetric about the centreline of the guide.

In this chapter we seek trapped modes in the Dirichlet problem containing a finite length thin plate on the centreline. The problem is equivalent to finding the Parker γ and δ modes considered in Evans and Linton (1994).

3.3 Formulation

We consider a two-dimensional waveguide with parallel sides a width d apart which contains a plate of length $2a$ situated on the centre line, as shown in figure 3.1.

The problem is set up so that the x -axis is along the plate and the y -axis passes midway through the plate. The symmetry of the problem allows us to seek modes

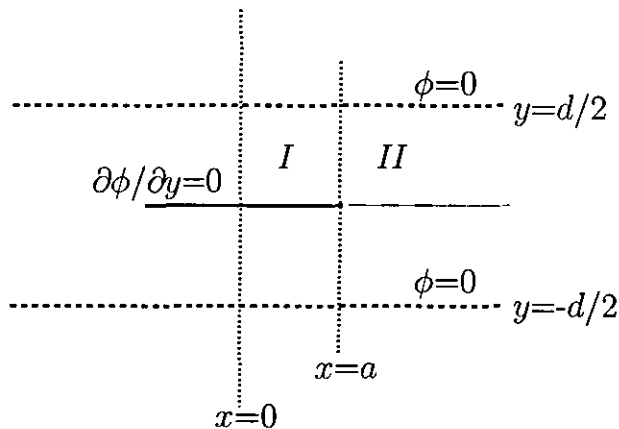


Figure 3.1: Definition sketch.

antisymmetric about the centreline of the guide by adding a Dirichlet condition on the line $y = 0$, away from the plate and considering only the upper-half of the waveguide. The geometry of the problem also allows us to express any solution as the sum of solutions which are either even or odd about $x = 0$. For the initial work we seek a solution which is symmetric about $x = 0$ by placing a Neumann condition on the line $x = 0$, $0 < y < d/2$. We consider the region $x > 0$, $0 < y < d/2$ and look for non-trivial solutions $\phi(x, y)$ which satisfy

$$\frac{\partial \phi}{\partial x} = 0 \text{ on } x = 0, \quad 0 < y < d/2. \quad (3.3.1)$$

The solution must also satisfy the Helmholtz equation within the waveguide

$$(\nabla^2 + k^2)\phi = 0, \quad 0 < y < d/2, \quad x > 0, \quad (3.3.2)$$

for some wavenumber k , subject to Neumann boundary conditions on the plate and Dirichlet boundary conditions on the guide wall and the extension of the plate

$$\frac{\partial \phi}{\partial y} = 0 \text{ on } y = 0, \quad 0 < x < a, \quad (3.3.3)$$

$$\phi = 0 \text{ on } y = 0, \quad x > a, \quad (3.3.4)$$

$$\phi = 0 \text{ on } y = d/2, \quad x > 0, \quad (3.3.5)$$

and we require a radiation condition specifying that no wave can propagate out to infinity:

$$\phi \rightarrow 0 \text{ as } x \rightarrow \infty. \quad (3.3.6)$$

We finally assume that ϕ is non-singular, but that

$$\nabla\phi = O(r^{-\frac{1}{2}}) \text{ as } r \equiv \{(x-a)^2 + y^2\}^{\frac{1}{2}} \rightarrow 0, \quad (3.3.7)$$

anticipating singular behaviour in the velocity field at the edge of the plate.

Any solutions to this problem can be extended to a solution in the whole guide using the symmetry relations

$$\phi(x, -y) = -\phi(x, y), \quad (3.3.8)$$

$$\phi(-x, y) = \phi(x, y), \quad (3.3.9)$$

and the resulting potential ϕ is a solution to the problem described in the previous chapter, with $b = d/2$.

It is useful to split the domain into two regions. Region *I* is $0 < y < d/2$, $0 < x < a$ and region *II* is $0 < y < d/2$, $x > a$, again shown in figure 3.1. We can represent the function ϕ by a function ϕ_i ($i = 1, 2$) in each region, with the following continuity conditions applied at each regions boundary:

$$\phi_1 = \phi_2, \quad \frac{\partial\phi_1}{\partial x} = \frac{\partial\phi_2}{\partial x}, \quad \text{on } x = a, \quad 0 < y < d/2. \quad (3.3.10)$$

Separation of variables reveals that

$$\phi_1(x, y) = \sum_{n=0}^{\infty} U_n^{(1)} \frac{\cosh \alpha_n x}{\alpha_n \sinh \alpha_n a} \Psi_n^{(1)}(y), \quad (3.3.11)$$

$$\phi_2(x, y) = \sum_{n=1}^{\infty} U_n^{(2)} \frac{e^{-\beta_n(x-a)}}{-\beta_n} \Psi_n^{(2)}(y), \quad (3.3.12)$$

where

$$\alpha_n = (\mu_n^2 - k^2)^{1/2}, \quad \beta_n = (\nu_n^2 - k^2)^{1/2}, \quad (3.3.13)$$

and we have introduced complete orthonormal sets

$$\Psi_n^{(1)}(y) = 2^{1/2} \sin \mu_n \left(\frac{d}{2} - y \right), \quad \mu_n = \frac{\pi}{d} (2n + 1), \quad n \in \mathbb{N}_0, \quad (3.3.14)$$

$$\Psi_n^{(2)}(y) = 2^{1/2} \sin \nu_n y, \quad \nu_n = \frac{2n\pi}{d}, \quad n \in \mathbb{N}, \quad (3.3.15)$$

which satisfy

$$\frac{2}{d} \int_{L_1} \Psi_n^{(i)}(y) \Psi_m^{(i)}(y) dy = \delta_{mn}, \quad i = 1, 2, \quad (3.3.16)$$

where L_1 is $x = a$, $0 < y < d/2$ and δ_{mn} is the Kronecker delta.

The condition that prevents waves propagating to infinity is that β_n , $n \in \mathbb{N}$, are real and positive and this implies $kd < 2\pi$. In terms of the spectral theory of operators the lowest point of the continuous spectrum for the Laplacian operator subject to the boundary conditions (3.3.3)–(3.3.6) is $4\pi^2/d^2$. We now seek modes whose frequencies are both above and below this cut-off. We do not, however, seek trapped modes above the second cut-off because the geometry is defined by one less parameter than in the previous chapter.

3.4 Trapped modes below the first cut-off

In this section we seek trapped modes whose frequencies are below the threshold of the continuous spectrum. We expect nothing new in terms of results in this section, just confirmation of the $b/d = 0.5$ results shown in figure 2.5. If $kd < 2\pi$ then the values α_n , $n \in \mathbb{N}$ will also be real and positive and so the corresponding modes will not have wave-like behaviour in the inner region. The only mode with possible wave-like behaviour will be the one corresponding to α_0 . To allow α_0 to have wave-like behaviour it must be purely imaginary and this implies $kd > \pi$. We therefore anticipate that a necessary condition for the existence of trapped modes is

$$\pi < kd < 2\pi. \quad (3.4.1)$$

We now formulate a solution using the modified residue calculus technique.

3.4.1 Modified residue calculus method

Matching $\phi_1 = \phi_2$ and $\partial\phi_1/\partial x = \partial\phi_2/\partial x$ along L_1 we obtain

$$\sum_{n=0}^{\infty} U_n^{(1)} \frac{\coth \alpha_n a}{\alpha_n} \Psi_n^{(1)}(y) = \sum_{n=1}^{\infty} U_n^{(2)} \frac{\Psi_n^{(2)}(y)}{-\beta_n}, \quad (3.4.2)$$

$$\sum_{n=0}^{\infty} U_n^{(1)} \Psi_n^{(1)}(y) = \sum_{n=1}^{\infty} U_n^{(2)} \Psi_n^{(2)}(y). \quad (3.4.3)$$

We can convert (3.4.2) and (3.4.3) into an infinite system of linear algebraic equations by multiplying both by $\Psi_m^{(1)}$, $m \in \mathbb{N}_0$, and integrating over L_1 to produce

$$U_m^{(1)} \frac{\coth \alpha_m a}{\alpha_m} = \sum_{n=1}^{\infty} \frac{U_n^{(2)}}{-\beta_n} d_{nm}, \quad m \in \mathbb{N}_0, \quad (3.4.4)$$

$$U_m^{(1)} = \sum_{n=1}^{\infty} U_n^{(2)} d_{nm}, \quad m \in \mathbb{N}_0, \quad (3.4.5)$$

where we have defined

$$d_{nm} = \frac{2}{d} \int_{L_1} \Psi_n^{(2)}(y) \Psi_m^{(1)}(y) dy. \quad (3.4.6)$$

Evaluating the integral d_{nm} , we find

$$\begin{aligned} d_{nm} &= \frac{2}{d} \int_0^{d/2} 2 \sin \nu_n y \sin \mu_m \left(\frac{d}{2} - y \right) dy, \\ &= \frac{4}{d(\nu_n^2 - \mu_m^2)} \left[\nu_n \sin \frac{\mu_m d}{2} - \mu_m \sin \frac{\nu_n d}{2} \right], \end{aligned} \quad (3.4.7)$$

provided $\nu_n \neq \mu_m$. It is simple to see from (3.3.14) and (3.3.15) that $\nu_n \neq \mu_m$ and hence (3.4.7) always holds. Since m and n are both integers we have $\sin \nu_n d/2 = 0$, and $\sin \mu_m d/2 = (-1)^{m+1}$. Substituting these results and $\nu_n^2 = \beta_n^2 + k^2$, and $\mu_m^2 = \alpha_m^2 + k^2$, into (3.4.7), we find that

$$d_{nm} = \frac{4\nu_n(-1)^m}{d(\alpha_m^2 - \beta_n^2)}, \quad m \in \mathbb{N}_0, \quad n \in \mathbb{N}. \quad (3.4.8)$$

We can now proceed by either eliminating $U_m^{(1)}$ or $U_n^{(2)}$ from (3.4.4) and (3.4.5). In order to use the modified residue calculus method we eliminate $U_m^{(1)}$ and use (3.4.8) to obtain

$$\sum_{n=1}^{\infty} U_n \left(\frac{1}{\beta_n - \alpha_m} + \frac{\zeta_m}{\beta_n + \alpha_m} \right) = 0, \quad m \in \mathbb{N}_0, \quad (3.4.9)$$

where we have defined

$$U_n = \frac{U_n^{(2)} \nu_n}{\beta_n} \quad \text{and} \quad \zeta_m = e^{-2\alpha_m a}. \quad (3.4.10)$$

Using a similar method to that shown in section 2.4.1 we also require

$$U_n = O(n^{-\frac{1}{2}}) \quad \text{as} \quad n \rightarrow \infty, \quad (3.4.11)$$

to ensure that the edge condition (3.3.7) is satisfied by $\phi_2(x, y)$.

We could devise an approximate solution by neglecting ζ_m , $m \in \mathbb{N}$, but instead we will proceed directly to the full solution by considering the integrals

$$I_m = \lim_{N \rightarrow \infty} \frac{1}{2\pi i} \int_{C_N} f(z) \left(\frac{1}{z - \alpha_m} + \frac{\zeta_m}{z + \alpha_m} \right) dz, \quad m \in \mathbb{N}_0, \quad (3.4.12)$$

where C_N is a sequence of contours on which $z \rightarrow \infty$ as $N \rightarrow \infty$ and $f(z)$ is a meromorphic function which has the following properties:

P1. $f(z)$ is an analytic function of z except for simple poles at $z = \beta_n$, $n \in \mathbb{N}$;

P2. $f(z) = O(z^{-\frac{1}{2}})$ as $|z| \rightarrow \infty$ on C_N as $N \rightarrow \infty$.

The main step in obtaining solutions by the modified residue calculus method involves the construction of $f(z)$.

Construction of $f(z)$

Following the same reasoning used in section 2.4.1 we would like to choose

$$f(z) = g(z)h(z), \quad (3.4.13)$$

where

$$g(z) = \prod_{n=1}^{\infty} \frac{1 - z/\alpha_n}{1 - z/\beta_n}, \quad h(z) = 1 + \sum_{n=1}^{\infty} \frac{A_n}{z - \alpha_n}, \quad (3.4.14)$$

and the coefficients A_n are to be determined. The function $f(z)$ is chosen to have the correct poles to satisfy P1. The function $h(z)$ is chosen so that the zeros of $g(z)$ at α_n are cancelled by the poles of $h(z)$ at these points.

To satisfy P2 we need to obtain the behaviour of $g(z)$ as $|z| \rightarrow \infty$. We therefore consider the following product

$$g(z) = \prod_{n=1}^{\infty} \frac{1 - z/\alpha_n}{1 - z/\mu_n} \prod_{n=1}^{\infty} \frac{1 - z/\nu_n}{1 - z/\beta_n} \prod_{n=1}^{\infty} \frac{1 - z/\mu_n}{1 - z/\nu_n}. \quad (3.4.15)$$

Following section 2.4.1 we have

$$\prod_{n=1}^{\infty} \frac{1 - z/\alpha_n}{1 - z/\mu_n} = \prod_{n=1}^{\infty} \left(1 - \frac{k^2}{\mu_n^2}\right)^{-\frac{1}{2}} \prod_{n=1}^{\infty} \left(1 + \frac{k^2}{(z - \mu_n)(\mu_n + \alpha_n)}\right), \quad (3.4.16)$$

and

$$\prod_{n=1}^{\infty} \frac{1 - z/\nu_n}{1 - z/\beta_n} = \prod_{n=1}^{\infty} \left(1 - \frac{k^2}{\nu_n^2}\right)^{\frac{1}{2}} \prod_{n=1}^{\infty} \left(1 - \frac{k^2}{(z - \beta_n)(\beta_n + \nu_n)}\right). \quad (3.4.17)$$

As all the terms α_n and β_n , $n \in \mathbb{N}$, are of the form $An + O(n^{-1})$ as $n \rightarrow \infty$, with A a constant, a comparison between the final products in (3.4.16) and (3.4.17), and $\sum_{n=1}^{\infty} n^{-2}$, shows that (3.4.16) and (3.4.17) are uniformly convergent on any compact set excluding $z = \beta_n$ and $z = \mu_n$. Provided $z \rightarrow \infty$ through a sequence of values which avoids these points we have

$$g(z) \sim \frac{\pi^2 \sin kd}{kd\pi^2 - (kd)^3} \prod_{n=1}^{\infty} \frac{1 - z/\mu_n}{1 - z/\nu_n}, \quad (3.4.18)$$

where Gradshteyn and Ryzhik (1980) eqn 1.431(4) has been used. We can expand the remaining product using (2.4.43) as

$$\prod_{n=1}^{\infty} \frac{1 - z/\mu_n}{1 - z/\nu_n} = \prod_{n=1}^{\infty} \frac{1 - zd/(2n+1)\pi}{1 - zd/2n\pi} = \frac{e^{\gamma zd/2\pi} \Gamma(3/2)}{\Gamma(3/2 - zd/2\pi)} \cdot \frac{\Gamma(1 - zd/2\pi)}{e^{\gamma zd/2\pi} \Gamma(1)}. \quad (3.4.19)$$

After using (2.4.45), we find after some simplification that as $|z| \rightarrow \infty$, $z \neq |z|$,

$$g(z) \sim \frac{\pi^2 \sin kd}{kd\pi^2 - (kd)^3} \left(\frac{-z}{2\pi}\right)^{-\frac{1}{2}}. \quad (3.4.20)$$

For the case when z is real and positive we use the reflection properties of the Gamma function, see (2.4.48), and the asymptotic behaviour can be shown to be

$$g(z) \sim \frac{\pi^2 \sin kd}{kd\pi^2 - (kd)^3} \cot\left(\frac{zd}{2}\right) \left(\frac{z}{2\pi}\right)^{-\frac{1}{2}}, \quad \text{as } z \rightarrow \infty, \quad z \neq -|z|. \quad (3.4.21)$$

If we choose C_N to be a sequence of circles with centre at the origin and radius $R_N = (N + 1/4)\pi$ then using these results we obtain

$$g(z) = O(z^{-\frac{1}{2}}), \quad \text{as } |z| \rightarrow \infty \text{ on } C_N \text{ as } N \rightarrow \infty, \quad (3.4.22)$$

and hence P2 is satisfied.

Applying Cauchy's residue theorem to (3.4.12) we obtain

$$\sum_{n=1}^{\infty} R(f : \beta_n) \left(\frac{1}{\beta_n - \alpha_m} + \frac{\zeta_m}{\beta_n + \alpha_m} \right) + f(\alpha_m) + \zeta_m f(-\alpha_m) = 0, \quad m \in \mathbb{N}_0. \quad (3.4.23)$$

A comparison with (3.4.9) shows our solution is given by $U_n = R(f : \beta_n)$ provided

$$f(\alpha_m) + \zeta_m f(-\alpha_m) = 0, \quad m \in \mathbb{N}_0. \quad (3.4.24)$$

For $m \in \mathbb{N}$, these equations can be solved by an appropriate choice of the coefficients A_n . We have for $m \in \mathbb{N}$

$$f(\alpha_m) = - \left(\frac{A_m}{\alpha_m(1 - \alpha_m/\beta_m)} \right) \prod_{\substack{n=1 \\ n \neq m}}^{\infty} \frac{1 - \alpha_m/\alpha_n}{1 - \alpha_m/\beta_n}, \quad (3.4.25)$$

and

$$f(-\alpha_m) = \left(1 - \sum_{n=1}^{\infty} \frac{A_n}{\alpha_m + \alpha_n} \right) \left(\frac{2}{1 + \alpha_m/\beta_m} \right) \prod_{\substack{n=1 \\ n \neq m}}^{\infty} \frac{1 + \alpha_m/\alpha_n}{1 + \alpha_m/\beta_n}. \quad (3.4.26)$$

Substituting (3.4.25) and (3.4.26) into (3.4.24) we obtain

$$A_m + B_m \sum_{n=1}^{\infty} \frac{A_n}{\alpha_m + \alpha_n} = B_m, \quad m \in \mathbb{N}, \quad (3.4.27)$$

where

$$B_m = \frac{2\alpha_m \zeta_m (\beta_m - \alpha_m)}{(\beta_m + \alpha_m)} \prod_{\substack{n=1 \\ n \neq m}}^{\infty} \frac{(1 + \alpha_m/\alpha_n)(1 - \alpha_m/\beta_n)}{(1 - \alpha_m/\alpha_n)(1 + \alpha_m/\beta_n)}. \quad (3.4.28)$$

The presence of the rapidly decaying factor ζ_m in equation (3.4.28) for B_m means that the system of equations (3.4.27) converges very quickly provided a/d is not too small. As in section 2.4.1 a sufficient condition for the infinite system (3.4.27) to have a unique solution with $\sum_{n=1}^{\infty} A_n^2 < \infty$ is that a/d is sufficiently large.

To satisfy the edge condition, U_n must satisfy the condition given by (3.4.11). Earlier we have shown that $U_m = R(f : \beta_m)$ and hence

$$U_m = -\beta_m \left(1 + \sum_{n=1}^{\infty} \frac{A_n}{\beta_m - \alpha_n} \right) \prod_{n=1}^{\infty} (1 - \beta_m/\alpha_n) / \prod_{\substack{n=1 \\ n \neq m}}^{\infty} (1 - \beta_m/\beta_n). \quad (3.4.29)$$

Using (3.4.15) we can expand this to

$$U_m = -\beta_m \left(1 - \frac{\beta_m d}{2m\pi} \right) \left(1 + \sum_{n=1}^{\infty} \frac{A_n}{\beta_m - \alpha_n} \right) \prod_{n=1}^{\infty} \frac{(1 - \beta_m/\alpha_n)}{(1 - \beta_m d/\pi(2n+1))} \\ \times \prod_{\substack{n=1 \\ n \neq m}}^{\infty} \frac{(1 - \beta_m d/2n\pi)}{(1 - \beta_m/\beta_n)} \prod_{n=1}^{\infty} \frac{(1 - \beta_m/\mu_n)}{(1 - \beta_m/\nu_n)}. \quad (3.4.30)$$

The first two infinite products can be rearranged in the form shown in (3.4.16) and (3.4.17) and hence are $O(1)$ as $m \rightarrow \infty$. From (3.4.21) we have

$$\prod_{n=1}^{\infty} \frac{(1 - \beta_m/\mu_n)}{(1 - \beta_m/\nu_n)} \sim \frac{\pi^2 \sin kd}{kd\pi^2 - (kd)^3} \cot \left(\frac{\beta_m d}{2} \right) \left(\frac{\beta_m}{2\pi} \right)^{-\frac{1}{2}} \\ \sim \frac{\pi^2 \sin kd}{kd\pi^2 - (kd)^3} \cot \left(m\pi - \frac{(kd)^2}{4m\pi} + O(m^{-2}) \right) \left(\frac{2m\pi}{d} \right)^{-\frac{1}{2}} \left(1 + O(m^{-2}) \right), \\ \sim \frac{\pi^2 \sin kd}{kd\pi^2 - (kd)^3} \left(\frac{8m\pi}{k^4 d^3} \right)^{\frac{1}{2}} + O(m^{-\frac{1}{2}}), \quad (3.4.31)$$

since

$$\beta_m \sim \frac{2m\pi}{d} - \frac{k^2 d}{4m\pi} + O(m^{-2}) \quad (3.4.32)$$

as $m \rightarrow \infty$.

As $m \rightarrow \infty$ we also have

$$\left(1 - \frac{\beta_m d}{2m\pi} \right) \sim \frac{1}{2} \left(\frac{kd}{2m\pi} \right)^2 + O(m^{-3}). \quad (3.4.33)$$

Using (3.4.31)–(3.4.33) we can see that U_n is $O(n^{-\frac{1}{2}})$ as $n \rightarrow \infty$, which is the required asymptotics to take account of the expected singularity in the velocity field near the plate edge.

Trapped mode condition

We can now return to the one condition still to be satisfied, namely (3.4.24) with $m = 0$. If we let $\alpha_0 = -i\alpha'$, where $\alpha' = (k^2 - \mu_0^2)^{\frac{1}{2}} = (k^2 - (\pi/d)^2)^{\frac{1}{2}}$, this condition reduces to

$$e^{2i\alpha'a} = -\frac{f(-i\alpha')}{f(i\alpha')}. \quad (3.4.34)$$

Using (3.4.14) we have

$$\frac{g(-i\alpha')}{g(i\alpha')} = e^{2i\chi}, \quad \frac{h(-i\alpha'_m)}{h(i\alpha'_m)} = e^{2i\sigma}, \quad (3.4.35)$$

where we have defined

$$\chi = \sum_{n=1}^{\infty} \left(\tan^{-1} \left(\frac{\alpha'}{\alpha_n} \right) - \tan^{-1} \left(\frac{\alpha'}{\beta_n} \right) \right), \quad (3.4.36)$$

and

$$\sigma = \arg \left(h(-i\alpha') \right) = \arg \left(1 - \sum_{n=1}^{\infty} \frac{A_n}{\alpha_n + i\alpha'} \right). \quad (3.4.37)$$

The condition for the existence of trapped modes, (3.4.34), reduces to

$$\alpha'a = \chi + \sigma + \left(n - \frac{1}{2} \right) \pi, \quad n \text{ an integer}, \quad (3.4.38)$$

where χ and σ are given by (3.4.36) and (3.4.37). Had we attempted an approximate solution for large a/d the condition would have been similar to (3.4.38), but without the σ term, and the results would be the same as those shown in Evans and Linton (1994).

As $a/d \rightarrow \infty$ we showed earlier that $A_n \rightarrow 0$ and hence from (3.4.37) $\sigma \rightarrow 0$. Thus given any $\epsilon > 0$ we can choose a/d sufficiently large so that $|\sigma| < \epsilon$. If we now consider the series $-\chi$, where χ is defined by (3.4.36), we see that it is made up of decreasing terms of alternate sign because \tan^{-1} is monotonic and

$$\beta_n < \alpha_n < \beta_{n+1}, \quad \text{for } n \in \mathbb{N}. \quad (3.4.39)$$

It is also clear that $-\chi$ is bounded below by zero and above by the first positive term, $\tan^{-1}(\alpha'/\beta_1)$. As \tan^{-1} is bounded above by $\pi/2$ the following inequality holds,

$$0 < -\chi < \tan^{-1}(\alpha'/\beta_1) < \pi/2, \quad (3.4.40)$$

and for $kd \in (\pi, 2\pi)$, we can fix a/d sufficiently large so that

$$0 < \pi/2 + \chi + \sigma \equiv C < \pi/2. \quad (3.4.41)$$

With this choice of a/d the right-hand side of (3.4.38) becomes

$$\chi + \sigma + \left(n - \frac{1}{2} \right) \pi = C + (n - 1)\pi. \quad (3.4.42)$$

Letting $n = N$, where N is a positive integer, we see that the right-hand side of (3.4.38) is bounded by two non-negative values $(N - 1)\pi$ and $(N - \frac{1}{2})\pi$. As kd increases from

π to 2π the left-hand side of (3.4.38) varies continuously between 0 and $\sqrt{3}\pi a/d$. To provide a solution to (3.4.38) we choose a/d sufficiently large so that $a/d \geq (N - \frac{1}{2})/\sqrt{3}$. With this choice of a/d we can see that there will be a value of kd in the range $(\pi, 2\pi)$ for which (3.4.38) is satisfied. Moreover as we choose different integers N there is an infinity of solutions for any fixed frequency. As a/d increases for fixed kd the value of σ decreases and the difference between successive solutions tends to $\pi/d\alpha'$.

Antisymmetry about $x = 0$

For the case of antisymmetry about $x = 0$, the condition (3.3.1) is replaced by

$$\phi = 0 \text{ on } x = 0, \quad 0 < y < d/2, \quad (3.4.43)$$

and hence the cosh and sinh terms in (3.3.11) are interchanged. The equation equivalent to (3.4.9) is

$$\sum_{n=1}^{\infty} U_n \left(\frac{1}{\beta_n - \alpha_m} - \frac{\zeta_m}{\beta_n + \alpha_m} \right) = 0, \quad m \in \mathbb{N}_0. \quad (3.4.44)$$

Equation (3.4.24) therefore becomes

$$f(\alpha_m) - \zeta_m f(-\alpha_m) = 0, \quad m \in \mathbb{N}_0, \quad (3.4.45)$$

with the infinite system (3.4.27) being

$$-A_m + B_m \sum_{n=1}^{\infty} \frac{A_n}{\alpha_m + \alpha_n} = B_m, \quad m \in \mathbb{N}. \quad (3.4.46)$$

The condition for antisymmetric modes, equivalent to (3.4.38), is therefore

$$\alpha' a = \chi + \sigma' + n\pi, \quad n \text{ an integer}, \quad (3.4.47)$$

where σ' is the argument of $h(-i\alpha')$ with the A_n coefficients coming from (3.4.46) and χ is defined in (3.4.36).

Results

In figure 3.2 the trapped-mode wavenumbers, kd/π , are plotted against a/d . The results were computed with the systems of equations (3.4.27) and (3.4.46) truncated with a truncation parameter of 5. The solid lines correspond to modes symmetric about $x = 0$ and the dashed lines correspond to modes antisymmetric about $x = 0$. We see that as a/d increases the number of modes increases and the modes appear alternatively

symmetric and antisymmetric from the cut-off $kd = 2\pi$ and decrease towards $kd = \pi$. The right-hand end points of the curves are for $a/d = 3$ and correspond to the left-hand end points in figure 2.5.

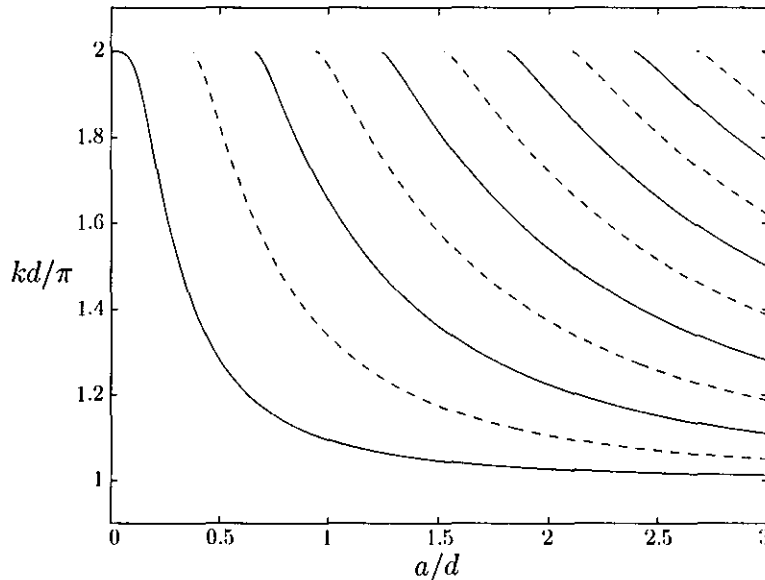


Figure 3.2: A comparison of the trapped-mode wavenumbers for modes symmetric (—) and antisymmetric (---) about $x = 0$ plotted against a/d .

In the quantum mechanics situation similar curves obtained using a mode-matching technique and showing the bound-state energies (when $\hbar^2/2m = 1$) against the plate length are presented by Exner et al. (1996).

Conclusion

In this section we have used the modified residue calculus method to prove the existence and compute the frequencies of Dirichlet modes occurring below the cut-off $kd = 2\pi$ in the two-dimensional waveguide containing a thin plate on the centreline. The proof is valid only when the plate length is sufficiently large but computations suggest that modes exist for all plate lengths. The trapped modes appear alternatively symmetric and antisymmetric about the line perpendicular to and through the midpoint of the plate, and exist for any length plate.

3.4.2 Variational methods

Estimates of trapped-mode frequencies

In this section we follow the work in section 2.4.2 to make estimates for the trapped-mode frequencies occurring below the cut-off $kd = 2\pi$ in a parallel-plate waveguide containing a plate on the centreline.

Using the same notation as before, we take $\lambda < 4\pi^2/d^2$, place a Neumann condition on $x = 0$, and compute the eigenvalues in region I with Dirichlet or Neumann conditions on $x = a$ as

$$\{\lambda_{(j)}^{I,D}\}_{j=1}^{\infty} = \left\{ \frac{(n-1/2)^2\pi^2}{a^2} + \frac{(2m-1)^2\pi^2}{d^2} \right\}_{n,m=1}^{\infty}, \quad (3.4.48)$$

$$\{\lambda_{(j)}^{I,N}\}_{j=1}^{\infty} = \left\{ \frac{(n-1)^2\pi^2}{a^2} + \frac{(2m-1)^2\pi^2}{d^2} \right\}_{n,m=1}^{\infty}. \quad (3.4.49)$$

The only value of m to give eigenvalues below $\lambda = 4\pi^2/d^2$ is $m = 1$. There are no eigenvalues in region II . Putting $m = 1$ into (3.4.48) and (3.4.49) we can produce the following inequality that holds for all j for which $\lambda_{(j),s} < 4\pi^2/d^2$,

$$\frac{\pi^2}{a^2}(j-1)^2 \leq \lambda_{(j),s} - \frac{\pi^2}{d^2} \leq \frac{\pi^2}{a^2}(j-1/2)^2. \quad (3.4.50)$$

Replacing the Neumann condition on $x = 0$ by a Dirichlet condition, we can recalculate the eigenfunction expansions and eigenvalues and the inequality similar to (3.4.50) is

$$\frac{\pi^2}{a^2}(j-1/2)^2 \leq \lambda_{(j),a} - \frac{\pi^2}{d^2} \leq \frac{\pi^2}{a^2}j^2. \quad (3.4.51)$$

Each interval of (3.4.50) and (3.4.51) whose right-end point is less than $3\pi^2/d^2$ contains only one eigenvalue. Notice that these estimations are exactly the same as the estimations made for the laterally coupled waveguide, (2.4.107) and (2.4.108).

The result of superimposing these intervals onto figure 3.2 is shown in figure 3.3. Although each mode appears between two estimates, it can be seen that as a/d increases along each mode, the estimate coming from the upper bound gives a better approximation to the frequency of the trapped mode.

Proof of existence of a trapped mode

To prove the existence of a trapped mode we need the right-hand side of (3.4.50) or (3.4.51) to be less than $3\pi^2/d^2$. Putting $j = 1$ into both (3.4.50) and (3.4.51) we can prove that a trapped mode exists provided $a/d > 1/\sqrt{12}$ when a Neumann condition

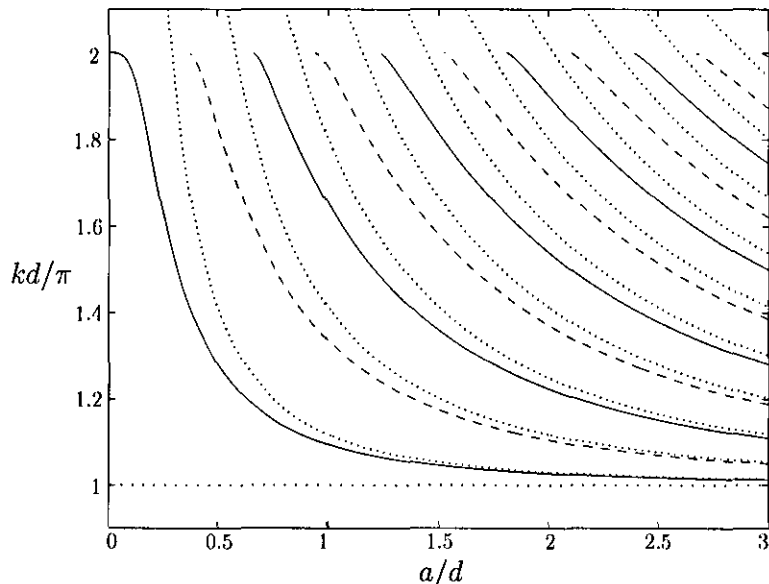


Figure 3.3: A comparison of the trapped-mode wavenumbers, kd/π , for modes symmetric and antisymmetric about $x = 0$ for the full solution, (solid) and (dashed) and the estimated intervals (dotted), plotted against a/d .

is placed on $x = 0$, and $a/d > 1/\sqrt{3}$ when a Dirichlet condition is on $x = 0$. These conditions are equivalent to (2.4.110) and (2.4.111) with $b/d = 1/2$.

3.5 Trapped modes below the second cut-off

In this section we seek Dirichlet modes whose frequencies are embedded in the continuous spectrum for the problem discussed earlier. In section 3.4 Dirichlet modes were found with a frequency $\pi < kd < 2\pi$. This cut-off allowed only one mode to propagate in the region containing the plate and all other modes to decay down the waveguide. When seeking the embedded trapped modes we look for modes with frequencies $kd > 2\pi$, as the continuous spectrum occupies the semi-interval $[4\pi^2/d^2, \infty)$.

In section 2.5 we found embedded trapped modes in the frequency range $2\pi < kd < d\pi/(d - b)$, when $1/2 < b/d \leq 2/3$. These modes do not exist when $b/d = 1/2$. In this section the symmetry of the problem allows embedded modes to be found in a higher frequency range.

We shall use the same modified residue calculus method as in section 2.5.2.

3.5.1 Formulation

The reasoning in section 3.4 that the frequency should be restricted to $\pi < kd < 2\pi$ was that α_0 would be purely imaginary whereas α_n and β_n would be real and positive for $n \in \mathbb{N}$. For the embedded case here we restrict the frequency to

$$3\pi < kd < 4\pi, \quad (3.5.1)$$

so that α_0, α_1 (and β_1) are purely imaginary whereas $\alpha_n, \beta_n, n \geq 2$ are real and positive.

We begin by seeking trapped modes symmetric about $x = 0$ and write the eigenfunction expansions for the two regions similar to (3.3.11) and (3.3.12) as

$$\phi_1(x, y) = \sum_{n=0}^{\infty} U_n^{(1)} \frac{\cosh \alpha_n x}{\alpha_n \sinh \alpha_n a} \Psi_n^{(1)}(y), \quad \alpha_n = (\mu_n^2 - k^2)^{1/2}, \quad (3.5.2)$$

$$\phi_2(x, y) = \sum_{n=2}^{\infty} U_n^{(2)} \frac{e^{-\beta_n(x-a)}}{-\beta_n} \Psi_n^{(2)}(y), \quad \beta_n = (\nu_n^2 - k^2)^{1/2}, \quad (3.5.3)$$

where ϕ_1 and ϕ_2 are defined as before and $\Psi_n^{(i)}(y), i = 1, 2$, are given by (3.3.14) and (3.3.15). Note that the summation for ϕ_2 starts from $n = 2$, as we set the amplitude of the wave-mode corresponding to an imaginary β_1 in the outer region to zero.

3.5.2 Modified residue calculus method

Matching $\phi_1 = \phi_2$ and $\partial\phi_i/\partial x = \partial\phi_3/\partial x$ along L_1 , as in section 3.4.1, we obtain

$$\sum_{n=2}^{\infty} U_n \left(\frac{1}{\beta_n - \alpha_m} + \frac{\zeta_m}{\beta_n + \alpha_m} \right) = 0, \quad m \in \mathbb{N}_0, \quad (3.5.4)$$

where U_n and ζ_m are given by (3.4.10). The edge condition (3.4.11) remains the same for the embedded case.

We now formulate a solution to (3.5.4) by considering the integrals

$$I_m = \lim_{N \rightarrow \infty} \frac{1}{2\pi i} \int_{C_N} f(z) \left(\frac{1}{z - \alpha_m} + \frac{\zeta_m}{z + \alpha_m} \right) dz, \quad m \in \mathbb{N}_0, \quad (3.5.5)$$

where C_N is a sequence of contours on which $z \rightarrow \infty$ as $N \rightarrow \infty$ and $f(z)$ is a meromorphic function which has the following properties:

P1. $f(z)$ is an analytic function of z except for simple poles at $z = \beta_n, n \geq 2$;

P2. $f(z) = O(z^{-\frac{1}{2}})$ as $|z| \rightarrow \infty$ on C_N as $N \rightarrow \infty$.

Construction of $f(z)$

We choose

$$f(z) = g(z)h(z), \quad (3.5.6)$$

where

$$g(z) = \prod_{n=2}^{\infty} \frac{1 - z/\alpha_n}{1 - z/\beta_n}, \quad h(z) = 1 + \sum_{n=2}^{\infty} \frac{A_n}{z - \alpha_n}. \quad (3.5.7)$$

It should be noted that the function $g(z)$ is the same as (3.4.14) except that one term has been removed from both the numerator and denominator. The asymptotics for large z remain the same and so P2 is satisfied if we choose the same contours C_N as in section 3.4.1.

Applying Cauchy's residue theorem to (3.5.5) we obtain

$$\sum_{n=2}^{\infty} R(f : \beta_n) \left(\frac{1}{\beta_n - \alpha_m} + \frac{\zeta_m}{\beta_n + \alpha_m} \right) + f(\alpha_m) + \zeta_m f(-\alpha_m) = 0, \quad m \in \mathbb{N}_0. \quad (3.5.8)$$

A comparison with (3.5.4) shows our solution is given by $U_n = R(f : \beta_n)$, provided

$$f(\alpha_m) + \zeta_m f(-\alpha_m) = 0, \quad m \in \mathbb{N}_0. \quad (3.5.9)$$

In order to solve (3.5.9) the coefficients $A_n, n \geq 2$, in (3.5.6) can be found from the infinite system of equations

$$A_m + B_m \sum_{n=2}^{\infty} \frac{A_n}{\alpha_m + \alpha_n} = B_m, \quad (3.5.10)$$

where

$$B_m = \frac{2\alpha_m \zeta_m (\beta_m - \alpha_m)}{(\beta_m + \alpha_m)} \prod_{\substack{n=2 \\ n \neq m}}^{\infty} \frac{(1 + \alpha_m/\alpha_n)(1 - \alpha_m/\beta_n)}{(1 - \alpha_m/\alpha_n)(1 + \alpha_m/\beta_n)}. \quad (3.5.11)$$

Trapped mode condition

We now have two conditions still to be satisfied simultaneously, namely (3.5.9) with $m = 0$ and $m = 1$. If we let $\alpha_0 = -i\alpha'_0$, where $\alpha'_0 = (k^2 - \mu_0^2)^{\frac{1}{2}} = (k^2 - (\pi/d)^2)^{\frac{1}{2}}$, and $\alpha_1 = -i\alpha'_1$, where $\alpha'_1 = (k^2 - \mu_1^2)^{\frac{1}{2}} = (k^2 - (3\pi/d)^2)^{\frac{1}{2}}$, these conditions reduce to

$$e^{2i\alpha'_j a} = -\frac{f(-i\alpha'_j)}{f(i\alpha'_j)}, \quad j = 0, 1. \quad (3.5.12)$$

Following the work in section 3.4.1 we find the condition for trapped modes is that

$$\alpha'_j a = \chi_j + \sigma_j + \left(n_j - \frac{1}{2}\right)\pi, \quad j = 0, 1, \quad (3.5.13)$$

are both satisfied simultaneously, where

$$\chi_j = \sum_{n=2}^{\infty} \left(\tan^{-1} \left(\frac{\alpha'_j}{\alpha_n} \right) - \tan^{-1} \left(\frac{\alpha'_j}{\beta_n} \right) \right), \quad (3.5.14)$$

$$\sigma_j = \arg \left(h(-i\alpha'_j) \right) = \arg \left(1 - \sum_{n=2}^{\infty} \frac{A_n}{\alpha_n + i\alpha'_j} \right), \quad (3.5.15)$$

and n_0 and n_1 are an arbitrary pair of integers.

As $a/d \rightarrow \infty$ it is easy to see that $A_n \rightarrow 0$ in (3.5.10) because of the exponential decay of B_n and hence from (3.5.15) $\sigma_j \rightarrow 0$, $j = 0, 1$. In a similar way to that shown in section 3.4.1, given an $\epsilon > 0$, we can choose a/d sufficiently large so that $\max(|\sigma_0|, |\sigma_1|) < \epsilon$. The series $-\chi_j$, $j = 0, 1$, with χ_j given by (3.5.15) consists of decreasing terms of alternating sign. Using (3.4.40) we can show that the following inequalities hold

$$0 < -\chi_j < \tan^{-1}(\alpha'_j/\beta_1) < \pi/2, \quad j = 0, 1, \quad (3.5.16)$$

and for $kd \in (3\pi, 4\pi)$, we can fix a/d sufficiently large so that,

$$0 < \pi/2 + \chi_j + \sigma_j \equiv C_j < \pi/2, \quad j = 0, 1. \quad (3.5.17)$$

As α'_0 is always greater than $\sqrt{8\pi}/d$ for $kd \in (3\pi, 4\pi)$ it can be seen from (3.5.13) that requiring a/d to be sufficiently large is equivalent to requiring n_0 to be sufficiently large. This is not the case for n_1 as α'_1 can be close to zero as $kd \rightarrow 3\pi$. If we eliminate a from the two trapped-mode conditions (3.5.13) we find

$$(\Lambda n_0 - n_1)\pi = (C_1 - \pi) + (\pi - C_0)\Lambda, \quad (3.5.18)$$

where $\Lambda = \alpha'_1/\alpha'_0$.

If we vary kd between 3π and 4π , $\Lambda \in (0, \sqrt{7/15})$ and so the value of the left-hand side of (3.5.18) lies between $-n_1\pi$ and $(\sqrt{7/15}n_0 - n_1)\pi$, whereas if we fix a/d (or n_0) sufficiently large, the right-hand side always lies between $-\pi$ and $(\sqrt{7/15} - 1/2)\pi$. We now fix $n_1 \in \mathbb{N}$, and choose n_0 sufficiently large so that $\sqrt{7/15}n_0 - n_1 > \sqrt{7/15} - 1/2$ and (3.5.17) both hold for $j = 0, 1$. We now find that there a value of kd in the range $(3\pi, 4\pi)$ which satisfies (3.5.18), with the corresponding value of a/d found from (3.5.17).

When seeking trapped modes with antisymmetry about $x = 0$, the conditions change to

$$\alpha'_j a = \chi_j + \sigma'_j + n_j \pi, \quad j = 0, 1, \quad (3.5.19)$$

where σ'_j is the argument of $h(-i\alpha'_j)$ with the A_n coefficients coming from

$$-A_m + B_m \sum_{n=2}^{\infty} \frac{A_n}{\alpha_m + \alpha_n} = B_m, \quad m = 2, 3, \dots \quad (3.5.20)$$

Results

For the results in this section a truncation parameter $N = 5$ was used on the infinite systems of equations (3.5.10) and (3.5.20). In figure 3.4 the trapped-mode wavenumbers, kd/π , are plotted against a/d , with a close-up of a number of points shown in figure 3.5. In both figures the modes symmetric about $x = 0$ are shown by a cross and the modes antisymmetric about $x = 0$ by a circle. The modes appear between the two cut-offs $kd = 3\pi$ and $kd = 4\pi$.

In figure 3.5 the lines corresponding to the solutions of (3.5.13) for $j = 0$ and $j = 1$ are shown together with the integer values for n_0 and n_1 . The trapped-mode frequencies are the intersection of the solid or dashed lines.

It can be seen in figure 3.4 that there are no trapped modes present when a/d is below some critical value and trapped modes occur only for specific values of the plate length. As a/d increases the number of trapped modes present in a small a/d interval also increases.

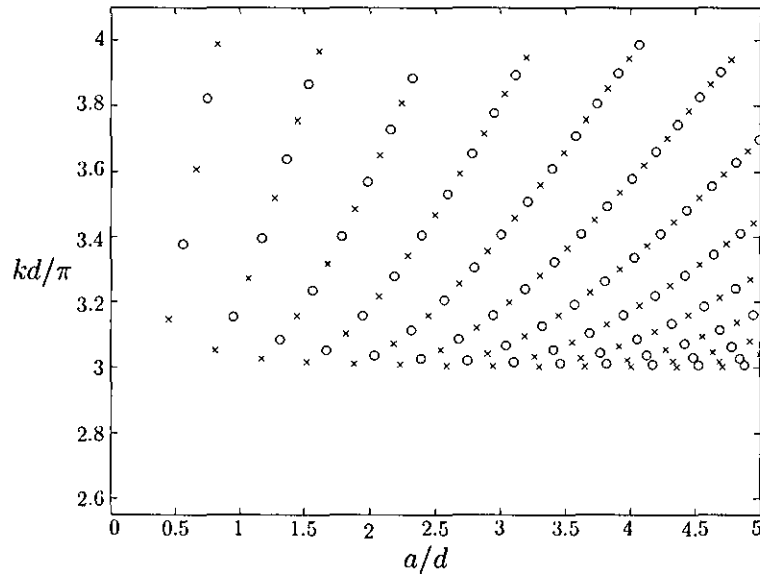


Figure 3.4: Trapped-mode wavenumbers, kd/π , for modes symmetric (\times) and antisymmetric (\circ) about $x = 0$ plotted against a/d .

Conclusion

In this section we have investigated Dirichlet modes for a rigid plate on the centreline of a guide whose frequencies are above the first cut-off for wave propagation down the

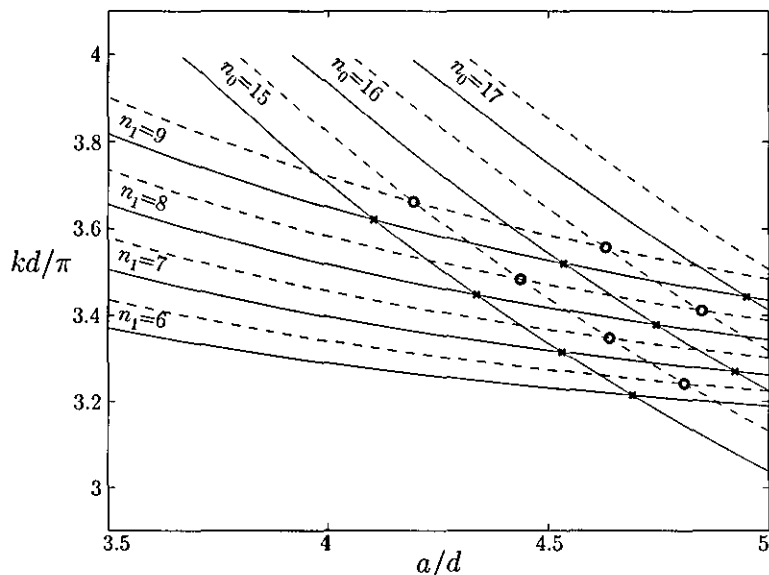


Figure 3.5: A detailed view of part of figure 3.4 showing the curves corresponding to the solutions of (3.5.13) for $j = 0$ and $j = 1$, labelled with the corresponding n_0 and n_1 values. The solid curves correspond to modes symmetric about $x = 0$ and the dashed to modes antisymmetric about $x = 0$. The embedded trapped modes, denoted by \times (symmetric) and \circ (antisymmetric), are solutions for both j values and are where the solid or dashed lines cross.

waveguide. The frequency was restricted so that one wave-like mode appeared in the outer region and two wave-like modes appeared in the inner region. The amplitude of the mode in the outer region was set to zero and a modified residue calculus technique used to produce a pair of conditions that needed to be solved simultaneously for the existence of trapped modes. We also proved that trapped modes exist provided the plate length is sufficiently large. The results plotted from this method show that the trapped modes correspond to the intersection of two sets of lines. The trapped modes only appear for specific values of the plate length, a feature that was apparent for the embedded trapped modes in chapter 2.

3.6 Summary

In this chapter we have investigated the trapped modes that can occur in a two-dimensional parallel-plate waveguide containing a finite length plate placed on the centreline of the guide. Dirichlet boundary conditions are placed on the waveguide walls

and a Neumann boundary condition on the plate. A Dirichlet condition is placed on the line which is an extension of the plate as modes are sought which are antisymmetric about the mid-line of the waveguide. The trapped modes found, which are known as Dirichlet modes, are either symmetric or antisymmetric about the line perpendicular to and through the centre of the plate.

After forming eigenfunction expansions for the problem, a cut-off was introduced below which modes cannot propagate to infinity. The chapter was then split into two sections, the first sought modes whose frequencies were below this cut-off and the second sought modes with frequencies above the cut-off.

Below the cut-off a modified residue calculus technique was used to prove the existence of Dirichlet modes when the plate is sufficiently long and compute the frequencies. These frequencies are shown to be the same as the frequencies coming from the laterally coupled waveguide in the limit as $b/d \rightarrow 1/2$. A variational principle was also used to provide estimates for the frequencies of the Dirichlet modes and prove the existence of a single mode for a sufficiently long plate. The Dirichlet modes were shown numerically to exist for any length plate and the number of modes increased as the length of the plate increased.

Above the cut-off a modified residue calculus technique is again used to prove the existence of Dirichlet modes for a sufficiently long plate. The modes only appear for specific values of the plate length and only when the plate is longer than a certain value.

Chapter 4

Two-dimensional waveguides containing an off-centre plate

4.1 Introduction to the problem

In this chapter we modify the work done in chapter 3 by moving the plate off the centreline of the waveguide.

The problem consists of a two dimensional parallel-plate waveguide with Dirichlet conditions on the guide walls containing a finite length thin Neumann plate parallel to the waveguide walls and off the centreline of the guide. Using the previous terminology we are seeking Dirichlet trapped modes in the guide, as in chapter 3 .

The chapter is divided as follows. We discuss previous work concerning off-centre bodies in parallel-plate waveguides in section 4.2. The problem is formulated in section 4.3 and we find that the geometry of the problem is described by two parameters corresponding to the length of the plate and the off-set of the plate. When formulating the problem an initial cut-off in the frequency is introduced below which modes cannot propagate to infinity.

In section 4.4 we seek Dirichlet modes whose frequencies are below this cut-off. The frequency is restricted in such a way that only one wave-like mode local to the plate appears in the model. The trapped-mode frequencies are computed in section 4.4.1 using a modified residue calculus technique. Below the first cut-off modes are shown to occur for any length plate and for any off-set. A variational principle is used in section 4.4.2 to provide estimates to the trapped mode frequencies and prove the existence of a single trapped mode for a sufficiently long plate.

In section 4.5 trapped modes are sought above the first cut-off and below the second cut-off using a modified residue calculus technique. Between the two cut-offs two wave-like modes local to the plate and one propagating mode exist in the model. When looking between the first and second cut-offs we set the amplitude of the propagating mode to zero and the solution corresponds to the intersection of two sets of lines. The range of frequency restriction in this section is depends on the off-set of the plate. Between the first and second cut-offs trapped modes appear for any off-set of the plate, except when the plate is three-quarters of the way up the guide, but only for specific values of the plate length.

The off-centre plate problem contains a third cut-off below which two modes can propagate down the guide. In section 4.6 trapped modes are sought between the second and third cut-offs using a modified residue calculus method. The amplitudes of both propagating modes are set to zero and the inner region now contains three wave-like modes. The range that the frequency is restricted to again depends on the off-set of the plate and trapped modes only occur when the off-set is below a certain value. The trapped modes correspond to the intersection of three sets of lines and only occur for specific combinations of the off-set and the plate length.

A summary of the chapter is presented in section 4.7 together with a plot of the lowest frequency mode in each of the three frequency bands.

4.2 Background

Previously work concerning the occurrence of trapped modes in two-dimensional parallel-plate waveguides containing off-centre obstacles has not been vast. As discussed in the previous chapter, if the geometry is symmetric about the centreline of the waveguide a natural cut-off can be introduced below which modes cannot propagate to infinity down the guide. If the obstacle is off the centreline the symmetry is removed and the problem is not as straightforward.

In the water wave context Linton and Evans (1991) used a matched eigenfunction expansion method to provide numerical evidence of trapped modes above a submerged horizontal plate of finite width in water of constant depth. The field equation for this example was, however, $(\nabla^2 - k^2)\phi = 0$, a mixed boundary condition was placed on the surface and Neumann conditions placed on the plate and on the bottom.

The Neumann problem of an off-centre thin plate was considered by Evans, Linton, and Ursell (1993). In the paper the authors used a modified residue calculus technique to prove the existence of Neumann modes for a sufficiently long thin plate. The problem is similar to the one considered in this chapter except that here we investigate Dirichlet modes.

It was later proved by Davies and Parnowski (1998), and also Groves (1998) and Linton and McIver (1998a) that the geometry considered by Evans, Linton, and Ursell (1993) is an example of a very general class of geometries for which Neumann modes exist. A more detailed explanation of the ideas in these papers is given in section 2.4.2.

The investigation into Neumann modes for an off-centre thin plate placed parallel to the walls in a parallel-plate waveguide was given by Linton et al. (2002). The geometry of the off-centre thin plate is defined by two non-dimensional parameters corresponding to the off-set of the plate compared to the width of the whole guide and the length of the plate compared to the width of the whole guide. The Neumann modes can be found below the first cut-off for any value of either parameter, as shown in Evans, Linton, and Ursell (1993). In Linton et al. (2002) Neumann modes found between the second and third cut-offs are shown to occur only for specific combinations of the two parameters. In this chapter we consider the Dirichlet problem and seek trapped modes below the first, second and third cut-offs.

4.3 Formulation

We consider a two-dimensional waveguide with parallel sides a width d apart containing a parallel plate of length $2a$ which is situated off the centreline of the waveguide. Cartesian axes are chosen so that the x -axis coincides with the lower boundary of the waveguide and the y -axis is chosen so that the waveguide is symmetric about $x = 0$. We set up the problem so that the plate is a distance b from the lower boundary of the waveguide and assume $b > d/2$, as shown in figure 4.1.

We begin by formulating a solution which is symmetric about $x = 0$ by considering the region $x > 0$ and seeking a non-trivial function $\phi(x, y)$ which satisfies

$$\frac{\partial \phi}{\partial x} = 0 \text{ on } x = 0, \quad 0 < y < d. \quad (4.3.1)$$

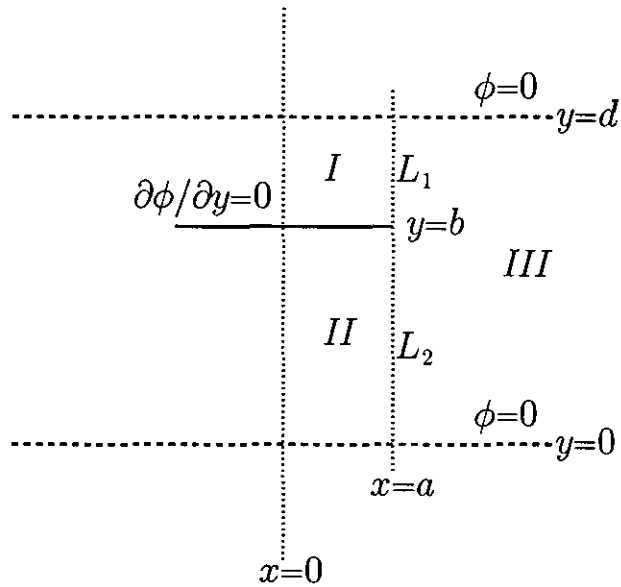


Figure 4.1: Definition sketch.

The function $\phi(x, y)$ must also satisfy the Helmholtz equation within the waveguide

$$(\nabla^2 + k^2)\phi = 0, \quad 0 < y < d, \quad x > 0 \text{ except on } y = b, \quad 0 < x < a, \quad (4.3.2)$$

subject to Dirichlet conditions on the waveguide walls and a Neumann condition on the plate,

$$\phi = 0 \text{ on } y = 0, \quad x > 0, \quad (4.3.3)$$

$$\phi = 0 \text{ on } y = d, \quad x > 0, \quad (4.3.4)$$

$$\frac{\partial \phi}{\partial y} = 0 \text{ on } y = b, \quad 0 < x < a, \quad (4.3.5)$$

and a radiation condition requiring no propagating modes at infinity,

$$\phi \rightarrow 0 \text{ as } x \rightarrow \infty. \quad (4.3.6)$$

We finally assume that ϕ is non-singular, but that

$$\nabla \phi = O(r^{-\frac{1}{2}}) \text{ as } r \equiv \{(x - a)^2 + (y - b)^2\}^{\frac{1}{2}} \rightarrow 0, \quad (4.3.7)$$

anticipating singular behaviour in the velocity field at the edge of the plate.

It is useful to split the domain into three regions. Region *I* is $b < y < d$, $0 < x < a$, region *II* is $0 < y < b$, $0 < x < a$, and region *III* is $0 < y < d$, $x > a$. We can represent the function ϕ by a function ϕ_i ($i = 1, 2, 3$) in each region with the following continuity

condition applied at each regions boundaries:

$$\phi_i = \phi_3, \quad \frac{\partial \phi_i}{\partial x} = \frac{\partial \phi_3}{\partial x}, \quad \text{on } L_i, \quad i = 1, 2, \quad (4.3.8)$$

where L_1 is $x = a, b < y < d$, L_2 is $x = a, 0 < y < b$ and L_3 is $L_1 \cup L_2$, as in figure 4.1.

Separation of variables reveals that

$$\phi_1(x, y) = \sum_{n=1}^{\infty} U_n^{(1)} \frac{\cosh \alpha_n x}{\alpha_n \sinh \alpha_n a} \Psi_n^{(1)}(y), \quad (4.3.9)$$

$$\phi_2(x, y) = \sum_{n=0}^{\infty} U_n^{(2)} \frac{\cosh \beta_n x}{\beta_n \sinh \beta_n a} \Psi_n^{(2)}(y), \quad (4.3.10)$$

$$\phi_3(x, y) = \sum_{n=1}^{\infty} U_n^{(3)} \frac{e^{-\gamma_n(x-a)}}{-\gamma_n} \Psi_n^{(3)}(y), \quad (4.3.11)$$

where

$$\alpha_n = (\nu_n^2 - k^2)^{1/2}, \quad \beta_n = (\mu_n^2 - k^2)^{1/2}, \quad \gamma_n = (\lambda_n^2 - k^2)^{1/2}, \quad (4.3.12)$$

and we have introduced complete orthonormal sets

$$\Psi_n^{(1)}(y) = 2^{1/2} \sin \nu_n(d - y), \quad \nu_n = \frac{\pi}{c} \left(n - \frac{1}{2} \right), \quad n \in \mathbb{N}, \quad (4.3.13)$$

$$\Psi_n^{(2)}(y) = 2^{1/2} \sin \mu_n y, \quad \mu_n = \frac{\pi}{b} \left(n + \frac{1}{2} \right), \quad n \in \mathbb{N}_0, \quad (4.3.14)$$

$$\Psi_n^{(3)}(y) = 2^{1/2} \sin \lambda_n y, \quad \lambda_n = \frac{n\pi}{d}, \quad n \in \mathbb{N}, \quad (4.3.15)$$

which satisfy

$$\frac{1}{|L_i|} \int_{L_i} \Psi_n^{(i)}(y) \Psi_m^{(i)}(y) dy = \delta_{mn}, \quad i = 1, 2, 3, \quad (4.3.16)$$

where δ_{mn} is the Kronecker delta and $c = d - b$.

We now restrict the frequency so that all modes in region *III* decay exponentially to zero, i.e. we need $\gamma_n, n \in \mathbb{N}$ to be real and positive. The first cut-off for this problem is therefore $kd = \pi$.

4.4 Trapped modes below the first cut-off

In this section we restrict the frequency so that only one wave-like mode is present in the inner region $x < a$, and so we require either α_1 or β_0 to be purely imaginary. To restrict the frequency so that α_1 is purely imaginary we have to have $k > \pi/2c > \pi/d$, which is not possible. We therefore require β_0 to be purely imaginary which implies

$kb > \pi/2$, and anticipate that a necessary condition for the existence of trapped modes is

$$\frac{\pi d}{2b} < kd < \pi. \quad (4.4.1)$$

It is important to note that trapped modes do not exist in this frequency range when $b/d = 1/2$. To compare this waveguide to the one in the previous chapter we need to examine the case when $b = d$. When $b = d$ we can reflect the waveguide about the line $x = d$ and consider a waveguide of width $2d$ containing a plate on the centreline. The two frequency ranges (3.4.1) and (4.4.1) are therefore equivalent, when $b = d$, if we replace d by $2d$ in (3.4.1).

We now apply the continuity conditions (4.3.8).

4.4.1 Modified residue calculus method

Matching the eigenfunction expansions $\phi_i = \phi_3$ on $L_i, i = 1, 2$, we obtain

$$\sum_{n=1}^{\infty} U_n^{(3)} \frac{\Psi_n^{(3)}(y)}{-\gamma_n} = \begin{cases} \sum_{n=1}^{\infty} U_n^{(1)} \frac{\coth \alpha_n a}{\alpha_n} \Psi_n^{(1)}(y), & y \in L_1, \\ \sum_{n=0}^{\infty} U_n^{(2)} \frac{\coth \beta_n a}{\beta_n} \Psi_n^{(2)}(y), & y \in L_2. \end{cases} \quad (4.4.2)$$

Similarly matching the x -derivatives $\partial\phi_i/\partial x = \partial\phi_3/\partial x$ on $L_i, i = 1, 2$, we find

$$\sum_{n=1}^{\infty} U_n^{(3)} \Psi_n^{(3)}(y) = \begin{cases} \sum_{n=1}^{\infty} U_n^{(1)} \Psi_n^{(1)}(y), & y \in L_1, \\ \sum_{n=0}^{\infty} U_n^{(2)} \Psi_n^{(2)}(y), & y \in L_2. \end{cases} \quad (4.4.3)$$

If we multiply (4.4.2) by $\Psi_m^{(i)}, m \in \mathbb{N}$, when $i = 1$ and $m \in \mathbb{N}_0$, when $i = 2$, and integrate over $L_i, i = 1, 2$, we have,

$$U_m^{(1)} = \sum_{n=1}^{\infty} U_n^{(3)} d_{nm}, \quad m \in \mathbb{N}, \quad (4.4.4)$$

$$U_m^{(2)} = \sum_{n=1}^{\infty} U_n^{(3)} e_{nm}, \quad m \in \mathbb{N}_0, \quad (4.4.5)$$

where we have defined

$$d_{nm} = \frac{1}{c} \int_{L_1} \Psi_n^{(3)}(y) \Psi_m^{(1)}(y) dy, \quad m \in \mathbb{N}, \quad (4.4.6)$$

$$e_{nm} = \frac{1}{b} \int_{L_2} \Psi_n^{(3)}(y) \Psi_m^{(2)}(y) dy, \quad m \in \mathbb{N}_0. \quad (4.4.7)$$

In a similar way from (4.4.3) we obtain

$$U_m^{(1)} \frac{\coth \alpha_m a}{\alpha_m} = \sum_{n=1}^{\infty} \frac{U_n^{(3)}}{-\gamma_n} d_{nm}, \quad m \in \mathbb{N}, \quad (4.4.8)$$

$$U_m^{(2)} \frac{\coth \beta_m a}{\beta_m} = \sum_{n=1}^{\infty} \frac{U_n^{(3)}}{-\gamma_n} e_{nm}, \quad m \in \mathbb{N}_0, \quad (4.4.9)$$

Evaluating the integrals d_{nm} and e_{nm} , we have

$$d_{nm} = \frac{2\lambda_n(-1)^{m+1} \cos \lambda_n b}{c(\gamma_n^2 - \alpha_m^2)}, \quad e_{nm} = \frac{2\lambda_n(-1)^{m+1} \cos \lambda_n b}{b(\gamma_n^2 - \beta_m^2)}, \quad (4.4.10)$$

provided $\gamma_n \neq \alpha_m$ and $\gamma_n \neq \beta_m$. Eliminating $U_m^{(1)}$ from (4.4.4) and (4.4.8), $U_m^{(2)}$ from (4.4.5) and (4.4.9) and using (4.4.10) we find

$$\sum_{n=1}^{\infty} U_n \left(\frac{1}{\gamma_n - \alpha_m} + \frac{\zeta_m}{\gamma_n + \alpha_m} \right) = 0, \quad m \in \mathbb{N}, \quad (4.4.11)$$

$$\sum_{n=1}^{\infty} U_n \left(\frac{1}{\gamma_n - \beta_m} + \frac{\xi_m}{\gamma_n + \beta_m} \right) = 0, \quad m \in \mathbb{N}_0, \quad (4.4.12)$$

where we have defined

$$U_n = \frac{U_n^{(3)} \lambda_n \cos \lambda_n c}{\gamma_n}, \quad \zeta_m = e^{-2\alpha_m a}, \quad \text{and} \quad \xi_m = e^{-2\beta_m a}. \quad (4.4.13)$$

The condition to ensure that (4.3.7) is satisfied by $\phi_3(x, y)$ is

$$U_n = O(n^{-\frac{1}{2}}) \text{ as } n \rightarrow \infty, \quad (4.4.14)$$

which is found as in section 2.4.1.

We could devise an approximate solution by neglecting α_m and β_m , $m \in \mathbb{N}$, but instead proceed directly to the full solution by considering the following contour integrals

$$I_m = \lim_{N \rightarrow \infty} \frac{1}{2\pi i} \int_{C_N} f(z) \left(\frac{1}{z - \alpha_m} + \frac{\zeta_m}{z + \alpha_m} \right) dz, \quad m \in \mathbb{N}, \quad (4.4.15)$$

$$J_m = \lim_{N \rightarrow \infty} \frac{1}{2\pi i} \int_{C_N} f(z) \left(\frac{1}{z - \beta_m} + \frac{\xi_m}{z + \beta_m} \right) dz, \quad m \in \mathbb{N}_0, \quad (4.4.16)$$

where C_N is a sequence of contours on which $z \rightarrow \infty$ as $N \rightarrow \infty$ and $f(z)$ is a meromorphic function which has the following properties:

P1. $f(z)$ is an analytic function of z except for simple poles at $z = \gamma_n$, $n \in \mathbb{N}$;

P2. $f(z) = O(z^{-\frac{1}{2}})$ as $|z| \rightarrow \infty$ on C_N as $N \rightarrow \infty$.

The main step in obtaining solutions for the modified residue calculus method involves the construction of $f(z)$.

Construction of $f(z)$

We would like to choose $f(z)$ in the form

$$f(z) = g(z)h(z), \quad (4.4.17)$$

where

$$g(z) = \prod_{n=1}^{\infty} \frac{(1 - z/\alpha_n)(1 - z/\beta_n)}{(1 - z/\gamma_n)}, \quad (4.4.18)$$

$$h(z) = 1 + \sum_{n=1}^{\infty} \left(\frac{A_n}{z - \alpha_n} + \frac{B_n}{z - \beta_n} \right), \quad (4.4.19)$$

and the coefficients A_n and B_n are to be determined. The function $f(z)$ is chosen to have the correct poles to satisfy P1 and the function $h(z)$ is chosen so that the zeros of $g(z)$ at α_n and β_n are cancelled by the poles of $h(z)$ at these points.

To satisfy P2, we need to work out the behaviour of (4.4.18) as $|z| \rightarrow \infty$. We begin by expanding $g(z)$ as

$$\hat{g}(z) = \prod_{n=1}^{\infty} \frac{1 - z/\alpha_n}{1 - z/\nu_n} \prod_{n=1}^{\infty} \frac{1 - z/\beta_n}{1 - z/\mu_n} \prod_{n=1}^{\infty} \frac{1 - z/\lambda_n}{1 - z/\gamma_n} \prod_{n=1}^{\infty} \frac{(1 - z/\mu_n)(1 - z/\nu_n)}{(1 - z/\lambda_n)}. \quad (4.4.20)$$

Following section 2.4.1 we can expand the infinite products as

$$\prod_{n=1}^{\infty} \frac{1 - z/\alpha_n}{1 - z/\nu_n} = \prod_{n=1}^{\infty} \left(1 - \frac{k^2}{\nu_n^2} \right)^{-\frac{1}{2}} \prod_{n=1}^{\infty} \left(1 + \frac{k^2}{(z - \nu_n)(\nu_n + \alpha_n)} \right), \quad (4.4.21)$$

$$\prod_{n=1}^{\infty} \frac{1 - z/\beta_n}{1 - z/\mu_n} = \prod_{n=1}^{\infty} \left(1 - \frac{k^2}{\mu_n^2} \right)^{-\frac{1}{2}} \prod_{n=1}^{\infty} \left(1 - \frac{k^2}{(z - \mu_n)(\mu_n + \beta_n)} \right), \quad (4.4.22)$$

and

$$\prod_{n=1}^{\infty} \frac{1 - z/\lambda_n}{1 - z/\gamma_n} = \prod_{n=1}^{\infty} \left(1 - \frac{k^2}{\lambda_n^2} \right)^{\frac{1}{2}} \prod_{n=1}^{\infty} \left(1 - \frac{k^2}{(z - \gamma_n)(\gamma_n + \lambda_n)} \right). \quad (4.4.23)$$

As all the terms α_n , β_n and γ_n are of the form $An + O(n^{-1})$ as $n \rightarrow \infty$, with A a constant, a comparison between the final products in (4.4.21)–(4.4.23), and $\sum_{n=1}^{\infty} n^{-2}$, shows that (4.4.21)–(4.4.23) are uniformly convergent on any compact set excluding $z = \nu_n$, $z = \mu_n$ and $z = \gamma_n$. Provided $z \rightarrow \infty$ through a sequence of values which avoids these points we have

$$g(z) \sim \left(\frac{\sin kd}{kd \cos kb \cos kc} \right)^{\frac{1}{2}} \prod_{n=1}^{\infty} \frac{(1 - z/\mu_n)(1 - z/\nu_n)}{(1 - z/\lambda_n)}. \quad (4.4.24)$$

Using the result (2.4.43) in (4.4.24) we have

$$\prod_{n=1}^{\infty} \frac{(1 - z/\mu_n)(1 - z/\nu_n)}{(1 - z/\lambda_n)} = \frac{e^{\gamma zb/\pi} \Gamma(3/2)}{\Gamma(3/2 - zb/\pi)} \cdot \frac{e^{\gamma zc/\pi} \Gamma(1/2)}{\Gamma(1/2 - zc/\pi)} \cdot \frac{\Gamma(1 - zd/\pi)}{e^{\gamma zd/\pi} \Gamma(1)}. \quad (4.4.25)$$

Using (2.4.45) in (4.4.25) we see, after some simplification, that as $z \rightarrow \infty$, $z \neq |z|$,

$$g(z) \sim \left(\frac{-kdz \cos kb \cos kc}{\pi \sin kd} \right)^{-\frac{1}{2}} \exp \left\{ \frac{-z}{\pi} (b \ln(d/b) + c \ln(d/c)) \right\}. \quad (4.4.26)$$

For the case when z is real and positive we use the reflection properties of the Gamma function, see (2.4.48), and the asymptotic behaviour can be shown to be

$$g(z) \sim \left(\frac{\cos zb \cos zc}{\sin zd} \right) \left(\frac{k dz \cos kb \cos kc}{\pi \sin kd} \right)^{-\frac{1}{2}} \exp \left\{ \frac{-z}{\pi} (b \ln(d/b) + c \ln(d/c)) \right\}, \quad (4.4.27)$$

as $|z| \rightarrow \infty$, $z \neq -|z|$. If we take C_N to be a sequence of circles with centre at the origin and radius R_N which avoids the points $z = \mu_n$, $z = \nu_n$ and $z = \gamma_n$, $n \in \mathbb{N}$, we can, instead of using (4.4.18), consider the function

$$g(z) = \exp \left\{ \frac{z}{\pi} (b \ln(d/b) + c \ln(d/c)) \right\} \prod_{n=1}^{\infty} \frac{(1 - z/\alpha_n)(1 - z/\beta_n)}{(1 - z/\gamma_n)}, \quad (4.4.28)$$

which is $O(z^{-\frac{1}{2}})$ as $|z| \rightarrow \infty$ on C_N as $N \rightarrow \infty$, and hence P2 is satisfied.

Applying Cauchy's residue theorem to (4.4.15) and (4.4.16) we have

$$\sum_{n=1}^{\infty} R(f : \gamma_n) \left(\frac{1}{\gamma_n - \alpha_m} + \frac{\zeta_m}{\gamma_n + \alpha_m} \right) + f(\alpha_m) + \zeta_m f(-\alpha_m) = 0, \quad m \in \mathbb{N}, \quad (4.4.29)$$

$$\sum_{n=1}^{\infty} R(f : \gamma_n) \left(\frac{1}{\gamma_n - \beta_m} + \frac{\xi_m}{\gamma_n + \beta_m} \right) + f(\beta_m) + \xi_m f(-\beta_m) = 0, \quad m \in \mathbb{N}_0. \quad (4.4.30)$$

A comparison with (4.4.11) and (4.4.12) shows our solution is given by $U_n = R(f : \gamma_n)$ provided

$$f(\alpha_m) + \zeta_m f(-\alpha_m) = 0, \quad m \in \mathbb{N}, \quad (4.4.31)$$

$$f(\beta_m) + \xi_m f(-\beta_m) = 0, \quad m \in \mathbb{N}_0. \quad (4.4.32)$$

For $m \in \mathbb{N}$ these equations can be solved with an appropriate choice of the coefficients A_m and B_m . For $m \in \mathbb{N}$ we have

$$f(\alpha_m) = - \exp \left\{ \frac{\alpha_m}{\pi} (b \ln(d/b) + c \ln(d/c)) \right\} \left(\frac{A_m (1 - \alpha_m/\beta_m)}{\alpha_m (1 - \alpha_m/\gamma_m)} \right) \times \prod_{\substack{n=1 \\ n \neq m}}^{\infty} \frac{(1 - \alpha_m/\alpha_n)(1 - \alpha_m/\beta_n)}{(1 - \alpha_m/\gamma_n)}, \quad (4.4.33)$$

$$f(-\alpha_m) = \left(1 - \sum_{n=1}^{\infty} \left(\frac{A_n}{\alpha_m + \alpha_n} + \frac{B_n}{\alpha_m + \beta_n} \right) \right) \exp \left\{ - \frac{\alpha_m}{\pi} (b \ln(d/b) + c \ln(d/c)) \right\} \times \left(\frac{2(1 + \alpha_m/\beta_m)}{1 + \alpha_m/\gamma_m} \right) \prod_{\substack{n=1 \\ n \neq m}}^{\infty} \frac{(1 + \alpha_m/\alpha_n)(1 + \alpha_m/\beta_n)}{(1 + \alpha_m/\gamma_n)}, \quad (4.4.34)$$

$$f(\beta_m) = -\exp\left\{\frac{\beta_m}{\pi}(b \ln(d/b) + c \ln(d/c))\right\} \left(\frac{B_m(1 - \beta_m/\alpha_m)}{\beta_m(1 - \beta_m/\gamma_m)}\right) \\ \times \prod_{\substack{n=1 \\ n \neq m}}^{\infty} \frac{(1 - \beta_m/\alpha_n)(1 - \beta_m/\beta_n)}{(1 - \beta_m/\gamma_n)}, \quad (4.4.35)$$

and

$$f(-\beta_m) = \left(1 - \sum_{n=1}^{\infty} \left(\frac{A_n}{\beta_m + \alpha_n} + \frac{B_n}{\beta_m + \beta_n}\right)\right) \exp\left\{-\frac{\beta_m}{\pi}(b \ln(d/b) + c \ln(d/c))\right\} \\ \times \left(\frac{2(1 + \beta_m/\alpha_m)}{1 + \beta_m/\gamma_m}\right) \prod_{\substack{n=1 \\ n \neq m}}^{\infty} \frac{(1 + \beta_m/\alpha_n)(1 + \beta_m/\beta_n)}{(1 + \beta_m/\gamma_n)}. \quad (4.4.36)$$

Substituting (4.4.33)-(4.4.36) into (4.4.31) and (4.4.32) we obtain,

$$A_m + C_m \sum_{n=1}^{\infty} \left(\frac{A_n}{\alpha_m + \alpha_n} + \frac{B_n}{\alpha_m + \beta_n}\right) = C_m, \quad (4.4.37)$$

$$B_m + D_m \sum_{n=1}^{\infty} \left(\frac{A_n}{\beta_m + \alpha_n} + \frac{B_n}{\beta_m + \beta_n}\right) = D_m, \quad (4.4.38)$$

where

$$C_m = \left(\frac{2\alpha_m(\gamma_m - \alpha_m)(\beta_m + \alpha_m)}{(\gamma_m + \alpha_m)(\beta_m - \alpha_m)}\right) \exp\left\{-\frac{2\alpha_m}{\pi}(b \ln(d/b) + c \ln(d/c) + a\pi)\right\} \\ \times \prod_{\substack{n=1 \\ n \neq m}}^{\infty} \frac{(1 + \alpha_m/\alpha_n)(1 + \alpha_m/\beta_n)(1 - \alpha_m/\gamma_n)}{(1 - \alpha_m/\alpha_n)(1 - \alpha_m/\beta_n)(1 + \alpha_m/\gamma_n)}, \quad (4.4.39)$$

$$D_m = \left(\frac{2\beta_m(\gamma_m - \beta_m)(\alpha_m + \beta_m)}{(\gamma_m + \beta_m)(\alpha_m - \beta_m)}\right) \exp\left\{-\frac{2\beta_m}{\pi}(b \ln(d/b) + c \ln(d/c) + a\pi)\right\} \\ \times \prod_{\substack{n=1 \\ n \neq m}}^{\infty} \frac{(1 + \beta_m/\alpha_n)(1 + \beta_m/\beta_n)(1 - \beta_m/\gamma_n)}{(1 - \beta_m/\alpha_n)(1 - \beta_m/\beta_n)(1 + \beta_m/\gamma_n)}. \quad (4.4.40)$$

and $m \in \mathbb{N}$, in all cases.

Because of the presence of the rapidly decaying factors ζ_m in (4.4.39) for C_m and ξ_m in (4.4.40) for D_m , the system of equations (4.4.37) and (4.4.38) converge very quickly provided a/d is not too small and provide a very efficient method for computing the unknowns A_m and B_m .

To satisfy the edge condition U_n must satisfy the condition given by (4.4.14). Earlier we have shown that $U_m = R(f : \gamma_m)$ and hence

$$U_m = -\gamma_m \left[1 + \sum_{n=1}^{\infty} \left(\frac{A_n}{\gamma_m + \alpha_n} + \frac{B_n}{\gamma_m + \beta_n}\right)\right] \exp\left\{\frac{\gamma_m}{\pi}(b \ln(d/b) + c \ln(d/c))\right\} \\ \times \prod_{n=1}^{\infty} (1 - \gamma_m/\alpha_n)(1 - \gamma_m/\beta_n) / \prod_{\substack{n=1 \\ n \neq m}}^{\infty} (1 - \gamma_m/\gamma_n). \quad (4.4.41)$$

Using (4.4.20) we can expand this to

$$\begin{aligned}
U_m = & -\gamma_m \left(1 - \frac{\gamma_m d}{m\pi}\right) \left[1 + \sum_{n=1}^{\infty} \left(\frac{A_n}{\gamma_m + \alpha_n} + \frac{B_n}{\gamma_m + \beta_n}\right)\right] \exp\left\{\frac{\gamma_m}{\pi} (b \ln(d/b) + c \ln(d/c))\right\} \\
& \times \prod_{n=1}^{\infty} \frac{(1 - \gamma_m/\alpha_n)}{(1 - \gamma_m c/\pi(n - 1/2))} \prod_{n=1}^{\infty} \frac{(1 - \gamma_m/\beta_n)}{(1 - \gamma_m b/\pi(n + 1/2))} \prod_{\substack{n=1 \\ n \neq m}}^{\infty} \frac{(1 - \gamma_m d/n\pi)}{(1 - \gamma_m/\gamma_n)} \\
& \times \prod_{n=1}^{\infty} \frac{(1 - \gamma_m/\mu_n)(1 - \gamma_m/\nu_n)}{(1 - \gamma_m/\lambda_n)}. \tag{4.4.42}
\end{aligned}$$

The first three infinite products can be rearranged in the form shown in (4.4.21)–(4.4.23) and are therefore $O(1)$ as $m \rightarrow \infty$. Using (4.4.27) on the final infinite product we have

$$\begin{aligned}
& \exp\left\{\frac{\gamma_m}{\pi} (b \ln(d/b) + c \ln(d/c))\right\} \prod_{n=1}^{\infty} \frac{(1 - \gamma_m/\mu_n)(1 - \gamma_m/\nu_n)}{(1 - \gamma_m/\lambda_n)} \\
& \sim \frac{\cos \gamma_m b \cos \gamma_m c}{\sin \gamma_m d} \gamma_m^{-\frac{1}{2}}, \\
& \sim \cos \gamma_m b \cos \gamma_m c \operatorname{cosec}\left(m\pi - \frac{(kd)^2}{2m\pi} + O(m^{-2})\right) \left(\frac{m\pi}{d}\right)^{-\frac{1}{2}} \left(1 + O(m^{-2})\right), \\
& \sim \frac{2\pi^{1/2} \cos \gamma_m b \cos \gamma_m c}{k^2 d^{3/2}} m^{\frac{1}{2}} \left(1 + O(m^{-1})\right), \tag{4.4.43}
\end{aligned}$$

as $m \rightarrow \infty$, since

$$\gamma_m \sim \frac{n\pi}{d} - \frac{k^2 d}{2n\pi} + O(m^{-2}). \tag{4.4.44}$$

As $m \rightarrow \infty$ we also have

$$\left(1 - \frac{\gamma_m d}{m\pi}\right) \sim \frac{1}{2} \left(\frac{kd}{m\pi}\right)^2 + O(m^{-3}). \tag{4.4.45}$$

Combining (4.4.42)–(4.4.45) we can see that U_n is $O(n^{-\frac{1}{2}})$ as $n \rightarrow \infty$, which is the required asymptotics to take account of the edge condition (4.3.7).

Trapped mode condition

We can now return to the one condition still to be satisfied, namely (4.4.32) with $m = 0$. If we let $\beta_0 = -i\beta'$, where $\beta' = (k^2 - \mu_0^2)^{\frac{1}{2}} = (k^2 - (\pi/2b)^2)^{\frac{1}{2}}$, this condition reduces to

$$e^{2i\beta' a} = -\frac{f(-i\beta')}{f(i\beta')}. \tag{4.4.46}$$

Using (4.4.28) and (4.4.19) we have

$$\frac{g(-i\beta')}{g(i\beta')} = e^{2i(x - \beta'\Theta)}, \quad \frac{h(-i\beta')}{h(i\beta')} = e^{2i\sigma}, \tag{4.4.47}$$

where we have defined

$$\chi = \sum_{n=1}^{\infty} \left(\tan^{-1} \left(\frac{\beta'}{\alpha_n} \right) + \tan^{-1} \left(\frac{\beta'}{\beta_n} \right) - \tan^{-1} \left(\frac{\beta'}{\gamma_n} \right) \right), \quad (4.4.48)$$

$$\Theta = \frac{1}{\pi} \left(b \ln(d/b) + c \ln(d/c) \right), \quad (4.4.49)$$

and

$$\sigma = \arg \left(h(-i\beta') \right) = \arg \left(1 - \sum_{n=1}^{\infty} \left(\frac{A_n}{\alpha_n + i\beta'} + \frac{B_n}{\beta_n + i\beta'} \right) \right). \quad (4.4.50)$$

The condition for the existence of trapped modes, (4.4.46), reduces to

$$\beta'(a + \Theta) = \chi + \sigma + \left(n - \frac{1}{2} \right) \pi, \quad n \text{ an integer}, \quad (4.4.51)$$

where χ , Θ and σ are given by (4.4.48)-(4.4.50). Had we attempted an approximate solution for large a/d the condition would have been similar to (4.4.51), but without the σ term.

Antisymmetry about $x = 0$

For the case of antisymmetry about $x = 0$, we replace condition (4.3.1) by

$$\phi = 0 \text{ on } x = 0, \quad 0 < y < d. \quad (4.4.52)$$

The changes caused by this condition are that equations (4.4.11) and (4.4.12) become,

$$\sum_{n=1}^{\infty} U_n \left(\frac{1}{\gamma_n - \alpha_m} - \frac{\zeta_m}{\gamma_n + \alpha_m} \right) = 0, \quad m \in \mathbb{N}, \quad (4.4.53)$$

$$\sum_{n=1}^{\infty} U_n \left(\frac{1}{\gamma_n - \beta_m} - \frac{\xi_m}{\gamma_n + \beta_m} \right) = 0, \quad m \in \mathbb{N}_0. \quad (4.4.54)$$

The condition for antisymmetric modes, equivalent to (4.4.51) is,

$$\beta'(a + \Theta) = \chi + \sigma' + n\pi, \quad n \text{ an integer}, \quad (4.4.55)$$

where χ and Θ are defined earlier, and σ' is the argument of $h(-i\beta')$ with the A_n and B_n coefficients coming from

$$-A_m + C_m \sum_{n=1}^{\infty} \left(\frac{A_n}{\alpha_m + \alpha_n} + \frac{B_n}{\alpha_m + \beta_n} \right) = C_m, \quad (4.4.56)$$

$$-B_m + D_m \sum_{n=1}^{\infty} \left(\frac{A_n}{\beta_m + \alpha_n} + \frac{B_n}{\beta_m + \beta_n} \right) = D_m, \quad (4.4.57)$$

with $m \in \mathbb{N}$, in both cases.

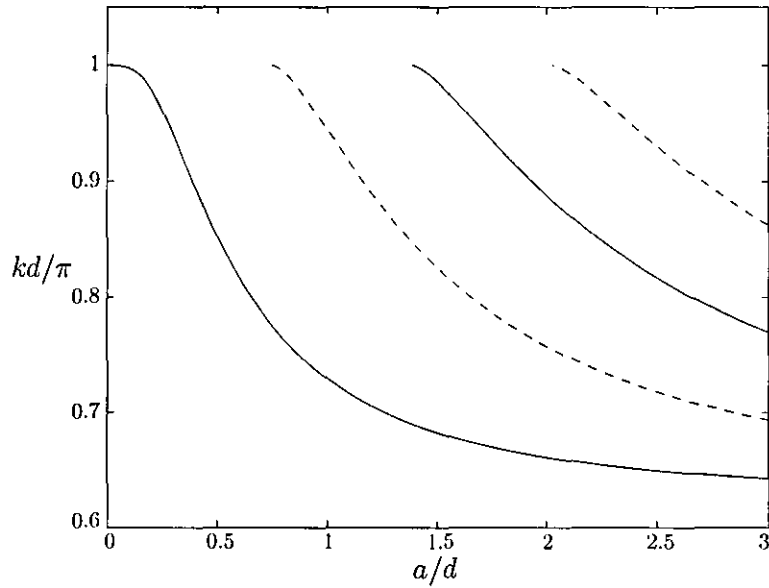


Figure 4.2: A comparison of the trapped-mode wavenumbers kd/π for modes symmetric (—) and antisymmetric (---) about $x = 0$ plotted against a/d when $b/d = 0.8$.

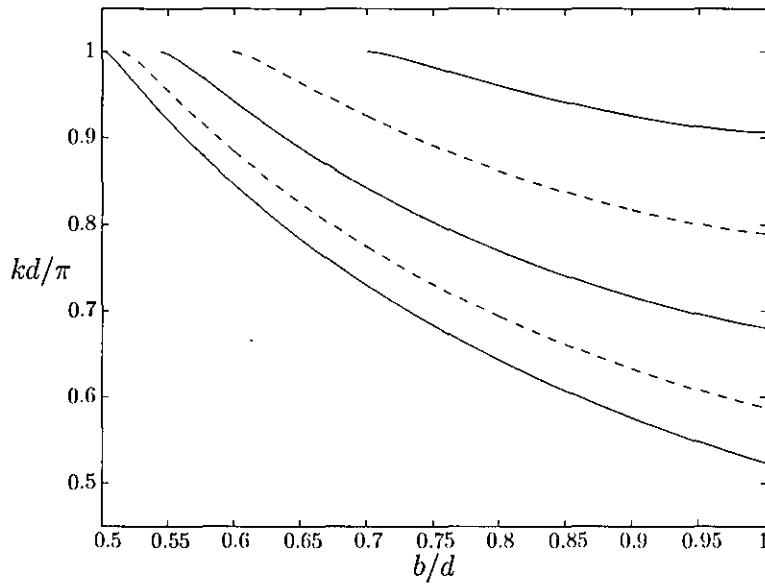


Figure 4.3: A comparison of the trapped-mode wavenumbers, kd/π , for modes symmetric (—) and antisymmetric (---) about $x = 0$ plotted against b/d when $a/d = 3$.

Results

For the results in this section the systems of equations (4.4.37)–(4.4.38) and (4.4.56)–(4.4.57) were truncated with a truncation parameter $N = 5$.

In figure 4.2 a typical set of trapped-mode wavenumbers, kd/π , are plotted against a/d when $b/d = 0.8$. The solid lines correspond to modes symmetric about $x = 0$ and

the dashed lines correspond to modes antisymmetric about $x = 0$. As a/d increases we see that the number of modes present increases and the modes appear alternatively symmetric and antisymmetric from the cut-off $kd = \pi$ and decrease towards $kd = \pi d/2b = 0.625\pi$.

The variation of trapped-mode wavenumbers, kd/π , plotted against b/d when $a/d = 3$ is shown in figure 4.3. The solid lines represent modes symmetric about $x = 0$ and the dashed lines modes antisymmetric about $x = 0$. It is clear that as b/d increases from 0.5 the number of modes present increases and also that modes exist for any off-set.

A comparison between figures 4.3 and 3.2 can be made if the axes on figure 3.2 are changed to $2kd/\pi$ and $a/2d$ (i.e. replacing d by $2d$). The right-hand end points of figure 4.3 correspond to the points when $a/2d = 1.5$ on figure 3.2.

Conclusion

In this section we have computed the frequencies of Dirichlet modes occurring below the cut-off $kd = \pi$ for the waveguide containing a thin plate located off the centreline of the guide. The Dirichlet modes satisfy the Helmholtz equation within the waveguide and are either symmetric or antisymmetric about the line through the midpoint of the plate perpendicular to the waveguide walls. The results computed show that trapped-mode frequencies can be found for any length plate and any off-set. It can be also seen that the number of modes present increases as the plate gets further away from the centreline.

4.4.2 Variational methods

Estimates of trapped-mode frequencies

In this section we follow the work in section 2.4.2 to provide estimates for the trapped-mode frequencies occurring below the cut-off $kd = \pi$ in a parallel-plate waveguide containing an off-centre plate.

Using the same notation as before, we take $\lambda < \pi^2/d^2$, place a Neumann condition on $x = 0$, and compute the eigenvalues in region *I* and *II* with Dirichlet or Neumann

conditions on $x = a$ as

$$\{\lambda_{(j)}^{I,D}\}_{j=1}^{\infty} = \left\{ \frac{(n-1/2)^2\pi^2}{a^2} + \frac{(m-1/2)^2\pi^2}{c^2} \right\}_{n,m=1}^{\infty}, \quad (4.4.58)$$

$$\{\lambda_{(j)}^{II,D}\}_{j=1}^{\infty} = \left\{ \frac{(n-1/2)^2\pi^2}{a^2} + \frac{(m-1/2)^2\pi^2}{b^2} \right\}_{n,m=1}^{\infty}, \quad (4.4.59)$$

$$\{\lambda_{(j)}^{I,N}\}_{j=1}^{\infty} = \left\{ \frac{(n-1)^2\pi^2}{a^2} + \frac{(m-1/2)^2\pi^2}{c^2} \right\}_{n,m=1}^{\infty}, \quad (4.4.60)$$

$$\{\lambda_{(j)}^{II,N}\}_{j=1}^{\infty} = \left\{ \frac{(n-1)^2\pi^2}{a^2} + \frac{(m-1/2)^2\pi^2}{b^2} \right\}_{n,m=1}^{\infty}. \quad (4.4.61)$$

There are no eigenvalues in region *III*. The only value of m to give eigenvalues below $\lambda = \pi^2/d^2$ is $m = 1$ in region *II*. As expected there are no eigenvalues in region *I* below the cut-off. Putting $m = 1$ into (4.4.59) and (4.4.61) we can produce the following inequality that holds for all j , provided $\lambda_{(j),s} < \pi^2/d^2$,

$$\frac{\pi^2}{a^2}(j-1)^2 + \frac{\pi^2}{4b^2} \leq \lambda_{(j),s} \leq \frac{\pi^2}{a^2}(j-1/2)^2 + \frac{\pi^2}{4b^2}. \quad (4.4.62)$$

Replacing the Neumann condition on $x = 0$ by a Dirichlet condition we can recalculate the eigenfunction expansions and eigenvalues and the inequality similar to (4.4.62) is

$$\frac{\pi^2}{a^2}(j-1/2)^2 + \frac{\pi^2}{4b^2} \leq \lambda_{(j),a} \leq \frac{\pi^2}{a^2}j^2 + \frac{\pi^2}{4b^2}. \quad (4.4.63)$$

Each interval of (4.4.62) and (4.4.63) whose right-end point is less than π^2/d^2 contains only one eigenvalue.

The result of superimposing these intervals onto figure 4.2 is shown in figure 4.4. Although each mode appears between two estimates, it can be seen that as a/d increases along each mode, the estimate coming from the upper bound gives a better approximation to the frequency of the trapped mode.

Proof of existence of a trapped mode

To prove the existence of a trapped mode we need the value of the right-hand side of (4.4.62) or (4.4.63) to be less than π^2/d^2 . Putting $j = 1$ into (4.4.62) and rearranging we find that a trapped mode symmetric about $x = 0$ exists provided

$$a/d > \left[4 - (d/b)^2 \right]^{-\frac{1}{2}}. \quad (4.4.64)$$

The similar condition for a single antisymmetric trapped mode is that

$$a/d > \left[1 - (d/2b)^2 \right]^{-\frac{1}{2}}. \quad (4.4.65)$$

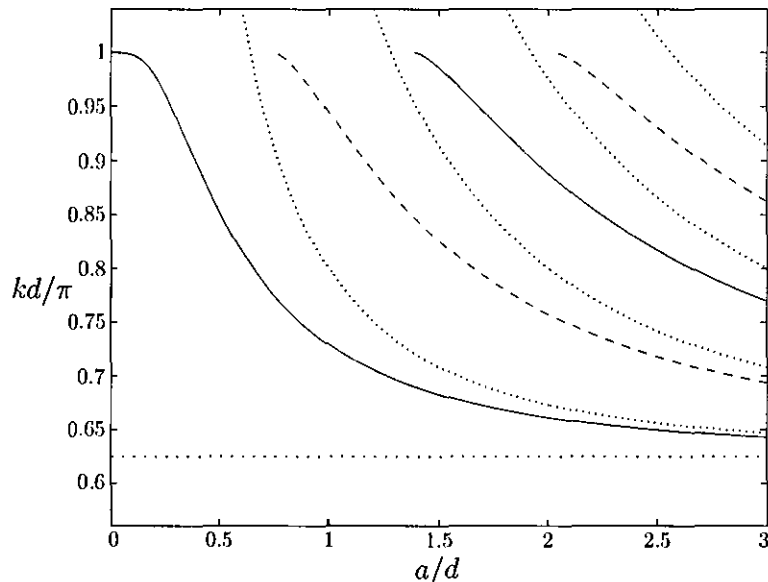


Figure 4.4: A comparison of the trapped-mode wavenumbers, kd/π , for modes symmetric and antisymmetric about $x = 0$ for the full solution, (solid) and (dashed) and the estimated intervals (dotted), plotted against a/d when $b/d = 0.8$.

As $b/d \rightarrow 1$ the value of the right-hand side of (4.4.64) tends to $1/\sqrt{3}$. For the antisymmetric case this value tends to $2/\sqrt{3}$. Both values are exactly the same as those found in the previous chapter if d is replaced by $d/2$ in the right-hand side of (4.4.64) and (4.4.65). As the plate is moved closer towards the centreline of the guide the value of both right-hand sides increases. As $b/d \rightarrow 1/2$ for both cases the required value of $a/d \rightarrow \infty$.

4.5 Trapped modes below the second cut-off

In section 4.3 we introduced a cut-off, $kd = \pi$, corresponding to the lowest point of the continuous spectrum. The cut-off was defined so that modes with frequencies below the cut-off cannot propagate to infinity. In this section we seek trapped modes whose frequencies are embedded in the continuous spectrum.

4.5.1 Formulation

In this section we restrict the frequency so that one mode can propagate in the region III and two modes propagate in the inner region $x < a$, i.e. one mode in region I and one in region II , two modes in region I and none in region II or vice versa. Only one

mode appears in the outer region if we restrict the frequency such that $kd < 2\pi$. The lower cut-off that allows two modes in the inner regions is dependent on the value of b/d . If $1/2 < b/d < 3/4$ we can restrict the frequency to $kc > \pi/2$, which allows one mode to appear below the plate and one mode to appear above the plate. If $3/4 < b/d < 1$ we can restrict the frequency to $kb > 3\pi/2$, which allows two modes to appear below the plate and none above the plate. We therefore restrict the frequency in such a way that

$$\frac{d\pi}{2c} < kd < 2\pi, \quad \text{when } 1/2 < b/d < 3/4, \quad (4.5.1)$$

$$\frac{3d\pi}{2b} < kd < 2\pi, \quad \text{when } 3/4 < b/d < 1. \quad (4.5.2)$$

Notice that trapped modes do not occur in this frequency range when $b/d = 3/4$. We define the upper value to both inequalities, $kd = 2\pi$ is the second cut-off for the problem.

The eigenfunction expansions for the three regions are

$$\phi_1(x, y) = \sum_{n=1}^{\infty} U_n^{(1)} \frac{\cosh \alpha_n x}{\alpha_n \sinh \alpha_n a} \Psi_n^{(1)}(y), \quad \alpha_n = (\nu_n^2 - k^2)^{1/2}, \quad (4.5.3)$$

$$\phi_2(x, y) = \sum_{n=0}^{\infty} U_n^{(2)} \frac{\cosh \beta_n x}{\beta_n \sinh \beta_n a} \Psi_n^{(2)}(y), \quad \beta_n = (\mu_n^2 - k^2)^{1/2}, \quad (4.5.4)$$

$$\phi_3(x, y) = \sum_{n=2}^{\infty} U_n^{(3)} \frac{e^{-\gamma_n(x-a)}}{-\gamma_n} \Psi_n^{(3)}(y), \quad \gamma_n = (\lambda_n^2 - k^2)^{1/2}, \quad (4.5.5)$$

where $\Psi_n^{(i)}(y)$, $i = 1, 2, 3$, are given by (4.3.13)–(4.3.15). These eigenfunctions are the same as (4.3.9)–(4.3.11) except the sum in region *III* starts from $n = 2$, as we set the amplitude of the mode corresponding to the imaginary γ_1 to zero.

4.5.2 Modified residue calculus method

We now formulate a solution using the modified residue calculus technique.

Following (4.4.2) to (4.4.12) we can match $\phi_i = \phi_3$ and their x -derivatives along L_i , $i = 1, 2$, convert the results into an infinite system of equations and eliminate $U_m^{(3)}$ to arrive at

$$\sum_{n=2}^{\infty} U_n \left(\frac{1}{\gamma_n - \alpha_m} + \frac{\zeta_m}{\gamma_n + \alpha_m} \right) = 0, \quad m \in \mathbb{N}, \quad (4.5.6)$$

$$\sum_{n=2}^{\infty} U_n \left(\frac{1}{\gamma_n - \beta_m} + \frac{\xi_m}{\gamma_n + \beta_m} \right) = 0, \quad m \in \mathbb{N}_0, \quad (4.5.7)$$

where U_n , ζ_m and ξ_m are given by (4.4.13). Note the only difference between (4.5.6)–(4.5.7) and (4.4.11)–(4.4.12) is the summation for U_n and V_n starts at $n = 2$ instead of $n = 1$. The edge condition (4.4.14) remains the same below the second cut-off.

We now formulate a solution by considering the following contour integrals

$$I_m = \lim_{N \rightarrow \infty} \frac{1}{2\pi i} \int_{C_N} f(z) \left(\frac{1}{z - \alpha_m} + \frac{\zeta_m}{z + \alpha_m} \right) dz \quad m \in \mathbb{N}, \quad (4.5.8)$$

$$J_m = \lim_{N \rightarrow \infty} \frac{1}{2\pi i} \int_{C_N} f(z) \left(\frac{1}{z - \beta_m} + \frac{\xi_m}{z + \beta_m} \right) dz \quad m \in \mathbb{N}_0, \quad (4.5.9)$$

where C_N is a sequence of contours on which $z \rightarrow \infty$ as $N \rightarrow \infty$ and $f(z)$ is a meromorphic function which has the following properties:

P1. $f(z)$ is an analytic function of z except for simple poles at $z = \gamma_n$, $n \geq 2$;

P2. $f(z) = O(z^{-\frac{1}{2}})$ as $|z| \rightarrow \infty$ on C_N as $N \rightarrow \infty$.

Construction of $f(z)$

The function we choose is dependent upon the value of b/d . If $1/2 < b/d < 3/4$, as in the previous section we choose

$$f(z) = \exp(z\Theta)g_1(z)h_1(z), \quad (4.5.10)$$

where Θ is defined by (4.4.49),

$$g_1(z) = (1 - z/\beta_1) \prod_{n=2}^{\infty} \frac{(1 - z/\alpha_n)(1 - z/\beta_n)}{1 - z/\gamma_n}, \quad (4.5.11)$$

and

$$h_1(z) = 1 + \sum_{n=2}^{\infty} \frac{A_n}{z - \alpha_n} + \sum_{n=1}^{\infty} \frac{B_n}{z - \beta_n}. \quad (4.5.12)$$

Similarly if $3/4 < b/d < 1$ we choose

$$f(z) = \exp(z\Theta)g_2(z)h_2(z), \quad (4.5.13)$$

where

$$g_2(z) = (1 - z/\alpha_1) \prod_{n=2}^{\infty} \frac{(1 - z/\alpha_n)(1 - z/\beta_n)}{1 - z/\gamma_n}, \quad (4.5.14)$$

and

$$h_2(z) = 1 + \sum_{n=1}^{\infty} \frac{A_n}{z - \alpha_n} + \sum_{n=2}^{\infty} \frac{B_n}{z - \beta_n}. \quad (4.5.15)$$

The functions $g_1(z)$ and $g_2(z)$ are chosen to have the correct poles to satisfy P1. The functions $h_1(z)$ and $h_2(z)$ are chosen so that the zeros of $g_1(z)$ and $g_2(z)$ at $z = \alpha_n$ and $z = \beta_n$ are cancelled by the poles of $h_1(z)$ and $h_2(z)$.

If we replace β_{n-1} by $\tilde{\beta}_n$ and B_{n-1} by \tilde{B}_n in (4.5.11) and (4.5.12), we have

$$g_1(z) = \prod_{n=2}^{\infty} \frac{(1 - z/\alpha_n)(1 - z/\tilde{\beta}_n)}{1 - z/\gamma_n}, \quad h_1(z) = 1 + \sum_{n=2}^{\infty} \frac{A_n}{z - \alpha_n} + \frac{\tilde{B}_n}{z - \tilde{\beta}_n}. \quad (4.5.16)$$

Similarly if we replace α_{n-1} by $\tilde{\alpha}_n$ and A_{n-1} by \tilde{A}_n in (4.5.14) and (4.5.15), we have

$$g_2(z) = \prod_{n=2}^{\infty} \frac{(1 - z/\tilde{\alpha}_n)(1 - z/\beta_n)}{1 - z/\gamma_n}, \quad h_2(z) = 1 + \sum_{n=2}^{\infty} \frac{\tilde{A}_n}{z - \tilde{\alpha}_n} + \frac{B_n}{z - \beta_n}. \quad (4.5.17)$$

Notice that the frequency constraints (4.5.1) and (4.5.2) lead to functions $g_1(z)$ and $g_2(z)$ which are the same order as $z \rightarrow \infty$ as that given in (4.4.18) since one factor has been removed from the numerator and the denominator. The functions given by (4.5.10) and (4.5.13) therefore satisfy P2.

Applying Cauchy's residue theorem to (4.5.8) and (4.5.9) we obtain

$$\sum_{n=2}^{\infty} R(f : \gamma_n) \left(\frac{1}{\gamma_n - \alpha_m} + \frac{\zeta_m}{\gamma_n + \alpha_m} \right) + f(\alpha_m) + \zeta_m f(-\alpha_m) = 0, \quad m \in \mathbb{N}, \quad (4.5.18)$$

$$\sum_{n=2}^{\infty} R(f : \gamma_n) \left(\frac{1}{\gamma_n - \beta_m} + \frac{\xi_m}{\gamma_n + \beta_m} \right) + f(\beta_m) + \xi_m f(-\beta_m) = 0, \quad m \in \mathbb{N}_0, \quad (4.5.19)$$

A comparison with (4.5.6) and (4.5.7) shows our solution is given by $U_n = R(f : \gamma_n)$ provided both

$$f(\alpha_m) + \zeta_m f(-\alpha_m) = 0, \quad m \in \mathbb{N}, \quad (4.5.20)$$

$$f(\beta_m) + \xi_m f(-\beta_m) = 0, \quad m \in \mathbb{N}_0. \quad (4.5.21)$$

We now formulate the trapped mode condition for the case when $1/2 < b/d < 3/4$ using the function $f(z) = g_1(z) h_1(z)$. The changes caused by using $g_2(z)$ and $h_2(z)$ will be discussed later.

In order to solve (4.5.20) and (4.5.21) the coefficients A_n and $\tilde{B}_n, n = 2, 3, \dots$, in (4.5.16) can be found from the infinite system of equations

$$A_m + C_m \sum_{n=2}^{\infty} \left(\frac{A_n}{\alpha_m + \alpha_n} + \frac{\tilde{B}_n}{\alpha_m + \tilde{\beta}_n} \right) = C_m, \quad (4.5.22)$$

$$\tilde{B}_m + D_m \sum_{n=2}^{\infty} \left(\frac{A_n}{\tilde{\beta}_m + \alpha_n} + \frac{\tilde{B}_n}{\tilde{\beta}_m + \tilde{\beta}_n} \right) = D_m, \quad (4.5.23)$$

where $m = 2, 3, \dots$, and

$$C_m = \left(\frac{2\alpha_m(\gamma_m - \alpha_m)(\tilde{\beta}_m + \alpha_m)}{(\gamma_m + \alpha_m)(\tilde{\beta}_m - \alpha_m)} \right) \exp \left(-2\alpha_m(\Theta + a) \right) \\ \times \prod_{\substack{n=2 \\ n \neq m}}^{\infty} \frac{(1 + \alpha_m/\alpha_n)(1 + \alpha_m/\tilde{\beta}_n)(1 - \alpha_m/\gamma_n)}{(1 - \alpha_m/\alpha_n)(1 - \alpha_m/\tilde{\beta}_n)(1 + \alpha_m/\gamma_n)}, \quad (4.5.24)$$

$$D_m = \left(\frac{2\tilde{\beta}_m(\gamma_m - \tilde{\beta}_m)(\alpha_m + \tilde{\beta}_m)}{(\gamma_m + \tilde{\beta}_m)(\alpha_m - \tilde{\beta}_m)} \right) \exp \left(-2\tilde{\beta}_m(\Theta + a) \right) \\ \times \prod_{\substack{n=2 \\ n \neq m}}^{\infty} \frac{(1 + \tilde{\beta}_m/\alpha_n)(1 + \tilde{\beta}_m/\tilde{\beta}_n)(1 - \tilde{\beta}_m/\gamma_n)}{(1 - \tilde{\beta}_m/\alpha_n)(1 - \tilde{\beta}_m/\tilde{\beta}_n)(1 + \tilde{\beta}_m/\gamma_n)}. \quad (4.5.25)$$

Trapped mode condition

We now have two conditions still to be satisfied simultaneously. When $1/2 < b/d < 3/4$ these conditions are (4.5.20) with $m = 1$ and (4.5.21) with $m = 0$. When $3/4 < b/d < 1$ a similar set of results to (4.5.22)–(4.5.25) can be produced with the A_n , \tilde{B}_n , α_m and $\tilde{\beta}_m$ terms replaced by \tilde{A}_n , B_n , $\tilde{\alpha}_m$ and β_m . The two conditions to be satisfied when $3/4 < b/d < 1$ are (4.5.21) with $m = 0$ and $m = 1$.

Continuing with the case of $1/2 < b/d < 3/4$, we let $\alpha_1 = -i\alpha'$, where $\alpha' = (k^2 - \nu_1^2)^{\frac{1}{2}} = (k^2 - (\pi/2c)^2)^{\frac{1}{2}}$, and $\beta_0 = -i\beta'_0$, where $\beta'_0 = (k^2 - \mu_0^2)^{\frac{1}{2}} = (k^2 - (\pi/2b)^2)^{\frac{1}{2}}$. Substituting these into (4.5.20) and (4.5.21) we have the following conditions which need to be satisfied simultaneously,

$$e^{2i\alpha'a} = -\frac{f(-i\alpha')}{f(i\alpha')}, \quad (4.5.26)$$

$$e^{2i\beta'_0a} = -\frac{f(-i\beta'_0)}{f(i\beta'_0)}. \quad (4.5.27)$$

Following the work in section 4.4.1, we find the condition for the existence of trapped modes when $1/2 < b/d < 3/4$ is that

$$\alpha'(a + \Theta) = \chi_1(\alpha') + \sigma_1(\alpha') + \left(n_1 - \frac{1}{2}\right)\pi, \quad (4.5.28)$$

$$\beta'_0(a + \Theta) = \chi_1(\beta'_0) + \sigma_1(\beta'_0) + \left(n_2 - \frac{1}{2}\right)\pi, \quad (4.5.29)$$

are both satisfied simultaneously for pairs of integers n_1 and n_2 , where we have defined

$$\chi_1(x) = \sum_{n=2}^{\infty} \left(\tan^{-1} \left(\frac{x}{\alpha_n} \right) + \tan^{-1} \left(\frac{x}{\tilde{\beta}_n} \right) - \tan^{-1} \left(\frac{x}{\gamma_n} \right) \right), \quad (4.5.30)$$

$$\sigma_1(x) = \arg(h_1(-ix)) = \arg \left(1 - \sum_{n=2}^{\infty} \left(\frac{A_n}{\alpha_n + ix} + \frac{\tilde{B}_n}{\tilde{\beta}_n + ix} \right) \right), \quad (4.5.31)$$

and Θ is given by (4.4.49).

For the case of $3/4 < b/d < 1$, we let $\beta_1 = -i\beta'_1$, where $\beta'_1 = (k^2 - \mu_1^2)^{\frac{1}{2}} = (k^2 - (3\pi/2b)^2)^{\frac{1}{2}}$ and the trapped mode condition becomes

$$\beta'_j(a + \Theta) = \chi_2(\beta'_j) + \sigma_2(\beta'_j) + \left(n_j - \frac{1}{2}\right)\pi, \quad j = 0, 1, \quad (4.5.32)$$

where n_0 and n_1 are integers and

$$\chi_2(x) = \sum_{n=2}^{\infty} \left(\tan^{-1} \left(\frac{x}{\tilde{\alpha}_n} \right) + \tan^{-1} \left(\frac{x}{\beta_n} \right) - \tan^{-1} \left(\frac{x}{\gamma_n} \right) \right), \quad (4.5.33)$$

$$\sigma_2(x) = \arg(h_2(-ix)) = \arg \left(1 - \sum_{n=2}^{\infty} \left(\frac{\tilde{A}_n}{\tilde{\alpha}_n + ix} + \frac{B_n}{\beta_n + ix} \right) \right), \quad (4.5.34)$$

For the case of antisymmetry about $x = 0$, the conditions change to

$$\alpha'(a + \Theta) = \chi_1(\alpha') + \sigma'_1(\alpha') + n_1\pi, \quad (4.5.35)$$

$$\beta'_0(a + \Theta) = \chi_1(\beta'_0) + \sigma'_1(\beta'_0) + n_2\pi, \quad (4.5.36)$$

when $1/2 < b/d < 3/4$, and

$$\beta'_j(a + \Theta) = \chi_2(\beta'_j) + \sigma'_2(\beta'_j) + n_j\pi, \quad j = 0, 1, \quad (4.5.37)$$

when $3/4 < b/d < 1$. The $\sigma'_j(x)$, $j = 1, 2$, terms are similar to those in (4.5.31) and (4.5.34) with the A_n and B_n coefficients coming from either

$$-A_m + C_m \sum_{n=2}^{\infty} \left(\frac{A_n}{\alpha_m + \alpha_n} + \frac{\tilde{B}_n}{\alpha_m + \tilde{\beta}_n} \right) = C_m, \quad (4.5.38)$$

$$-\tilde{B}_m + D_m \sum_{n=2}^{\infty} \left(\frac{A_n}{\tilde{\beta}_m + \alpha_n} + \frac{\tilde{B}_n}{\tilde{\beta}_m + \tilde{\beta}_n} \right) = D_m, \quad (4.5.39)$$

when $1/2 < b/d < 3/4$, or

$$-\tilde{A}_m + C_m \sum_{n=2}^{\infty} \left(\frac{\tilde{A}_n}{\tilde{\alpha}_m + \tilde{\alpha}_n} + \frac{B_n}{\tilde{\alpha}_m + \beta_n} \right) = C_m, \quad (4.5.40)$$

$$-B_m + D_m \sum_{n=2}^{\infty} \left(\frac{\tilde{A}_n}{\beta_m + \tilde{\alpha}_n} + \frac{B_n}{\beta_m + \beta_n} \right) = D_m, \quad (4.5.41)$$

when $3/4 < b/d < 1$, with $m = 2, 3, \dots$, in all cases.

Results

For the results presented in this section the system of equations (4.5.22)–(4.5.23) and (4.5.38)–(4.5.41) were truncated with a truncation parameter of $N = 5$.

In figure 4.5 a typical set of trapped-mode frequencies, kd/π , are plotted against a/d when $b/d = 0.6$, for which the relevant frequency range is $d\pi/2c = 1.25\pi < kd < 2\pi$. The trapped modes are the intersection of two sets of lines corresponding to the solutions of (4.5.28)–(4.5.29) and (4.5.35)–(4.5.36). A more detailed view of some of the modes in figure 4.5 are shown in figure 4.6 along with some of the corresponding values of n_1 and n_2 . In both figures the modes symmetric about $x = 0$ are represented by a cross and the modes antisymmetric about $x = 0$ are represented by a circle. It can be seen in figure 4.5 that as the plate length increases the number of modes appearing in a small a/d -interval also increases.

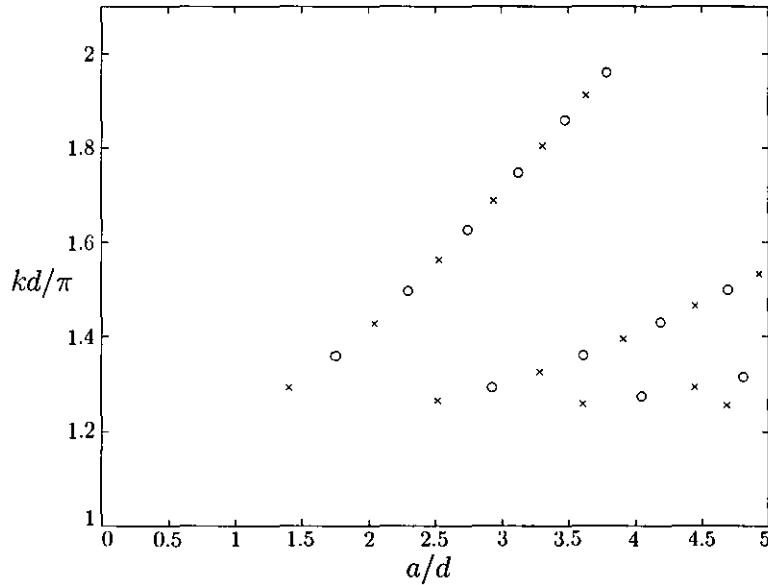


Figure 4.5: Trapped-mode wavenumbers, kd/π , for modes symmetric (\times) and antisymmetric (\circ) about $x = 0$ plotted against a/d , when $b/d = 0.6$.

The results for modes symmetric about $x = 0$ obtained by keeping the integers n_1 and n_2 , used in (4.5.28)–(4.5.29), and n_0 and n_1 , used in (4.5.32), constant and varying either kd/π in (a) or a/d in (b) against b/d are shown in figure 4.7. The vertical dotted line corresponds to the value $b/d = 3/4$. The modes to the left of this line were computed using the frequency range (4.5.1) and the modes to the right of this line were computed using the frequency range (4.5.2). The two dotted lines either side of $b/d = 0.75$ correspond to the lower cut-offs $kc = \pi/2$ for $b/d < 0.75$ and $kb = 3\pi/2$ for $b/d > 0.75$. The trapped modes generally appear when b/d is in the range $(0.5, p_1) \cup (p_2, 1)$ where $p_1 (< 3/4)$ and $p_2 (> 3/4)$ depend on the two integers chosen. If the two integers (n_1, n_2) or (n_0, n_1) are chosen in the form (N, M) with $N \gg M$ then

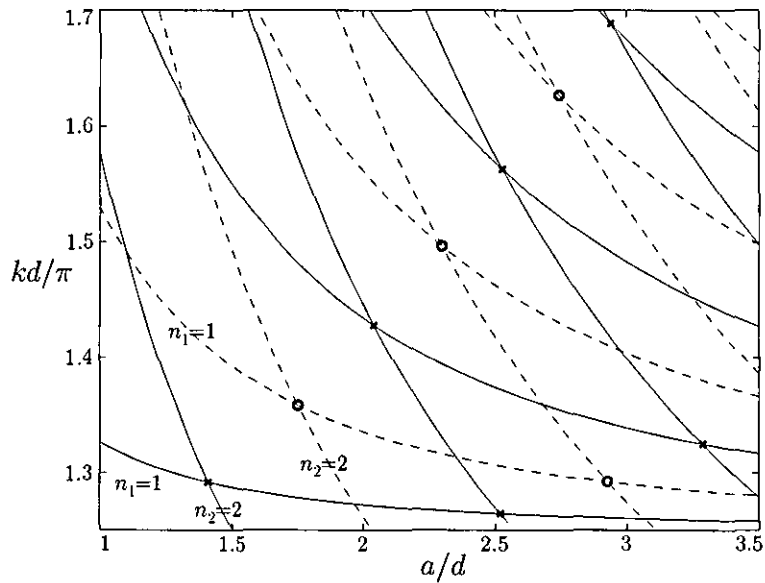


Figure 4.6: A detailed view of part of figure 4.5 showing the curves corresponding to the solutions of (4.5.28), (4.5.29), (4.5.35) and (4.5.36), along with some corresponding n_1 and n_2 values. The solid curves correspond to modes symmetric about $x = 0$ and the dashed to modes antisymmetric about $x = 0$. The embedded trapped modes, denoted by \times (symmetric) and \circ (antisymmetric), are where the solid or dashed lines cross.

$p_1 \rightarrow 3/4-$ and $p_2 \rightarrow 3/4+$, and hence trapped modes appear for all values of b/d except when $b/d = 3/4$.

From 4.7(b) we can see that trapped modes do not exist when the plate length is small. We can also see that as $b/d \rightarrow 0.5$ the corresponding values of a/d becomes large. When looking at figure 4.7(a) we see however that trapped modes do not exist when $b/d = 0.5$ and as $b/d \rightarrow 0.5$ the range of kd becomes very small.

Conclusion

In this section we have computed the frequencies of Dirichlet modes below the second cut-off for wave propagation down the guide using the modified residue calculus method. The modes found are either symmetric or antisymmetric about the line perpendicular to and through the centre of the plate.. The frequency is restricted so that two wave-like modes appear in the inner region and one mode can propagate down the guide. The range that the frequency has to be restricted to depends on the off-set of the plate

The results computed show that the trapped modes correspond to the intersection of two sets of lines, one from each of the wave-like modes in the inner region. The modes

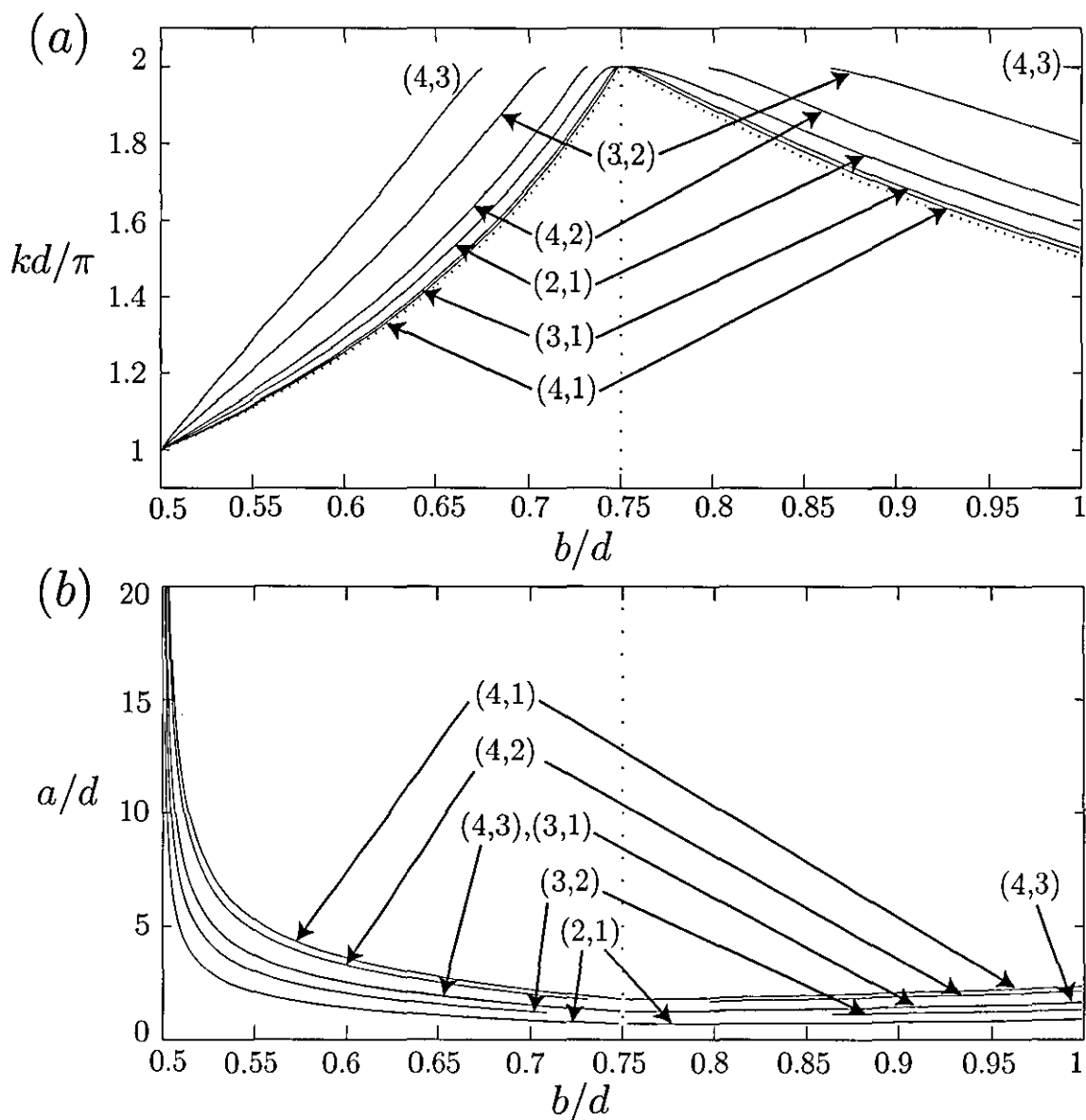


Figure 4.7: Variation of (a) kd/π and (b) a/d with b/d for modes symmetric about $x = 0$. The curves are labelled with the values of (n_1, n_2) , from (4.5.28)–(4.5.29), and (n_0, n_1) , from (4.5.32), which are used to generate them.

can appear for any off-set of the plate, except when the plate is $3/4$ of the way up the guide, but only for specific values of the plate length.

4.6 Trapped modes below the third cut-off

In the previous two sections we have found trapped modes in the ranges $\pi d/2b < kd < \pi$, and either $\pi d/2c < kd < 2\pi$, or $3\pi d/2b < kd < 2\pi$. As the trapped-mode frequencies have increased we have seen clear changes in the form of the results. The results for

frequencies between $\pi d/2b < kd < \pi$ show that trapped modes can be found for any length plate and for any off-set, so appear as continuous lines in the plots shown. When looking below the second cut-off we see that the modes can appear for any off-set, except when the plate is 3/4 of the way up the guide, but for only discrete lengths of the plate and appear as the intersection of two lines in the plots. This tends to suggest that if we look below the next cut-off, we may find trapped modes for only specific combinations of the plate length and off-set.

4.6.1 Formulation

When formulating the model, we need to restrict the frequency in such a way that the asymptotics of the function $f(z)$ used previously remain unchanged, i.e. we require one more wave-like mode in the inner region than in the outer region. As in section 4.5 the restricted frequency depends upon the value of b/d .

If $1/2 < b/d \leq 3/4$ we can restrict the frequency to

$$\frac{3d\pi}{2b} < kd < 3\pi, \quad (4.6.1)$$

and if $3/4 \leq b/d < 5/6$ we can restrict the frequency to

$$\frac{d\pi}{2c} < kd < 3\pi. \quad (4.6.2)$$

Both the frequency restrictions produce the results that $\alpha_1, \beta_0, \beta_1, \gamma_1$ and γ_2 are purely imaginary whereas all the other values of α_n, β_n and γ_n are real and positive.

When the value of b/d is between 5/6 and 1 the resulting trapped mode condition, found later, becomes inconsistent and no trapped modes can be found using the method discussed in this section. A similar occurrence happened in chapter 2 for all values of b/d .

The eigenfunction expansions in the three regions are

$$\phi_1(x, y) = \sum_{n=1}^{\infty} U_n^{(1)} \frac{\cosh \alpha_n x}{\alpha_n \sinh \alpha_n a} \Psi_n^{(1)}(y), \quad \alpha_n = (\nu_n^2 - k^2)^{1/2}, \quad (4.6.3)$$

$$\phi_2(x, y) = \sum_{n=0}^{\infty} U_n^{(2)} \frac{\cosh \beta_n x}{\beta_n \sinh \beta_n a} \Psi_n^{(2)}(y), \quad \beta_n = (\mu_n^2 - k^2)^{1/2}, \quad (4.6.4)$$

$$\phi_3(x, y) = \sum_{n=3}^{\infty} U_n^{(3)} \frac{e^{-\gamma_n(x-a)}}{-\gamma_n} \Psi_n^{(3)}(y), \quad \gamma_n = (\lambda_n^2 - k^2)^{1/2}, \quad (4.6.5)$$

where $\Psi_n^{(i)}$, $i = 1, 2, 3$ are defined previously. In this section we set the amplitudes of the modes corresponding to the imaginary γ_1 and γ_2 to zero. Following the work in section

4.5 we arrive at equations similar to (4.5.8) and (4.5.9) except that the summation now starts at $n = 3$ instead of $n = 2$. We now solve the problem using the modified residue calculus technique.

4.6.2 Modified residue calculus method

By considering the integrals shown in section 4.5.2, where the function $f(z)$ is required to have poles at $z = \gamma_n$, $n \geq 3$, we can consider the following function

$$f(z) = \exp(z\Theta)g(z)h(z), \quad (4.6.6)$$

where Θ is defined in (4.4.49),

$$g(z) = (1 - z/\alpha_2)(1 - z/\beta_2) \prod_{n=3}^{\infty} \frac{(1 - z/\alpha_n)(1 - z/\beta_n)}{1 - z/\gamma_n}, \quad (4.6.7)$$

and

$$h(z) = 1 + \sum_{n=2}^{\infty} \left(\frac{A_n}{z - \alpha_n} + \frac{B_n}{z - \beta_n} \right). \quad (4.6.8)$$

Redefining $\alpha_{n-1} = \tilde{\alpha}_n$, $\beta_{n-1} = \tilde{\beta}_n$, $A_{n-1} = \tilde{A}_n$ and $B_{n-1} = \tilde{B}_n$ we have

$$g(z) = \prod_{n=3}^{\infty} \frac{(1 - z/\tilde{\alpha}_n)(1 - z/\tilde{\beta}_n)}{1 - z/\gamma_n}, \quad h(z) = 1 + \sum_{n=3}^{\infty} \left(\frac{\tilde{A}_n}{z - \tilde{\alpha}_n} + \frac{\tilde{B}_n}{z - \tilde{\beta}_n} \right). \quad (4.6.9)$$

It is useful to notice that $g(z)$ has the same ratio of poles to zeros as (4.5.11) and can therefore be shown to have the correct behaviour as $|z| \rightarrow \infty$. The solution to the problem is given by $U_n = R(f : \gamma_n)$ provided both

$$f(\alpha_m) + \zeta_m f(-\alpha_m) = 0 \quad m \in \mathbb{N}, \quad (4.6.10)$$

$$f(\beta_m) + \xi_m f(-\beta_m) = 0 \quad m \in \mathbb{N}_0 \quad (4.6.11)$$

For $m \geq 2$, following the previous work (4.6.10) and (4.6.11) lead to an exponentially converging infinite system of real equations similar to (4.5.22) and (4.5.23).

Trapped mode condition

For the case of seeking trapped modes above the second cut-off we now have to satisfy three conditions simultaneously. These conditions are (4.6.10) with $m = 1$ and (4.6.11) with $m = 0, 1$. If we let $\alpha_1 = -i\alpha'$, where $\alpha' = (k^2 - \nu_1^2)^{\frac{1}{2}} = (k^2 - (\pi/2c)^2)^{\frac{1}{2}}$, $\beta_0 = -i\beta'_0$,

where $\beta'_0 = (k^2 - \mu_0^2)^{\frac{1}{2}} = (k^2 - (\pi/2b)^2)^{\frac{1}{2}}$ and $\beta_1 = -i\beta'_1$, where $\beta'_1 = (k^2 - \mu_1^2)^{\frac{1}{2}} = (k^2 - (3\pi/2b)^2)^{\frac{1}{2}}$ the three conditions reduce to

$$e^{2i\alpha'a} = -\frac{f(-i\alpha')}{f(i\alpha')}, \quad (4.6.12)$$

$$e^{2i\beta'_j a} = -\frac{f(-i\beta'_j)}{f(i\beta'_j)}, \quad j = 0, 1, \quad (4.6.13)$$

which need to be satisfied simultaneously. If we define

$$\chi(x) = \sum_{n=3}^{\infty} \left(\tan^{-1} \left(\frac{x}{\tilde{\alpha}_n} \right) + \tan^{-1} \left(\frac{x}{\tilde{\beta}_n} \right) - \tan^{-1} \left(\frac{x}{\tilde{\gamma}_n} \right) \right) \quad (4.6.14)$$

and

$$\sigma(x) = \arg \left(1 - \sum_{n=3}^{\infty} \left(\frac{\tilde{A}_n}{\tilde{\alpha}_n + ix} + \frac{\tilde{B}_n}{\tilde{\beta}_n + ix} \right) \right), \quad (4.6.15)$$

we find the conditions for the existence of trapped modes are that

$$\alpha'(a + \Theta) = \chi(\alpha') + \sigma(\alpha') + \left(n_1 - \frac{1}{2} \right) \pi, \quad (4.6.16)$$

$$\beta'_0(a + \Theta) = \chi(\beta'_0) + \sigma(\beta'_0) + \left(n_2 - \frac{1}{2} \right) \pi, \quad (4.6.17)$$

$$\beta'_1(a + \Theta) = \chi(\beta'_1) + \sigma(\beta'_1) + \left(n_3 - \frac{1}{2} \right) \pi, \quad (4.6.18)$$

are all satisfied simultaneously for sets of integers n_1 , n_2 and n_3 .

As $a/d \rightarrow \infty$, due to the exponential convergence of \tilde{A}_n and \tilde{B}_n , $\sigma(x)$ tends quickly to zero. In section 4.5 the trapped modes computed did not exist when the plate length was small. As will be shown later trapped modes are not found below the third cut-off when $a/d < 1$. The computed σ values below the third cut-off are hence insignificant and will be ignored from now on.

To help simplify matters we now make what turns out to be a quite accurate approximation to (4.6.16)–(4.6.18) by using a similar estimate to the earlier variational approach. If we place a Dirichlet condition on $x = a$, $0 < y < d$ and assume that the potential in region *III* is identically zero then the eigenfunctions (4.6.3)–(4.6.4) for the wave-like modes will take the form

$$\phi_1(x, y) = U_1^{(1)} \cos(n_1 - 1/2) \frac{\pi x}{a} \sin \frac{\pi(d-y)}{2c}, \quad (4.6.19)$$

$$\phi_2(x, y) = U_0^{(2)} \cos(n_2 - 1/2) \frac{\pi x}{a} \sin \frac{\pi y}{2b} + U_1^{(2)} \cos(n_3 - 1/2) \frac{\pi x}{a} \sin \frac{3\pi y}{2b}, \quad (4.6.20)$$

where n_j , $j = 1, 2, 3$ are non-negative integers. Note that these solutions would not satisfy the original equations as these solutions do not have a continuous derivative

across $x = a$. To enable the solutions (4.6.19)–(4.6.20) to satisfy the Helmholtz equation for the same frequency parameter we need

$$k^2 = (n_1 - 1/2)^2 \frac{\pi^2}{a^2} + \frac{\pi^2}{4c^2} = (n_2 - 1/2)^2 \frac{\pi^2}{a^2} + \frac{\pi^2}{4b^2} = (n_3 - 1/2)^2 \frac{\pi^2}{a^2} + \frac{9\pi^2}{4b^2}. \quad (4.6.21)$$

Rearranging these we have

$$\alpha'a = (n_1 - \frac{1}{2})\pi, \quad \beta'_0 a = (n_2 - \frac{1}{2})\pi, \quad \beta'_1 a = (n_3 - \frac{1}{2})\pi, \quad (4.6.22)$$

which are just (4.6.16)–(4.6.18) without the Θ , χ and σ terms. Eliminating k and a from (4.6.21) we have

$$\frac{(n_2 - 1/2)^2 - (n_3 - 1/2)^2}{(n_1 - 1/2)^2 - (n_2 - 1/2)^2} = \frac{8(d - b)^2}{9d^2 - 18db + 8b^2}. \quad (4.6.23)$$

Now if $1/2 < b/d < 3/4$ then the value of the right-hand side of (4.6.23) is strictly greater than one and hence a necessary condition for a right-hand side value greater than one is that

$$n_2 > n_1 > n_3 > 0. \quad (4.6.24)$$

If b/d lies in the range $(3/4, 5/6)$ this condition changes to

$$n_2 > n_3 > n_1 > 0. \quad (4.6.25)$$

If we find a set of integers that satisfy (4.6.24) or (4.6.25) we can simply find the corresponding value of b/d from (4.6.23). If this value of b/d lies within the correct range then the kd and a/d values corresponding to the off-set can quickly be found from (4.6.21).

Results

Results plotted from the full solution (4.6.16)–(4.6.18) compared to the approximate solution (4.6.22) when $a/d < 4$ are shown in figure 4.8. It is clear that a good approximation can be made by removing the Θ , χ and σ terms from (4.6.16)–(4.6.18). Another approximation can be made by placing a Neumann condition on $x = a$ and setting the outer region to zero so that the derivative of the potential is continuous but not the potential itself. The results computed for such an approximation are found not to be as good as those shown here.

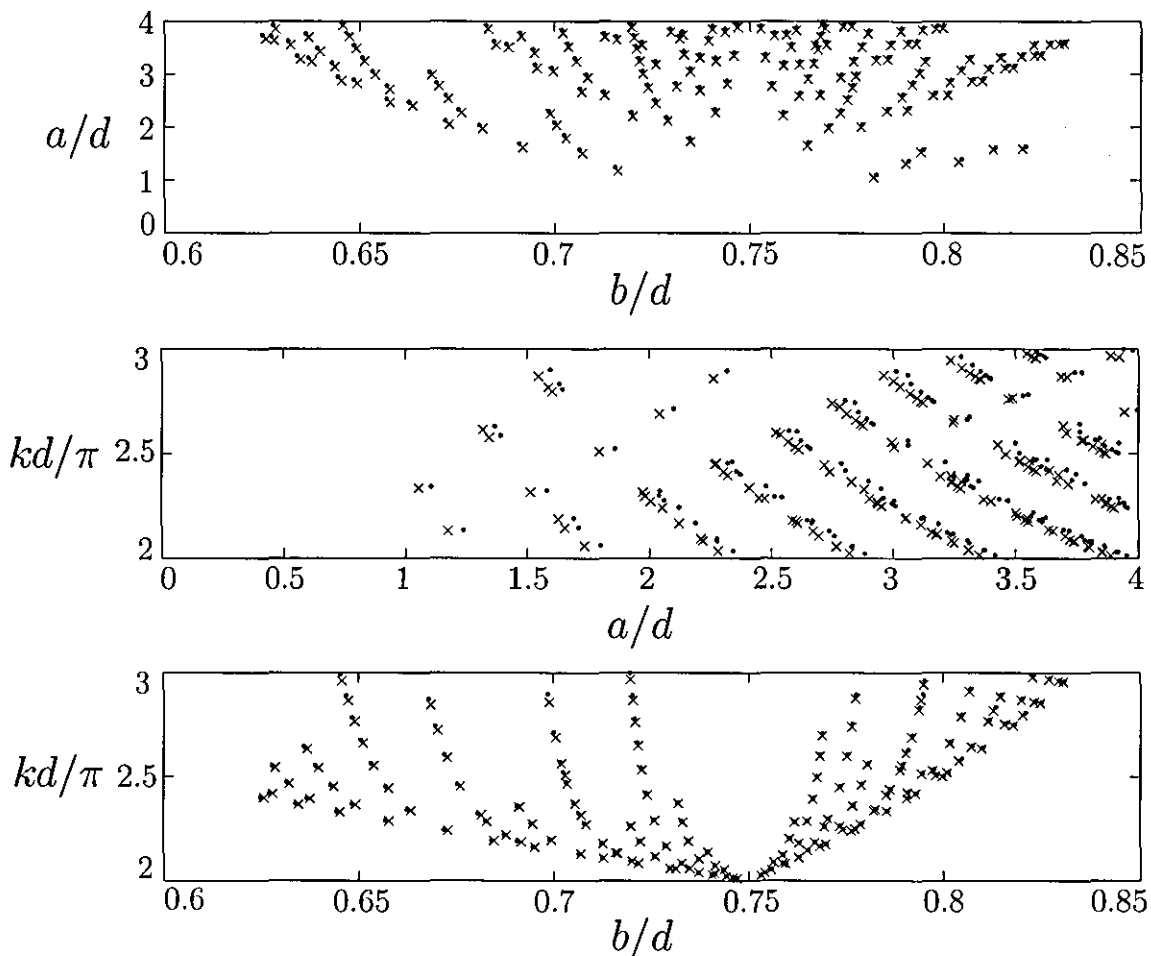


Figure 4.8: Solutions $(a/d, b/d, kd/\pi)$, with $a/d < 4$ for trapped modes symmetric about $x = 0$ below the third cut-off for an off-centre plate. The dots are results from the approximate solution (4.6.22) and the crosses from the full solution (4.6.16)–(4.6.18).

The results shown in figure 4.8 are for $a/d < 4$ and only required $n_2 \leq 12$. If results are needed for a larger value of a/d then the value of n_2 has to be increased, because kd varies between 2π and 3π and so from (4.6.17) a large value of a/d implies a large value of n_2 . If $n_2 \leq 12$ then all the trapped modes below $a/d = 4$ are found and hence the top two panels of figure 4.8 are complete, but the bottom panel contains more and more points as the value of n_2 is increased. Figure 4.9 shows the bottom panel of figure 4.8 with $n_2 \leq 50$.

Conclusion

In this section we have found trapped modes whose frequencies are below the third cut-off for the problem of an off-centre plate using a modified residue calculus method. The

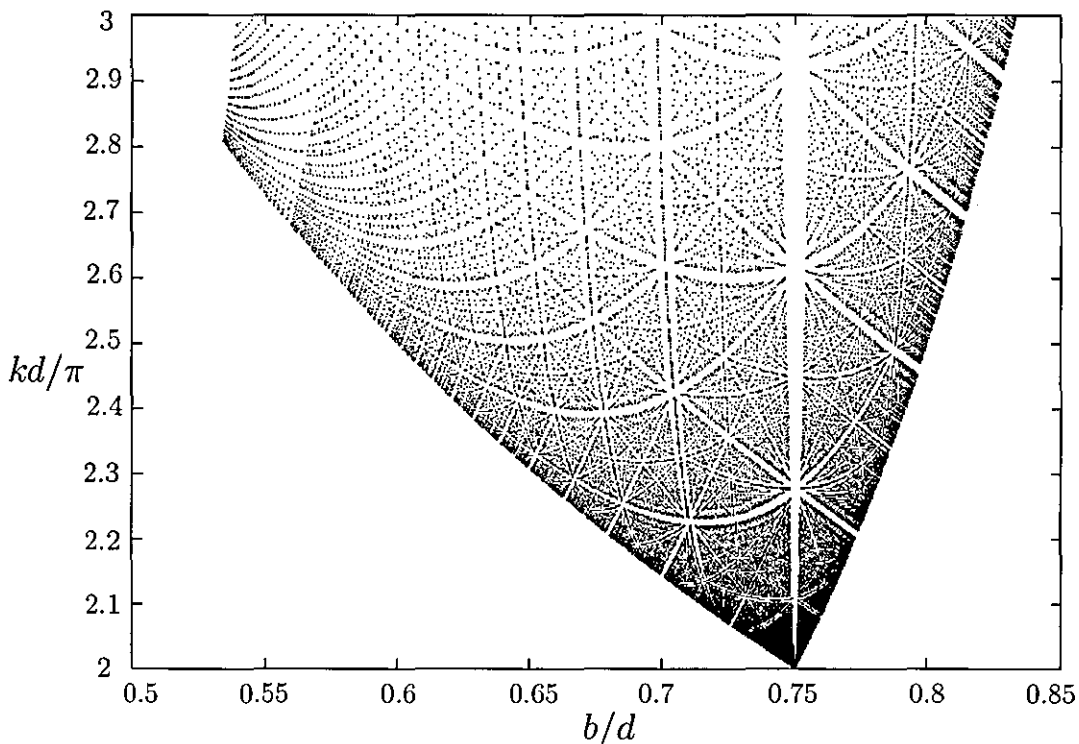


Figure 4.9: Results from the approximate solution (4.6.22) for modes symmetric about $x = 0$, with $n_2 \leq 50$.

third cut-off is defined as the frequency below which only two wave-like modes appear in the region outside the plate.

The modes computed are symmetric about the line perpendicular to and through the centre of the plate. The frequency restriction depends on the off-set of the plate and modes were only found when the plate was below five-sixths of the way up the guide. Below the third cut-off three wave-like modes appear local to the plates and the modes correspond to the solution of three conditions which have to be solved simultaneously. To simplify matters an approximation to the three conditions, coming from a similar idea to the variational methods, is given allowing simple computation of the modes.

As expected from the discussion in section 4.2 the results show that the modes appear only for specific combinations of the off-set and plate length.

4.7 Summary

In this chapter we have investigated the occurrence of Dirichlet modes in a parallel-plate waveguide containing a thin off centre plate. The modes were found in various frequency bands each defined by an upper cut-off which restricted the amount of modes in the region outside the plate. The geometry of the problem was defined by two parameters corresponding to the off-set of the plate and the length of the plate.

In section 4.4 trapped modes were found below the first cut-off using a modified residue calculus method and estimates to the frequencies were given using a variational method. We were also able to prove the existence of a single trapped mode using the variational method for a sufficiently long plate. The results plotted show that trapped modes occur for any off-set and for any plate length.

Trapped modes below the second cut-off were found in section 4.5 using a modified residue calculus. The results showed that trapped modes can occur for any off-set except when the plate was three-quarters of the way up the guide, but only for specific plate lengths. Below the third cut-off trapped modes were found using a modified residue calculus method and the results showed that the modes occurred for specific combinations of the plate length and the off-set.

Figure 4.10 shows a comparison of the three lowest frequency modes below each cut-off. The mode below the first cut-off appears as a plane, the mode below the second cut-off appears as a line and the mode below the third cut-off appears as a point.

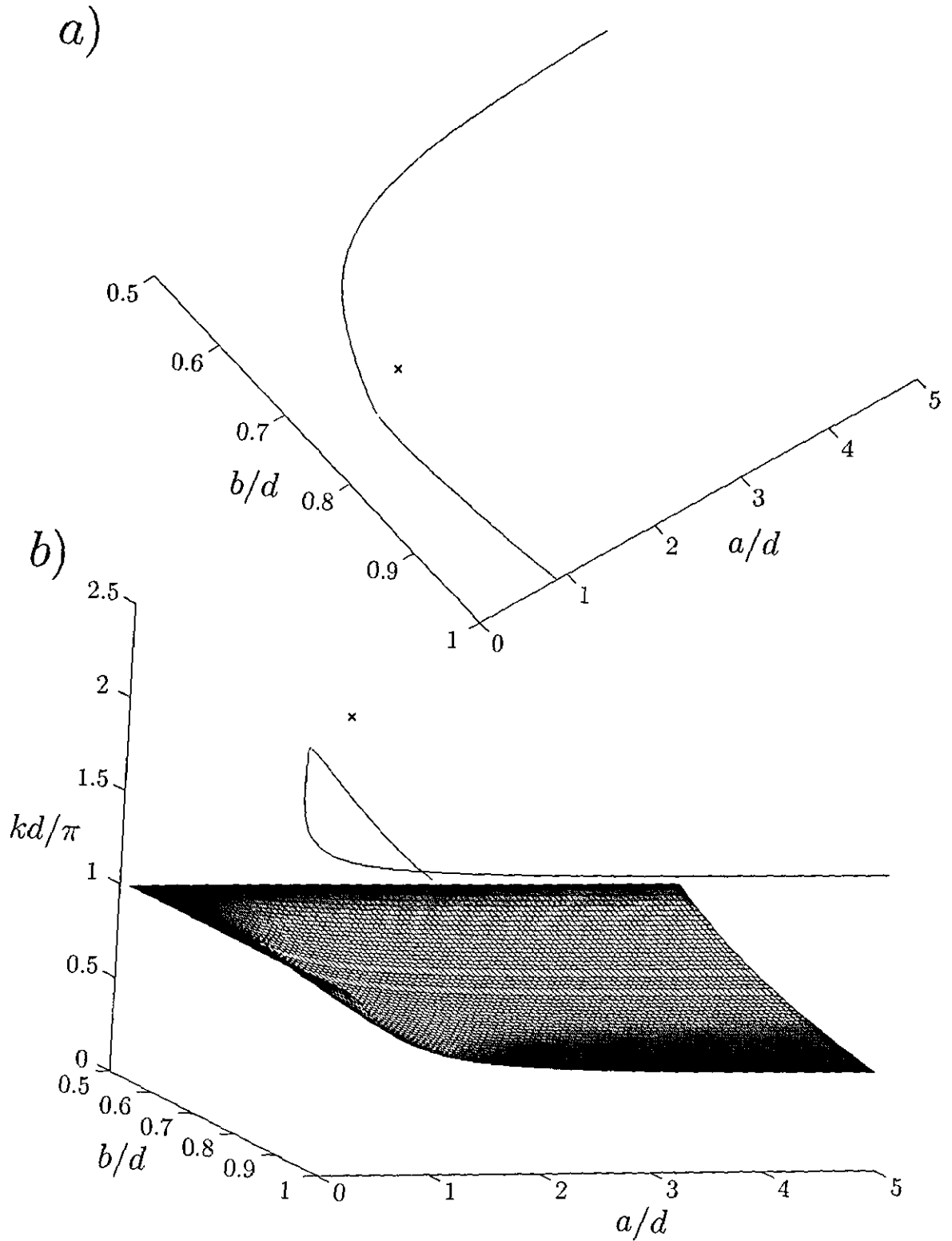


Figure 4.10: A comparison of the three lowest frequency modes in the various cut-off regions. Figure (a) is a plan view of figure (b).

Chapter 5

Two-dimensional array of parallel plates containing finite gaps

5.1 Introduction to the problem

In this chapter we seek a different type of trapped mode to those considered previously. The trapped modes sought in this chapter travel along an array of identical obstacles and decay away from the obstacles. We seek trapped modes (or as defined later Rayleigh-Bloch waves) in a two dimensional array of parallel plates, with each plate containing an equal length finite gap. We place Dirichlet boundary conditions on each plate and set up the array so that the plates are an equal distance apart and the line of symmetry passes through the centre-point of each gap. The trapped modes sought travel through the row of gaps and decay down the plates.

The chapter is presented in the following manner. In section 5.2 we review previous work concerning the occurrence of trapped modes near an array of identical obstacles. We formulate the problem in section 5.3 and see that the problem is characterised by two non-dimensional parameters corresponding to the length of the gap compared to the width between the plates and the propagation or Bloch constant compared to the width between the plates (defined later a/d and $\beta'd$ respectively). We also introduce the first cut-off of the problem in this section. The cut-off, which depends on the propagation constant, is defined so that modes with frequencies below the cut-off cannot propagate to infinity.

In section 5.4 we seek trapped modes below the first cut-off using a modified residue calculus method. Below the first cut-off we see that the problem contains only one

wave-like mode which travels through the gaps in the plates. The results show that the trapped modes occur for any length plate and any value of the propagation constant.

We seek trapped modes whose frequencies are above the first cut-off and below the second cut-off in section 5.5. The second cut-off is defined as the frequency below which only one mode can propagate to infinity along the plates. In this section we use a modified residue calculus technique and set the amplitude of the propagating mode to zero. We find that the problem has two wave-like modes in the gaps and the solution corresponds to the intersection of two sets of lines. The trapped modes are found for any value of the propagation constant but only for specific values of the gap length.

As the problem is specified by two parameters, as in the previous chapter, we seek trapped modes above the second cut-off and below the third cut-off in section 5.6. In this section we restrict the frequency so that two propagating modes and three wave-like modes appear in the problem. As in the previous chapter we use a very accurate approximation to provide a solution to the full problem. The solutions are found to be the intersection of three sets of lines and appear as specific combinations of the two parameters in $(a/d, \beta'd)$ space.

A summary of the chapter is provided in section 5.7.

5.2 Background

The investigations into trapped modes occurring locally to an array of equivalent structures periodic in one dimension has been vast. This is due to the problem having many relevant applications in the fields of acoustics, water waves, optics and electromagnetism.

The first example of a trapped mode in such a geometry was found by Stokes (1846), who constructed a non-trivial solution describing a water-wave travelling along a uniform sloping beach which decays exponentially out to sea. Such waves have since been named edge waves. In the electromagnetic theory of diffraction gratings these edge waves are known as Rayleigh-Bloch waves and are characterised by a dominant wavenumber of motion, β' , along the array. A general discussion of the electromagnetic theory of gratings is given in Petit (1980), with a more mathematical approach in Wilcox (1984). We shall refer to the trapped modes appearing in this chapter as Rayleigh-Bloch waves to distinguish them from the trapped modes occurring in waveguides with parallel walls.

An area of research of great interest from an acoustical point of view is that of a duct

containing a series of equally spaced thin parallel plates. As discussed earlier the acoustic resonances found by Parker (1966) and (1967) were local to a similar duct. Later work by Franklin (1972) used a method involving Green functions and an approximation based on a variational formulation to calculate the acoustic resonances occurring in the same problem. Later Koch (1983) used a Wiener-Hopf technique to compute the resonant acoustic frequencies for the modes found by Parker. The author also presented results for the staggered cascade and when the mean flow was non-zero. The acoustic scattering from an array of parallel Neumann plates was considered by Linton and Evans (1993) using a similar residue calculus method to the one we use in this chapter.

In the context of water waves Evans and Linton (1993) proved the existence of Rayleigh-Bloch waves travelling along a periodic coastline consisting of a straight and vertical cliff face from which protrudes an infinite number of sufficiently long identical thin barriers, each extending throughout the water depth. The depth dependence can be separated out and the problem is reduced to the solution of the two-dimensional Helmholtz equation with Neumann conditions on all boundaries. The proof uses the modified residue calculus method, similar to problems investigated in this part of the thesis.

In a later paper Evans and Fernyhough (1995) extended the problem and provided numerical evidence for the existence of Rayleigh-Bloch waves when the barriers were rectangular blocks. Neumann conditions were placed on the blocks and the method of solution is based on a Galerkin approximation to an integral representation of the problem. Rayleigh-Bloch waves have also been found local to arrays of circular cylinders, but this will be discussed in greater depth in chapter 7.

Porter and Evans (2002) have recently provided numerical results for Rayleigh-Bloch waves occurring above the first cut-off along periodic rectangular arrays. Neumann conditions were placed on the rectangles and embedded Rayleigh-Bloch waves were found using a similar method to that in Evans and Fernyhough (1995). In the paper the authors also gave strong numerical evidence for the existence of Rayleigh-Bloch waves occurring above the second cut-off for a single family of rectangular cross-section.

Rayleigh-Bloch waves were also recently found along arrays of parallel Neumann plates above the first cut-off for wave propagation down the guide by Evans and Porter (2002). Using a similar method to that used by Linton and Evans (1993) the authors were able to prove the existence of solutions for sufficiently long plates.

There is no general existence proof for Rayleigh-Bloch waves, i.e. no result equivalent to that given by Evans, Levitin, and Vassiliev (1994), although if an array of thin finite-length Dirichlet obstacles are considered Bonnet-Bendhia and Starling (1994) proved that Rayleigh-Bloch waves do not occur.

5.3 Formulation

We consider the case of an array of parallel thin plates of equal widths d apart situated so that the x -axis lies along one of the plates. Each plate contains an equal length finite gap located between $x = -a$ and $x = a$, as shown in figure 5.1. The plates therefore occupy $|x| > a, y = md, m = 0, \pm 1 \dots$. The symmetry of the problem allows any solution to be expressed as the sum of solutions which are either symmetric or antisymmetric about the y -axis. We begin by looking for a solution symmetric about $x = 0$, by considering the region $x > 0$ and seeking a non-trivial solution $\phi(x, y)$ which satisfies

$$(\nabla^2 + k^2)\phi = 0, \quad x > 0 \text{ except on } |x| > a, y = md, m \text{ an integer}, \quad (5.3.1)$$

subject to the symmetry condition

$$\frac{\partial \phi}{\partial x} = 0 \text{ on } x = 0, \quad (5.3.2)$$

Dirichlet boundary conditions on the plates

$$\phi = 0 \text{ on } y = md, x > a, m \text{ an integer}, \quad (5.3.3)$$

and a condition which requires the solution to decay down the plates

$$\phi \rightarrow 0 \text{ as } x \rightarrow \infty. \quad (5.3.4)$$

The radiation condition (5.3.4) again comes from the idea that Rayleigh-Bloch waves possess finite energy down the plates. We finally assume that ϕ is non-singular and

$$\nabla \phi = O(r^{-\frac{1}{2}}) \text{ as } r \equiv \{(x - a)^2 + (y - md)^2\}^{\frac{1}{2}} \rightarrow 0, m \text{ an integer}, \quad (5.3.5)$$

anticipating singular behaviour in the velocity field at the plates edges.

We now make use of the periodicity of the plates d , by assuming that a potential at $y + d$ can only differ from a potential at y by a shift in phase, denoted by the multiplicative factor $e^{i\beta'd}$, where $\beta'd$ is some real parameter. This technique is commonly

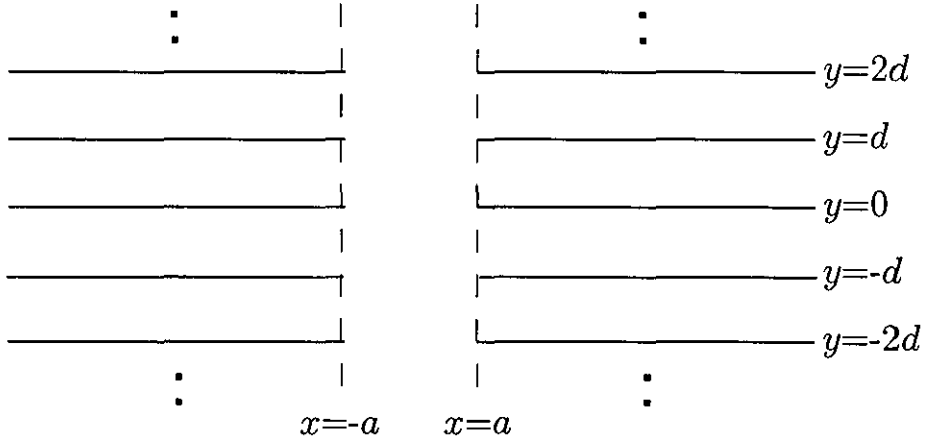


Figure 5.1: Definition sketch

used for arrays of structures, with periodicity in one dimension only, see for example Evans and Linton (1993). The parameter β' is sometimes known as the propagation or Bloch constant. Using this definition the total potential may be written

$$\phi(x, y + md) = e^{im\beta'd} \phi(x, y) \quad m \in \mathbb{Z}. \quad (5.3.6)$$

For $0 < y < d$ (5.3.6) is satisfied by

$$\phi(x, y) = e^{i\beta'y} \psi(x, y) \quad (5.3.7)$$

where $\psi(x, y)$ and its derivative with respect to y , are periodic in y with period d . We now only need to consider the region $0 < y < d$, as equation (5.3.6) provides an extension of the solution outside this region.

It is now useful to split the domain $0 < y < d$ into two regions. Region *I* is the area not containing the plates, i.e. $0 < x < a$, $0 < y < d$, and region *II* is the remainder, $x > a$, $0 < y < d$. We can represent the function ϕ by a function ϕ_i ($i = 1, 2$) in each region, with the following continuity conditions applied at each regions boundary,

$$\phi_1 = \phi_2, \quad \frac{\partial \phi_1}{\partial x} = \frac{\partial \phi_2}{\partial x}, \quad \text{on } x = a, \quad 0 < y < d. \quad (5.3.8)$$

Separation of variables reveals that

$$\phi_1(x, y) = \sum_{n=-\infty}^{\infty} U_n^{(1)} \frac{\cosh \alpha_n x}{\alpha_n \sinh \alpha_n a} e^{i\beta_n y}, \quad \alpha_n = (\beta_n^2 - k^2)^{1/2}, \quad (5.3.9)$$

$$\phi_2(x, y) = \sum_{n=1}^{\infty} U_n^{(2)} \frac{e^{-\gamma_n(x-a)}}{-\gamma_n} \sin \lambda_n y, \quad \gamma_n = (\lambda_n^2 - k^2)^{1/2}, \quad (5.3.10)$$

where

$$\beta_n = \beta' + \frac{2n\pi}{d}, \quad \text{and} \quad \lambda_n = \frac{n\pi}{d}. \quad (5.3.11)$$

Without loss of generality we assume that

$$0 \leq \beta'd < 2\pi. \quad (5.3.12)$$

When $\beta'd = 0$ the problem reduces to the Neumann case of a thin finite length plate placed on the centreline of a two-dimensional parallel-plate waveguide, as in Evans (1992). Note that the functions $e^{i\beta_n y}$ satisfy the orthogonality condition

$$\frac{1}{d} \int_0^d e^{iy(\beta_n - \beta_m)} dy = \delta_{mn}, \quad (5.3.13)$$

where δ_{mn} is the Kronecker delta.

The condition that prevents waves propagating to infinity is that γ_n is real and positive for all $n \in \mathbb{N}$. The first cut-off for this problem is therefore $kd = \pi$, and in the next section we seek Rayleigh-Bloch waves whose frequencies are below this cut-off.

5.4 Rayleigh-Bloch waves below the first cut-off

In this section we seek Rayleigh-Bloch waves whose frequencies are below the first cut-off $kd = \pi$. With this restriction of frequency we find that α_n , $|n| \in \mathbb{N}$, are all real and positive, and so the only possible wave-like mode that can appear in the problem is the one corresponding to α_0 . We require α_0 to be purely imaginary for it to be wave-like in region I and so $k > \beta'$. We therefore anticipate that a necessary condition for the existence of Rayleigh-Bloch waves is

$$\beta'd < kd < \pi. \quad (5.4.1)$$

Notice that although we vary $\beta'd \in [0, 2\pi)$ with this restriction we expect modes to exist only if $\beta'd \in [0, \pi)$. We now formulate a solution using the modified residue calculus technique discussed in previous chapters.

5.4.1 Modified residue calculus method

Using (5.3.8) we match $\phi_1 = \phi_2$ and $\partial\phi_1/\partial x = \partial\phi_2/\partial x$ along $x = a$, $0 < y < d$ and obtain

$$\sum_{n=-\infty}^{\infty} U_n^{(1)} \frac{\coth \alpha_n a}{\alpha_n} e^{i\beta_n y} = \sum_{n=1}^{\infty} U_n^{(2)} \frac{\sin \lambda_n y}{-\gamma_n}, \quad (5.4.2)$$

$$\sum_{n=-\infty}^{\infty} U_n^{(1)} e^{i\beta_n y} = \sum_{n=1}^{\infty} U_n^{(2)} \sin \lambda_n y. \quad (5.4.3)$$

If we multiply (5.4.2) and (5.4.3) by $e^{-i\beta_m y}$, $m \in \mathbb{Z}$, integrate over $0 < y < d$, and use (5.3.13), we have

$$\frac{U_m^{(1)} \coth \alpha_m a}{\alpha_m} = \sum_{n=1}^{\infty} \frac{U_n^{(2)}}{-\gamma_n} d_{nm}, \quad (5.4.4)$$

$$U_m^{(1)} = \sum_{n=1}^{\infty} U_n^{(2)} d_{nm}, \quad (5.4.5)$$

where we have defined

$$d_{nm} = \frac{1}{d} \int_0^d \sin \lambda_n y e^{-i\beta_m y} dy, \quad m \in \mathbb{Z}. \quad (5.4.6)$$

Evaluating the integral d_{nm} , we find

$$d_{nm} = \frac{1}{2di} \int_0^d (e^{i\lambda_n y} - e^{-i\lambda_n y}) e^{-i\beta_m y} dy = \frac{\lambda_n (1 - e^{-i\beta'} (-1)^n)}{d(\gamma_n^2 - \alpha_m^2)}, \quad (5.4.7)$$

provided $\gamma_n \neq \alpha_m$, where $n \in \mathbb{N}$, $m \in \mathbb{Z}$ and (5.3.11) has been used.

Eliminating $U_m^{(1)}$ from (5.4.4) and (5.4.5) we find after some rearrangement that

$$\sum_{n=1}^{\infty} U_n \left(\frac{1}{\gamma_n - \alpha_m} + \frac{\zeta_m}{\gamma_n + \alpha_m} \right) = 0, \quad m \in \mathbb{Z}, \quad (5.4.8)$$

where we have defined

$$U_n = \frac{U_n^{(2)} \lambda_n (1 - e^{-i\beta'} (-1)^n)}{\gamma_n}, \quad \text{and} \quad \zeta_m = e^{-2\alpha_m a}. \quad (5.4.9)$$

To ensure that the edge condition (5.3.5) is satisfied by $\phi_2(x, y)$, we also require

$$U_n = O(n^{-\frac{1}{2}}) \text{ as } n \rightarrow \infty. \quad (5.4.10)$$

We now consider the integrals

$$I_m = \lim_{N \rightarrow \infty} \frac{1}{2\pi i} \int_{C_N} f(z) \left(\frac{1}{z - \alpha_m} + \frac{\zeta_m}{z + \alpha_m} \right) dz, \quad m \in \mathbb{Z}, \quad (5.4.11)$$

where C_N is a sequence of contours on which $z \rightarrow \infty$ as $N \rightarrow \infty$ and $f(z)$ is a meromorphic function which has the following properties:

P1. $f(z)$ is an analytic function of z except for simple poles at $z = \gamma_n$, $n \in \mathbb{N}$.

P2. $f(z) = O(z^{-\frac{1}{2}})$ as $|z| \rightarrow \infty$ on C_N as $N \rightarrow \infty$.

Construction of $f(z)$

Following the work in previous sections we would like to choose a function of the form

$$f(z) = g(z)h(z), \quad (5.4.12)$$

where

$$g(z) = \prod_{n=1}^{\infty} \frac{(1 - z/\alpha_n)(1 - z/\alpha_{-n})}{(1 - z/\gamma_n)}, \quad h(z) = 1 + \sum_{\substack{n=-\infty \\ n \neq 0}}^{\infty} \frac{A_n}{z - \alpha_n}. \quad (5.4.13)$$

The function $f(z)$ is chosen to have the correct poles to satisfy P1 and the function $h(z)$ is chosen so that the zeros of $g(z)$ at $z = \alpha_n$ and $z = \alpha_{-n}$ are cancelled by the poles of $h(z)$ at these points.

To satisfy P2 we need to obtain the behaviour of $g(z)$ as $|z| \rightarrow \infty$. We obtain this behaviour by firstly considering the following product

$$g(z) = \prod_{n=1}^{\infty} \frac{1 - z/\alpha_n}{1 - z/\beta_n} \prod_{n=1}^{\infty} \frac{1 - z/\alpha_{-n}}{1 - z/\beta_{-n}} \prod_{n=1}^{\infty} \frac{1 - z/\lambda_n}{1 - z/\gamma_n} \prod_{n=1}^{\infty} \frac{(1 - z/\beta_n)(1 - z/\beta_{-n})}{(1 - z/\lambda_n)}. \quad (5.4.14)$$

Following section 2.4.1 we have

$$\prod_{n=1}^{\infty} \frac{1 - z/\alpha_{\pm n}}{1 - z/\beta_{\pm n}} = \prod_{n=1}^{\infty} \left(1 - \frac{k^2}{\beta_{\pm n}^2}\right)^{-\frac{1}{2}} \prod_{n=1}^{\infty} \left(1 + \frac{k^2}{(z - \beta_{\pm n})(\beta_{\pm n} + \alpha_{\pm n})}\right), \quad (5.4.15)$$

and

$$\prod_{n=1}^{\infty} \frac{1 - z/\lambda_n}{1 - z/\gamma_n} = \prod_{n=1}^{\infty} \left(1 - \frac{k^2}{\lambda_n^2}\right)^{\frac{1}{2}} \prod_{n=1}^{\infty} \left(1 - \frac{k^2}{(z - \gamma_n)(\gamma_n + \lambda_n)}\right). \quad (5.4.16)$$

As all the terms $\beta_{\pm n}$ and γ_n , $n \in \mathbb{N}$, are of the form $An + O(n^{-1})$ as $n \rightarrow \infty$, with A a constant, a comparison between the final products in (5.4.15) and (5.4.16), and $\sum_{n=1}^{\infty} n^{-2}$, shows that (5.4.15) and (5.4.16) are uniformly convergent on any compact set excluding $z = \gamma_n$ and $z = \beta_{\pm n}$. Thus provided $z \rightarrow \infty$ through a sequence of values which avoids these points we have

$$g(z) \sim \frac{\alpha_0 \sin \beta' d}{\beta'} \left(\frac{2 \sin kd}{kd(\cos kd - \cos \beta' d)} \right)^{\frac{1}{2}} \prod_{n=1}^{\infty} \frac{(1 - z/\beta_n)(1 - z/\beta_{-n})}{(1 - z/\lambda_n)}, \quad (5.4.17)$$

where Gradshteyn and Ryzhik (1980) eqn 1.432(1) has been used. Expanding (5.4.17) using (2.4.43) we can show that

$$\prod_{n=1}^{\infty} \frac{(1 - z/\beta_n)(1 - z/\beta_{-n}) e^{zd/n\pi}}{(1 - z/\lambda_n) e^{zd/n\pi}} = \frac{e^{\gamma z d/2\pi} \Gamma(1)}{\Gamma(1 - zd/2\pi)} \frac{e^{\gamma z d/2\pi} \Gamma(1)}{\Gamma(1 - zd/2\pi)} \frac{\Gamma(1 - zd/\pi)}{e^{\gamma z d/\pi} \Gamma(1)}. \quad (5.4.18)$$

Using (2.4.45) we see that as $z \rightarrow \infty, z \neq |z|$,

$$\prod_{n=1}^{\infty} \frac{(1 - z/\beta_n)(1 - z/\beta_{-n})}{(1 - z/\lambda_n)} \sim (-z)^{-\frac{1}{2}} \left(\frac{\alpha_0^2 \sin^2 \beta' d \sin kd}{k(\beta' d)^2 (\cos kd - \cos \beta' d)} \right)^{\frac{1}{2}} \exp \left\{ -\frac{zd}{\pi} \ln 2 \right\}. \quad (5.4.19)$$

For the case when z is real and positive we use the reflection properties of the Gamma function, see (2.4.48), and the asymptotic behaviour can be shown to be

$$\prod_{n=1}^{\infty} \frac{(1 - z/\beta_n)(1 - z/\beta_{-n})}{(1 - z/\lambda_n)} \sim \frac{z^{-\frac{1}{2}} \sin^2 zd/2}{\sin zd} \times \left(\frac{\alpha_0^2 \sin^2 \beta' d \sin kd}{k(\beta' d)^2 (\cos kd - \cos \beta' d)} \right)^{\frac{1}{2}} \exp \left\{ -\frac{zd}{\pi} \ln 2 \right\}, \quad (5.4.20)$$

as $z \rightarrow \infty, z \neq -|z|$. If we choose C_N to be a sequence of circles with centre at the origin and radius $R_N = (N + 1/4)\pi$ then using (5.4.19) and (5.4.20) we can consider the function

$$g(z) = \exp \left\{ \frac{zd}{\pi} \ln 2 \right\} \prod_{n=1}^{\infty} \frac{(1 - z/\alpha_n)(1 - z/\alpha_{-n})}{(1 - z/\gamma_n)}, \quad (5.4.21)$$

which is $O(z^{-\frac{1}{2}})$ as $|z| \rightarrow \infty$ on C_N as $N \rightarrow \infty$ and hence P2 is satisfied.

Applying Cauchy's residue theorem to (5.4.11) we obtain

$$\sum_{n=1}^{\infty} R(f : \gamma_n) \left(\frac{1}{\gamma_n - \alpha_m} + \frac{\zeta_m}{\gamma_n + \alpha_m} \right) + f(\alpha_m) + \zeta_m f(-\alpha_m) = 0, \quad m \in \mathbb{Z}. \quad (5.4.22)$$

A comparison with (5.4.8) shows our solution is given by $U_n = R(f : \gamma_n)$ provided

$$f(\alpha_m) + \zeta_m f(-\alpha_m) = 0, \quad m \in \mathbb{Z}. \quad (5.4.23)$$

For $|m| \in \mathbb{N}$, these equation can be solved by an appropriate choice of the coefficients A_n . We have for $|m| \in \mathbb{N}$,

$$f(\alpha_m) = -\exp \left\{ \frac{\alpha_m d}{\pi} \ln 2 \right\} \left(\frac{A_m}{\alpha_m (1 - \alpha_m/\gamma_m)} \right) \prod_{\substack{n=-\infty \\ n \neq 0, m}}^{\infty} (1 - \alpha_m/\alpha_n) \prod_{\substack{n=1 \\ n \neq m}}^{\infty} \frac{1}{1 - \alpha_m/\gamma_n}, \quad (5.4.24)$$

and

$$f(-\alpha_m) = \left(1 - \sum_{\substack{n=-\infty \\ n \neq 0}}^{\infty} \frac{A_n}{\alpha_m + \alpha_n} \right) \exp \left\{ \frac{-\alpha_m d}{\pi} \ln 2 \right\} \times \left(\frac{2}{(1 + \alpha_m/\gamma_m)} \right) \prod_{\substack{n=-\infty \\ n \neq 0, m}}^{\infty} (1 + \alpha_m/\alpha_n) \prod_{\substack{n=1 \\ n \neq m}}^{\infty} \frac{1}{1 + \alpha_m/\gamma_n}. \quad (5.4.25)$$

Substituting (5.4.24) and (5.4.25) into (5.4.23) and rearranging we find

$$A_m + B_m \sum_{\substack{n=-\infty \\ n \neq 0}}^{\infty} \frac{A_n}{\alpha_m + \alpha_n} = B_m \quad |m| \in \mathbb{N}, \quad (5.4.26)$$

where

$$B_m = \left(\frac{2\alpha_m(\gamma_m - \alpha_m)}{(\gamma_m + \alpha_m)} \right) \exp \left\{ \frac{-2\alpha_m}{\pi} (d \ln 2 + a\pi) \right\} \\ \times \prod_{\substack{n=-\infty \\ n \neq 0, m}}^{\infty} \frac{(1 + \alpha_m/\alpha_n)}{(1 - \alpha_m/\alpha_n)} \prod_{\substack{n=1 \\ n \neq m}}^{\infty} \frac{(1 - \alpha_m/\gamma_n)}{(1 + \alpha_m/\gamma_n)}. \quad (5.4.27)$$

Because of the presence of the rapidly decaying factor ζ_m in equation (5.4.27) for B_m , the system of equations (5.4.26) converge very quickly provided a/d is sufficiently large and provide a very efficient method for computing the unknowns A_m .

To satisfy the edge condition, U_n must satisfy the condition given by (5.4.10). Earlier we have shown that $U_m = R(f : \gamma_m)$ and hence

$$U_m = -\gamma_m \left(1 + \sum_{\substack{n=-\infty \\ n \neq 0}}^{\infty} \frac{A_n}{\gamma_m - \alpha_n} \right) \exp \left\{ \frac{\gamma_m d}{\pi} \ln 2 \right\} \\ \times \prod_{n=1}^{\infty} (1 - \gamma_m/\alpha_n)(1 - \gamma_m/\alpha_{-n}) / \prod_{\substack{n=1 \\ n \neq m}}^{\infty} (1 - \gamma_m/\gamma_n). \quad (5.4.28)$$

Using (5.4.14) we can expand this to

$$U_m = -\gamma_m \left(1 - \frac{\gamma_m d}{m\pi} \right) \left(1 + \sum_{\substack{n=-\infty \\ n \neq 0}}^{\infty} \frac{A_n}{\gamma_m - \alpha_n} \right) \exp \left\{ \frac{\gamma_m d}{\pi} \ln 2 \right\} \\ \times \prod_{n=1}^{\infty} \frac{(1 - \gamma_m/\alpha_n)(1 - \gamma_m/\alpha_{-n})}{(1 - \gamma_m/(\beta' + 2n\pi/d))(1 - \gamma_m/(\beta' - 2n\pi/d))} \\ \times \prod_{\substack{n=1 \\ n \neq m}}^{\infty} \frac{(1 - \gamma_m d/n\pi)}{(1 - \gamma_m/\gamma_n)} \prod_{n=1}^{\infty} \frac{(1 - \gamma_m/\beta_n)(1 - \gamma_m/\beta_{-n})}{(1 - \gamma_m/\lambda_n)}. \quad (5.4.29)$$

The first two infinite products can be rearranged in the form shown in (5.4.15) and (3.4.17) and hence are $O(1)$ as $m \rightarrow \infty$. From (5.4.20) we have

$$\exp \left\{ \frac{\gamma_m d}{\pi} \ln 2 \right\} \prod_{n=1}^{\infty} \frac{(1 - \gamma_m/\beta_n)(1 - \gamma_m/\beta_{-n})}{(1 - \gamma_m/\lambda_n)} \\ \sim C \sin^2(\gamma_m d/2) \operatorname{cosec} \left(m\pi - \frac{(kd)^2}{m\pi} + O(m^{-2}) \right) \left(\frac{m\pi}{d} \right)^{-\frac{1}{2}} \left(1 + O(m^{-2}) \right), \\ \sim \frac{C\pi^{1/2} \sin^2(\gamma_m d/2)}{k^2 d^{3/2}} m^{\frac{1}{2}} + \left(1 + O(m^{-1}) \right), \quad (5.4.30)$$

as $m \rightarrow \infty$, where

$$C = \left(\frac{\alpha_0^2 \sin^2 \beta' d \sin kd}{k(\beta' d)^2 (\cos kd - \cos \beta' d)} \right)^{\frac{1}{2}}, \quad (5.4.31)$$

and we have used

$$\gamma_m \sim \frac{m\pi}{d} - \frac{k^2 d}{2m\pi} + O(m^{-2}), \quad (5.4.32)$$

as $m \rightarrow \infty$.

As $m \rightarrow \infty$ we also have

$$\left(1 - \frac{\gamma_m d}{m\pi}\right) \sim \frac{1}{2} \left(\frac{kd}{m\pi}\right)^2 + O(m^{-3}). \quad (5.4.33)$$

Using (5.4.30)-(5.4.33) we can see that U_n is $O(n^{-\frac{1}{2}})$ as $n \rightarrow \infty$, which is the required asymptotics to take account of the expected singularity in the velocity field near the plate edge.

Rayleigh-Bloch wave condition

We can now return to the one condition still to be satisfied, namely (5.4.23) with $m = 0$.

If we let $\alpha_0 = -i\alpha'$, where $\alpha' = (k^2 - (\beta')^2)^{\frac{1}{2}}$, this condition reduces to

$$e^{2i\alpha'a} = -\frac{f(-i\alpha')}{f(i\alpha')}. \quad (5.4.34)$$

Using (5.4.13) we have

$$\frac{g(-i\alpha')}{g(i\alpha')} = e^{2i(\chi - \alpha'\Theta)}, \quad \frac{h(-i\alpha'_m)}{h(i\alpha'_m)} = e^{2i\sigma}, \quad (5.4.35)$$

where we have defined

$$\chi = \sum_{n=1}^{\infty} \left(\tan^{-1} \left(\frac{\alpha'}{\alpha_n} \right) + \tan^{-1} \left(\frac{\alpha'}{\alpha_{-n}} \right) - \tan^{-1} \left(\frac{\alpha'}{\gamma_n} \right) \right), \quad (5.4.36)$$

$$\Theta = \frac{d}{\pi} \ln 2, \quad (5.4.37)$$

and

$$\sigma = \arg \left(1 - \sum_{\substack{n=-\infty \\ n \neq 0}}^{\infty} \frac{A_n}{\alpha_n + i\alpha'} \right). \quad (5.4.38)$$

The condition for the existence of Rayleigh-Bloch waves, (5.4.34), reduces to

$$\alpha'(a + \Theta) = \chi + \sigma + \left(n - \frac{1}{2}\right)\pi, \quad n \text{ an integer}, \quad (5.4.39)$$

where χ , Θ and σ are given by (5.4.36), (5.4.37) and (5.4.38).

Antisymmetry about $x = 0$

For the case of antisymmetry about $x = 0$ the boundary condition (5.3.2) is replaced by

$$\phi = 0 \text{ on } x = 0, \quad 0 < y < d. \quad (5.4.40)$$

The condition for antisymmetric Rayleigh-Bloch waves, equivalent to (5.4.39), is

$$\alpha'(a + \Theta) = \chi + \sigma' + n\pi, \quad n \text{ an integer}, \quad (5.4.41)$$

where χ and Θ are defined by (5.4.36) and (5.4.37) and σ' is the argument of $h(-i\alpha')$ with the A_n coefficients coming from

$$-A_m + B_m \sum_{\substack{n=-\infty \\ n \neq 0}}^{\infty} \frac{A_n}{\alpha_m + \alpha_n} = B_m, \quad |m| \in \mathbb{N}. \quad (5.4.42)$$

Results

For the results produced in this section the systems of equations (5.4.26) and (5.4.42) are truncated with a truncation parameter of 5, i.e. 5 negative and 5 positive terms are used.

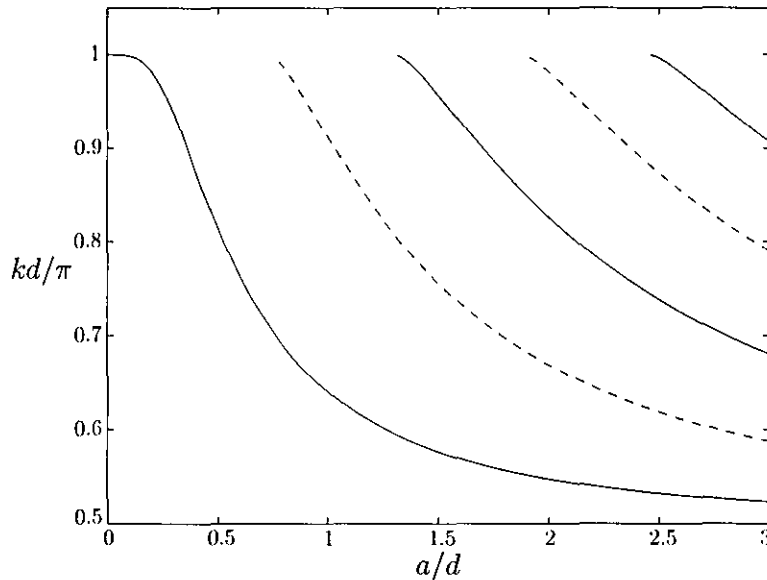


Figure 5.2: A comparison of the Rayleigh-Bloch wave wavenumbers for waves symmetric (—) and antisymmetric (---) about $x = 0$ plotted against a/d when $\beta'd = \pi/2$.

In figure 5.2 a typical set of trapped-mode wavenumbers, kd/π , are plotted against a/d when $\beta'd = \pi/2$. The solid lines correspond to waves symmetric about $x = 0$ and

the dashed lines correspond to waves antisymmetric about $x = 0$. We see that as a/d increases the number of waves increases as they appear alternatively symmetric and antisymmetric from the cut-off $kd = \pi$ and decrease towards $kd = \beta'd = \pi/2$.

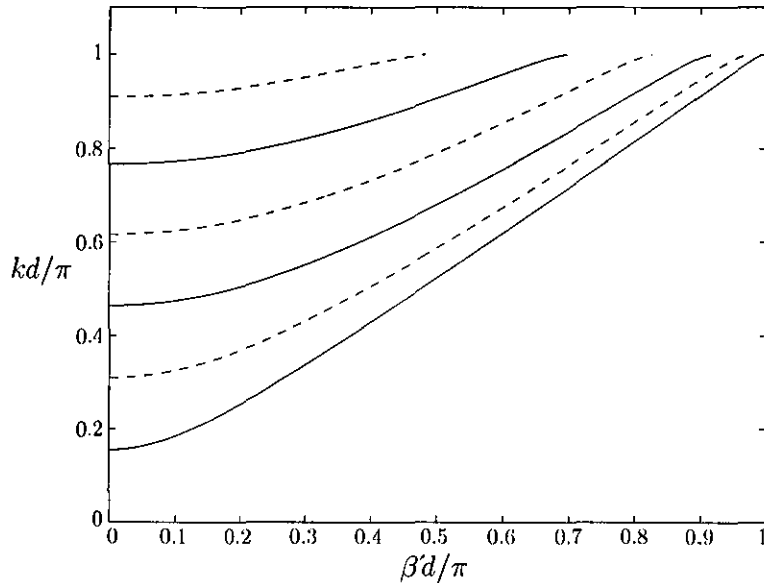


Figure 5.3: A comparison of the Rayleigh-Bloch wave wavenumbers for waves symmetric (—) and antisymmetric (---) about $x = 0$ plotted against $\beta'd/\pi$ when $a/d = 3.0$.

The variation of Rayleigh-Bloch wave wavenumbers, kd/π , plotted against $\beta'd/\pi$ when $a/d = 3$ is shown in figure 5.3. The solid lines represent waves symmetric about $x = 0$ and the dashed lines waves antisymmetric about $x = 0$. It is clear that as $\beta'd/\pi$ increases from zero the number of waves present decreases, but waves appear for all values of the propagation constant. The frequencies on the left-hand side of figure 5.3 correspond to the modes found when the Neumann problem of a thin finite plate on the centreline is considered.

Conclusion

In this section we have used the modified residue calculus method to compute the frequencies of Rayleigh-Bloch waves occurring below the cut-off $kd = \pi$ for the case of an array of equally spaced thin plates, each containing a finite length gap of the same size. The plates are aligned in such a way that the line of symmetry perpendicular to the plates cuts across the midpoint of each gap. The waves satisfy the Helmholtz equation within the fluid and Dirichlet conditions on the plates. The Rayleigh-Bloch

waves travel along the row of gaps and are characterised by a propagation constant β' , where $0 \leq \beta' d < 2\pi$.

The Rayleigh-Bloch waves appear either alternatively symmetric and antisymmetric about the line through the mid-point of the gaps. The results plotted show that Rayleigh-Bloch waves are present for any length gap and for any propagation constant in the range $0 \leq \beta' d < \pi$.

5.5 Rayleigh-Bloch waves below the second cut-off

In this section we seek Rayleigh-Bloch waves whose frequencies are above the first cut-off $kd = \pi$. As in previous chapters we restrict the frequency in such a way that there are two wave-like modes in the inner region containing the gap and one propagating mode in the outer region containing the plates and use a modified residue calculus technique.

5.5.1 Formulation

We set up the problem with the same geometry as shown in figure 5.1, and again seek non-trivial solutions to the Helmholtz equations subject to the boundary conditions (5.3.3)–(5.3.5). To ensure that only one propagating mode appears in the problem we need to restrict the frequency so that $kd < 2\pi$. The frequency $kd = 2\pi$ is the second cut-off of the problem. With this restriction γ_1 is purely imaginary whereas γ_n , $n \geq 2$ are all real and positive. To produce two wave-like modes in the inner region we need $kd > |\beta' d - 2\pi| = 2\pi - \beta' d$, as then α_0 and α_{-1} will be purely imaginary and all the other values of α_n will be real and positive. We anticipate that a natural condition for the existence of Rayleigh-Bloch waves is

$$\pi < 2\pi - \beta' d < kd < 2\pi, \quad (5.5.1)$$

as with this restriction two wave-like modes exist in the gap between two sets of adjacent parallel plates in the array. The reason why this works is that we can now use a function similar to that used in section 5.4, with one factor removed from the top and bottom of the product, and hence the product retains the required asymptotics for large z . Following section 5.3 we can construct the following eigenfunction expansions in regions

I and *II*.

$$\phi_1(x, y) = \sum_{n=-\infty}^{\infty} U_n^{(1)} \frac{\cosh \alpha_n x}{\alpha_n \sinh \alpha_n a} e^{i\beta_n y}, \quad \alpha_n = (\beta_n^2 - k^2)^{1/2}, \quad (5.5.2)$$

$$\phi_2(x, y) = \sum_{n=2}^{\infty} U_n^{(2)} \frac{e^{-\gamma_n(x-a)}}{-\gamma_n} \sin \lambda_n y, \quad \gamma_n = (\lambda_n^2 - k^2)^{1/2}. \quad (5.5.3)$$

Notice that the summation in region *II* starts from $n = 2$ as we set the amplitude of the wave-like mode corresponding to the imaginary γ_1 to zero.

We now formulate a solution using the modified residue calculus method.

5.5.2 Modified residue calculus method

Following (5.4.2) to (5.4.8) we can match the two eigenfunction expansions and their x -derivatives along $x = a$, convert the results into an infinite set of equations and eliminate one set of unknowns to arrive at

$$\sum_{n=2}^{\infty} U_n \left(\frac{1}{\gamma_n - \alpha_m} + \frac{\zeta_m}{\gamma_n + \alpha_m} \right) = 0, \quad m \in \mathbb{Z}, \quad (5.5.4)$$

where U_n and ζ_m as defined as in (5.4.9). The edge condition (5.4.10) remains the same above the first-cut off.

We now consider the integrals

$$I_m = \lim_{N \rightarrow \infty} \frac{1}{2\pi i} \int_{C_N} f(z) \left(\frac{1}{z - \alpha_m} + \frac{\zeta_m}{z + \alpha_m} \right) dz, \quad m \in \mathbb{Z}, \quad (5.5.5)$$

where C_N is a sequence of contours on which $z \rightarrow \infty$ as $N \rightarrow \infty$ and $f(z)$ is a meromorphic function which has the following properties:

P1. $f(z)$ is an analytic function of z except for simple poles at $z = \gamma_n$, $n \geq 2$.

P2. $f(z) = O(z^{-\frac{1}{2}})$ as $|z| \rightarrow \infty$ on C_N as $N \rightarrow \infty$.

Construction of $f(z)$

As in the previous section we choose

$$f(z) = \exp(z\Theta)g(z)h(z), \quad (5.5.6)$$

where Θ is defined in (5.4.37) and

$$g(z) = (1 - z/\alpha_1) \prod_{n=2}^{\infty} \frac{(1 - z/\alpha_n)(1 - z/\alpha_{-n})}{(1 - z/\gamma_n)}, \quad h(z) = 1 + \sum_{\substack{n=-\infty \\ n \neq 0, -1}}^{\infty} \frac{A_n}{z - \alpha_n}. \quad (5.5.7)$$

As the function $g(z)$ is the same as (5.4.13), with one term removed from the top and bottom, the asymptotics for large z remain the same and so P2 is satisfied.

Applying Cauchy's residue theorem to (5.5.5) we obtain

$$\sum_{n=2}^{\infty} R(f : \gamma_n) \left(\frac{1}{\gamma_n - \alpha_m} + \frac{\zeta_m}{\gamma_n + \alpha_m} \right) + f(\alpha_m) + \zeta_m f(-\alpha_m) = 0, \quad m \in \mathbb{Z}. \quad (5.5.8)$$

A comparison with (5.5.4) shows our solution is given by $U_n = R(f : \gamma_n)$ provided

$$f(\alpha_m) + \zeta_m f(-\alpha_m) = 0, \quad m \in \mathbb{Z}. \quad (5.5.9)$$

In order to solve (5.5.9) the coefficients A_n , $n = 1, \pm 2, \dots$, can be found from the infinite system of equations

$$A_m + B_m \sum_{\substack{n=-\infty \\ n \neq 0, -1}}^{\infty} \frac{A_n}{\alpha_m + \alpha_n} = B_m, \quad m = 1, \pm 2, \dots, \quad (5.5.10)$$

where

$$B_m = \left(\frac{2\alpha_m(\gamma_m - \alpha_m)}{(\gamma_m + \alpha_m)} \right) \exp \left(-2\alpha_m(\Theta + a) \right) \times \prod_{\substack{n=-\infty \\ n \neq 0, -1, m}}^{\infty} \frac{(1 + \alpha_m/\alpha_n)}{(1 - \alpha_m/\alpha_n)} \prod_{\substack{n=2 \\ n \neq m}}^{\infty} \frac{(1 - \alpha_m/\gamma_n)}{(1 + \alpha_m/\gamma_n)}. \quad (5.5.11)$$

Rayleigh-Bloch wave condition

We now have two conditions to be satisfied simultaneously, namely (5.5.9) with $m = 0$ and $m = -1$. If we let $\alpha_0 = -i\alpha'_0$, where $\alpha'_0 = (k^2 - (\beta')^2)^{\frac{1}{2}}$ and $\alpha_{-1} = -i\alpha'_{-1}$, where $\alpha'_{-1} = (k^2 - \beta_{-1}^2)^{\frac{1}{2}}$, these conditions reduce to

$$e^{2i\alpha'_j a} = -\frac{f(-i\alpha'_j)}{f(i\alpha'_j)}, \quad j = -1, 0. \quad (5.5.12)$$

Following the work in section 5.4 we find that the condition for the existence of Rayleigh-Bloch waves is that

$$\alpha'_j(a + \Theta) = \chi_j + \sigma_j + \left(n_j - \frac{1}{2}\right)\pi, \quad j = -1, 0, \quad (5.5.13)$$

are satisfied simultaneously, where Θ is given by (5.4.37), n_0 and n_{-1} are integers,

$$\chi_j = \tan^{-1} \left(\frac{\alpha'_j}{\alpha_1} \right) + \sum_{n=2}^{\infty} \left(\tan^{-1} \left(\frac{\alpha'_j}{\alpha_n} \right) + \tan^{-1} \left(\frac{\alpha'_j}{\alpha_{-n}} \right) - \tan^{-1} \left(\frac{\alpha'_j}{\gamma_n} \right) \right), \quad (5.5.14)$$

and

$$\sigma_j = \arg \left(1 - \sum_{\substack{n=-\infty \\ n \neq 0, -1}}^{\infty} \frac{A_n}{\alpha_n + i\alpha'_j} \right). \quad (5.5.15)$$

For the case of antisymmetry about $x = 0$ the conditions change to

$$\alpha'_j(a + \Theta) = \chi_j + \sigma'_j + n_j\pi, \quad j = -1, 0, \quad (5.5.16)$$

where σ'_j are the arguments of $h(-i\alpha'_j)$ with the A_n coefficients coming from

$$-A_m + B_m \sum_{\substack{n=-\infty \\ n \neq 0}}^{\infty} \frac{A_n}{\alpha_m + \alpha_n} = B_m, \quad m = 1, \pm 2, \dots, \quad (5.5.17)$$

and the χ_j and Θ are as defined earlier.

Results

The results in this section are computed with the infinite systems of equations (5.5.10) and (5.5.17) truncated with the parameter $N = 5$. In figure 5.4 Rayleigh-Bloch wave wavenumbers, kd/π , are plotted against a/d when $\beta'd = \pi/2$, for which the relevant frequency range is $3/2 < kd/\pi < 2$. The waves symmetric about $x = 0$ are denoted by a cross and the waves antisymmetric about $x = 0$ are denoted by a circle. It can be seen that for this value of $\beta'd$, no waves appear when the gap length is sufficiently small.

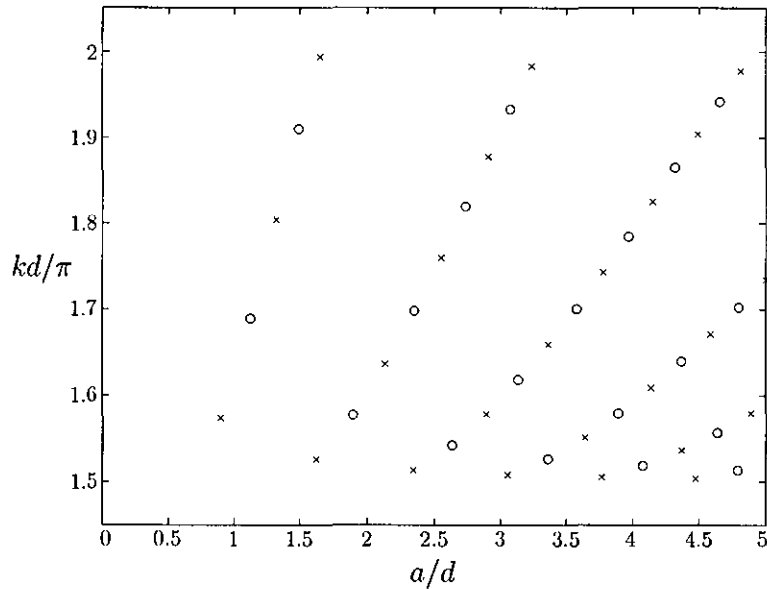


Figure 5.4: Rayleigh-Bloch wave wavenumbers, kd/π , for waves symmetric (\times) and antisymmetric (\circ) about $x = 0$ plotted against a/d , when $\beta'd = \pi/2$.

In figure 5.5 the waves symmetric about $x = 0$ obtained from keeping the integers n_0 and n_{-1} constant and varying (a) kd/π and (b) a/d with $\beta'd/\pi$ are shown. The dotted line in figure 5.5(a) corresponds to the lower cut-off $kd = 2\pi - \beta'd$. Only a selection of

the waves are shown along with the values of n_0 and n_{-1} . It can be seen from (a) that for certain combinations of the two integers waves do not occur for all values of $\beta'd$ in the range $(0, \pi)$. However if we fix $n_{-1} \in \mathbb{N}$, then as n_0 is increased the interval of $\beta'd$ for which the solutions exist does tend to $(0, \pi)$. Following a similar pattern to previous chapters we have from (5.5.13) that large n_0 implies large a/d . Using figure 5.5(b) we find that Rayleigh-Bloch waves do not exist when the value of a/d is below about 0.65. As $\beta'd$ is increased from zero the value of a/d also increases for each mode. As $\beta'd \rightarrow \pi$ we see from figure 5.5(b) that the value of a/d becomes large for each mode, but figure 5.5(a) shows that Rayleigh-Bloch waves do not exist when $\beta'd = \pi$.

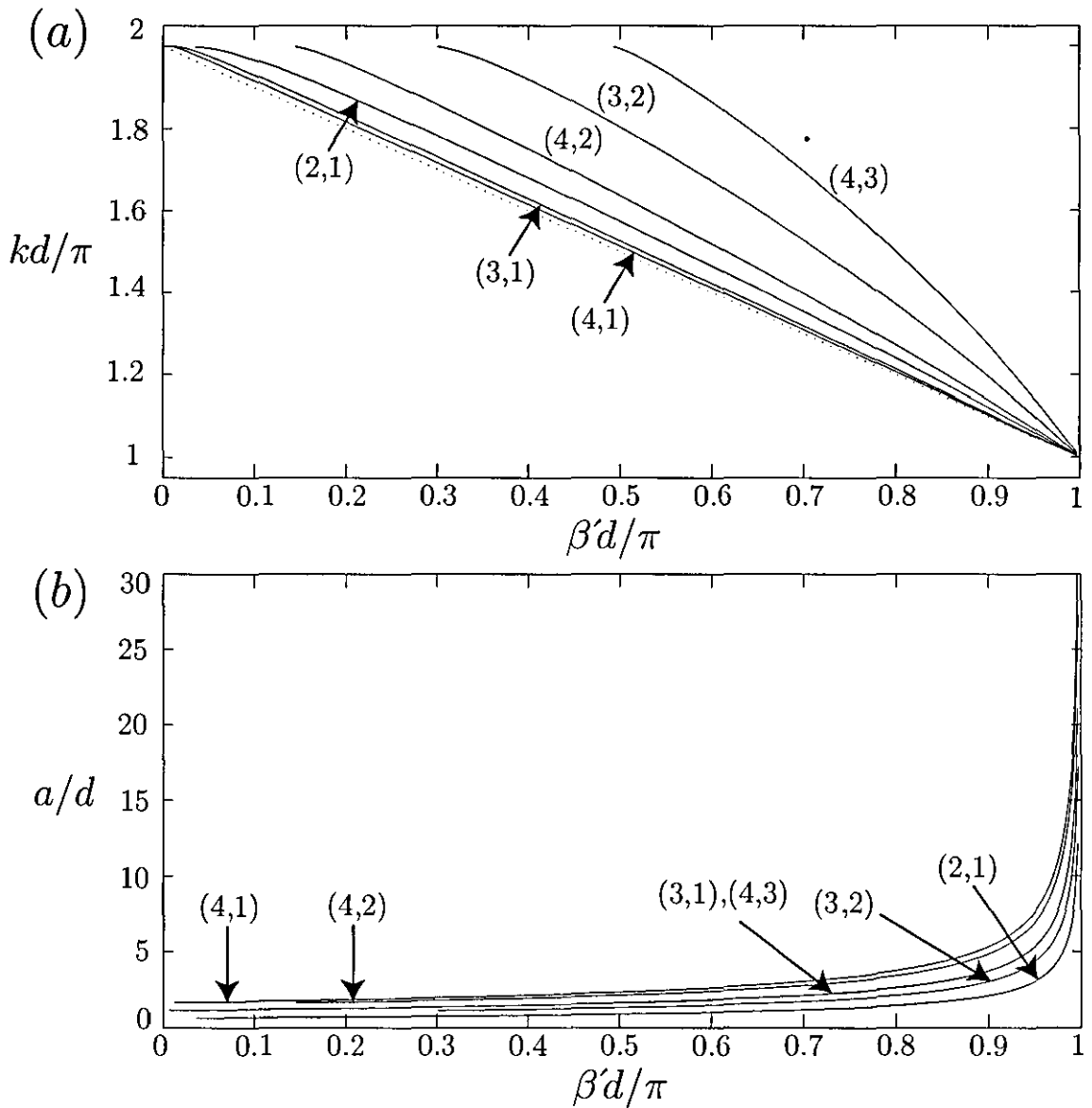


Figure 5.5: Variation of (a) kd/π and (b) a/d with $\beta'd/\pi$ for waves symmetric about $x = 0$. The curves are labelled with the values of (n_0, n_{-1}) used to generate them.

Conclusion

In this section we have used a modified residue calculus method to compute the frequencies of Rayleigh-Bloch waves above the first cut-off for wave propagation down the guide. The Rayleigh-Bloch waves are either symmetric or antisymmetric about the line of symmetry through the centre-point of each gap.

The results show that solutions only occur when the gap is above a certain length and only for specific lengths. It can also be seen that the range of the propagation constant β' is dependent upon the length of the gap. If the gap length becomes large waves can be found for all values of $\beta'd$ in the range $(0, \pi)$.

5.6 Rayleigh-Bloch waves below the third cut-off

As the problem we are considering in this chapter is defined by two parameters we may expect to find Rayleigh-Bloch waves in three frequency bands.

In this section we seek Rayleigh-Bloch waves whose frequencies are above the second cut-off $kd = 2\pi$. As in the previous chapter we restrict the frequency in such a way that three wave-like modes appear when $x < a$ and two propagating modes appear when $x > a$ and use a modified residue calculus technique.

5.6.1 Formulation

If $kd < 3\pi$ then both γ_1 and γ_2 are purely imaginary whereas γ_n , $n \geq 2$ are real and positive. If we also restrict the frequency so that $kd > 2\pi + \beta'd$, then α_0 , α_{-1} and α_1 are purely imaginary and α_n , $|n| \geq 2$ are real and positive. We therefore anticipate that a natural condition for the existence of Rayleigh-Bloch waves is

$$2\pi + \beta'd < kd < 3\pi. \quad (5.6.1)$$

This restriction will allow us to use a similar function to that used in the previous two sections.

The eigenfunction expansions in the two regions are

$$\phi_1(x, y) = \sum_{n=-\infty}^{\infty} U_n^{(1)} \frac{\cosh \alpha_n x}{\alpha_n \sinh \alpha_n a} e^{i\beta_n y}, \quad \alpha_n = (\beta_n^2 - k^2)^{1/2}, \quad (5.6.2)$$

$$\phi_2(x, y) = \sum_{n=3}^{\infty} U_n^{(2)} \frac{e^{-\gamma_n(x-a)}}{-\gamma_n} \sin \lambda_n y, \quad \gamma_n = (\lambda_n^2 - k^2)^{1/2}. \quad (5.6.3)$$

Notice that the summation in region II starts from $n = 3$ as we set the amplitude of the propagating modes corresponding to the imaginary γ_1 and γ_2 to zero. Following the work in section 5.5 we arrive at a similar equation to (5.5.4) except the summation starts at $n = 3$. We now consider the integrals (5.5.5) where $f(z)$ is now a meromorphic function which has the following properties:

- P1. $f(z)$ is an analytic function of z except for simple poles at $z = \gamma_n$, $n \geq 3$.
P2. $f(z) = O(z^{-\frac{1}{2}})$ as $|z| \rightarrow \infty$ on C_N as $N \rightarrow \infty$.

Construction of $f(z)$

We construct the function $f(z)$ in the form

$$f(z) = \exp(z\Theta)g(z)h(z), \quad (5.6.4)$$

where Θ is defined in (5.4.37) and

$$g(z) = \prod_{n=2}^{\infty} \frac{(1 - z/\alpha_n)(1 - z/\alpha_{-n})}{(1 - z/\gamma_n)}, \quad h(z) = 1 + \sum_{\substack{n=-\infty \\ n \neq 0, -1, 1}}^{\infty} \frac{A_n}{z - \alpha_n}. \quad (5.6.5)$$

The function $g(z)$ has the same asymptotic behaviour for large z as (5.4.21), since a single factor is removed from both the numerator and denominator. The function given by (5.6.4) therefore satisfies P2.

After applying Cauchy's residue theorem we find that our solution is given by $U_n = R(f : \gamma_n)$ provided both

$$f(\alpha_m) + \zeta_m f(-\alpha_m) = 0, \quad m \in \mathbb{Z}. \quad (5.6.6)$$

For $|m| \geq 2$, following the previous work, (5.6.6) leads to an exponentially converging infinite system of real equations similar to (5.5.10).

Rayleigh-Bloch wave condition

As in section 4.6 we now have three conditions that need to be satisfied simultaneously. These conditions are given by (5.6.6), with $m = 0$, $m = -1$ and $m = 1$. If we let $\alpha_0 = -i\alpha'_0$, where $\alpha'_0 = (k^2 - \beta'^2)^{\frac{1}{2}}$, $\alpha_{-1} = -i\alpha'_{-1}$, where $\alpha'_{-1} = (k^2 - \beta_{-1}^2)^{\frac{1}{2}}$ and $\alpha_1 = -i\alpha'_1$, where $\alpha'_1 = (k^2 - \beta_1^2)^{\frac{1}{2}}$ we can reduce these conditions to

$$e^{2i\alpha'_j a} = -\frac{f(-i\alpha'_j)}{f(i\alpha'_j)}, \quad j = -1, 0, 1. \quad (5.6.7)$$

If we define

$$\chi(x) = \sum_{n=2}^{\infty} \left(\tan^{-1} \left(\frac{x}{\alpha_n} \right) + \tan^{-1} \left(\frac{x}{\alpha_{-n}} \right) - \tan^{-1} \left(\frac{x}{\gamma_n} \right) \right) \quad (5.6.8)$$

and

$$\sigma(x) = \arg \left(1 - \sum_{\substack{n=-\infty \\ n \neq 0, -1, 1}}^{\infty} \frac{A_n}{\tilde{\alpha}_n + ix} \right), \quad (5.6.9)$$

we find the conditions for the existence of Rayleigh-Bloch waves are that

$$\alpha'_0(a + \Theta) = \chi(\alpha'_0) + \sigma(\alpha'_0) + \left(n_0 - \frac{1}{2} \right) \pi, \quad (5.6.10)$$

$$\alpha'_{-1}(a + \Theta) = \chi(\alpha'_{-1}) + \sigma(\alpha'_{-1}) + \left(n_{-1} - \frac{1}{2} \right) \pi, \quad (5.6.11)$$

$$\alpha'_1(a + \Theta) = \chi(\alpha'_1) + \sigma(\alpha'_1) + \left(n_1 - \frac{1}{2} \right) \pi, \quad (5.6.12)$$

are all satisfied simultaneously for sets of integers n_0 , n_{-1} and n_1 .

As $a/d \rightarrow \infty$, due to the exponential convergence of A_n , $\sigma(x)$ tends quickly to zero and so the computed σ values below the third cut-off are insignificant and will be ignored from now on. We now make a similar approximation to that in section 4.6 and ignore the Θ and χ terms in (5.6.10)–(5.6.12) to obtain

$$\alpha'_0 a = \left(n_0 - \frac{1}{2} \right) \pi, \quad \alpha'_{-1} a = \left(n_{-1} - \frac{1}{2} \right) \pi, \quad \alpha'_1 a = \left(n_1 - \frac{1}{2} \right) \pi. \quad (5.6.13)$$

Eliminating k and a from (5.6.13) we find

$$\frac{\left(n_0 - 1/2 \right)^2 - \left(n_1 - 1/2 \right)^2}{\left(n_{-1} - 1/2 \right)^2 - \left(n_1 - 1/2 \right)^2} = \frac{\pi + \beta' d}{\pi - \beta' d} > 1, \quad (5.6.14)$$

since $0 < \beta' d < \pi$. As the value of both sides of (5.6.14) is strictly greater than one this implies that

$$n_0 > n_{-1} \geq n_1 > 0. \quad (5.6.15)$$

If a set of integers can be found that satisfy (5.6.15), then it is easy to find the corresponding value of $\beta' d$ from (5.6.14) as the right-hand side is monotonically increasing. The values of kd and a/d can then be found quickly from (5.6.13) and providing the value of kd is in the correct range a good estimate to the Rayleigh-Bloch waves can be found.

Results

Results plotted from the full solution (4.6.16)–(4.6.18) compared to the approximate solution (5.6.13) when $a/d < 3$ are shown in figure 5.6. The waves coming from the full solution are represented with crosses and the waves from the approximate solution are represented with dots. It can be seen from figure 5.6 that the approximation made is very good as the dots and crosses are close together.

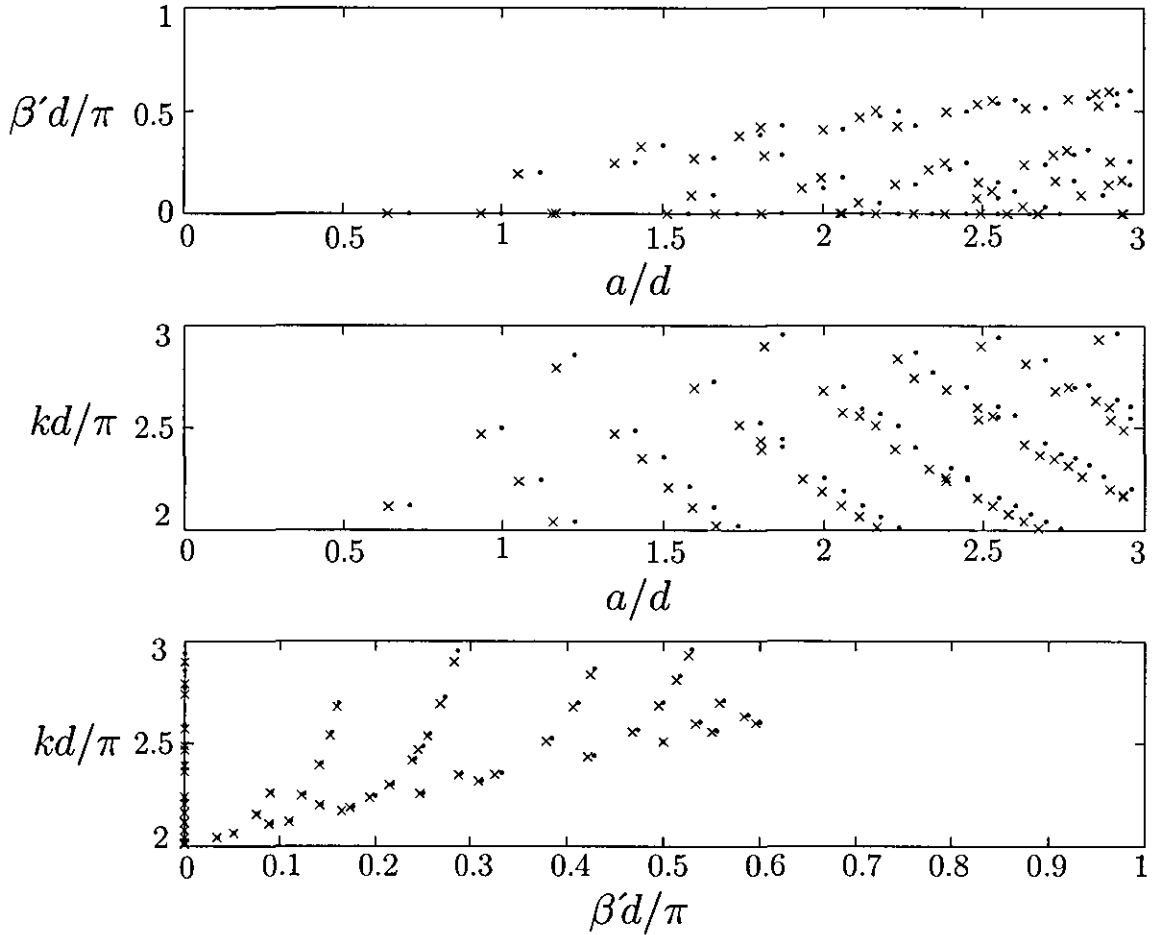


Figure 5.6: Solutions $(a/d, \beta'd/\pi, kd/\pi)$, with $a/d < 3$ for Rayleigh-Bloch waves symmetric about $x = 0$ below the third cut-off for an array of plates each containing an equal length finite gap. The dots are results from the approximate solution (4.6.22) and the crosses from the full solution (4.6.16)–(4.6.18).

The waves shown in figure 5.6 are for $a/d < 3$ and only require $n_0 \leq 9$. If Rayleigh-Bloch waves are needed with $a/d > 3$ the value of n_0 has to be increased. It can be seen from the bottom panel of figure 5.6 that when $a/d \leq 3$ Rayleigh-Bloch waves are only found for $\beta'd/\pi < 0.6$. This means that waves with a larger propagation constant

correspond to larger values of gap length (a similar phenomenon was found below the second cut-off). If $n_0 \leq 9$ all the Rayleigh-Bloch waves below $a/d = 3$ are found and hence the top two panels of figure 5.6 are complete. The bottom panel would contain more and more points as the value of n_0 is increased. Figure 5.7 shows the bottom panel of figure 5.6 with $n_0 \leq 50$.

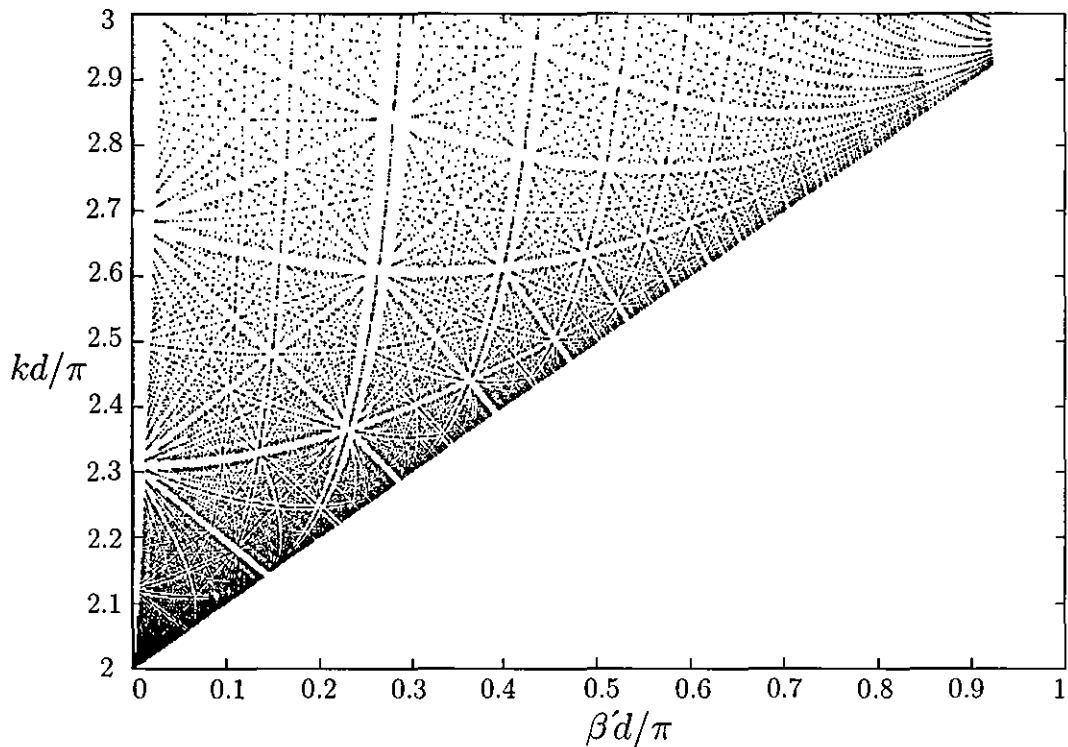


Figure 5.7: Results from the approximate solution (4.6.22) for waves symmetric about $x = 0$, with $n_0 \leq 50$.

Conclusion

In this section we have found Rayleigh-Bloch waves whose frequencies are below the third cut-off for an array of equally spaced parallel plates each containing an equal length finite gap. The third cut-off is defined as the frequency below which two propagating modes appear in the model. The Rayleigh-Bloch waves are found either symmetric or antisymmetric about the line of symmetry through the centre-point of each gap.

Below the third cut-off the waves correspond to the solution of three conditions which have to be solved simultaneously. A simple approximation to these three conditions can

be made which requires three integers to satisfy a certain condition. If a set of integers can be found that satisfy this condition then the corresponding propagation constant, gap length and frequency can be quickly found. The waves are found only for specific values of gap length and propagation constant.

5.7 Summary

In this chapter we have found Rayleigh-Bloch waves in three frequency bands for the case of an array of parallel Dirichlet plates, each containing an equal length finite gap. The Rayleigh-Bloch waves differ from trapped modes found in previous chapters as the Rayleigh-Bloch waves propagate in one direction along an array of objects and decay in another direction away from the array.

When formulating the problem in section 5.3 we found that it was specified by two non-dimensional parameters corresponding to the gap length and propagation constant. In the lowest frequency band (i.e. below the first cut-off) Rayleigh-Bloch waves were found for all values of the two parameters. In the next frequency band we found Rayleigh-Bloch waves for all values of the propagation constant (provided the gap was sufficiently large), but only for specific values of gap length, and in the highest frequency band we found Rayleigh-Bloch waves only for specific combinations of the two parameters. This feature is consistent with that found for trapped modes in Dirichlet problems in previous chapters.

Part II

Three-Dimensional Waveguides

Chapter 6

Three-dimensional laterally coupled cylindrical waveguides

6.1 Introduction to the problem

In this chapter we consider the case where the two-dimensional laterally coupled waveguide discussed in chapter 2 is rotated about the x -axis to produce a three-dimensional waveguide. The waveguide consists of pair of concentric circular cylindrical guides coupled laterally by a finite gap along the axis of the inner cylinder. We seek trapped modes whose frequencies are below the first cut-off for wave propagation down the guide using the modified residue calculus technique described in section 2.4.1.

The chapter is presented in the following manner. A review of previous work concerning trapped modes in cylindrical waveguides is given in section 6.2. The problem is formulated in section 6.3 and a solution using the modified residue calculus method is provided in section 6.4. The trapped modes that are found have certain angular variations and are both symmetric and antisymmetric about the line through the centre of the gap. Results are computed in section 6.4.1 and conclusions drawn in section 6.5.

6.2 Background

Early work on trapped modes in circular cylindrical waveguides was done by Ursell (1991), who considered a cylinder with a sphere placed on the axis. Both the sphere and the cylinder had Neumann conditions on their boundaries. In this work the author restricted the attention to modes with a particular angular variation, thus introducing

a cut-off below which modes could not propagate to infinity. A method using multipole expansions was used to prove the existence of trapped modes provided the sphere was sufficiently small.

Evans and Linton (1994) used the residue calculus method to find acoustic resonances for the case of a infinitely long circular cylindrical tube containing a concentric inner open-ended circular cylinder of finite length. They developed an approximate for large inner cylinder length, similar to that shown in section 2.4.1, and showed it to be very accurate. Neumann boundary conditions were placed on both cylinders and various trapped-mode frequency plots were shown.

The authors also investigated the acoustic resonances occurring in a circular cylindrical waveguide of constant cross-section. A Neumann boundary condition was placed on the wall of the guide for a finite length and a Dirichlet condition placed on the remainder. The trapped modes for the duct were sought with an azimuthal dependence of the form $\cos m\theta$ and $\sin m\theta$, with $m \in \mathbb{N}_0$, as in Ursell (1991). The plotted frequencies showed that as the length of the section with a Neumann boundary condition was increased the frequencies became largely independent of m .

The non-existence of trapped modes in a large class of circular cylindrical acoustic waveguides containing certain obstacles was proved in McIver and Linton (1995). The method of proof relies on finding a strictly positive function that satisfies certain field and boundary inequalities within the guide, on the guide walls and the body surfaces. A vector identity is then used to relate this function to the the trapped-mode potential. If this potential can only equal zero within the guide then trapped modes cannot exist. Neumann and Dirichlet boundary conditions are used on the guide walls and on the obstacle placed in the guide. The authors also proved that trapped modes do not exist when the boundary of the obstacle satisfies certain geometrical conditions.

Linton and McIver (1998a) proved that trapped modes can exist when a thin sound-hard obstacle is placed in a sound-hard cylindrical waveguide of constant cross-section in such a way that its normal is everywhere perpendicular to the generators of the cylinder. Similar results were also given in Groves (1998). The authors proved that circular cylindrical waveguides containing objects with axisymmetric geometries have an infinite sequence of trapped modes corresponding to different angular variations. The example of a cylindrical sleeve inside a circular cylindrical waveguide with Neumann conditions on all boundaries considered in Evans and Linton (1994) was recalculated

using the residue calculus technique and extended to cover different angular variations.

The case of Dirichlet conditions placed on the walls of a cylindrical waveguide was considered in a very analytical paper by Witsch (1990). The author used the same idea of specifying the angular variation to produce a cut-off and then used a minimum-maximum principle to provide examples of eigenvalues that can occur in the waveguide. Witsch refers these eigenvalues back to the total operator and therefore calls them embedded eigenvalues, whereas we call them trapped modes below the first cut-off.

The case of the circular cylindrical guide containing a number of radial fins with Neumann conditions on all boundaries appearing in Linton and McIver (1998b) is discussed in greater detail in chapter 8.

We now formulate the problem of a three-dimensional laterally coupled waveguide.

6.3 Formulation

In this section we consider a rotation of the waveguide used in chapter 2 about the x -axis. We introduce cylindrical polar coordinates (r, θ, x) so that the outer surface of the guide is at $r = d$. Inside the guide is placed what can be thought of as an infinite cylinder of radius b ($< d$) which has a gap of length $2a$ along its axis. The inner cylinder is placed so that its surface is at $r = b$ and the gap is at $-a < x < a$, as shown in figure 6.1. The resulting geometry is axisymmetric about the line $r = 0$, hence we are able to look for modes with angular variation $\cos m\theta$, where $m \in \mathbb{N}_0$. The quantity m is to be regarded as fixed in what follows.

The geometry is symmetric about $x = 0$, allowing us only to consider the region $x > 0$ and seek modes which are either symmetric or antisymmetric about $x = 0$. We begin by seeking modes symmetric about $x = 0$ by looking for non-trivial solutions $\phi(r, \theta, x)$, which satisfy

$$\frac{\partial \phi}{\partial x} = 0 \text{ on } x = 0, \quad 0 < r < d. \quad (6.3.1)$$

The potential $\phi(r, \theta, x)$ must also satisfy the Helmholtz equation within the waveguide,

$$(\nabla^2 + k^2) \phi = 0, \quad 0 < r < d, x > 0 \text{ except on } r = b, x > a, \quad (6.3.2)$$

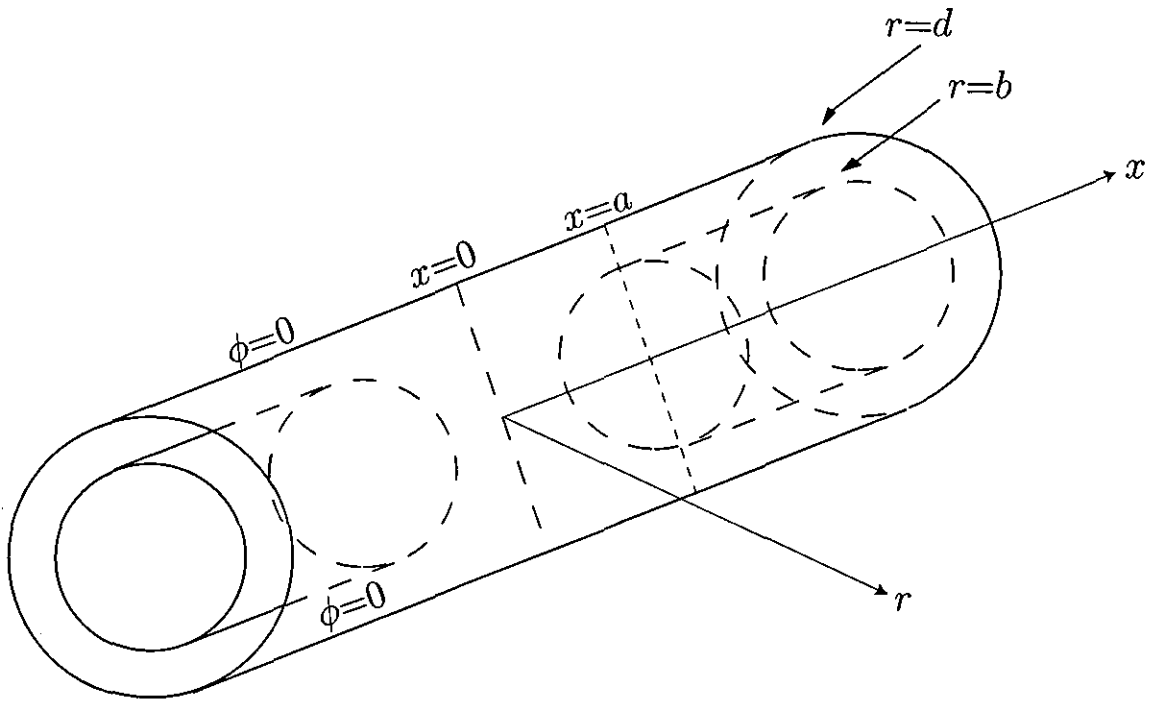


Figure 6.1: Definition sketch.

subject to Dirichlet boundary conditions on the cylinders

$$\phi = 0 \text{ on } r = b, x > a, \quad (6.3.3)$$

$$\phi = 0 \text{ on } r = d, x > 0, \quad (6.3.4)$$

and a radiation condition that stops waves propagating to infinity,

$$\phi \rightarrow 0 \text{ as } x \rightarrow \infty. \quad (6.3.5)$$

We finally assume that ϕ is non-singular and

$$\frac{\partial \phi}{\partial \rho} = O(\rho^{-\frac{1}{2}}) \text{ as } \rho = [(x-a)^2 + (r-b)^2]^{\frac{1}{2}} \rightarrow 0, \quad (6.3.6)$$

anticipating singular behaviour in the velocity field at the edge. The changes resulting from replacing (6.3.1) by an antisymmetric condition will be discussed later.

We now divide the region into three parts. Region *I* is the annular region between the outer and inner cylinders, i.e. $\{r, \theta, x : b < r < d, x > a\}$, region *II* is the interior of the inner cylinder, that is $\{r, \theta, x : 0 < r < b, x > a\}$ and region *III* is the gap of the inner cylinder, that is $\{r, \theta, x : 0 < r < d, 0 < x < a\}$. We can represent the function ϕ by a function $\phi_i(r, \theta, x) = \hat{\phi}_i(r, x) \cos m\theta$, ($i = 1, 2, 3$, $m \in \mathbb{N}_0$) in each region and apply the following continuity conditions at each regions boundary

$$\hat{\phi}_i = \hat{\phi}_3, \quad \frac{\partial \hat{\phi}_i}{\partial x} = \frac{\partial \hat{\phi}_3}{\partial x}, \quad \text{on } L_i, i = 1, 2, \quad (6.3.7)$$

where L_1 is $x = a, b < r < d$, L_2 is $x = a, 0 < r < b$ and L_3 is $L_1 \cup L_2$.

Expressing the Helmholtz equation (6.3.2) in cylindrical polar coordinates we obtain

$$\frac{1}{r} \frac{\partial}{\partial r} \left(r \frac{\partial \phi}{\partial r} \right) + \frac{1}{r^2} \frac{\partial^2 \phi}{\partial \theta^2} + \frac{\partial^2 \phi}{\partial x^2} + k^2 \phi = 0. \quad (6.3.8)$$

In each region we seek solutions of the form

$$\hat{\phi}_i(r, x) = U_i(r) V_i(x), \quad i = 1, 2, 3, \quad (6.3.9)$$

subject to the relevant boundary conditions. Substituting (6.3.9) into (6.3.8) we find

$$\frac{1}{U_i r} \frac{\partial}{\partial r} \left(r \frac{\partial U_i}{\partial r} \right) + k^2 - \frac{m^2}{r^2} = -\frac{1}{V_i} \frac{\partial^2 V_i}{\partial x^2}, \quad i = 1, 2, 3. \quad (6.3.10)$$

As the left-hand side of (6.3.10) is a function of r only whereas the right-hand side is a function of x , both sides must be equal to the same constant in each region.

In region I we require the solution to decay as $x \rightarrow \infty$, hence the constant is selected to be negative ($-\alpha^2$ say), with $\alpha > 0$, and we have

$$V_1(x) = A e^{-\alpha x}. \quad (6.3.11)$$

The left-hand side of (6.3.10) now becomes

$$\frac{1}{U_1 r} \frac{\partial}{\partial r} \left(r \frac{\partial U_1}{\partial r} \right) + k^2 + \alpha^2 - \frac{m^2}{r^2} = 0. \quad (6.3.12)$$

If we let $\eta^2 = k^2 + \alpha^2$, $r^* = \eta r$ and $U_1^*(r^*) = U_1(r)$, we can rewrite (6.3.12) as

$$\frac{\partial}{\partial r^*} \left(r^* \frac{\partial U_1^*}{\partial r^*} \right) + U_1^* \left(r^* - \frac{m^2}{r^*} \right) = 0, \quad (6.3.13)$$

which is Bessel's equation of order m for $U_1^*(r^*)$. The general solution of (6.3.13) is

$$U_1^*(r^*) = U_1(r) = A J_m(\eta r) + B Y_m(\eta r), \quad (6.3.14)$$

and using the boundary condition (6.3.3) we obtain

$$A = -B Y_m(\eta b) / J_m(\eta b). \quad (6.3.15)$$

Substituting this back into (6.3.14) we produce

$$U_1(\eta r) = A_1 \{ J_m(\eta r) Y_m(\eta b) - Y_m(\eta r) J_m(\eta b) \}, \quad (6.3.16)$$

where $A_1 = -B / J_m(\eta b)$. Substituting the other boundary condition, (6.3.4), into (6.3.16) we have

$$U_1(\eta d) = A_1 \{ J_m(\eta d) Y_m(\eta b) - Y_m(\eta d) J_m(\eta b) \} = 0. \quad (6.3.17)$$

If we replace η by ν_{mn} , the n^{th} positive zero of the cross-product $J_m(\eta d) Y_m(\eta b) - Y_m(\eta d) J_m(\eta b)$, the function $\Psi_{mn}^{(1)}$, $n \in \mathbb{N}$, can be introduced, where

$$\Psi_{mn}^{(1)}(r) = p_{mn}^{(1)} [J_m(\nu_{mn} r) Y_m(\nu_{mn} b) - Y_m(\nu_{mn} r) J_m(\nu_{mn} b)]. \quad (6.3.18)$$

This function satisfies (6.3.3)–(6.3.4) and with $p_{mn}^{(1)}$ chosen to be, (see Jones (1986), p228)

$$p_{mn}^{(1)} = \frac{\nu_{mn} \pi^{\frac{1}{2}}}{2^{\frac{1}{2}}} \left(\frac{J_m^2(\nu_{mn} b)}{J_m^2(\nu_{mn} d)} - 1 \right)^{-\frac{1}{2}}, \quad (6.3.19)$$

we have the orthogonality condition

$$\int_{L_i} r \Psi_{mn}^{(i)}(r) \Psi_{ms}^{(i)}(r) dr = \delta_{ns}, \quad n, s \in \mathbb{N}, \quad (6.3.20)$$

with $i = 1$, where δ_{ns} is the Kronecker delta. Since $\eta^2 = k^2 - \alpha^2$, we have

$$\alpha_{mn} d = \left((\nu_{mn} d)^2 - (kd)^2 \right)^{\frac{1}{2}}. \quad (6.3.21)$$

For decay down the guide we require α_{mn} to be real and positive for all m and n and so

$$kd < \nu_{m1} d. \quad (6.3.22)$$

In region *II* we set the constant equal to $-\beta^2$ with $\beta > 0$. The solution for $V_2(x)$, similar to (6.3.11), is

$$V_2(x) = A e^{-\beta x}, \quad (6.3.23)$$

and the general solution for $U_2(r)$ is

$$U_2(r) = B J_m(\eta r). \quad (6.3.24)$$

Using the boundary condition (6.3.3) we let

$$\mu_{mn} b = j_{mn}, \quad n \in \mathbb{N}, \quad (6.3.25)$$

where j_{mn} is the n th non-negative zero of the Bessel function $J_m(x)$ and (6.3.24) becomes

$$U_2(r) = B J_m(\mu_{mn} r). \quad (6.3.26)$$

We define the function $\Psi_{mn}^{(2)}(r)$ as

$$\Psi_{mn}^{(2)}(r) = p_{mn}^{(2)} J_m(\mu_{mn} r), \quad n \in \mathbb{N}, \quad (6.3.27)$$

where

$$p_{mn}^{(2)} = \frac{2^{\frac{1}{2}}}{b J_{m+1}(\mu_{mn}b)}, \quad (6.3.28)$$

which satisfies the orthogonality condition (6.3.20) with $i = 2$. The relation $\eta^2 = k^2 - \beta^2$ becomes

$$\beta_{mn}d = \left((\mu_{mn}d)^2 - (kd)^2 \right)^{\frac{1}{2}}. \quad (6.3.29)$$

For decay down the guide we require β_{mn} to be real and positive for all m and n and hence

$$kd < \mu_{m1}d = j_{m1}\left(\frac{d}{b}\right), \quad n \in \mathbb{N}. \quad (6.3.30)$$

In region *III* we set the constant equal to $-\gamma^2$, with $\gamma > 0$, and the solution for V_3 is

$$V_3(x) = A \cosh \gamma x. \quad (6.3.31)$$

If we let

$$\lambda_{mn}d = j_{m,n+1} \quad n \in \mathbb{N}_0, \quad (6.3.32)$$

where j_{mn} is defined as before, then the solution for U_3 is

$$U_3(r) = B J_m(\lambda_{mn}r). \quad (6.3.33)$$

We can now define

$$\Psi_{mn}^{(3)}(r) = p_{mn}^{(3)} J_m(\lambda_{mn}r) \quad n \in \mathbb{N}_0, \quad (6.3.34)$$

where we have introduced the coefficient

$$p_{mn}^{(3)} = \frac{2^{\frac{1}{2}}}{d J_{m+1}(\lambda_{mn}d)} \quad (6.3.35)$$

and hence $\Psi_{mn}^{(3)}$ satisfies the orthogonality condition (6.3.20), with $i = 3$. In this case $\eta^2 = k^2 - \gamma^2$, so replacing η by λ_{mn} and rearranging, we obtain

$$\gamma_{mn}d = \left((\lambda_{mn}d)^2 - (kd)^2 \right)^{\frac{1}{2}}. \quad (6.3.36)$$

We require γ_{m0} to be purely imaginary for $m \in \mathbb{N}_0$, but γ_{mn} to be real and positive for all other values of m and n , to produce one wave-like mode in the inner region and hence

$$kd > \lambda_{m0}d > j_{m1}. \quad (6.3.37)$$

We therefore anticipate that a necessary condition for the existence of trapped modes is

$$j_{m1} < kd < \min\left(j_{m1}\left(\frac{d}{b}\right), \nu_{m1}d\right). \quad (6.3.38)$$

The appropriate eigenfunction expansions for $\hat{\phi}$ are now

$$\hat{\phi}_1(r, x) = \sum_{n=1}^{\infty} U_{mn}^{(1)} \frac{e^{-\alpha_{mn}(x-a)}}{-\alpha_{mn}} \Psi_{mn}^{(1)}(r), \quad \alpha_{mn} = (\nu_{mn}^2 - k^2)^{\frac{1}{2}}, \quad (6.3.39)$$

$$\hat{\phi}_2(r, x) = \sum_{n=1}^{\infty} U_{mn}^{(2)} \frac{e^{-\beta_{mn}(x-a)}}{-\beta_{mn}} \Psi_{mn}^{(2)}(r), \quad \beta_{mn} = (\mu_{mn}^2 - k^2)^{\frac{1}{2}}, \quad (6.3.40)$$

$$\hat{\phi}_3(r, x) = \sum_{n=0}^{\infty} U_{mn}^{(3)} \frac{\cosh \gamma_{mn}x}{\gamma_{mn} \sinh \gamma_{mn}a} \Psi_{mn}^{(3)}(r), \quad \gamma_{mn} = (\lambda_{mn}^2 - k^2)^{\frac{1}{2}}. \quad (6.3.41)$$

In the next section we seek trapped modes below the first cut-off using the modified residue calculus method.

6.4 Trapped modes below the first cut-off

We now use the continuity conditions (6.3.7) and match $\hat{\phi}_i = \hat{\phi}_3$ on L_i , $i = 1, 2$, to give

$$\sum_{n=0}^{\infty} U_{mn}^{(3)} \frac{\coth \gamma_{mn}a}{\gamma_{mn}} \Psi_{mn}^{(3)}(r) = \begin{cases} \sum_{n=1}^{\infty} U_{mn}^{(1)} \frac{\Psi_{mn}^{(1)}(r)}{-\alpha_{mn}}, & r \in L_1, \\ \sum_{n=1}^{\infty} U_{mn}^{(2)} \frac{\Psi_{mn}^{(2)}(r)}{-\beta_{mn}}, & r \in L_2. \end{cases} \quad (6.4.1)$$

Similarly matching $\partial\phi_i/\partial x = \partial\phi_3/\partial x$ on L_i , $i = 1, 2$, we have

$$\sum_{n=0}^{\infty} U_{mn}^{(3)} \Psi_{mn}^{(3)}(r) = \begin{cases} \sum_{n=1}^{\infty} U_{mn}^{(1)} \Psi_{mn}^{(1)}(r), & r \in L_1, \\ \sum_{n=1}^{\infty} U_{mn}^{(2)} \Psi_{mn}^{(2)}(r), & r \in L_2. \end{cases} \quad (6.4.2)$$

We can convert (6.4.1) and (6.4.2) into an infinite systems of linear algebraic equations by multiplying each by $\Psi_{ms}^{(3)}$, $s \in \mathbb{N}_0$, and integrating over L_3 . From (6.4.1) we have,

$$\int_{L_3} \sum_{n=0}^{\infty} U_{mn}^{(3)} \Psi_{mn}^{(3)}(r) \Psi_{ms}^{(3)}(r) dr = \int_{L_1} \sum_{n=1}^{\infty} U_{mn}^{(1)} \Psi_{mn}^{(1)}(r) \Psi_{ms}^{(3)}(r) dr + \int_{L_2} \sum_{n=1}^{\infty} U_{mn}^{(2)} \Psi_{mn}^{(2)}(r) \Psi_{ms}^{(3)}(r) dr, \quad s \in \mathbb{N}_0. \quad (6.4.3)$$

We can rewrite (6.4.3) as

$$U_{ms}^{(3)} = \sum_{n=1}^{\infty} U_{mn}^{(1)} d_{ns} + \sum_{n=1}^{\infty} U_{mn}^{(2)} e_{ns}, \quad s \in \mathbb{N}_0, \quad (6.4.4)$$

where we have defined

$$d_{ns} = \frac{1}{d} \int_{L_1} \Psi_{mn}^{(1)}(r) \Psi_{ms}^{(3)}(r) dr, \quad (6.4.5)$$

$$e_{ns} = \frac{1}{d} \int_{L_2} \Psi_{mn}^{(2)}(r) \Psi_{ms}^{(3)}(r) dr. \quad (6.4.6)$$

In a similar way to (6.4.2) we obtain

$$U_{ms}^{(3)} \frac{\coth \gamma_{ms} a}{\gamma_{ms}} = \sum_{n=1}^{\infty} \left(\frac{U_{mn}^{(1)}}{-\alpha_{mn}} d_{ns} + \frac{U_{mn}^{(2)}}{-\beta_{mn}} e_{ns} \right), \quad s \in \mathbb{N}_0. \quad (6.4.7)$$

The integral d_{ns} can be evaluated as

$$\begin{aligned} d_{ns} &= \int_b^d r \Psi_{mn}^{(1)}(r) \Psi_{ms}^{(3)}(r) dr = \frac{p_{mn}^{(1)} p_{ms}^{(3)}}{\nu_{mn}^2 - \lambda_{ms}^2} \times \\ &\left(Y_m(\nu_{mn} b) \left[\lambda_{ms} d J_m(\nu_{mn} d) J_{m-1}(\lambda_{ms} d) - \nu_{mn} d J_{m-1}(\nu_{mn} d) J_m(\lambda_{ms} d) \right. \right. \\ &\quad \left. \left. - \lambda_{ms} b J_m(\nu_{mn} b) J_{m-1}(\lambda_{ms} b) + \nu_{mn} b J_{m-1}(\nu_{mn} b) J_m(\lambda_{ms} b) \right] \right. \\ &\quad \left. - J_m(\nu_{mn} b) \left[\lambda_{ms} d Y_m(\nu_{mn} d) J_{m-1}(\lambda_{ms} d) - \nu_{mn} d Y_{m-1}(\nu_{mn} d) J_m(\lambda_{ms} d) \right. \right. \\ &\quad \left. \left. - \lambda_{ms} b Y_m(\nu_{mn} b) J_{m-1}(\lambda_{ms} b) + \nu_{mn} b Y_{m-1}(\nu_{mn} b) J_m(\lambda_{ms} b) \right] \right), \quad (6.4.8) \end{aligned}$$

provided $\nu_{mn} \neq \lambda_{ms}$, where $s \in \mathbb{N}_0$, $n \in \mathbb{N}$, and Gradshteyn and Ryzhik (1980), eqn 5.54(1) has been used. Using the definition of λ_{ms} given in (6.3.32) and the identities

$$J_{m-1}(\nu_{mn} r) = -J_{m+1}(\nu_{mn} r) + \frac{2m}{\nu_{mn} r} J_m(\nu_{mn} r), \quad (6.4.9)$$

$$J_{m-1}(\lambda_{ms} d) = -J_{m+1}(\lambda_{ms} d), \quad (6.4.10)$$

and

$$Y_m(\nu_{mn} b) J_{m+1}(\nu_{mn} b) - J_m(\nu_{mn} b) Y_{m+1}(\nu_{mn} b) = \frac{2}{\pi \nu_{mn} b}, \quad (6.4.11)$$

(see Watson (1944) p77), we find that provided $\nu_{mn} \neq \lambda_{ms}$, $s \in \mathbb{N}_0$, $n \in \mathbb{N}$,

$$d_{ns} = -\frac{2 p_{mn}^{(1)} p_{ms}^{(3)} \nu_{mn} b J_m(\lambda_{ms} b)}{(\nu_{mn}^2 - \lambda_{ms}^2) \pi \nu_{mn} b}. \quad (6.4.12)$$

Substituting the values of $p_{mn}^{(1)}$ and $p_{ms}^{(3)}$ from (6.3.19) and (6.3.35) into (6.4.12) we have

$$d_{ns} = -\frac{2 \nu_{mn} J_m(\lambda_{ms} b)}{(\nu_{mn}^2 - \lambda_{ms}^2) \pi^{\frac{1}{2}} d J_{m+1} \lambda_{ms} d} \left(\frac{J_m^2(\nu_{mn} b)}{J_m^2(\nu_{mn} d)} - 1 \right)^{-\frac{1}{2}}, \quad s \in \mathbb{N}_0, n \in \mathbb{N}, \quad (6.4.13)$$

provided $\nu_{mn} \neq \lambda_{ms}$. Evaluating the integral e_{ns} in a similar way we find

$$e_{ns} = \frac{2 \mu_{mn} J_m(\lambda_{ms} b)}{d J_{m+1}(\lambda_{ms} d) (\mu_{mn}^2 - \lambda_{ms}^2)}, \quad s \in \mathbb{N}_0, n \in \mathbb{N}, \quad (6.4.14)$$

provided $\mu_{mn} \neq \lambda_{ms}$.

Eliminating $U_{mn}^{(3)}$ from (6.4.4) and (6.4.7) and using (6.4.13) and (6.4.14), we obtain after some simplification

$$\sum_{n=1}^{\infty} U_{mn} \left(\frac{1}{\alpha_{mn} - \gamma_{ms}} + \frac{\zeta_{ms}}{\alpha_{mn} + \gamma_{ms}} \right) - \sum_{n=1}^{\infty} V_{mn} \left(\frac{1}{\beta_{mn} - \gamma_{ms}} + \frac{\zeta_{ms}}{\beta_{mn} + \gamma_{ms}} \right) = 0, \quad (6.4.15)$$

where $s \in \mathbb{N}_0$ and we have defined

$$U_{mn} = \frac{U_{mn}^{(1)} \nu_{mn}}{\pi^{\frac{1}{2}} \alpha_{mn}} \left(\frac{J_m^2(\nu_{mn}b)}{J_m^2(\nu_{mn}d)} - 1 \right)^{-\frac{1}{2}}, \quad V_{mn} = \frac{U_{mn}^{(2)} \mu_{mn}}{\beta_{mn}}, \quad \text{and } \zeta_{ms} = e^{-2\gamma_{ms}a}. \quad (6.4.16)$$

The singular behaviour required by condition (6.3.6) again influences the asymptotic behaviour of U_{mn} and V_{mn} as $n \rightarrow \infty$. Following a similar method to (2.4.18)–(2.4.24) the edge condition is satisfied if both $U_{mn} = O(n^{-\frac{1}{2}})$ and $V_{mn} = O(n^{-\frac{1}{2}})$ as $n \rightarrow \infty$.

We now consider the following contour integrals

$$I_s = \lim_{N \rightarrow \infty} \frac{1}{2\pi i} \int_{C_N} f(z) \left(\frac{1}{z - \gamma_{ms}} + \frac{\zeta_{ms}}{z + \gamma_{ms}} \right) dz, \quad s \in \mathbb{N}_0, \quad (6.4.17)$$

where C_N is a sequence of contours (to be determined) on which $z \rightarrow \infty$ as $N \rightarrow \infty$ and $f(z)$ is a meromorphic function satisfying the following properties:

P1. $f(z)$ is an analytic function of z except for simple poles at $z = \alpha_{mn}$ and $z = \beta_{mn}$, $n \in \mathbb{N}$.

P2. $f(z) = O(z^{-\frac{1}{2}})$ as $|z| \rightarrow \infty$ on C_N as $N \rightarrow \infty$.

Construction of $f(z)$

Following the work in section 2.4.1 we choose

$$f(z) = g(z)h(z), \quad (6.4.18)$$

where $g(z)$ is

$$g(z) = \prod_{n=1}^{\infty} \frac{(1 - z/\gamma_{mn})}{(1 - z/\alpha_{mn})(1 - z/\beta_{mn})}, \quad (6.4.19)$$

and

$$h(z) = 1 + \sum_{n=1}^{\infty} \frac{A_{mn}}{(z - \gamma_{mn})}. \quad (6.4.20)$$

The function $g(z)$ is chosen as it satisfies property P1 stated earlier and is the appropriate function to employ when solving the problem in the limit as $a/d \rightarrow \infty$. The function $h(z)$ is chosen so that the zeros of $g(z)$ at γ_{mn} , are cancelled by the poles of $h(z)$ at these points.

To satisfy P2 we need to work out the behaviour of (6.4.19) as $|z| \rightarrow \infty$. This can be done by examining the behaviour of $g(z)$ for large z . With this in mind we write

$$g(z) = \prod_{n=1}^{\infty} \frac{1 - z/\nu_{mn}}{1 - z/\alpha_{mn}} \prod_{n=1}^{\infty} \frac{1 - z/\mu_{mn}}{1 - z/\beta_{mn}} \prod_{n=1}^{\infty} \frac{1 - z/\gamma_{mn}}{1 - z/\lambda_{mn}} \prod_{n=1}^{\infty} \frac{(1 - z/\lambda_{mn})}{(1 - z/\mu_{mn})(1 - z/\nu_{mn})}. \quad (6.4.21)$$

The first three products in (6.4.21) can be expanded as

$$\prod_{n=1}^{\infty} \frac{1 - z/\nu_{mn}}{1 - z/\alpha_{mn}} = \prod_{n=1}^{\infty} \left(1 - \frac{k^2}{\nu_{mn}^2}\right)^{\frac{1}{2}} \prod_{n=1}^{\infty} \left(1 - \frac{k^2}{(z - \alpha_{mn})(\alpha_{mn} + \nu_{mn})}\right), \quad (6.4.22)$$

$$\prod_{n=1}^{\infty} \frac{1 - z/\mu_{mn}}{1 - z/\beta_{mn}} = \prod_{n=1}^{\infty} \left(1 - \frac{k^2}{\mu_{mn}^2}\right)^{\frac{1}{2}} \prod_{n=1}^{\infty} \left(1 - \frac{k^2}{(z - \beta_{mn})(\beta_{mn} + \mu_{mn})}\right), \quad (6.4.23)$$

and

$$\prod_{n=1}^{\infty} \frac{1 - z/\gamma_{mn}}{1 - z/\lambda_{mn}} = \prod_{n=1}^{\infty} \left(1 - \frac{k^2}{\lambda_{mn}^2}\right)^{-\frac{1}{2}} \prod_{n=1}^{\infty} \left(1 + \frac{k^2}{(z - \lambda_{mn})(\lambda_{mn} + \gamma_{mn})}\right). \quad (6.4.24)$$

We now make use of the results from Abramowitz and Stegun (1972), eqn 9.5.12 and eqn 9.5.27. We have as $n \rightarrow \infty$,

$$\lambda_{mn}d = j_{m,n+1} \sim (n + m/2 + 3/4)\pi + O(1/n), \quad (6.4.25)$$

$$\mu_{mn}b = j_{mn} \sim (n + m/2 - 1/4)\pi + O(1/n), \quad (6.4.26)$$

$$\nu_{mn}(d - b) \sim n\pi + O(1/n). \quad (6.4.27)$$

Using these results we can compare the final products in (6.4.22)–(6.4.24) with $\sum_{n=1}^{\infty} n^{-2}$, and see that (6.4.22)–(6.4.24) are uniformly convergent on any compact set excluding $z = \alpha_{mn}$, $z = \beta_{mn}$ and $z = \lambda_{mn}$ respectively. Thus provided $z \rightarrow \infty$ through a sequence of values which avoids these points we have

$$\begin{aligned} g(z) &\sim C_m \prod_{n=1}^{\infty} \frac{1 - z/\gamma_{mn}}{1 - z/\lambda_{mn}} \prod_{n=1}^{\infty} \frac{(1 - z/\lambda_{mn})}{(1 - z/\mu_{mn})(1 - z/\nu_{mn})} \\ &\sim C_m \prod_{n=1}^{\infty} \frac{\left(1 - \frac{zd}{(n+m/2+3/4)\pi}\right)}{\left(1 - \frac{zc}{n\pi}\right)\left(1 - \frac{zb}{(n+m/2-1/4)\pi}\right)}, \end{aligned} \quad (6.4.28)$$

where C_m is a constant dependent upon m and independent of z . Using (2.4.43) we can show

$$\prod_{n=1}^{\infty} \frac{\left(1 - \frac{zd}{(n+m/2+3/4)\pi}\right)}{\left(1 - \frac{zc}{n\pi}\right)\left(1 - \frac{zb}{(n+m/2-1/4)\pi}\right)} = \frac{\Gamma(m/2 + 7/4) \Gamma(1 - zc/\pi) \Gamma(m/2 + 3/4 - zb/\pi)}{\Gamma(m/2 + 7/4 - zd/\pi) \Gamma(m/2 + 3/4)}. \quad (6.4.29)$$

We then find the behaviour of (6.4.29) as $|z| \rightarrow \infty$, $z \neq |z|$ after using (2.4.45) to be

$$g(z)C_m \left(\frac{2\pi^2 c b^{(m-1/2)}}{(-z) d^{(m+5/2)}}\right)^{\frac{1}{2}} \exp\left[\frac{z}{\pi}(b \ln(d/b) + c \ln(d/c))\right]. \quad (6.4.30)$$

For the case when z is real and positive we use the reflection properties of the Gamma function, see (2.4.48), and the asymptotic behaviour can be found to be

$$\begin{aligned} g(z) &\sim C_m \left(\frac{(zd/\pi - m/2 - 7/4) \sin(m\pi/2 + 3\pi/4 - zb) \sin(m\pi/2 + 7\pi/4 - zd)}{(1 - zc/\pi)(m/2 + 3/4 - zb/\pi) \sin(zc)}\right) \\ &\times \left(\frac{z c^3 b^{(m+5/2)}}{d^{(m+9/2)}}\right)^{\frac{1}{2}} \exp\left[\frac{z}{\pi}(b \ln(d/b) + c \ln(d/c))\right], \end{aligned} \quad (6.4.31)$$

as $z \rightarrow \infty$, $z \neq -|z|$ through any sequence of values which avoids the points $z = n\pi/c$, $z \in \mathbb{N}$. If we choose the curves C_N to be a sequence of circles with centre at the origin and radius R_N not equal to any of the points mentioned previously we can consider the function

$$g(z) = \exp \left[-\frac{z}{\pi} (b \ln(d/b) + c \ln(d/c)) \right] \prod_{n=1}^{\infty} \frac{(1 - z/\gamma_{mn})}{(1 - z/\alpha_{mn})(1 - z/\beta_{mn})}, \quad (6.4.32)$$

which is $O(z^{-\frac{1}{2}})$ as $|z| \rightarrow \infty$ on C_N as $N \rightarrow \infty$, and hence P2 is satisfied. It is interesting to note that this function is very similar in form to the function (2.4.50) used in the two-dimensional case.

We now apply Cauchy's residue theorem to (6.4.17) to obtain

$$\sum_{n=1}^{\infty} R(f : \alpha_{mn}) \left(\frac{1}{\alpha_{mn} - \gamma_{ms}} + \frac{\zeta_{ms}}{\alpha_{mn} + \gamma_{ms}} \right) + \sum_{n=1}^{\infty} R(f : \beta_{mn}) \left(\frac{1}{\beta_{mn} - \gamma_{ms}} + \frac{\zeta_{ms}}{\beta_{mn} + \gamma_{ms}} \right) + f(\gamma_{ms}) + \zeta_{ms} f(-\gamma_{ms}) = 0, \quad s \in \mathbb{N}_0. \quad (6.4.33)$$

A comparison with (6.4.15) shows our solution is given by $U_{mn} = R(f : \alpha_{mn})$ and $V_{mn} = -R(f : \beta_{mn})$ provided

$$f(\gamma_{ms}) + \zeta_{ms} f(-\gamma_{ms}) = 0, \quad s \in \mathbb{N}_0. \quad (6.4.34)$$

For $s \in \mathbb{N}$ these equations can be solved by an appropriate choice of the coefficients A_{mn} . We have for $s \in \mathbb{N}$,

$$f(\gamma_{ms}) = -\exp \left\{ -\frac{\gamma_{ms}}{\pi} (b \ln(d/b) + c \ln(d/c)) \right\} \left(\frac{A_{ms}}{\gamma_{ms}(1 - \gamma_{ms}/\alpha_{ms})(1 - \gamma_{ms}/\beta_{ms})} \right) \times \prod_{\substack{n=1 \\ n \neq s}}^{\infty} \frac{1 - \gamma_{ms}/\gamma_{mn}}{(1 - \gamma_{ms}/\alpha_{mn})(1 - \gamma_{ms}/\beta_{mn})}, \quad (6.4.35)$$

and

$$f(-\gamma_{ms}) = \left(1 - \sum_{n=1}^{\infty} \frac{A_{mn}}{\gamma_{ms} + \gamma_{mn}} \right) \exp \left\{ \frac{\gamma_{ms}}{\pi} (b \ln(d/b) + c \ln(d/c)) \right\} \times \left(\frac{2}{(1 + \gamma_{ms}/\alpha_{ms})(1 + \gamma_{ms}/\beta_{ms})} \right) \prod_{\substack{n=1 \\ n \neq s}}^{\infty} \frac{1 + \gamma_{ms}/\gamma_{mn}}{(1 + \gamma_{ms}/\alpha_{mn})(1 + \gamma_{ms}/\beta_{mn})}. \quad (6.4.36)$$

Substituting both (6.4.35) and (6.4.36) into (6.4.34) we obtain,

$$A_{ms} + D_{ms} \sum_{n=1}^{\infty} \frac{A_{mn}}{\gamma_{ms} + \gamma_{mn}} = D_{ms}, \quad s \in \mathbb{N}, \quad (6.4.37)$$

where

$$D_{ms} = \left(\frac{2\gamma_{ms}(\alpha_{ms} - \gamma_{ms})(\beta_{ms} - \gamma_{ms})}{(\alpha_{ms} + \gamma_{ms})(\beta_{ms} + \gamma_{ms})} \right) \exp \left\{ \frac{2\gamma_{ms}}{\pi} (b \ln(d/b) + c \ln(d/c) - a\pi) \right\} \\ \times \prod_{\substack{n=1 \\ n \neq s}}^{\infty} \frac{(1 + \gamma_{ms}/\gamma_{mn})(1 - \gamma_{ms}/\alpha_{mn})(1 - \gamma_{ms}/\beta_{mn})}{(1 + \gamma_{ms}/\alpha_{mn})(1 + \gamma_{ms}/\beta_{mn})(1 - \gamma_{ms}/\gamma_{mn})}. \quad (6.4.38)$$

Trapped mode condition

We now return to the one condition still to be satisfied, namely (6.4.34) with $s = 0$. If we let $\gamma_{m0} = -i\gamma'_m$, where $\gamma'_m = (k^2 - \lambda_{m0}^2)^{\frac{1}{2}} = (k^2 - j_{m1}^2)^{\frac{1}{2}}$, this condition reduces to

$$e^{2i\gamma'_m a} = -\frac{f(-i\gamma'_m)}{f(i\gamma'_m)}. \quad (6.4.39)$$

From (6.4.32) and (6.4.20) we have

$$\frac{g(-i\gamma')}{g(i\gamma')} = e^{2i(\chi_m + \gamma'_m \Theta)}, \quad \frac{h(-i\gamma'_m)}{h(i\gamma'_m)} = e^{2i\sigma_m}, \quad (6.4.40)$$

where we have defined

$$\chi_m = \sum_{n=1}^{\infty} \left(\tan^{-1} \left(\frac{\gamma'_m}{\gamma_{mn}} \right) - \tan^{-1} \left(\frac{\gamma'_m}{\alpha_{mn}} \right) - \tan^{-1} \left(\frac{\gamma'_m}{\beta_{mn}} \right) \right), \quad (6.4.41)$$

$$\Theta = \frac{1}{\pi} (b \ln(d/b) + c \ln(d/c)), \quad (6.4.42)$$

and

$$\sigma_m = \arg \left(h(-i\gamma'_m) \right) = \arg \left(1 - \sum_{n=1}^{\infty} \frac{A_{mn}}{\gamma_{mn} + i\gamma'_m} \right). \quad (6.4.43)$$

The condition for the existence of trapped modes, (6.4.39), reduces to

$$\gamma'_m (a - \Theta) = \chi_m + \sigma_m + \left(n - \frac{1}{2} \right) \pi, \quad n \text{ an integer}, \quad (6.4.44)$$

where χ_m , Θ and σ_m are given by (6.4.41)–(6.4.43).

Antisymmetry about $x = 0$

If we seek trapped modes antisymmetric about $x = 0$ we replace the boundary condition (6.3.1) by

$$\phi = 0 \quad \text{on } x = 0, \quad 0 < r < d, \quad (6.4.45)$$

and hence the cosh and sinh terms in (6.3.41) are interchanged. Equation (6.4.15) becomes

$$\sum_{n=1}^{\infty} U_{mn} \left(\frac{1}{\alpha_{mn} - \gamma_{ms}} - \frac{\zeta_{ms}}{\alpha_{mn} + \gamma_{ms}} \right) - \sum_{n=1}^{\infty} V_{mn} \left(\frac{1}{\beta_{mn} - \gamma_{ms}} - \frac{\zeta_{ms}}{\beta_{mn} + \gamma_{ms}} \right) = 0, \quad (6.4.46)$$

where $s \in \mathbb{N}_0$. The equivalent condition to (6.4.44) is

$$\gamma'_m(a - \Theta) = \chi_m + \sigma'_m + n\pi, \quad n \text{ an integer}, \quad (6.4.47)$$

where χ_m and Θ are given by (6.4.41) and (6.4.42) and σ'_m is the argument of $h(-i\gamma'_m)$ with the A_{mn} coefficients coming from the system of equations

$$-A_{ms} + D_{ms} \sum_{n=1}^{\infty} \frac{A_{mn}}{\gamma_{ms} + \gamma_{mn}} = D_{ms} \quad s \in \mathbb{N}. \quad (6.4.48)$$

6.4.1 Results

The results in this section are computed with the systems of equations (6.4.37) and (6.4.48) truncated with a parameter $N = 5$. Typical results for the trapped-mode wavenumbers are shown in figure 6.2 and figure 6.3, for $m = 0$ and 1. In both figures the solid lines correspond to modes symmetric about $x = 0$ and the dashed lines to modes antisymmetric about $x = 0$.

In figure 6.2 trapped-mode wavenumbers are plotted against a/d when $b/d = 0.5$. We see that as a/d increases more and more modes appear alternatively symmetric and antisymmetric about $x = 0$ for each value of m . The upper and lower cut-offs for the existence of trapped modes are given by (6.3.38) are dependent on m . When $m = 0$ the modes appear from the cut-off given by the minimum of $kd = j_{01}/0.5 \approx 4.810$ and $kd = \nu_{01}d \approx 6.246$, i.e. $kd = j_{01}/0.5$, and tend to $kd = j_{01} \approx 2.405$ as a/d increases. This minimum value changes however when $m = 1$, as the upper cut-off becomes $kd = \nu_{11}d \approx 6.393$ which is less than $kd = 2j_{11} \approx 7.663$. As a/d increases the modes corresponding to $m = 1$ tend to $kd = j_{11} \approx 3.832$.

In figure 6.3 trapped-mode wavenumbers are plotted against b/d when $a/d = 3$. The upper plot corresponds to the case when $m = 1$ and the lower plot corresponds to the case $m = 0$. The dotted lines appearing on both plots are the upper and lower cut-offs for the two different m values and show where the frequency ranges lie with respect to each other. When $b/d \rightarrow 0$ the only upper cut-off present for both plots is

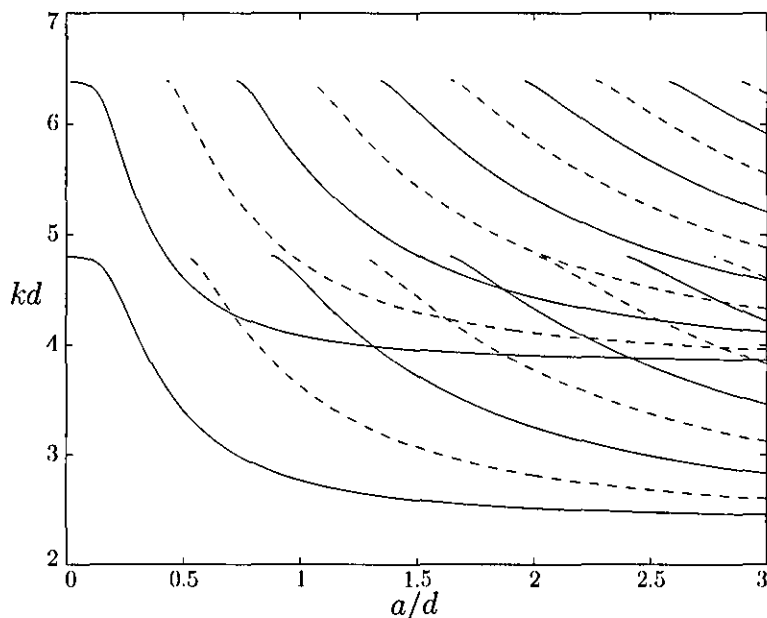


Figure 6.2: A comparison of the trapped-mode wavenumbers for modes symmetric (—) and antisymmetric (---) about $x = 0$ plotted against a/d when $b/d = 0.5$.

the one corresponding to $kd = \eta_{m1}$, whereas when $b/d \rightarrow 1$ the upper cut-off is shown by $kd = d j_{m1}/b$ for both values of m . When $m = 0$ the upper cut off changes from $kd = \eta_{01}d$ to $kd = j_{01}d/b$ when $b/d \approx 0.436$, and the largest number of modes appears at this value. As m increases the value of b/d when the upper cut-off changes also increases.

6.5 Summary

In this chapter we have considered the three dimensional laterally coupled waveguide. The waveguide consists of two concentric circular cylindrical waveguides coupled by a finite length gap along the axis of the inner cylinder and can be formed by rotating the waveguide considered in chapter 2 about the x -axis. We used a modified residue calculus method to computed trapped-mode frequencies below the first cut-off for wave propagation down the waveguide.

We were able to look for modes with an angular variation $\cos m\theta$, $m \in \mathbb{N}_0$, and the trapped modes found are either symmetric and antisymmetric about the line of symmetry perpendicular to the axis of the cylinder. During the formulation we found that the upper cut-off is dependent on the values of m and b/d (the ratio of the two

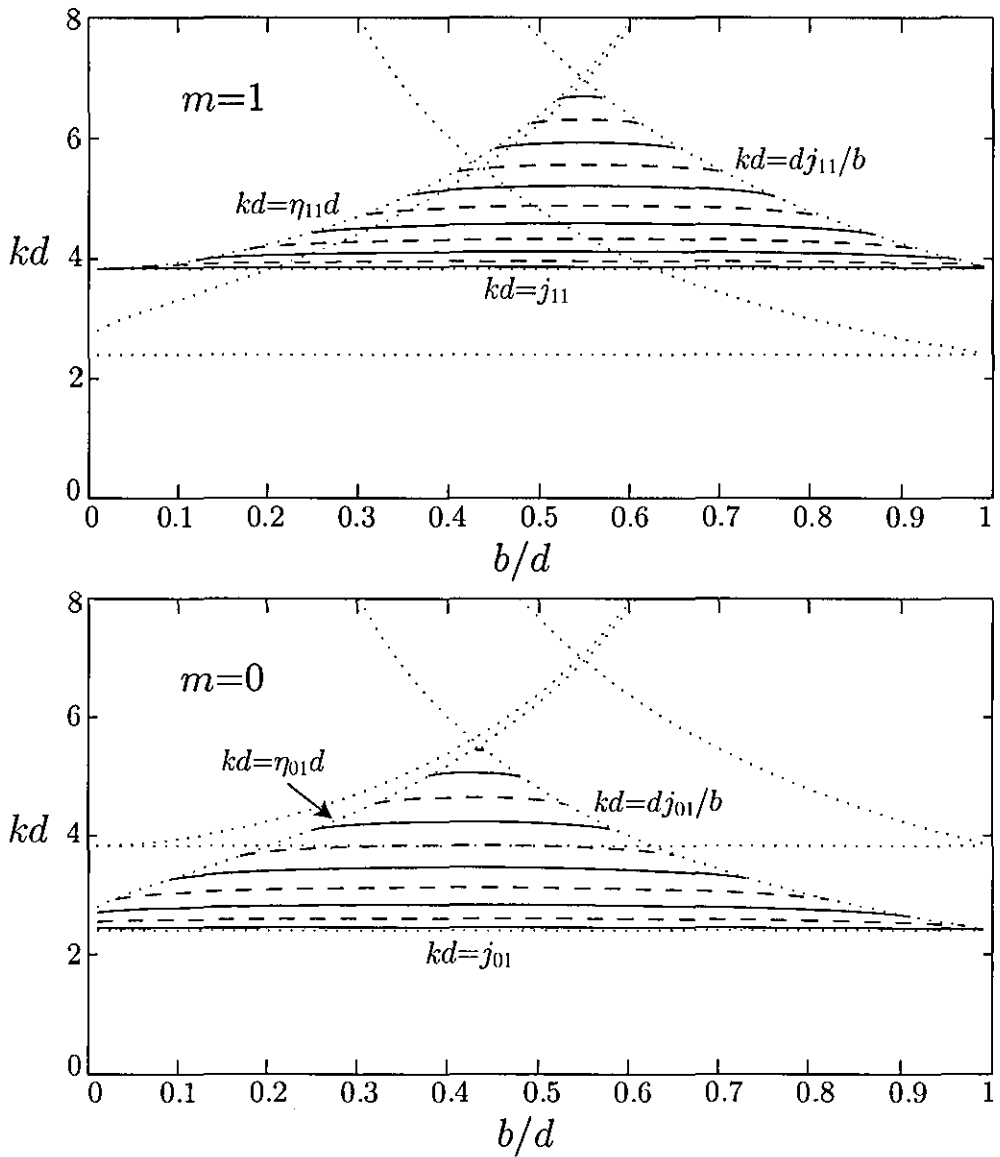


Figure 6.3: A comparison of the trapped-mode wavenumbers for modes symmetric (—) and antisymmetric (---) about $x = 0$ plotted against b/d when $a/d = 3$.

radii). The results presented in section 6.4.1 show that the trapped modes occur for any value of the gap length and ratio of radii (a/d and b/d) and the frequencies increase as m increases.

Chapter 7

Three-dimensional laterally coupled planar waveguides

7.1 Introduction to the problem

In this chapter we consider the case where the two-dimensional laterally coupled waveguide considered in chapter 2 is rotated about the y -axis to produce a three-dimensional waveguide. The waveguide consists of two planar layers of widths b and $d - b$ coupled laterally through a circular hole of radius a in the common boundary.

When the two planar layers are of equal width the problem reduces to a Neumann disc on the centreline (just as the two-dimensional laterally coupled waveguide reduced to a Neumann plate on the centreline). In this chapter we initially consider the case of a number of Neumann discs placed on the centreline of a planar waveguide, as the symmetry of the problem allows us to simplify the analysis. We return to the case of different width waveguides later in the chapter.

The chapter is presented in the following manner. In section 7.2 we review work done concerning trapped modes around thin circular discs and vertical cylinders. Vertical cylinders are considered as the plan view of both sets of problems is identical and so we expect the formulation in two coordinates to be similar. We formulate the problem for P circular discs on the centreline of a planar waveguide in section 7.3. This general formulation allows us to provide results for various configurations.

In section 7.4.1 we consider a single disc on the centreline. When one disc is considered a number of simplifications to the formulation can be made and results are presented for a typical radius. We investigate the case of two discs in section 7.4.2. Two

problems are considered, the case when the discs are identical and the case when they are different.

In section 7.4.3 we return to the problem of a laterally coupled planar waveguide. We reformulate the problem and consider the case when the waveguide is coupled by a single circular hole.

A summary of the chapter is provided in section 7.5.

7.2 Background

Although we are considering thin circular discs in planar waveguides, in this chapter, it can be seen from figure 7.1 that the plan view of the problem is equivalent to the plan view of a number of vertical circular cylinders. We thus may expect the formulation of the problem in this chapter to be similar to the formulation for a number of vertical cylinders in all but the depth coordinate. We therefore include work on trapped modes around vertical cylinders in this review along with work on thin circular discs.

There has not been a vast amount of work done so far on thin circular discs in three-dimensions, although from a physical viewpoint Farina and Martin (1998) note that the equivalent water-wave problem may find application in coastal engineering, perhaps as components in a breakwater or in a wave-focussing device.

Martin and Farina (1997) and Farina and Martin (1998) used a hypersingular integral equation to calculate the waves radiated from heave (vertical) oscillations of a thin circular disc and the scattering of water waves by a thin circular disc. In both cases Neumann conditions were placed on the disc and a mixed boundary condition on the surface.

Much of the work on trapped modes around vertical cylinders concerns parallel-plate waveguides containing a symmetrically-placed cylinder. As the cylinder is assumed to extend throughout the depth of the fluid the depth dependence can be factored out and we are left with a two-dimensional problem. As in chapter 3 the symmetry of the problem can be used to introduce a cut-off below which modes cannot propagate to infinity.

Callan, Linton, and Evans (1991) proved numerically using a multipole method that a trapped mode exists in a waveguide with such a geometry with Neumann conditions placed on all the boundaries. The mode was antisymmetric about the mid-plane of the

guide and symmetric about a line perpendicular to the guide walls and had a frequency below the cut-off for wave propagation down the guide. No mode was found in the paper that was both antisymmetric about the mid-plane and a line perpendicular to the walls, although such a mode has been subsequently found for sufficiently large radius cylinder by Evans and Porter (1999).

Trapped modes in the vicinity of multiple cylinders in a channel were considered by Evans and Porter (1997). The authors considered the case of a number of different-sized circular cylinders arbitrarily spaced along the centreline of the channel. Both Neumann and Dirichlet modes were sought using solution based on a multipole method and the use of addition theorems for Bessel functions. It was shown that there are up to N trapped-mode frequencies below the first cut-off corresponding to any configuration of N cylinders.

In this chapter we use a method based on a matched eigenfunction expansion to calculate the trapped-mode frequencies for a number of discs on the centreline of a planar waveguide. We begin by formulating a solution for P discs.

7.3 Formulation

In this section we consider P (≥ 1) discs placed on the centre-plane of a waveguide of total height d . We introduce $P + 1$ cylindrical polar coordinate systems, so that (r, θ, z) is centred at the origin and (r_j, θ_j, z) , $j = 1, \dots, P$, are centred at $(x_j, y_j, 0)$, the centre of the j^{th} disc of radius a_j . The outer walls of the waveguide are at $z = \pm d/2$ and the centre-plane is at $z = 0$. The various parameters relating to the relative positions and sizes of the discs when $P = 2$ are shown in figure 7.1.

The symmetry of the problem allows us to seek trapped modes which are antisymmetric about the centre-plane of the guide by adding a Dirichlet condition on the plane $z = 0$, away from each disc and considering only the upper-half of the waveguide. Condition (3.3.8) can then be used to extend the solution into the whole guide.

We now divide the domain up into $P + 1$ parts, ϕ_j^I , $j = 1, \dots, P$ is the potential above the j^{th} disc and ϕ^{II} is the potential exterior to the discs. We look for non-trivial solutions ϕ_j^I , $j = 1, \dots, P$ and ϕ^{II} , each of which satisfies the Helmholtz equation in the

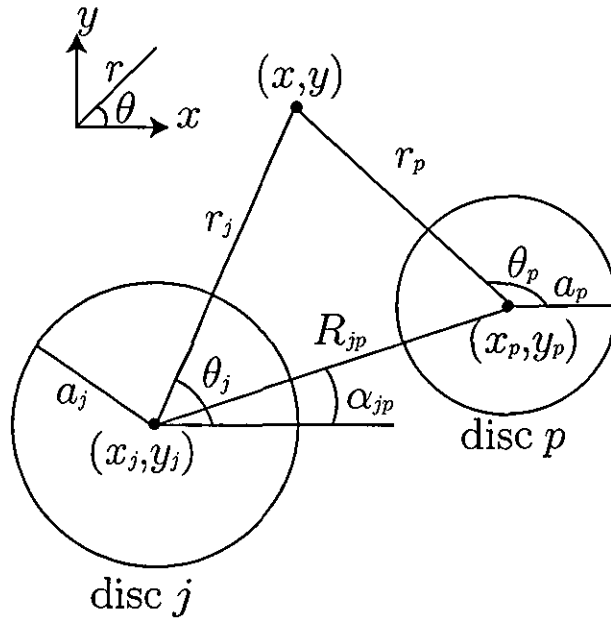


Figure 7.1: Plan view of two discs.

relevant set of cylindrical polar coordinates,

$$\frac{1}{r} \frac{\partial}{\partial r} \left(r \frac{\partial \phi}{\partial r} \right) + \frac{1}{r^2} \frac{\partial^2 \phi}{\partial \theta^2} + \frac{\partial^2 \phi}{\partial z^2} + k^2 \phi = 0, \quad 0 < z < d/2, \quad r > 0, \quad (7.3.1)$$

subject to Dirichlet boundary conditions on the planes

$$\phi^{II} = 0 \text{ on } z = 0, \quad (7.3.2)$$

$$\phi_j^I = \phi^{II} = 0 \text{ on } z = d/2, \quad j = 1, \dots, P, \quad (7.3.3)$$

Neumann condition on the discs

$$\frac{\partial \phi_j^I}{\partial z} = 0 \text{ on } z = 0, \quad r_j < a_j, \quad j = 1, \dots, P, \quad (7.3.4)$$

and a condition that stops waves radiating to infinity,

$$\phi^{II} \rightarrow 0 \text{ as } r \rightarrow \infty. \quad (7.3.5)$$

We also need to apply the following continuity conditions at each regions boundary

$$\phi_j^I = \phi^{II}, \quad \frac{\partial \phi_j^I}{\partial r_j} = \frac{\partial \phi^{II}}{\partial r_j} \quad \text{on } r_j = a_j, \quad j = 1, \dots, P. \quad (7.3.6)$$

Separation of variables reveals that the appropriate eigenfunction expansions are

$$\phi_j^I = \sum_{m=-\infty}^{\infty} \sum_{n=0}^{\infty} A_{mn}^j \frac{I_m(\alpha_n r_j) \Psi_n^{(1)}(z) e^{im\theta_j}}{\alpha_n I_m'(\alpha_n a_j)}, \quad j = 1, \dots, P, \quad (7.3.7)$$

$$\phi^{II} = \sum_{p=1}^P \sum_{m=-\infty}^{\infty} \sum_{n=0}^{\infty} B_{mn}^p \frac{K_m(\beta_n r_p) \Psi_n^{(2)}(z) e^{im\theta_p}}{\beta_n K_m'(\beta_n a_p)}, \quad (7.3.8)$$

where $I_m(z)$ and $K_m(z)$ are modified Bessel functions and $\alpha_n, \beta_n, \Psi_n^{(1)}(z)$ and $\Psi_n^{(2)}(z)$ are defined by (3.3.13), (3.3.14) and (3.3.15). As in section 3.4 we find that if we restrict the frequency so that

$$\pi < kd < 2\pi, \quad (7.3.9)$$

then α_0 is purely imaginary whereas α_n and $\beta_n, n \in \mathbb{N}$ will all be real and positive. This restriction allows the mode corresponding to $n = 0$ to become wave-like local to each disc, whereas all other modes decay as r becomes large.

In order to apply the continuity conditions (7.3.6) the eigenfunction expansion in region II must be written solely in terms of the coordinates r_j and θ_j . This can be achieved using Graf's addition theorem for Bessel functions, see Linton and McIver (2001) p169, which shows that provided $r_j < R_{jp}$ for all p , we can write

$$\begin{aligned} \phi^{II}(r_j, \theta_j, z) = & \sum_{m=-\infty}^{\infty} \sum_{n=1}^{\infty} B_{mn}^j \frac{K_m(\beta_n r_j) \Psi_n^{(2)}(z) e^{im\theta_j}}{\beta_n K'_m(\beta_n a_j)} \\ & + \sum_{\substack{p=1 \\ p \neq j}}^P \sum_{m=-\infty}^{\infty} \sum_{n=1}^{\infty} B_{mn}^p \frac{\Psi_n^{(2)}(z)}{\beta_n K'_m(\beta_n a_j)} \sum_{s=-\infty}^{\infty} I_s(\beta_n r_j) K_{m-s}(\beta_n R_{jp}) e^{is\theta_p} e^{i(m-s)\alpha_{jp}}, \end{aligned} \quad (7.3.10)$$

where R_{jp} is the distance between the centres of discs j and p , and α_{jp} is the angle of the centre of disc p from disc j , measured as shown in figure 7.1.

Matching $\phi_j^I = \phi^{II}$ on $r_j = a_j, j = 1, \dots, P$, we find

$$\begin{aligned} \sum_{m=-\infty}^{\infty} \sum_{n=0}^{\infty} A_{mn}^j \frac{I_m(\alpha_n a_j) \Psi_n^{(1)}(z) e^{im\theta_j}}{\alpha_n I'_m(\alpha_n a_j)} = & \sum_{m=-\infty}^{\infty} \sum_{n=1}^{\infty} B_{mn}^j \frac{K_m(\beta_n a_j) \Psi_n^{(2)}(z) e^{im\theta_j}}{\beta_n K'_m(\beta_n a_j)} \\ & + \sum_{\substack{p=1 \\ p \neq j}}^P \sum_{m=-\infty}^{\infty} \sum_{n=1}^{\infty} B_{mn}^p \frac{\Psi_n^{(2)}(z)}{\beta_n K'_m(\beta_n a_j)} \sum_{s=-\infty}^{\infty} I_s(\beta_n a_j) K_{m-s}(\beta_n R_{jp}) e^{is\theta_p} e^{i(m-s)\alpha_{jp}}. \end{aligned} \quad (7.3.11)$$

Similarly matching $\partial\phi_j^I/\partial r_j = \partial\phi^{II}/\partial r_j$ on $r_j = a_j, j = 1, \dots, P$, we have

$$\begin{aligned} \sum_{m=-\infty}^{\infty} \sum_{n=0}^{\infty} A_{mn}^j \Psi_n^{(1)}(z) e^{im\theta_j} = & \sum_{m=-\infty}^{\infty} \sum_{n=1}^{\infty} B_{mn}^j \Psi_n^{(2)}(z) e^{im\theta_j} \\ & + \sum_{\substack{p=1 \\ p \neq j}}^P \sum_{m=-\infty}^{\infty} \sum_{n=1}^{\infty} B_{mn}^p \frac{\Psi_n^{(2)}(z)}{K'_m(\beta_n a_j)} \sum_{s=-\infty}^{\infty} I'_s(\beta_n a_j) K_{m-s}(\beta_n R_{jp}) e^{is\theta_p} e^{i(m-s)\alpha_{jp}}. \end{aligned} \quad (7.3.12)$$

We can convert (7.3.11) and (7.3.12) into an infinite system of linear algebraic equations by multiplying each by $\Psi_t^{(1)}(z) e^{-iw\theta_j}, t \in \mathbb{N}_0, w \in \mathbb{Z}, j = 1, \dots, P$, and integrating over

$z = 0, d/2, \theta_j = 0, 2\pi$. From (7.3.11) and (7.3.12) we find

$$A_{wt}^j \frac{I_w(\alpha_t a_j)}{\alpha_t I'_w(\alpha_t a_j)} = \sum_{n=1}^{\infty} B_{wt}^j \frac{K_w(\beta_t a_j) d_{nt}}{\beta_t K'_w(\beta_t a_j)} + \sum_{\substack{p=1 \\ p \neq j}}^P \sum_{m=-\infty}^{\infty} \sum_{n=1}^{\infty} B_{mn}^p \frac{d_{nt} I_w(\beta_n a_j) K_{m-w}(\beta_n R_{jp}) e^{i(m-w)\alpha_{jp}}}{\beta_n K'_m(\beta_n a_j)}, \quad (7.3.13)$$

and

$$A_{wt}^j = \sum_{n=1}^{\infty} B_{wt}^j d_{nt} + \sum_{\substack{p=1 \\ p \neq j}}^P \sum_{m=-\infty}^{\infty} \sum_{n=1}^{\infty} B_{mn}^p \frac{d_{nt} I'_w(\beta_n a_j) K_{m-w}(\beta_n R_{jp}) e^{i(m-w)\alpha_{jp}}}{K'_m(\beta_n a_j)}, \quad (7.3.14)$$

where $t \in \mathbb{N}_0$, $w \in \mathbb{Z}$, $j = 1, \dots, P$ in both cases and from (3.4.8),

$$d_{nt} = \frac{2}{d} \int_0^{d/2} \Psi_n^{(2)}(z) \Psi_t^{(1)}(z) dz = \frac{4\nu_n(-1)^t}{d(\mu_t^2 - \nu_n^2)}. \quad (7.3.15)$$

Eliminating A_{wt}^j from both (7.3.13) and (7.3.14) we obtain

$$\begin{aligned} & \frac{I_w(\alpha_t a_j)}{\alpha_t I'_w(\alpha_t a_j)} \left(\sum_{n=1}^{\infty} B_{wt}^j d_{nt} + \sum_{\substack{p=1 \\ p \neq j}}^P \sum_{m=-\infty}^{\infty} \sum_{n=1}^{\infty} B_{mn}^p \frac{d_{nt} I'_w(\beta_n a_j) K_{m-w}(\beta_n R_{jp}) e^{i(m-w)\alpha_{jp}}}{K'_m(\beta_n a_j)} \right) \\ &= \sum_{n=1}^{\infty} B_{wt}^j \frac{K_w(\beta_t a_j) d_{nt}}{\beta_t K'_w(\beta_t a_j)} \sum_{\substack{p=1 \\ p \neq j}}^P \sum_{m=-\infty}^{\infty} \sum_{n=1}^{\infty} B_{mn}^p \frac{d_{nt} I_w(\beta_n a_j) K_{m-w}(\beta_n R_{jp}) e^{i(m-w)\alpha_{jp}}}{\beta_n K'_m(\beta_n a_j)}, \end{aligned} \quad (7.3.16)$$

which can be rearranged as

$$\begin{aligned} & \sum_{n=1}^{\infty} B_{wt}^j d_{nt} \left(\frac{I_w(\alpha_t a_j)}{\alpha_t I'_w(\alpha_t a_j)} - \frac{K_w(\beta_t a_j)}{\beta_t K'_w(\beta_t a_j)} \right) \\ & + \sum_{\substack{p=1 \\ p \neq j}}^P \sum_{m=-\infty}^{\infty} \sum_{n=1}^{\infty} B_{mn}^p \frac{d_{nt} K_{m-w}(\beta_n R_{jp}) I'_w(\beta_n a_j) e^{i(m-w)\alpha_{jp}}}{K'_m(\beta_n a_j)} \\ & \quad \times \left(\frac{I_w(\alpha_t a_j)}{\alpha_t I'_w(\beta_t a_j)} - \frac{I_w(\beta_n a_j)}{\beta_n I'_w(\beta_n a_j)} \right) = 0, \end{aligned} \quad (7.3.17)$$

where $t \in \mathbb{N}_0$, $w \in \mathbb{Z}$, and $j = 1, \dots, P$. If we define

$$X_{wntj} = d_{nt} \left(\frac{I_w(\alpha_t a_j)}{\alpha_t I'_w(\alpha_t a_j)} - \frac{K_w(\beta_t a_j)}{\beta_t K'_w(\beta_t a_j)} \right), \quad (7.3.18)$$

and

$$Y_{wntjmp} = \frac{d_{nt} K_{m-w}(\beta_n R_{jp}) I'_w(\beta_n a_j) e^{i(m-w)\alpha_{jp}}}{K'_m(\beta_n a_j)} \left(\frac{I_w(\alpha_t a_j)}{\alpha_t I'_w(\beta_t a_j)} - \frac{I_w(\beta_n a_j)}{\beta_n I'_w(\beta_n a_j)} \right) \quad (7.3.19)$$

we can simplify the left-hand side of (7.3.17) to

$$\sum_{\substack{p=1 \\ p \neq j}}^P \sum_{m=-\infty}^{\infty} \sum_{n=1}^{\infty} B_{mn}^p Z_{wntjmp} = 0 \quad (7.3.20)$$

where

$$Z_{wntjmp} = \begin{cases} X_{wntj}\delta_{mw} & p = j, \\ Y_{wntjmp} & p \neq j, \end{cases} \quad (7.3.21)$$

with δ_{mw} being the Kronecker delta and $t \in \mathbb{N}_0$ $w \in \mathbb{Z}$, and $j = 1, \dots, P$ in all cases.

We shall solve (7.3.21) by truncating m and w with a truncation parameter $\pm M$, n and $t + 1$ with a truncation parameter N , and write

$$\lambda_1 = n + N(m + M) + N(2M + 1)(p - 1), \quad (7.3.22)$$

$$\lambda_2 = 1 + t + N(w + M) + N(2M + 1)(j - 1), \quad (7.3.23)$$

so that any positive integer λ_i , $\lambda_i = 1, \dots, N(2M + 1)P$, corresponds to a unique triple, (n, m, p) for $i = 1$, or (t, w, j) for $i = 2$. To find a solution of (7.3.21) we are required to find frequencies kd so that the determinant of the matrix Z_{λ_1, λ_2} is zero.

We now consider the solution for different problems, starting with the case of one disc on the centreline.

7.4 Trapped modes below the first cut-off

7.4.1 One disc on the centreline

In this section we consider a single disc of radius a placed on the centreline of a planar waveguide of total width d , as shown in figure 7.2. We can use the work in the previous section if we take $P = 1$. If we take $P = 1$ then the matrix Z_{λ_1, λ_2} is simplified considerably as no Y_{λ_1, λ_2} terms appear, only X_{mnt1} . If we replace w by $-w$ in (7.3.18) we find that $X_{wntj} = X_{(-w)ntj}$, and so we only need to consider non-negative values of m (or w) for the single disc case.

Results

For the results computed in this section truncation parameters $N = 5$ and $M = 3$ were used. The differences between the results presented here and the results obtained using a truncation parameter $N = 10$ are less than 10^{-3} . The value of M has to be chosen sufficiently large enough so that all the possible trapped modes can be found. If M is chosen to be 3 then all the modes are found up to $a/d \approx 1$. If $a/d > 1$ a larger value of M is required to find all the trapped modes.

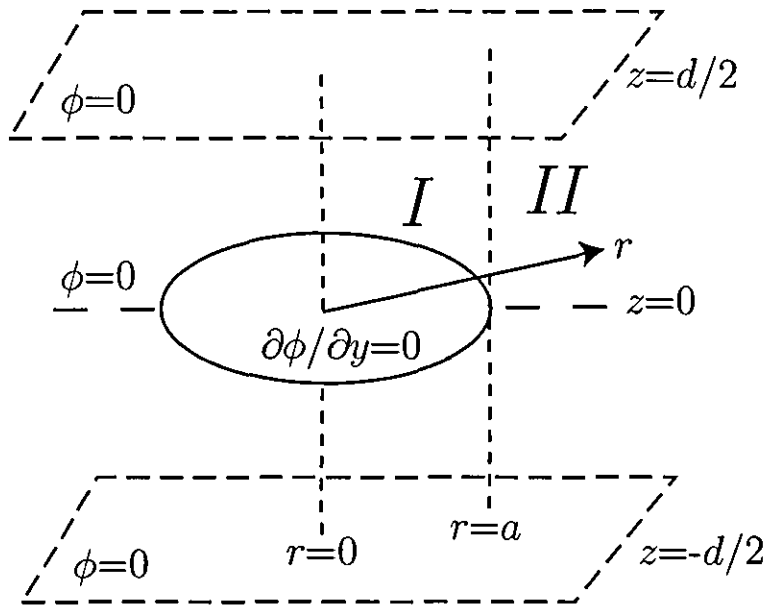


Figure 7.2: Definition sketch.

In figure 7.3 trapped-mode wavenumbers kd/π are plotted against a/d for $m = 0, \dots, \pm M$. The solid lines correspond to $m = 0$, the dashed lines to $m = \pm 1$, the dotted lines to $m = \pm 2$ and the dot-dashed lines to $m = \pm 3$. We see that as a/d increases the trapped modes appear from the cut-off $kd = 2\pi$ and tend to the cut-off $kd = \pi$.

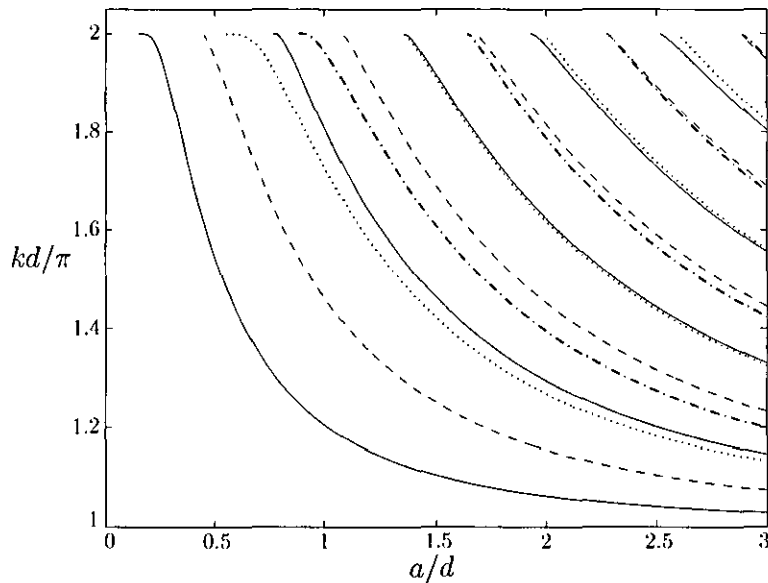


Figure 7.3: Trapped-mode wavenumbers, kd/π , plotted against a/d . The solid lines correspond to $m = 0$, the dashed lines to $m = \pm 1$, the dotted lines to $m = \pm 2$ and the dot-dashed lines to $m = \pm 3$.

The results plotted show that the $m = 0$ modes exist for all values of the radius except when the radius is small and as a/d increases the number of modes increases. As the value of $|m|$ is increased similar features occur and the value of a/d below which modes do not occur is increased for consecutive values of $|m|$.

The plot shown in figure 7.3 is complete when $a/d \leq 1$, but as a/d is increased a higher value of M must be chosen to produce all possible modes.

7.4.2 Two discs on the centreline

In this section we consider the case of two thin circular discs placed on the centreline of the waveguide. There are two problems to consider in this section, the case when both discs are identical and the case when they are not. When considering two discs the resulting trapped-mode frequencies should be independent of the angle between the centres of the two discs (α_{12} and α_{21} , in figure 7.1). If we multiply each term in the matrix Z_{wntjmp} defined in (7.3.21) by $\exp(-i(m\alpha_{jp} - w\alpha_{pj}))$, we find that we can remove the angle dependence from the Y_{wntjmp} terms defined by (7.3.19) and the X_{wntj} terms in (7.3.18) remain the same.

For the results provided in this section truncation parameters $N = 5$ and $M = 3$ were used to allow a comparison to be made with results in the previous section.

Equal radii discs

We consider the case of two identical thin circular discs placed on the centreline of the waveguide.

Figure 7.4 shows the trapped-mode wavenumbers, kd/π plotted against R/d for two identical circular thin discs of radii $a/d = 1$. The value R/d is the non-dimensional distance between the centres of the two discs. The dotted lines are the trapped-mode wavenumbers from the single disc case when $a/d = 1$ and are labelled with the appropriate values of m . The dotted lines can be interpreted as the case when $R/d \rightarrow \infty$ and the dashed line is the upper cut-off $kd = 2\pi$.

The value $a/d = 1$ is chosen because if we then use the truncation parameter $M = 3$ all possible modes will appear on the plot, as mentioned in the previous section. If we took a larger value of a/d we would have to use a larger truncation parameter M to guarantee all modes appear.

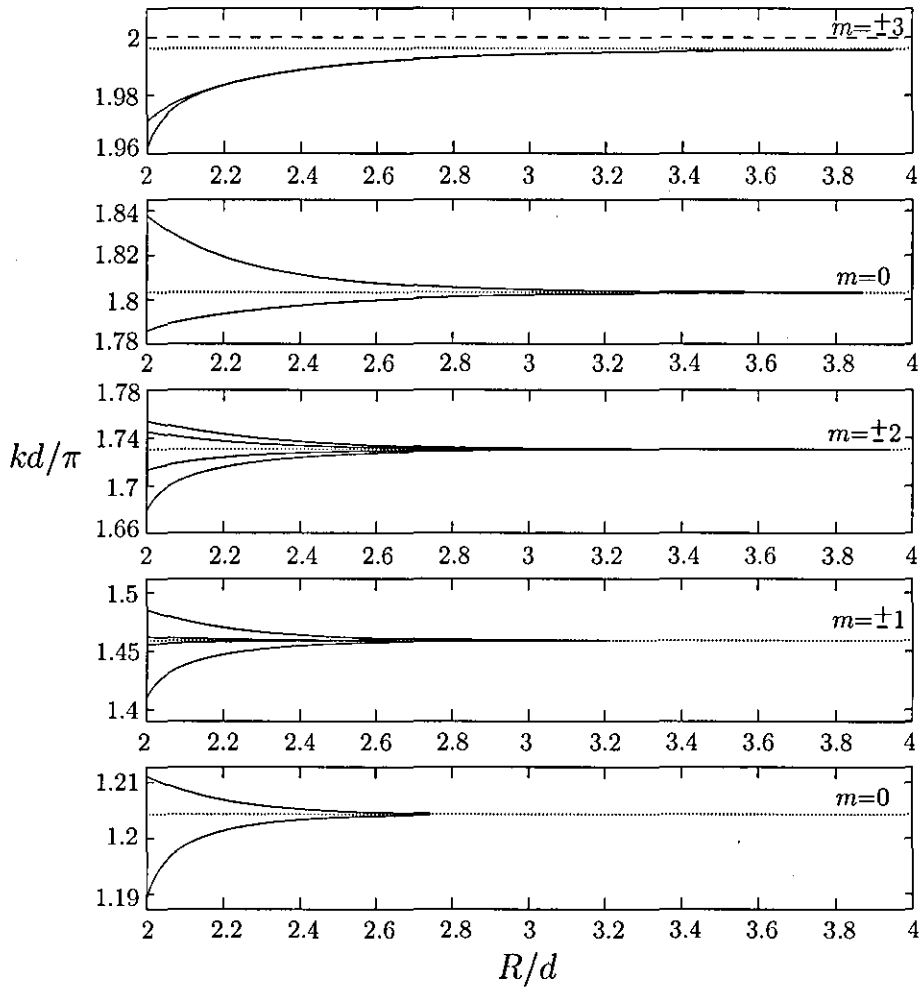


Figure 7.4: Trapped-mode wavenumbers, kd/π , plotted against R/d for the case of two identical thin discs of radii $a/d = 1$. The dotted lines correspond to the trapped modes from the single disc case with $a/d = 1$ and are labelled with the appropriate values of m . The dashed line corresponds to the upper cut-off.

We see that when the two discs are touching, i.e. when $R/d = 2$, there are fourteen trapped modes. We have two modes around each dotted line corresponding to $m = 0$ and four modes around the other dotted lines (two for the positive value of m and two for the negative value of m). The exception occurs when $m = \pm 3$ as this mode is close to the upper cut-off and so only a single mode appears below the dotted line for each m . As the value of R/d is increased, which means that the discs are moved apart, we find that each pair of modes converges towards the limiting case.

Different radii discs

We now consider the case of two different thin circular discs placed on the centreline of the waveguide.

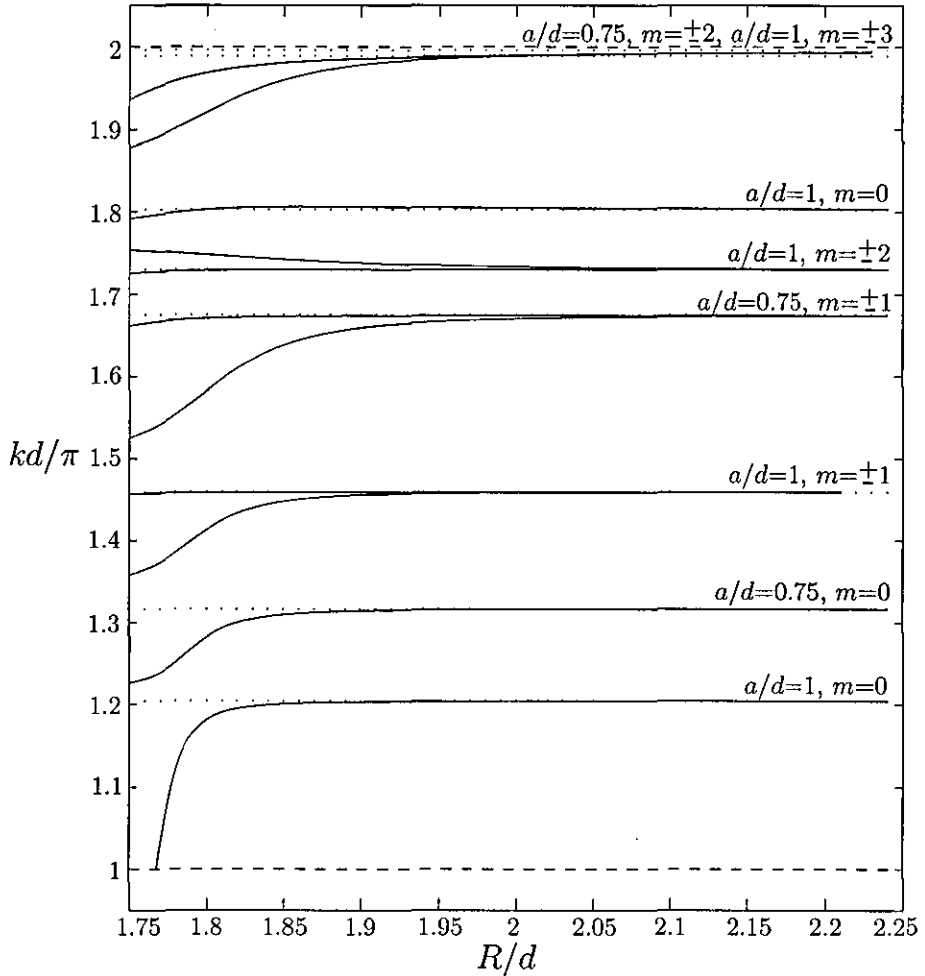


Figure 7.5: Trapped-mode wavenumbers, kd/π , plotted against R/d for the case of two thin discs of radii $a/d = 1$ and $a/d = 0.75$. The dotted lines correspond to the trapped modes from the single disc case with $a/d = 1$ and $a/d = 0.75$ and are labelled with the appropriate values of m . The dashed lines correspond to the upper and lower cut-offs.

Figure 7.5 shows the trapped-mode wavenumbers, kd/π plotted against R/d for two circular thin discs of radii $a/d = 1$ and $a/d = 0.75$. The dotted lines are the trapped-mode wavenumbers from the single disc cases when $a/d = 1$ and $a/d = 0.75$ and are labelled with the appropriate values of m . The dotted lines can be interpreted as the case when $R/d \rightarrow \infty$ and the dashed lines are the upper and lower cut-offs.

If we take discs of radii $a/d = 1$ and $a/d = 0.75$ then we can again use the truncation

parameter $M = 3$ and figure 7.5 will be complete. Between the two cut-offs we find that there are five modes from the single disc case with $a/d = 1$ and three modes from the single disc case when $a/d = 0.75$.

From figure 7.5 we find that a single trapped mode exists for each value of m from the single disc modes, apart from the highest frequency mode ($a/d = 0.75$, $m = \pm 2$) as this is very close to the cut-off and the lowest frequency mode ($a/d = 1$, $m = 0$) below $R/d \approx 1.768$.

When the two discs are touching, i.e. when $R/d = 1.75$, the modes appear away from the modes from the single disc cases. As the discs are moved further away from each other the modes tend towards the cases of single discs on the centreline.

7.4.3 Laterally coupled planar waveguides

Using the work in the previous sections we can formulate a solution for the case of a laterally coupled planar waveguide. The waveguide consists of two parallel planar waveguides of widths b and $d - b$ coupled laterally by a small circular hole of radius a in the common boundary. As in chapter 2 we assume for convenience that $b > d/2$.

As with the waveguide considered in this chapter 2 this waveguide has a physical relevance in quantum mechanics. Exner and Vugalter (1996) considered the case when the hole was sufficiently small so that only one eigenvalue occurred below the essential spectrum. The authors were then able to provide upper and lower asymptotic bounds on the gap between the eigenvalue and the essential spectrum.

Formulation

We introduce circular cylindrical polar coordinates (r, θ, z) so that the waveguide is axisymmetric about $r = 0$ and the planes lie at $z = 0$, $z = b$ and $z = d$. We have to find a non-trivial function $\phi(x, y)$ which satisfies the Helmholtz equation within the waveguide

$$(\nabla^2 + k^2)\phi = 0, \quad 0 < z < d, \quad r > 0 \text{ except on } x = b, \quad r > a, \quad (7.4.1)$$

subject to the boundary conditions

$$\phi = 0 \text{ on } z = 0, r > 0, \quad (7.4.2)$$

$$\phi = 0 \text{ on } z = b, r > a, \quad (7.4.3)$$

$$\phi = 0 \text{ on } z = d, r > 0, \quad (7.4.4)$$

and a radiation condition specifying that no waves propagate out to infinity,

$$\phi \rightarrow 0 \text{ as } r \rightarrow \infty. \quad (7.4.5)$$

As in chapter 2 we divide the region into three parts. Region *I* is the region above the plane outside the hole, i.e. $\{r, \theta, z : r > a, b < z < d\}$, region *II* is below the plane outside the hole, that is $\{r, \theta, z : r > a, 0 < z < b\}$ and region *III* is the hole, that is $\{r, \theta, z : r < a, 0 < z < d\}$. As the geometry is axisymmetric about $r = 0$, we are able to look for a mode with angular variation $\cos m\theta$, $m \in \mathbb{N}_0$. We can therefore represent the function $\phi_i(r, \theta, z)$ by a function $\hat{\phi}_i(r, z) \cos m\theta$, ($i = 1, 2, 3$), in each region and apply the following continuity conditions

$$\hat{\phi}_i = \hat{\phi}_3, \quad \frac{\partial \hat{\phi}_i}{\partial r} = \frac{\partial \hat{\phi}_3}{\partial r}, \quad \text{on } L_i, \quad i = 1, 2, \quad (7.4.6)$$

where L_1 is $r = a, b < z < d$, L_2 is $r = a, 0 < z < b$ and we write L_3 for $L_1 \cup L_2$.

Following section 7.3 we find that the eigenvalue expansions in each region are

$$\hat{\phi}_1(r, z) = \sum_{n=1}^{\infty} U_{mn}^{(1)} \frac{K_m(\alpha_n r) \Psi_n^{(1)}(z)}{\alpha_n K'_m(\alpha_n a)}, \quad (7.4.7)$$

$$\hat{\phi}_2(r, z) = \sum_{n=1}^{\infty} U_{mn}^{(2)} \frac{K_m(\beta_n r) \Psi_n^{(2)}(z)}{\beta_n K'_m(\beta_n a)}, \quad (7.4.8)$$

$$\hat{\phi}_3(r, z) = \sum_{n=0}^{\infty} U_{mn}^{(3)} \frac{I_m(\gamma_n r) \Psi_n^{(3)}(z)}{\gamma_n I'_m(\gamma_n a)}, \quad (7.4.9)$$

where $\alpha_n, \beta_n, \gamma_n$ and $\Psi_n^{(i)}(z)$, $i = 1, 2, 3$, are defined by (2.3.31)–(2.3.33) and (2.3.27)–(2.3.29). As in section 2.4 we anticipate a necessary condition for the existence of trapped modes to be

$$\pi < kd < \frac{d\pi}{b}, \quad (7.4.10)$$

as γ_0 will be purely imaginary whereas α_n, β_n and γ_n , $n \in \mathbb{N}$, will all be real and positive. The mode corresponding to γ_0 will therefore be oscillatory in region *III* and all the other modes will decay away from the hole. We now apply the continuity conditions (7.4.6).

Matching $\hat{\phi}_i = \hat{\phi}_3$ on L_i , $i = 1, 2$, we have

$$\sum_{n=0}^{\infty} U_{mn}^{(3)} \frac{I_m(\gamma_n a)}{\gamma_n I'_m(\gamma_n a)} \Psi_n^{(3)}(z) = \begin{cases} \sum_{n=1}^{\infty} U_{mn}^{(1)} \frac{K_m(\alpha_n a)}{\alpha_n K'_m(\alpha_n a)} \Psi_n^{(1)}(z), & z \in L_1, \\ \sum_{n=1}^{\infty} U_{mn}^{(2)} \frac{K_m(\beta_n a)}{\beta_n K'_m(\beta_n a)} \Psi_n^{(2)}(z), & z \in L_2. \end{cases} \quad (7.4.11)$$

Similarly matching $\partial \hat{\phi}_i / \partial x = \partial \hat{\phi}_3 / \partial x$ on L_i , $i = 1, 2$, we arrive at

$$\sum_{n=0}^{\infty} U_{mn}^{(3)} \Psi_n^{(3)}(z) = \begin{cases} \sum_{n=1}^{\infty} U_{mn}^{(1)} \Psi_n^{(1)}(z), & z \in L_1, \\ \sum_{n=1}^{\infty} U_{mn}^{(2)} \Psi_n^{(2)}(z), & z \in L_2. \end{cases} \quad (7.4.12)$$

We can convert (7.4.11) and (7.4.12) into an infinite system of linear algebraic equations by multiplying each by $\Psi_s^{(3)}$, $s \in \mathbb{N}_0$, and integrating over L_3 . From (7.4.11) and (7.4.12) we find

$$U_{ms}^{(3)} \frac{I_m(\gamma_s a)}{\gamma_s I'_m(\gamma_s a)} = \sum_{n=1}^{\infty} \frac{U_{mn}^{(1)} K_m(\alpha_n a)}{\alpha_n K'_m(\alpha_n a)} d_{ns} + \sum_{n=1}^{\infty} \frac{U_{mn}^{(2)} K_m(\beta_n a)}{\beta_n K'_m(\beta_n a)} e_{ns}, \quad s \in \mathbb{N}_0, \quad (7.4.13)$$

and

$$U_{ms}^{(3)} = \sum_{n=1}^{\infty} U_{mn}^{(1)} d_{ns} + \sum_{n=1}^{\infty} U_{mn}^{(2)} e_{ns}, \quad s \in \mathbb{N}_0, \quad (7.4.14)$$

where d_{ns} and e_{ns} are given by (2.4.10) and (2.4.12).

Eliminating $U_{ms}^{(3)}$ from (7.4.14) and (7.4.13) we obtain

$$\sum_{n=1}^{\infty} U_{mn}^{(1)} d_{ns} \left(\frac{I_m(\gamma_n a)}{\gamma_n I'_m(\gamma_n a)} - \frac{K_m(\alpha_n a)}{\alpha_n K'_m(\alpha_n a)} \right) + \sum_{n=1}^{\infty} U_{mn}^{(2)} e_{ns} \left(\frac{I_m(\gamma_n a)}{\gamma_n I'_m(\gamma_n a)} - \frac{K_m(\beta_n a)}{\beta_n K'_m(\beta_n a)} \right) = 0, \quad s \in \mathbb{N}_0. \quad (7.4.15)$$

We shall solve equation (7.4.15) by truncating the value of n and $s+1$ with a truncation parameter N . We therefore have to find the values of kd so that the determinant of a $2N \times 2N$ matrix is zero for each value of $m \in \mathbb{N}_0$.

Results

For the results shown in this section we use a truncation parameter $N = 5$.

Figure 7.6 shows a typical set of trapped-mode wavenumbers, kd/π , plotted against a/d when $b/d = 0.6$. The solid lines correspond to the modes when $m = 0$, the dashed lines are when $m = 1$, the dotted lines are when $m = 2$ and the dot-dashed lines are when $m = 3$. As the value of a/d is increased the trapped modes appear from the upper cut-off $kd = 5\pi/3$ and tend to the lower cut-off $kd = \pi$. The results show that that

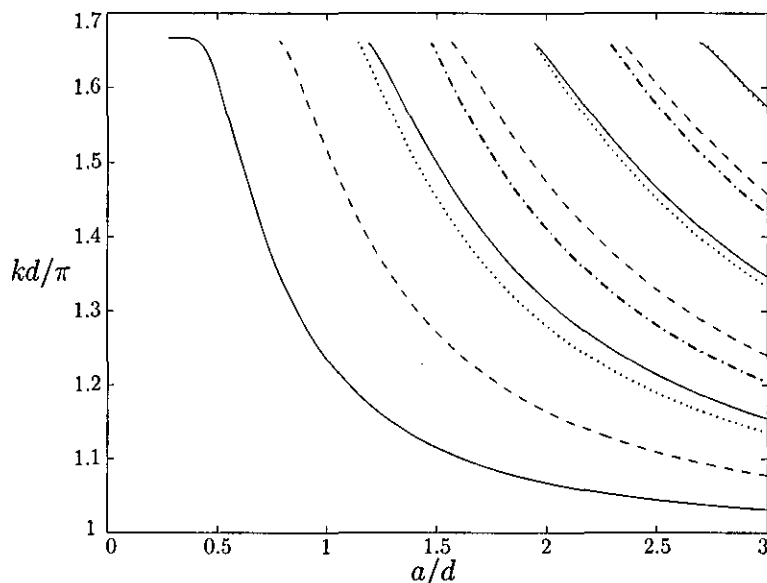


Figure 7.6: Trapped-mode wavenumbers, kd/π , plotted against a/d when $b/d = 0.6$. The solid lines correspond to $m = 0$, the dashed lines to $m = 1$, the dotted lines to $m = 2$ and the dot-dashed lines to $m = 3$.

trapped modes occur for all a/d except when the hole is small for $m = 0$. As the value of m is increased the value of a/d below which modes do not exist also increases.

In the paper by Exner and Vugalter (1997), the authors speculated that the asymptotic behaviour of the ground-state eigenvalue, kd , for small a is

$$kd(a) \approx \left(\frac{d}{b}\right) \left(\pi^2 - \exp(-c_1 a^{-3})\right)^{\frac{1}{2}}, \quad (7.4.16)$$

where c_1 is a positive constant. It is difficult to compare this conjecture to the results in this section as trapped modes were not found when a/d was below about 0.25.

It is fairly simple to extend the work above and consider the case of a pair of planar layers coupled laterally by a number of holes.

7.5 Summary

In this chapter we have considered the problem of a pair of planar layers laterally coupled by a number of circular holes. We initially considered the case when the planar layers are of equal width, a problem equivalent to that of an array of thin circular discs placed parallel to the walls and on the centreline of a planar waveguide. The planar waveguide had Dirichlet conditions placed on the walls and the thin discs were placed on

the centreline. The symmetry of the resulting problem allowed us to place a Neumann condition on the discs, a Dirichlet condition on the rest of the plane containing the discs and consider only the upper half-plane.

The problem was formulated in section 7.3 for a general array of P discs using a matched eigenfunction expansion method. The frequency was restricted so that one mode became wave-like local to each disc (this frequency restriction is the same as that found in chapter 3 as the geometry is the same in the z -axis). To find the trapped-mode wavenumbers we have to find the zeros of a determinant of an infinite matrix, which is done by truncation.

A number of results are presented in this chapter. In section 7.4.1 we consider the case of one disc on the centreline. For the one disc case we only need to consider $m \in \mathbb{N}_0$ as it is shown that the modes for negative m are equivalent to the modes for positive m . In section 7.4.2 we consider the cases of two identical discs and two different discs on the centreline. We find that when the discs are far apart the trapped modes are equivalent to those occurring in the single disc cases. When the discs are moved closer together we find that the total number of trapped modes present is independent of the distance between the centres.

In section 7.4.3 we return to the case when the planar layers have different widths and are coupled by a single hole. We reformulate the problem using ideas found in section 7.3 and compute trapped-mode frequencies with different angular variations.

Chapter 8

Annular waveguide.

8.1 Introduction to the problem.

One application explicitly mentioned in Parker and Stoneman (1989) is the case of axial-flow compressors in turbo-machinery. The geometry of these compressors is highly complicated but can be thought of, to a first approximation, as an infinite cylinder with annular cross-section containing thin radial fins of finite length in the axial direction distributed evenly around the guide.

The acoustic resonances that occur in engineering applications are excited by vortex-shedding from the blades, which will only occur if a mean flow is present. Work by Koch (1983) however has shown that for a flat plate cascade the resonant frequencies in the presence of mean flow are very close to those in zero mean flow, provided the Mach number of the flow is small.

A recent paper by Linton and McIver (1998b) presented a method, based on matched eigenfunction expansions, to determine the frequencies of trapped modes that occur in a circular cylindrical waveguide in the presence of a number of thin radial fins of finite length. The authors found that there were significant differences in the modes possible if the number of plates was even or odd and that when the number of fins passed a crucial value, a change in the qualitative behaviour of the resonance frequencies occurs. The paper also presents approximate formulas for low-frequency modes when the number of fins becomes large.

This chapter extends work done by Linton and McIver (1998b) by replacing the circular cross-section by an annular one to examine the possibility of trapped modes in the geometry discussed previously.

We begin in section 8.2 by reformulating the problem for the annular region. The results computed from the formulation are then discussed in section 8.3, together with curves displaying the variation of the frequency kd with blade length a/d , where d is the outer radius of the annular cross-section. We see that as the inner radius of the annular region and the number of blades increases past certain values a fundamental change in the curves occurs. We also show an approximate formula for the frequencies of low-frequency modes as the number of blades becomes large, and also see how varying the inner radius changes the frequencies. Conclusions are drawn in section 8.4.

8.2 Formulation

We consider a cylindrical guide with an annular cross-section of inner radius b and outer radius d and use cylindrical polar coordinates (r, θ, x) with the x -axis along centre of the guide. We consider $L(\geq 1)$ finite length identical thin plates placed at angles $\beta_i = 2i\pi/L, i = 0, \dots, L - 1$, around the guide. The plates are located at $\{\theta = \beta_i, b < r < d, -a < x < a\}$ so that the resulting geometry is symmetric about $x = 0$. Figure 8.1 shows a schematic representation of the configuration under investigation.

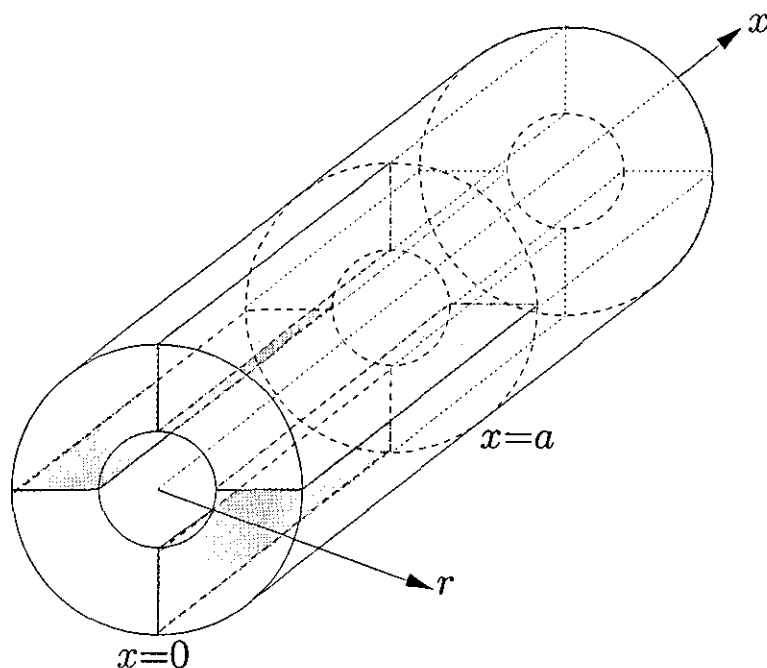


Figure 8.1: Definition sketch.

Initially we shall seek a solution which is even (symmetric) about $x = 0$, by consid-

ering the semi-infinite sector $\Omega = \{r, \theta, x : b < r < d, 0 < \theta < \beta_1, x > 0\}$ and seeking a function $\phi(x, y)$ which satisfies

$$\frac{\partial \phi}{\partial x} = 0 \text{ on } x = 0, \quad b < r < d. \quad (8.2.1)$$

The function $\phi(x, y)$ must also satisfy the Helmholtz equation within the sector

$$(\nabla^2 + k^2) \phi = 0, \quad \phi \in \Omega, \quad (8.2.2)$$

and Neumann boundary conditions on the inner and outer cylinders and the blades,

$$\frac{\partial \phi}{\partial r} = 0 \text{ on } r = b \text{ and } r = d, \quad (8.2.3)$$

$$\frac{\partial \phi}{\partial \theta} = 0 \text{ on } \theta = 0 \text{ and } \theta = \beta_1, \quad x < a. \quad (8.2.4)$$

In reality trapped modes are excited due to vortex shedding from the trailing edges of plates and this is consistent with an antisymmetry boundary condition on the plane which is an extension of the plates down the guide, (see Parker (1966) and Parker (1967)). Thus we can add an antisymmetry condition about the planes $\theta = 0$ and $\theta = \beta_1$:

$$\phi = 0 \text{ on } \theta = 0 \text{ and } \theta = \beta_1, \quad x > a. \quad (8.2.5)$$

The case of symmetry about these planes is uninteresting as these boundary conditions lead to a simple guide whose cross-section is an annular sector with Neumann conditions on all sides, and hence to a problem where trapped modes do not exist.

We require the trapped modes to be localised around the region of the blades and hence the solution must decay at infinity and so

$$\phi \rightarrow 0 \text{ as } x \rightarrow \infty. \quad (8.2.6)$$

We extend the solution to (8.2.2)–(8.2.6) into a solution in the whole semi-infinite guide $x > 0$ by writing $\alpha = n\beta_1 + \gamma$, for $\alpha \in [0, 2\pi)$, where $n \in \mathbb{N}_0$, and $\gamma \in [0, \beta_1)$, and defining

$$\phi|_{\theta=\alpha} = \begin{cases} -\phi|_{\theta=\beta_1-\gamma} & n \text{ odd,} \\ \phi|_{\theta=\gamma} & n \text{ even,} \end{cases} \quad (8.2.7)$$

which ensures continuity of ϕ between neighbouring sectors, although ϕ is allowed to be discontinuous across the plates themselves.

Figure 8.2 illustrates the above extension when $L = 4$ and with symmetry about the mid-plane of the sector. The plus/minus signs in figure 8.2 signify positive or negative values of ϕ . Each positive sector has negative adjacent sectors and vice-versa. For the case $x < a$ the solid horizontal and vertical lines represent the blades. For the case of $x > a$ these solid lines represent the planes across which ϕ changes sign, i.e. from (8.2.5) $\phi = 0$ on the planes.

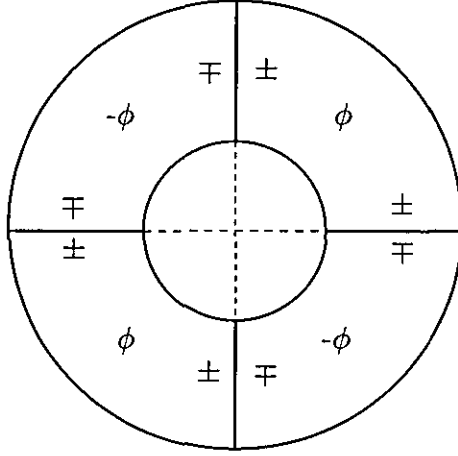


Figure 8.2: Continuity of ϕ throughout the fluid, but not necessarily across the plates. The figure shows the case when $L = 4$ of symmetry about the mid-plane of the sector.

To ensure continuity of the derivative of ϕ , it follows from (8.2.7) that

$$\frac{\partial \phi}{\partial \theta} \Big|_{\theta=\alpha} = \begin{cases} \frac{\partial \phi}{\partial \theta} \Big|_{\theta=\beta_1-\gamma} & n \text{ odd}, \\ \frac{\partial \phi}{\partial \theta} \Big|_{\theta=\gamma} & n \text{ even}. \end{cases} \quad (8.2.8)$$

Putting $\alpha = 2\pi$ into (8.2.8) we find that $n = L$ and $\gamma = 0$, and so

$$\frac{\partial \phi}{\partial \theta} \Big|_{\theta=2\pi} = \begin{cases} \frac{\partial \phi}{\partial \theta} \Big|_{\theta=\beta_1} & L \text{ odd}, \\ \frac{\partial \phi}{\partial \theta} \Big|_{\theta=0} & L \text{ even}. \end{cases} \quad (8.2.9)$$

Equation (8.2.9) shows that when L is even continuity of $\partial\phi/\partial\theta$ occurs, but when L is odd we need to ensure that $\partial\phi/\partial\theta$ has the same value on $\theta = 0$ and $\theta = \beta_1$ in $x > a$. Note that any ϕ that does not satisfy this condition will result in trapped modes that are a solution to the sector problem (8.2.2)–(8.2.6), but not for the full annular cylindrical guide.

Expanding the Helmholtz equation (8.2.2), in cylindrical polar coordinates (r, θ, x) gives

$$\frac{1}{r} \frac{\partial}{\partial r} \left(r \frac{\partial \phi}{\partial r} \right) + \frac{1}{r^2} \frac{\partial^2 \phi}{\partial \theta^2} + \frac{\partial^2 \phi}{\partial x^2} + k^2 \phi = 0, \quad (8.2.10)$$

and we seek solutions of the form

$$\phi(r, \theta, x) = U(r)V(\theta)W(x). \quad (8.2.11)$$

Substituting (8.2.11) into (8.2.10) we obtain

$$\frac{1}{Ur} \frac{\partial}{\partial r} \left(r \frac{\partial U}{\partial r} \right) + \frac{1}{Vr^2} \frac{\partial^2 V}{\partial \theta^2} + k^2 = -\frac{1}{W} \frac{\partial^2 W}{\partial x^2}. \quad (8.2.12)$$

Since the left hand side is a function of r and θ , whereas the right-hand side is a function of x only both sides must equal the same constant. As we require the solutions to decay as $x \rightarrow \infty$ we select the constant to be $-\alpha^2$, say with $\alpha > 0$. For the inner region $x < a$ we use the boundary condition (8.2.1) and hence

$$W(x) = A \cosh \alpha x, \quad x < a. \quad (8.2.13)$$

For the outer region $x > a$ we use (8.2.6) and find

$$W(x) = B e^{-\alpha x}, \quad x > a. \quad (8.2.14)$$

If we multiply (8.2.12) by r^2 , the term $\frac{1}{V} \frac{\partial^2 V}{\partial \theta^2}$ is a function of θ only and hence can be set equal to a constant. The conditions (8.2.4) and (8.2.5) require the solution and its derivative to be zero at $\theta = 0$ and $\theta = \beta_1$, so we need trigonometric solutions and hence the constant is chosen to be $-\sigma^2$, with $\sigma > 0$. For $x < a$ we use (8.2.4) to produce

$$V(\theta) = A \cos \sigma(m)\theta, \quad (8.2.15)$$

where

$$\sigma(m) = m\pi/\beta_1 = mL/2, \quad m \in \mathbb{N}_0. \quad (8.2.16)$$

Similarly in the outer region $x > a$ we use (8.2.5) and find that

$$V(\theta) = B \sin \sigma(m)\theta, \quad m \in \mathbb{N}. \quad (8.2.17)$$

If we substitute the chosen constants back into (8.2.12) we have

$$\frac{1}{rU} \frac{dU}{dr} + \frac{1}{U} \frac{d^2U}{dr^2} + k^2 + \alpha^2 - \frac{\sigma(m)^2}{r^2} = 0. \quad (8.2.18)$$

If we let $\lambda^2 = k^2 + \alpha^2$, $r^* = \lambda r$ and $U^*(r^*) = U(r)$, then (8.2.18) becomes

$$\frac{\partial}{\partial r^*} \left(r^* \frac{\partial U_1^*}{\partial r^*} \right) + U_1^* \left(1 - \frac{\sigma(m)^2}{r^{*2}} \right) = 0, \quad (8.2.19)$$

which is Bessel's equation for $U^*(r^*)$ of order $\sigma(m)$ and has general solution

$$U^*(r^*) = U(r) = A J_{\sigma(m)}(\lambda r) + B Y_{\sigma(m)}(\lambda r). \quad (8.2.20)$$

Using the first condition in (8.2.3) we obtain

$$U'(\lambda b) = A \lambda J'_{\sigma(m)}(\lambda b) + B \lambda Y'_{\sigma(m)}(\lambda b) = 0. \quad (8.2.21)$$

Substituting (8.2.21) into (8.2.20) and rearranging slightly we have

$$U(\lambda r) = A_1 \left\{ Y'_{\sigma(m)}(\lambda b) J_{\sigma(m)}(\lambda r) - J'_{\sigma(m)}(\lambda b) Y_{\sigma(m)}(\lambda r) \right\}. \quad (8.2.22)$$

Using the second condition we find that

$$U'(\lambda d) = A_1 \lambda \left\{ Y'_{\sigma(m)}(\lambda b) J'_{\sigma(m)}(\lambda d) - J'_{\sigma(m)}(\lambda b) Y'_{\sigma(m)}(\lambda d) \right\} = 0. \quad (8.2.23)$$

If λ is replaced by $\eta_{\sigma(m)n}/b$ and we define $\delta = d/b$, the function $\psi_{mn}(r)$ can be introduced, where $\psi_{01}(r) = 0$ and if $(m, n) \neq (0, 1)$

$$\psi_{mn}(r) = Y'_{\sigma(m)}(\eta_{\sigma(m)n}) J_{\sigma(m)}(\eta_{\sigma(m)n} r/b) - J'_{\sigma(m)}(\eta_{\sigma(m)n}) Y_{\sigma(m)}(\eta_{\sigma(m)n} r/b). \quad (8.2.24)$$

We define $\eta_{01} = 0$, and for $n > 1$ we let η_{0n} be the $(n-1)$ th positive zero of the function $Y'_0(x) J'_0(x\delta) - J'_0(x) Y'_0(x\delta)$. If $m \in \mathbb{N}$, then $\eta_{\sigma(m)n}$ is the n th positive zero of the function $Y'_{\sigma(m)}(x) J'_{\sigma(m)}(x\delta) - J'_{\sigma(m)}(x) Y'_{\sigma(m)}(x\delta)$. Returning to (8.2.12) we have

$$\alpha_{mn} d = \left[(\eta_{\sigma(m)n} \delta)^2 - (kd)^2 \right]^{\frac{1}{2}}. \quad (8.2.25)$$

The eigenvalue expansions in the regions $x < a$ and $x > a$ are

$$\phi(r, \theta, x) = \sum_{m=0}^{\infty} \sum_{n=1}^{\infty} a_{mn} \frac{\cosh \alpha_{mn} x}{\alpha_{mn} \sinh \alpha_{mn} a} \psi_{mn}(r) \cos \sigma(m) \theta, \quad x < a, \quad (8.2.26)$$

$$\phi(r, \theta, x) = \sum_{m=1}^{\infty} \sum_{n=1}^{\infty} b_{mn} \frac{e^{-\alpha_{mn}(x-a)}}{-\alpha_{mn}} \psi_{mn}(r) \sin \sigma(m) \theta, \quad x > a. \quad (8.2.27)$$

The function ϕ defined by (8.2.26) and (8.2.27) satisfies (8.2.3)–(8.2.5) and in order to satisfy (8.2.6), it is essential that all the α_{mn} , $m, n \in \mathbb{N}$ in (8.2.27) are real and positive.

We now match ϕ and the x -derivative across $x = a$ and get

$$\sum_{m=0}^{\infty} \sum_{n=1}^{\infty} a_{mn} \psi_{mn}(r) \cos \sigma(m) \theta = \sum_{m=1}^{\infty} \sum_{n=1}^{\infty} b_{mn} \psi_{mn}(r) \sin \sigma(m) \theta, \quad (8.2.28)$$

$$\sum_{m=0}^{\infty} \sum_{n=1}^{\infty} a_{mn} \frac{\coth \alpha_{mn} a}{\alpha_{mn}} \psi_{mn}(r) \cos \sigma(m) \theta = \sum_{m=1}^{\infty} \sum_{n=1}^{\infty} \frac{b_{mn}}{-\alpha_{mn}} \psi_{mn}(r) \sin \sigma(m) \theta, \quad (8.2.29)$$

with $b < r < d$ and $0 < \theta < \beta_1$ in both cases. We can convert these equations into an infinite system of linear algebraic equations by multiplying the first by $r \psi_{\mu\nu}(r) \sin \sigma(\mu)\theta$, $\mu, \nu \in \mathbb{N}$, the second by $r \psi_{\mu\nu}(r) \cos \sigma(\mu)\theta$, $\mu \in \mathbb{N}_0, \nu \in \mathbb{N}$ and integrating over the sector $b < r < d$ and $0 < \theta < \beta_1$, to give

$$\begin{aligned} \sum_{m=0}^{\infty} \sum_{n=1}^{\infty} \int_{\theta=0}^{\beta_1} \int_{r=b}^d a_{mn} \psi_{mn}(r) \psi_{\mu\nu}(r) \cos \sigma(m)\theta \sin \sigma(\mu)\theta r dr d\theta = \\ \sum_{m=1}^{\infty} \sum_{n=1}^{\infty} \int_{\theta=0}^{\beta_1} \int_{r=b}^d b_{mn} \psi_{mn}(r) \psi_{\mu\nu}(r) \sin \sigma(m)\theta \sin \sigma(\mu)\theta r dr d\theta, \end{aligned} \quad (8.2.30)$$

$$\begin{aligned} \sum_{m=0}^{\infty} \sum_{n=1}^{\infty} \int_{\theta=0}^{\beta_1} \int_{r=b}^d a_{mn} \psi_{mn}(r) \psi_{\mu\nu}(r) \cos \sigma(m)\theta \cos \sigma(\mu)\theta \frac{\coth \alpha_{mn} a}{\alpha_{mn}} r dr d\theta = \\ \sum_{m=1}^{\infty} \sum_{n=1}^{\infty} \int_{\theta=0}^{\beta_1} \int_{r=b}^d \frac{b_{mn}}{-\alpha_{mn}} \psi_{mn}(r) \psi_{\mu\nu}(r) \sin \sigma(m)\theta \cos \sigma(\mu)\theta r dr d\theta. \end{aligned} \quad (8.2.31)$$

We now introduce some notation to simplify matters. We write

$$I_{m\mu}^{n\nu} = \int_b^d \psi_{mn}(r) \psi_{\mu\nu}(r) r dr, \quad (8.2.32)$$

and use the result that

$$I_{\mu\mu}^{n\nu} = \delta_{n\nu} q_{\mu\nu}, \quad (8.2.33)$$

where, see Appendix A,

$$2d^{-2} q_{\mu\nu} = \left\{ \begin{aligned} & \left(\left\{ \left(Y'_{\sigma(\mu)}(\eta_{\sigma(\mu)\nu}) J'_{\sigma(\mu)}(\eta_{\sigma(\mu)\nu} \delta) - \right. \right. \right. \\ & \quad \left. \left. \left. J'_{\sigma(\mu)}(\eta_{\sigma(\mu)\nu}) Y'_{\sigma(\mu)}(\eta_{\sigma(\mu)\nu} \delta) \right)^2 \right. \right. \\ & + \left(Y'_{\sigma(\mu)}(\eta_{\sigma(\mu)\nu}) J_{\sigma(\mu)}(\eta_{\sigma(\mu)\nu} \delta) - \right. \\ & \quad \left. \left. J'_{\sigma(\mu)}(\eta_{\sigma(\mu)\nu}) Y_{\sigma(\mu)}(\eta_{\sigma(\mu)\nu} \delta) \right)^2 \right. \\ & \quad \left. \left[1 - \left(\frac{\sigma(\mu)}{\eta_{\sigma(\mu)\nu} \delta} \right)^2 \right] \right\} \\ & - \frac{1}{\delta^2} \left\{ \left(Y'_{\sigma(\mu)}(\eta_{\sigma(\mu)\nu}) J_{\sigma(\mu)}(\eta_{\sigma(\mu)\nu}) - \right. \right. \\ & \quad \left. \left. J'_{\sigma(\mu)}(\eta_{\sigma(\mu)\nu}) Y_{\sigma(\mu)}(\eta_{\sigma(\mu)\nu}) \right)^2 \right. \\ & \quad \left. \left[1 - \left(\frac{\sigma(\mu)}{\eta_{\sigma(\mu)\nu}} \right)^2 \right] \right\}, \quad (\sigma(\mu), \nu) \neq (0, 1), \\ & (1 - 1/\delta^2), \quad (\sigma(\mu), \nu) = (0, 1). \end{aligned} \right. \quad (8.2.34)$$

We also make use of the orthogonality condition

$$\int_0^{\beta_1} \cos \sigma(m)\theta \cos \sigma(\mu)\theta d\theta = \int_0^{\beta_1} \sin \sigma(m)\theta \sin \sigma(\mu)\theta d\theta = \frac{\beta_1}{\epsilon_\mu} \delta_{m\mu}, \quad (8.2.35)$$

where ϵ_μ is the Neumann symbol, defined by $\epsilon_0 = 1$, $\epsilon_\mu = 2$, $\mu \in \mathbb{N}$. As in Linton and McIver (1998b) eqn 2.21 we also define

$$T_{m\mu} = \frac{\pi}{\beta_1} \int_0^{\beta_1} \cos \sigma(m)\theta \sin \sigma(\mu)\theta \, d\theta = \begin{cases} 0 & m + \mu \text{ even,} \\ \frac{2\mu}{\mu^2 - m^2} & m + \mu \text{ odd.} \end{cases} \quad (8.2.36)$$

Substituting (8.2.35) and (8.2.36) into (8.2.30) we have

$$\sum_{m=0}^{\infty} \sum_{n=1}^{\infty} a_{mn} I_{m\mu}^{n\nu} T_{m\mu} \frac{\beta_1}{\pi} = \sum_{m=1}^{\infty} \sum_{n=1}^{\infty} \int_b^d b_{mn} \psi_{mn}(r) \psi_{\mu\nu}(r) \frac{\beta_1}{2} \delta_{m\mu} r \, dr, \quad \mu, \nu \in \mathbb{N}. \quad (8.2.37)$$

The right hand side of equation (8.2.37) is zero unless $m = \mu$ and so using (8.2.32) and (8.2.33) we have

$$\frac{2}{\pi} \sum_{m=0}^{\infty} \sum_{n=1}^{\infty} a_{mn} I_{m\mu}^{n\nu} T_{m\mu} = \sum_{n=1}^{\infty} b_{\mu n} I_{\mu\mu}^{n\nu} = b_{\mu\nu} q_{\mu\nu}. \quad (8.2.38)$$

In a similar way (8.2.31) becomes

$$\sum_{m=1}^{\infty} \sum_{n=1}^{\infty} \frac{b_{mn}}{-\alpha_{mn}} \frac{\beta_1}{\pi} I_{m\mu}^{n\nu} T_{\mu m} = \sum_{m=0}^{\infty} \sum_{n=1}^{\infty} \int_{r=b}^d a_{mn} \psi_{mn}(r) \psi_{\mu\nu}(r) \frac{\beta_1 \coth \alpha_{mn} a}{\epsilon_\mu \alpha_{mn}} \delta_{m\mu} r \, dr, \quad (8.2.39)$$

where $\mu \in \mathbb{N}_0$ and $\nu \in \mathbb{N}$. The left hand side of (8.2.39) is zero unless $m = \mu$ and hence

$$\sum_{m=1}^{\infty} \sum_{n=1}^{\infty} \frac{b_{mn}}{-\alpha_{mn}} \frac{\beta_1}{\pi} I_{m\mu}^{n\nu} T_{\mu m} = a_{\mu\nu} q_{\mu\nu} \frac{\beta_1 \coth \alpha_{\mu\nu} a}{\epsilon_\mu \alpha_{\mu\nu}}. \quad (8.2.40)$$

If the unknown coefficients $b_{\mu\nu}$ are eliminated from (8.2.38) and (8.2.40), we have

$$\frac{\pi^2 \coth \alpha_{\mu\nu} a}{2\epsilon_\mu \alpha_{\mu\nu}} a_{\mu\nu} q_{\mu\nu} = \sum_{r=1}^{\infty} \sum_{s=1}^{\infty} \left\{ \sum_{m=0}^{\infty} \sum_{n=1}^{\infty} a_{mn} \frac{I_{mr}^{ns} I_{r\mu}^{s\nu} T_{mr} T_{\mu r}}{-\alpha_{rs} q_{rs}} \right\}, \quad (8.2.41)$$

and changing the order of summation gives

$$\frac{\pi^2 \coth \alpha_{\mu\nu} a}{2\epsilon_\mu \alpha_{\mu\nu}} a_{\mu\nu} q_{\mu\nu} = \sum_{m=0}^{\infty} \sum_{n=1}^{\infty} a_{mn} \left\{ \sum_{r=1}^{\infty} \sum_{s=1}^{\infty} \frac{I_{mr}^{ns} I_{r\mu}^{s\nu} T_{mr} T_{\mu r}}{-\alpha_{rs} q_{rs}} \right\}, \quad \mu \in \mathbb{N}_0, \quad \nu \in \mathbb{N}. \quad (8.2.42)$$

The problem can now be restricted in one of two ways, as we can look for modes symmetric or antisymmetric about the mid-plane of the sector, $\theta = \beta_1/2$. For the symmetric case, we have

$$\frac{\partial \phi}{\partial \theta} = 0 \quad \text{on} \quad \theta = \frac{\beta_1}{2}, \quad (8.2.43)$$

and putting this into (8.2.26) and (8.2.27) we find

$$\left. \frac{\partial \phi}{\partial \theta} \right|_{\theta=\beta_1/2} = \sum_{m=0}^{\infty} \sum_{n=1}^{\infty} -a_{mn} \frac{\sigma(m) \cosh \alpha_{mn} x}{\alpha_{mn} \sinh \alpha_{mn} a} \psi_{mn}(r) \sin \left(\frac{m\pi}{2} \right) = 0, \quad x < a, \quad (8.2.44)$$

$$= \sum_{m=1}^{\infty} \sum_{n=1}^{\infty} b_{mn} \frac{\sigma(m) e^{-\alpha_{mn}(x-a)}}{-\alpha_{mn}} \psi_{mn}(r) \cos \left(\frac{m\pi}{2} \right) = 0, \quad x > a, \quad (8.2.45)$$

and hence $a_{mn} = 0$ if m is odd and $b_{mn} = 0$ if m is even. As the potential ϕ is symmetric about the mid-plane (8.2.43) implies that $\partial\phi/\partial\theta$ on $\theta = 0$ differs from $\partial\phi/\partial\theta$ on $\theta = \beta_1$ by a factor of -1 and so it follows from the continuity condition (8.2.9) that such modes do not exist when L is odd. The condition for antisymmetry about $\theta = \beta_1/2$ is

$$\phi = 0 \quad \text{on} \quad \theta = \frac{\beta_1}{2}. \quad (8.2.46)$$

Substituting (8.2.46) into (8.2.44) and (8.2.45) we have

$$\phi \Big|_{\theta=\beta_1/2} = \sum_{m=0}^{\infty} \sum_{n=1}^{\infty} a_{mn} \frac{\cosh \alpha_{mn} x}{\alpha_{mn} \sinh \alpha_{mn} a} \psi_{mn}(r) \cos \left(\frac{m\pi}{2} \right) = 0, \quad x < a, \quad (8.2.47)$$

$$= \sum_{m=1}^{\infty} \sum_{n=1}^{\infty} b_{mn} \frac{e^{-\alpha_{mn}(x-a)}}{-\alpha_{mn}} \psi_{mn}(r) \sin \left(\frac{m\pi}{2} \right) = 0, \quad x > a, \quad (8.2.48)$$

and so $a_{mn} = 0$ if m is even and $b_{mn} = 0$ if m is odd. For antisymmetry about the mid-plane the derivative $\partial\phi/\partial\theta$ on $\theta = 0$ is equal to $\partial\phi/\partial\theta$ on $\theta = \beta_1$ so we find that modes exist for both even and odd values of L .

For the case of symmetry about the mid-plane of the sector we require non-trivial solutions of (8.2.42), and so can assume that μ and m are even and hence from (8.2.36) it follows that r is odd. In this case b_{11} is non-zero and as we require exponential decay down the waveguide we need α_{11} to be real and positive. Using (8.2.25) we restrict kd so that $kd < \eta_{\sigma(1)1}\delta$. With this restriction we find that α_{mn} , $m, n \in \mathbb{N}$ are all real and positive and since $\eta_{01} = 0$ then α_{01} is purely imaginary, whereas α_{0n} , $n \in \mathbb{N}$ are either real and positive or purely imaginary depending on the value of L and kd . If $\eta_{\sigma(1)1} > \eta_{0n}$ then we define

$$\alpha_{0n}d = \begin{cases} [(\eta_{0n}\delta)^2 - (kd)^2]^{1/2}, & kd \leq \eta_{0n}\delta, \\ -i[(kd)^2 - (\eta_{0n}\delta)^2]^{1/2}, & \eta_{0n}\delta < kd < \eta_{\sigma(1)1}\delta. \end{cases} \quad (8.2.49)$$

We shall solve (8.2.42) using truncation. We introduce the truncation parameter N and write

$$\lambda = \frac{\mu}{2}N + \nu, \quad l = \frac{m}{2}N + n, \quad t = \frac{r-1}{2}N + s, \quad (8.2.50)$$

so that a given $\lambda \in \mathbb{N}$ corresponds to a unique pair μ, ν and similarly for l and t . If we write

$$g_\lambda = \frac{\pi^2 \coth \alpha_{\mu\nu} a}{2\epsilon_\mu \alpha_{\mu\nu}} q_{\mu\nu} \quad (8.2.51)$$

and

$$\tilde{a}_\lambda = a_{\mu\nu}, \quad \tilde{a}_l = a_{mn}, \quad \tilde{\alpha}_t = \alpha_{rs}, \quad \tilde{q}_t = q_{rs}, \quad \tilde{I}_{lt} = I_{mr}^{ns} T_{mr}, \quad (8.2.52)$$

we find from (8.2.42),

$$g_\lambda \tilde{a}_\lambda + \sum_{l=1}^{\infty} \tilde{a}_l \sum_{t=1}^{\infty} \frac{\tilde{I}_{lt} \tilde{I}_{\lambda t}}{\tilde{\alpha}_t \tilde{q}_t} = 0, \quad \lambda \in \mathbb{N}. \quad (8.2.53)$$

We can truncate this to an $NM \times NM$ system of equations

$$g_\lambda \tilde{a}_\lambda + \sum_{l=1}^{NM} \tilde{a}_l \sum_{t=1}^{\infty} \frac{\tilde{I}_{lt} \tilde{I}_{\lambda t}}{\tilde{\alpha}_t \tilde{q}_t} = 0, \quad \lambda = 1, 2, \dots, NM. \quad (8.2.54)$$

When truncated, the required trapped mode frequencies correspond to the values of kd for which the determinant of the matrix S whose elements are given by

$$S_{\lambda l} = g_\lambda \delta_{\lambda l} + \sum_{t=1}^{\infty} \frac{\tilde{I}_{lt} \tilde{I}_{\lambda t}}{\tilde{\alpha}_t \tilde{q}_t}, \quad \lambda, l = 1, 2, \dots, NM, \quad (8.2.55)$$

is zero. All terms can be evaluated using the previous workings, apart from the terms \tilde{I}_{lt} and $\tilde{I}_{\lambda t}$ in the summation which involve integrals of products of Bessel functions and must be evaluated numerically.

For the case of antisymmetry about the mid-plane of the sector, we obtain the same system of equations as (8.2.54), but find that m and μ are odd, r is even (starting with 2) and λ, l and t are given by

$$\lambda = \frac{\mu - 1}{2} N + \nu, \quad l = \frac{m - 1}{2} N + n, \quad t = \frac{r - 2}{2} N + s. \quad (8.2.56)$$

For the case of antisymmetry about the mid-plane we found that if m is odd then $b_{mn}, n \in \mathbb{N}$, is zero and so the boundary condition (8.2.6) is satisfied provided $kd < \eta_{\sigma(2)1}$. With this frequency restriction $\alpha_{mn}, m = 2, 3, \dots, n \in \mathbb{N}$ are all real and positive whereas $a_{0n}, n \in \mathbb{N}$, are all zero. To ensure wave-like modes occur in the inner region $x < a$ we need to restrict the frequency to the range $\eta_{\sigma(1)1} \delta < kd < \eta_{\sigma(2)1} \delta$. We then define

$$\alpha_{1n} d = \begin{cases} [(\eta_{1n} \delta)^2 - (kd)^2]^{1/2}, & kd \leq \eta_{1n} \delta, \\ -i[(kd)^2 - (\eta_{1n} \delta)^2]^{1/2}, & \eta_{1n} \delta < kd < \eta_{\sigma(2)1} \delta. \end{cases} \quad (8.2.57)$$

To reformulate the problem for modes antisymmetric about $x = 0$, we change (8.2.1) to

$$\phi = 0 \text{ on } x = 0. \quad (8.2.58)$$

The only alteration caused by this is to replace coth term in (8.2.51) by a tanh term.

8.3 Results

The results in this section were computed with truncation parameters $N = M = 8$ to give a 64×64 system of equations. In this work a large value of δ represents a case similar to that of the cylindrical waveguide considered by Linton and McIver (1998b). The results obtained with a large value of δ are equivalent to those provided by Linton and McIver.

Results for the trapped-mode frequencies, kd , with $L = 1$ and $\delta = 2$ are shown in figure 8.3, with figure 8.4 providing a schematic representation of the problem under discussion. Figure 8.4 shows cross-sections of the cylinder for the one-fin case, the solid lines represent the blade and the dashed lines represent the planes of antisymmetry ($\phi = 0$). Since L is odd only modes antisymmetric about $\theta = \pi$ exist, as mentioned previously. The solid lines in figure 8.3 represent modes which are symmetric about $x = 0$ and the dashed lines represent modes antisymmetric about this line. It can be seen that as a/d increases the trapped mode appear alternately symmetric and antisymmetric about $x = 0$. In figure 8.3 the modes appear from the cut-off $kd = \delta\eta_{11} \approx 1.3547$ and tend to the cut-off $kd = \delta\eta_{1/2,1} \approx 0.6792$ as $a/d \rightarrow \infty$.

As the value of δ is increased we find that both cut-offs increase to the values given by Linton and McIver. It can be shown, (see Appendix B), that as $\delta \rightarrow 1$, $\eta_{m1} \rightarrow m$, and so the upper cut-off tends to $\sigma(2) = L$ and the lower cut-off tends to $\sigma(1) = L/2$. The results when $L = 2$ and $\delta = 2$, which corresponds to a flat plate spanning the guide, are shown in figure 8.5, with the cross-section shown in figure 8.6. Since L is even modes both symmetric and antisymmetric about the mid-plane of the sector, $\theta = \pi/2$, exist. The modes symmetric about $\theta = \pi/2$ appear when $\delta = 2$ from the cut-off $kd = \delta\eta_{11}$ and tend to zero as a/d increases. The modes antisymmetric about $\theta = \pi/2$ appear from the cut-off $kd = \delta\eta_{21} \approx 2.6812$ and approach the cut-off $kd = \delta\eta_{11}$ as $a/d \rightarrow \infty$.

Figure 8.7 shows how the frequency of the lowest mode symmetric about $x = 0$, for the cases of both symmetry and antisymmetry about $\theta = \pi/2$ changes with a/d

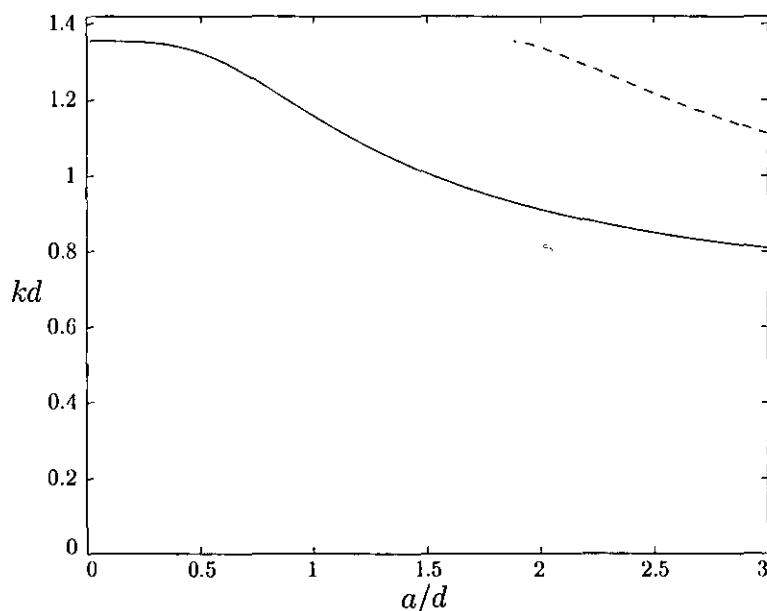


Figure 8.3: Trapped mode frequencies for modes symmetric (—) and antisymmetric (---) about $x = 0$ plotted against a/d when $L = 1$ and $\delta = 2$. The curves correspond to the cross-sections in figure 8.4.

for various δ . It can be seen that the mode symmetric about $\theta = \pi/2$ varies most as a function of δ when a/d is small, and as a/d becomes large the resulting frequency becomes independent δ . The mode that is antisymmetric about $\theta = \pi/2$, shows greater change because the frequency that the mode tends to as a/d becomes large depends on δ .

Results for $L = 4$ are shown in figures 8.8 and 8.9. The situation is qualitatively similar to the $L = 2$ case with the appropriate cut-offs changing to $kd = \delta\eta_{21}$ and $kd = \delta\eta_{41} \approx 5.1752$. If one compares figures 8.3, 8.5 and 8.8 it is plain to see that as a/d increases the number of modes appearing becomes greater for larger values of L .

The boundary conditions for these modes when $|x| > a$ are artificial and imposed just to reduce the problem to one in the sector $0 < \theta < \beta_1$. Figure 8.6(a) shows that some modes exist for both cases when $L = 2$ and $L = 4$, provided the value of δ remains the same. In figure 8.10 curves corresponding to the geometries in figures 8.6(a) and 8.9(a) with $\delta = 2$ are shown superimposed. In practice the modes corresponding to 8.6(a) are unlikely to be generated if 4 fins are present since they do not have a condition of antisymmetry on the plane that is an extension of the fins down the guide, and this is the natural condition since the resonances are usually excited by vortex shedding. The

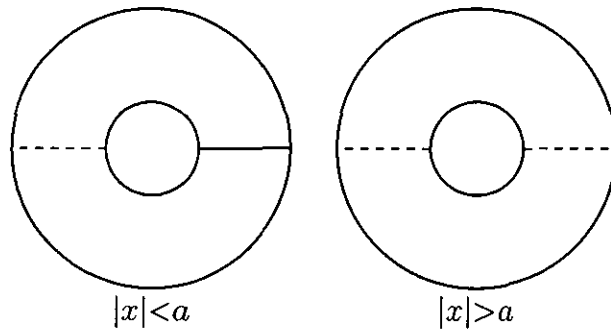


Figure 8.4: Cross-sections for the results plotted in figure 8.3. The solid radial line represents the single fin and Dirichlet conditions are applied on surfaces represented by dashed lines.

$L = 4$ modes satisfy $\partial\phi/\partial\theta = 0$ on $\theta = 0, \pi$ and look as though they would be solutions for the $L = 2$ case also, provided δ was the same. This is not however the case as the $L = 4$ modes have discontinuities in ϕ which would be within the fluid for the $L = 2$ case, for example on $\theta = \pi/2, |x| < a$.

When $L = 4$ and with symmetry about the mid-plane of the sector imposed we find that for any value of δ , we have $\eta_{\sigma(1)1} < \eta_{02}$ and so from (8.2.49), $\alpha_{0n}, n \in \mathbb{N}$ are real and positive. Similarly for antisymmetry about $\theta = \beta_1/2$ we find that $\eta_{\sigma(2)1} < \eta_{\sigma(1)2}$ for any value of δ and so $\alpha_{1n}, n \in \mathbb{N}$ are real and positive. As the value of L is increased we find however that this situation changes. We now consider the $L = 8$ case and find that this change can produce a qualitative change in the behaviour of the trapped mode frequencies.

For the 8-blade case with $\delta = 5$, we have $\delta\eta_{\sigma(1)1} \approx 5.3173 > \delta\eta_{02} \approx 4.2357$ and $\delta\eta_{\sigma(2)1} \approx 9.6474 > \delta\eta_{\sigma(1)2} \approx 9.2734$, whereas with $\delta = 1.001$, $\delta\eta_{41} \approx 4.0020 < \delta\eta_{02} \approx 3144.7$ and $\delta\eta_{81} \approx 8.0040 < \delta\eta_{42} \approx 3144.7$. These cut-offs show that as δ decreases from 5, i.e. the inner radius of the annular region increases compared to the outer radius, there will be a certain value of δ that causes $\delta\eta_{41} > \delta\eta_{02}$ and/or $\delta\eta_{81} > \delta\eta_{42}$. The results for $\delta = 5$ and $\delta = 1.001$ are shown in figures 8.11 and 8.12 with the corresponding schematic representation of the problem given in figure 8.13. If we compare the curves in figure 8.11 to the solid lines in figures 8.3, 8.5 and 8.8, there is a fundamental change for the $L = 8$ case.

We now consider the lower set of curves in figures 8.11 and 8.12, i.e. those that correspond to figure 8.13(a). Earlier work on trapped modes in two-dimensional acoustic

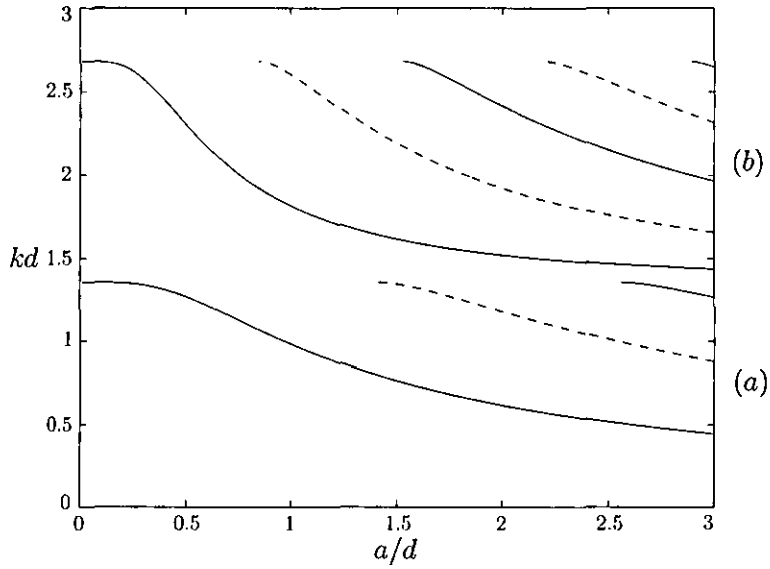


Figure 8.5: Trapped mode frequencies for modes symmetric (—) and antisymmetric (---) about $x = 0$ plotted against a/d when $L = 2$ and $\delta = 2$. The lower set of curves correspond to the cross-sections in figure 8.6(a), whereas the upper set of curves corresponds to the cross-sections in figure 8.6(b).

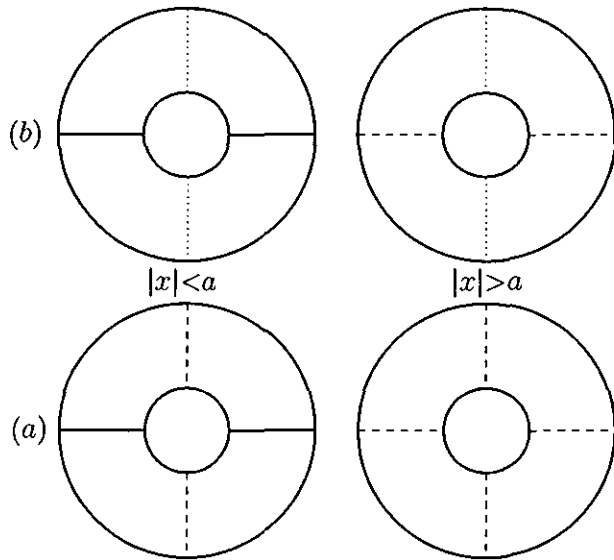


Figure 8.6: Cross-sections for the results plotted in figure 8.5. The solid radial line represents the fins whereas the dotted lines represent surfaces on which Neumann conditions are applied, and Dirichlet conditions are applied on surfaces represented by dashed lines. The modes are continuous across the dashed and the dotted lines but need not be across solid lines.

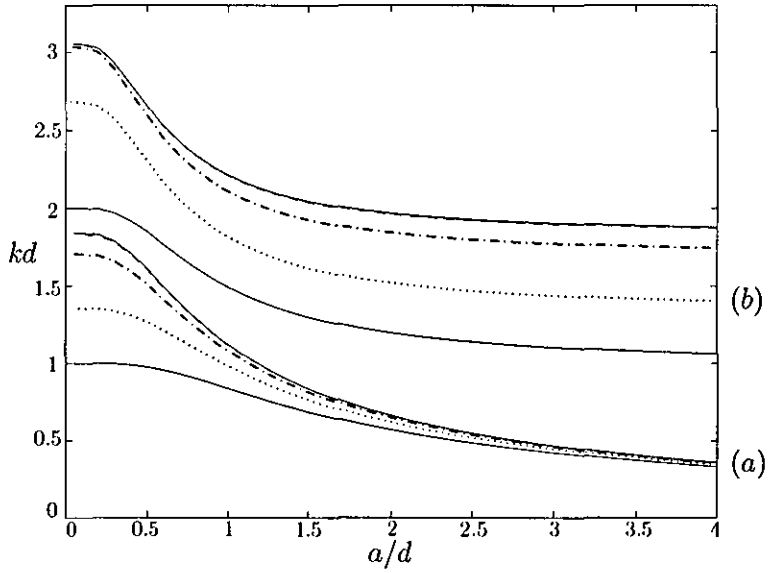


Figure 8.7: Trapped mode frequencies for the lowest frequency mode symmetric about $x = 0$, for modes symmetric and antisymmetric about $\theta = \pi/2$, plotted against a/d when $L = 2$ for various δ . The lower set of curves correspond to the mode symmetric about $\theta = \pi/2$, whereas the upper set of curves corresponds to the mode antisymmetric about $\theta = \pi/2$. For both sets of curves the lower solid line corresponds to $\delta = 1.001$, the dotted line corresponds to $\delta = 2$, the dot-dash line corresponds to $\delta = 5$, the dashed line corresponds to $\delta = 25$ and the upper solid line corresponds to the cylinder case.

waveguides by Evans and Linton (1991) showed how trapped-mode frequencies could be found as the intersection of a tan curve and a positive curve, leading to the regular spacing seen in the figures for lower numbers of blades. This simple behaviour still remains when $L = 8$ and $\delta = 1.001$, but is lost as δ increases to 5 between the frequencies $\delta\eta_{02} < kd < \delta\eta_{41}$. When $\delta = 5$, $\delta\eta_{\sigma(1)1} > \delta\eta_{02}$, and therefore from (8.2.51), we find that instead of only g_1 having zeros and singularities, g_2 now shows similar features. For the 8-fin case it can be shown that $\delta\eta_{41} \approx \delta\eta_{02}$ when $\delta \approx 2.5823$, and hence when $\delta > 2.5823$ and $kd > 5.2891$ the phenomenon seen in figure 8.11 will occur. When $L = 8$ we find that a smaller value of δ is needed for the modes antisymmetric about $\theta = \beta_1/2$ to display the phenomenon seen in figure 8.11. As the number of blades is increased the value of δ at which this phenomenon for both modes symmetric and antisymmetric about $\theta = \beta_1/2$ occurs tends to one. This implies that when L is large $\eta_{\sigma(1)1} > \eta_{02}$ and $\eta_{\sigma(2)1} > \eta_{\sigma(1)2}$ for all δ .

If the lower set of curves in figure 8.11 are not examined too closely it appears

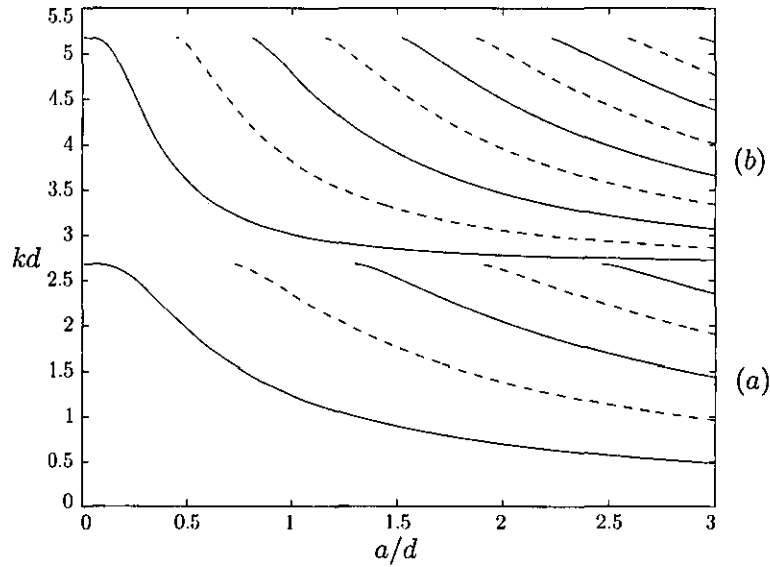


Figure 8.8: Trapped mode frequencies for modes symmetric (—) and antisymmetric (---) about $x = 0$ plotted against a/d when $L = 4$ and $\delta = 2$. The lower set of curves correspond to the cross-sections in figure 8.9(a), whereas the upper set of curves corresponds to the cross-sections in figure 8.9(b).

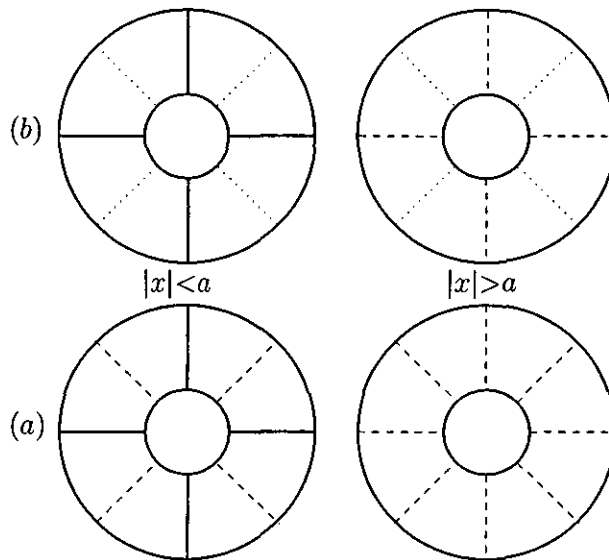


Figure 8.9: Cross-sections for the results plotted in figure 8.8. The solid radial line represents the fins whereas the dotted lines represent surfaces on which Neumann conditions are applied, and Dirichlet conditions are applied on surfaces represented by dashed lines. The modes are continuous across the dashed and the dotted lines but need not be across solid lines.

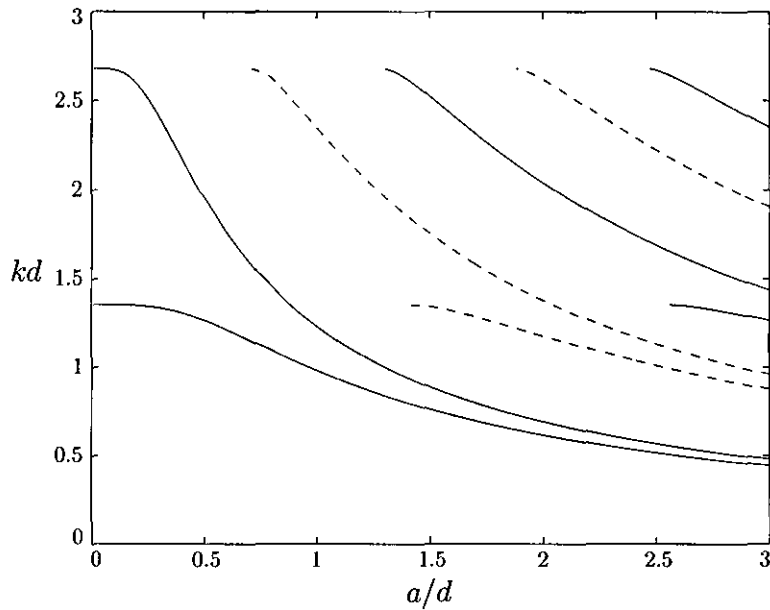


Figure 8.10: Trapped mode frequencies for modes symmetric (—) and antisymmetric (---) about $x = 0$ plotted against a/d with $\delta = 2$. The lower set of curves correspond to the cross-sections in figure 8.6(a) whereas the upper set of curves corresponds to the cross-sections in figure 8.9(a).

that there are two sets of curves present, one of which is associated with $\lambda = 1$ in (8.2.51) containing curves appearing from the cut-off, $kd = \delta\eta_{41}$, and tending to zero as $a/d \rightarrow \infty$, and the other associated with $\lambda = 2$ in (8.2.51) containing modes that appear from the cut-off $kd = \delta\eta_{41}$ and tend to $kd = \delta\eta_{02}$ as $a/d \rightarrow \infty$. A similar occurrence is present in the upper set of curves as one set of modes corresponding to $\lambda = 1$ appears to start from the cut-off $kd = \delta\eta_{81}$ and tends to zero as $a/d \rightarrow \infty$, and the second set of modes associated with $\lambda = 2$ appear from $kd = \delta\eta_{81}$ and tend to $kd = \delta\eta_{42}$ as $a/d \rightarrow \infty$.

If figure 8.11 is examined closer however, it is clear that the curves *do not* cross, and this would appear to be the case at all possible intersections. Similar examples of near intersections can be found in eigenvalue curves given by Berry and Wilkinson (1984) and Karim-Panahi (1983). Berry and Wilkinson examined eigenvalues dependent on two geometrical parameters, one of which was fixed and the other allowed to vary. Similar near-crossing behaviour was shown to occur and the authors explained that close to a near intersection the eigenvalue curves are hyperbolas—the intersection of a plane with a double cone. Karim-Panahi studied the dispersion relation of harmonic shear waves in an infinite, elastic, and periodically triple-layered media.

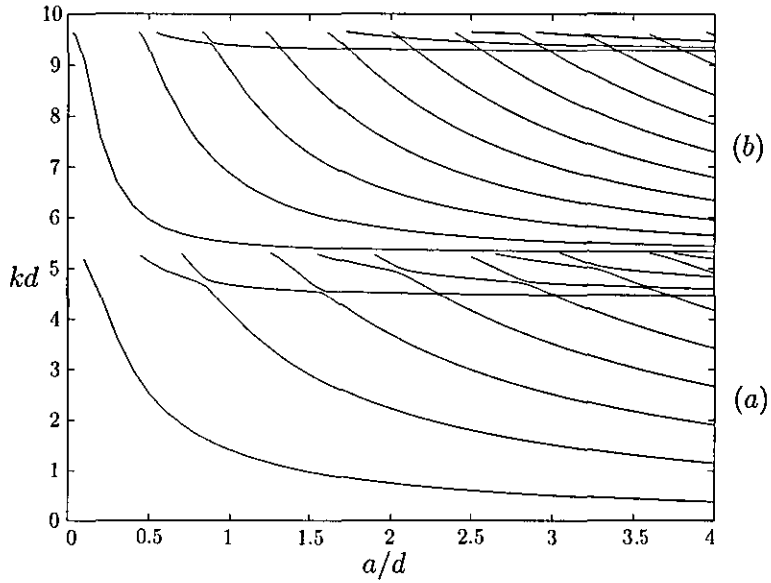


Figure 8.11: Trapped mode frequencies for modes symmetric about $x = 0$ plotted against a/d when $L = 8$ and $\delta = 5$. The lower set of curves correspond to the cross-sections in figure 8.13(a), whereas the upper set of curves corresponds to the cross-sections in figure 8.13(b).

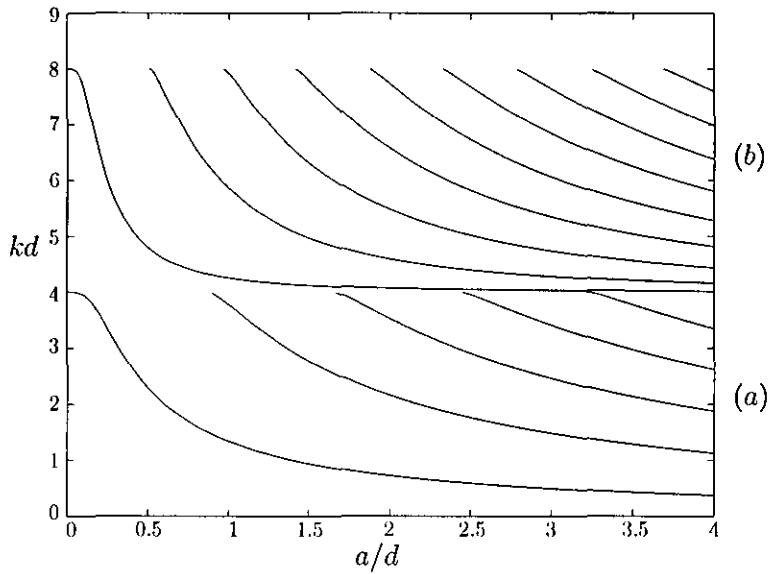


Figure 8.12: Trapped mode frequencies for modes symmetric about $x = 0$ plotted against a/d when $L = 8$ and $\delta = 1.001$. The lower set of curves correspond to the cross-sections in figure 8.13(a), whereas the upper set of curves corresponds to the cross-sections in figure 8.13(b).

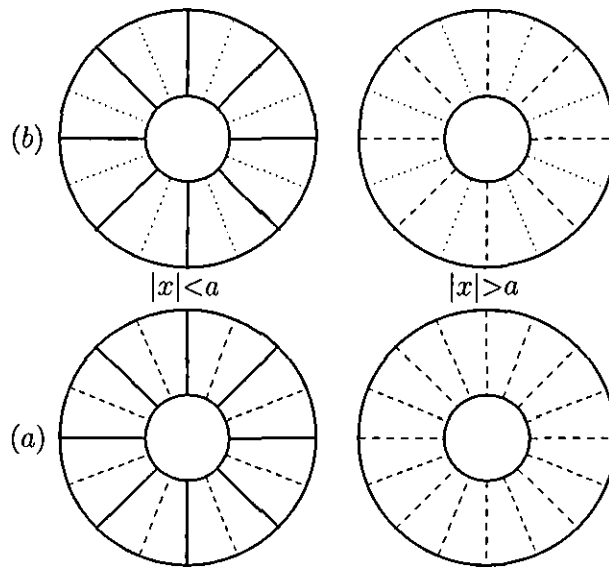


Figure 8.13: Cross-sections for the results plotted in figures 8.11 and 8.12. The solid radial line represents the fins whereas the dotted lines represent surfaces on which Neumann conditions are applied, and Dirichlet conditions are applied on surfaces represented by dashed lines. The modes are continuous across the dashed and the dotted lines but need not be across solid lines.

We now examine one near-crossing occurring when $L = 8$ and $\delta = 3$ near to $a/d \approx 1.4$, $kd \approx 5.0$. The two geometrical parameters in our problem are a/d and β_1 . If we fix a/d and allow β_1 to vary, which is possible by changing L because $\beta_1 = 2\pi/L$, we can see that the eigenvalue curves behave in a similar way to those in Berry and Wilkinson (1984). The numerical results suggest that as the number of blades increases, i.e. as β_1 decreases, the two eigenvalue curves do not meet, as shown in figure 8.14. Figure 8.14 shows that as β_1 is halved the two eigenvalue curves get closer and closer while the crossing point increases slowly to a larger value of a/d .

Analysing the elements in the matrix (8.2.55) we see that as $L \rightarrow \infty$ the value of the summation tends to zero, indicating that the eigenvalue curves will become simply the zeros of $S_{\lambda l} = g_{\lambda} \delta_{\lambda l}$. These of course are the solutions of $g_{\lambda} = 0$, and as previously mentioned when $L = 8$ and $\delta > 2.58$ both g_1 and g_2 have zeros. The solutions to $g_1 = 0$ are the solutions to $\coth \alpha_{01} a = \cot ka = 0$ and so

$$ka = \left(m - \frac{1}{2}\right)\pi \quad m \in \mathbb{N}. \quad (8.3.1)$$

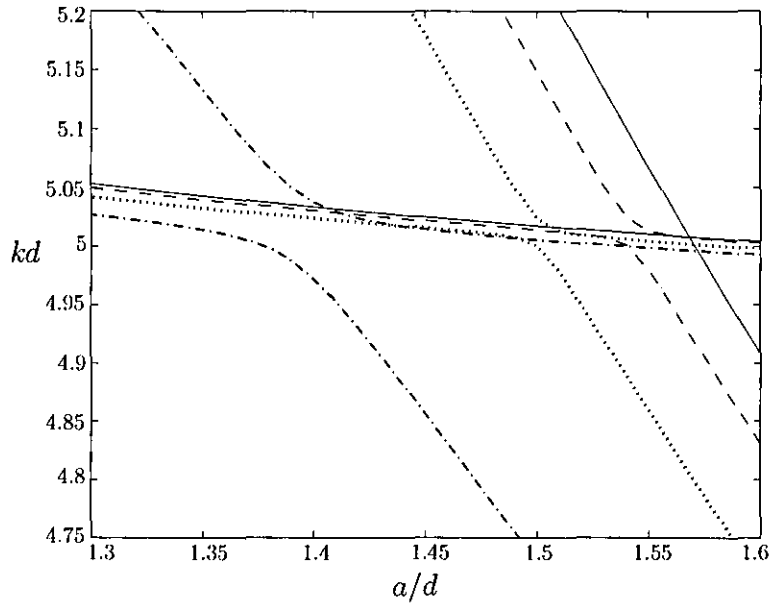


Figure 8.14: An enlarged view of one of the near-crossings for $\delta = 3$. The different curves demonstrate the effect of decreasing the angle β_1 , (dot-dashed) $L = 8$, (dotted) $L = 16$, (dashed) $L = 32$. The solid line represents the limiting values as $L \rightarrow \infty$ ($\beta_1 \rightarrow 0$).

The solutions to $g_2 = 0$ are

$$ka = \left[\left(\left(m - \frac{1}{2} \right) \pi \right)^2 + \left(\frac{\eta_{0n} a}{b} \right)^2 \right]^{1/2}, \quad m \in \mathbb{N}. \quad (8.3.2)$$

The solid lines in figure 8.14 correspond to (8.3.1) with $m = 3$ and (8.3.2) with $m = 1$. It appears that the Berry and Wilkinson phenomenon does not occur in the $(a/d, \beta_1)$ parameter space in this problem but may exist when $\beta_1 \rightarrow 0$ at the edge of this space. It is important to see that the solutions as $L \rightarrow \infty$ given in (8.3.1) and (8.3.2) do not depend on L , but do depend on δ .

Figure 8.15 shows a comparison between the 8-fin case with $\delta = 5$ and the large blade approximation from (8.3.1) and (8.3.2). It is clear that the large blade curves produce all the features required of the eight blade case (although as shown previously the curves do not cross) and the approximation gets better as a/d increases and the results move away from the cut-off $\delta\eta_{41}$.

For antisymmetry about $x = 0$ we can produce similar solutions to (8.3.1) and (8.3.2), but the zeros of $g_1 = 0$ are now

$$ka = m\pi \quad m \in \mathbb{N}, \quad (8.3.3)$$

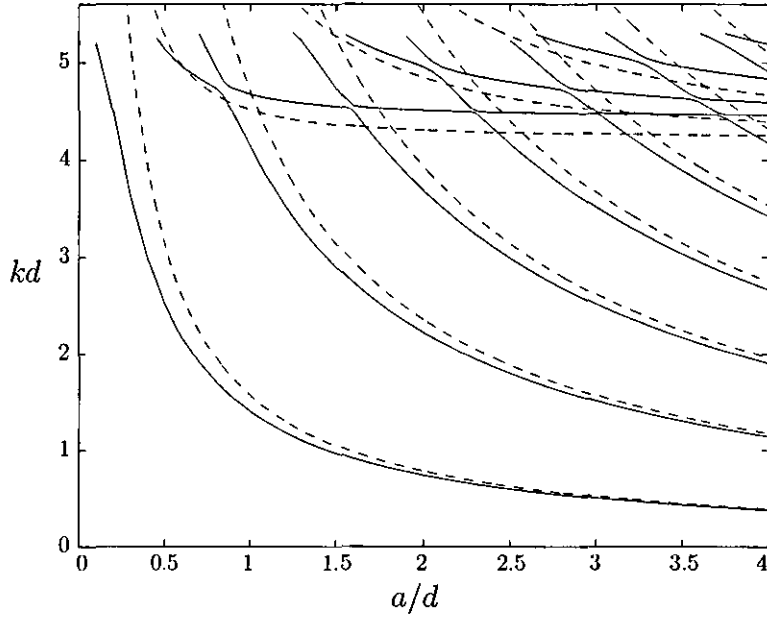


Figure 8.15: Trapped mode frequencies for modes symmetric about $x = 0$ and $\theta = \beta_1/2$ plotted against a/d when $\delta = 5$. The solid curves represent the case when $L = 8$ and the dashed lines represent the large L approximation.

and those of $g_2 = 0$ are

$$ka = \left[(m\pi)^2 + \left(\frac{\eta_{0n}a}{b} \right)^2 \right]^{1/2}, \quad m \in \mathbb{N}. \quad (8.3.4)$$

The results (8.3.1)–(8.3.4) are all for the case of symmetry about the mid-plane of the sector. The case of antisymmetry about $\beta_1/2$ is not of practical importance as the number of blades becomes large since the frequency of the modes satisfy $kd > \delta\eta_{\sigma(1)1}$ and so become large as L becomes large.

If a/d is fixed it is possible to see how the trapped mode frequencies vary as δ is changed. Figure 8.16 shows the case for modes symmetric about $x = 0$, with $L = 8$ and $a/d = 4$. The modes symmetric about the midplane $\theta = \beta_1/2$ appear below the lower dotted line corresponding to the cut-off $kd = \delta\eta_{\sigma(1)1}$. The modes antisymmetric about $\theta = \beta_1/2$ appear between the upper dotted line, corresponding to the cut-off $kd = \delta\eta_{\sigma(2)1}$, and the lower dotted line. The upper dashed line corresponds to the value $\delta\eta_{\sigma(1)2}$ and the lower dashed line corresponds to the value $\delta\eta_{02}$.

If we look at the modes symmetric about the mid-plane of the sector it is clear that the frequency of the modes below $\delta\eta_{02}$ is independent of δ . The modes appear as almost horizontal lines at regular intervals. The frequency of these acoustic resonances are the

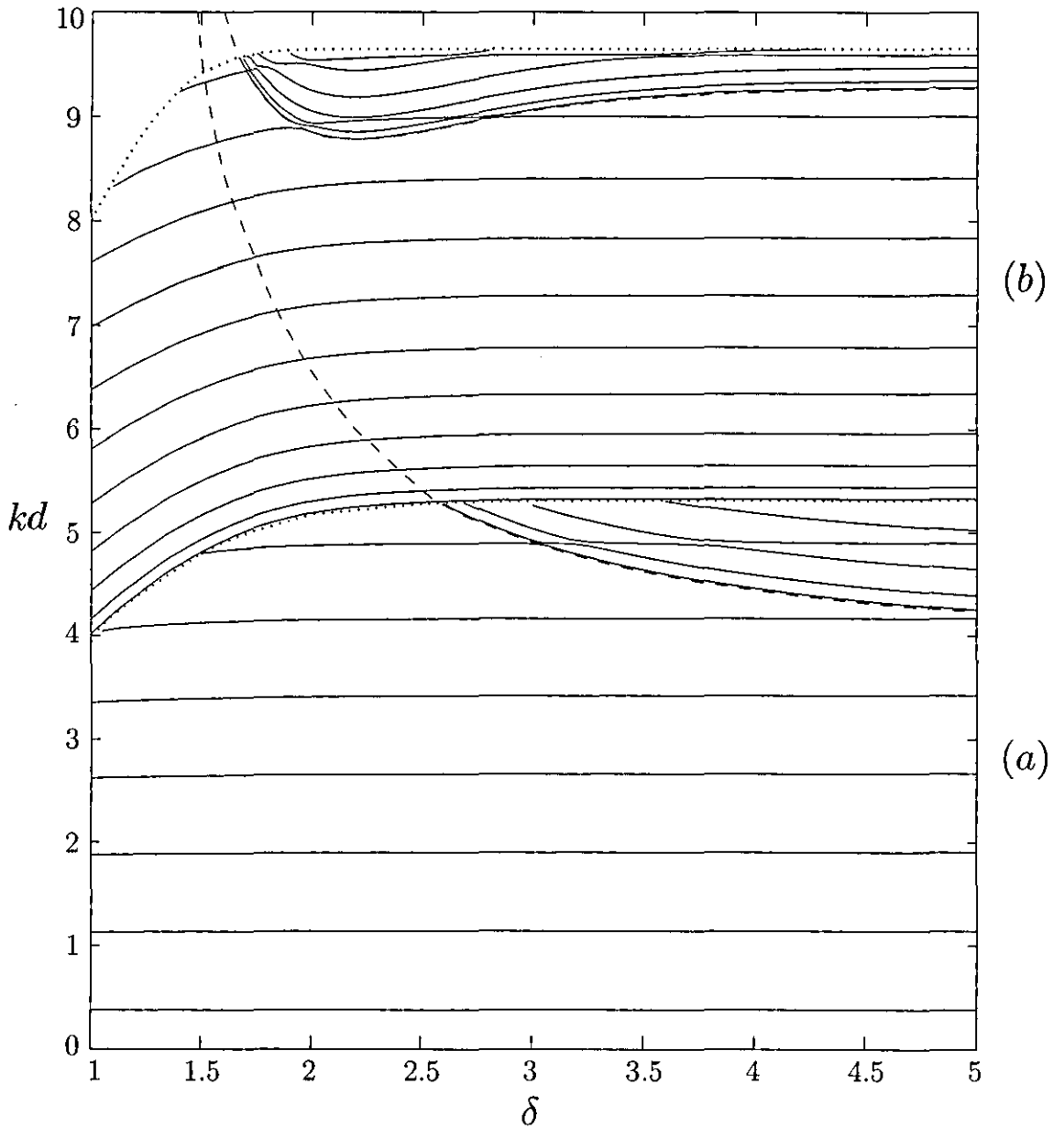


Figure 8.16: Trapped mode frequencies for modes symmetric about $x = 0$ plotted against δ when $L = 8$ and $a/d = 4$. The lower dotted line corresponds to the cut-off $\delta\eta_{\sigma(1)1}$ and the lower dashed line corresponds to the value $\delta\eta_{02}$. The upper dotted line corresponds to the cut-off $\delta\eta_{\sigma(2)1}$ and the upper dashed line corresponds to the value $\delta\eta_{\sigma(1)2}$. The lower set of curves correspond to the cross-sections in figure 8.13(a), whereas the upper set of curves corresponds to the cross-sections in figure 8.13(b).

solutions of $g_1 = 0$ in (8.2.51) with $a = 4$, i.e.

$$kd = (2m - 1)\frac{\pi}{4} \quad m \in \mathbb{N}. \quad (8.3.5)$$

We previously noted that when $\delta > 2.58$ the value $\eta_{02} < \eta_{41}$ and so when the trapped-modes frequencies are above $kd = \delta\eta_{02}$ with $\delta > 2.58$ there is a qualitative change in the curves. If one does not look too closely at the lower curves in figure 8.16 it appears that there are two sets of curves. One set corresponds to the results in (8.3.5) with $m = 7$ and the other set follows the trend of the value $kd = \delta\eta_{02}$ with an even spacing between each successive line. The second set of lines is a solution to the equation $g_2 = 0$ in (8.2.51) with $a = 4$, i.e. from (8.3.2)

$$kd = \left[\left((2m - 1)\frac{\pi}{8} \right)^2 + (\delta\eta_{02})^2 \right]^{1/2}, \quad m \in \mathbb{N}. \quad (8.3.6)$$

Figure 8.17 shows a close up of this region and it appears that the curves do not cross but show the same phenomenon discussed earlier.

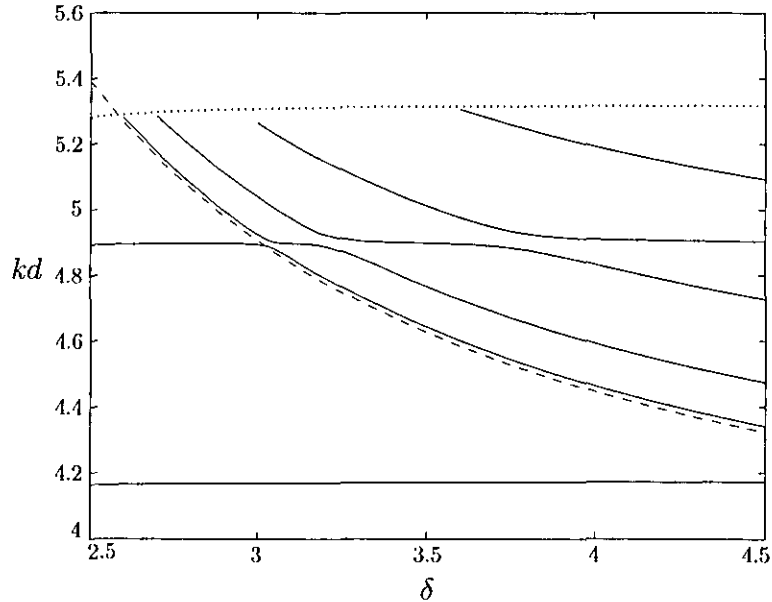


Figure 8.17: Trapped mode frequencies for modes symmetric about $x = 0$ and $\theta = \beta_1/2$ plotted against δ when $L = 8$ and $a/d = 4$. The dotted line corresponds to the cut-off $\delta\eta_{\sigma(1)1}$ and the dashed line corresponds to the value $\delta\eta_{02}$.

The modes asymmetrical about the mid-plane $\theta = \beta_1/2$ show similar properties as the symmetrical modes. The trapped-mode frequencies for the two sets of curves are

$$kd = \left[\left((2m - 1)\frac{\pi}{8} \right)^2 + (\delta\eta_{41})^2 \right]^{1/2}, \quad m \in \mathbb{N}, \quad (8.3.7)$$

for the lower modes and

$$kd = \left[\left((2m-1) \frac{\pi}{8} \right)^2 + (\delta\eta_{42})^2 \right]^{1/2}, \quad m \in \mathbb{N}, \quad (8.3.8)$$

for the modes appearing above $kd = \delta\eta_{42}$.

8.4 Summary

In this chapter we have extended the work done by Linton and McIver (1998b) by formulating the problem for a cylinder with an annular cross-section. We have provided a simple theory that allows the prediction of the trapped mode frequencies that are present in the case of a number of blades evenly placed around a cylindrical guide with annular cross-section.

The results computed in section 8.3 allow us to make a comparison between the annular case with small inner radius and the cylinder case with circular cross-section, and also show how the frequencies of the trapped modes change as the inner radius is increased.

We have been able to show that many of the features associated with the circular cross-section case continue to occur in the annular case. Firstly we see that the nature of modes occurring depends on whether the number of blades is even or odd. If we have an odd number of blades, we can only find modes which are antisymmetric about the mid-plane of the sector, whereas if we have an even number of blades, it is possible to find modes either symmetric or antisymmetric about the mid-plane.

We have also found that as the number of blades and the inner radius increase above certain values a fundamental change occurs in the trapped-mode curves plotted. For a large number of blades we can provide an accurate simple approximation to the trapped-mode frequencies. We also showed that for an annular region with a large number of blades increasing the inner radius compared to the outer radius has little effect on the low frequency modes.

Chapter 9

Conclusion

In this thesis we have investigated the occurrence of trapped modes in the presence of thin obstacles. The thesis has been split into two parts. In part I we consider two-dimensional problems, with three-dimensional problems considered in part II. In this chapter we shall draw conclusions from the work presented.

The work in chapters 2–4 concerns two-dimensional parallel-plate waveguides containing thin obstacles. In chapters 2 and 4 the geometries of the problems are defined by two parameters, whereas in chapter 3 the problem can be simplified due to symmetry and has a geometry defined by a single parameter. The number of parameters defining the geometry is important as we found that if a geometry was defined by N parameters, we were able to find trapped modes in $N + 1$ frequency bands. The exception occurred in chapter 2 as trapped modes were not found in the highest frequency band. In each band a modified residue calculus method was used to calculate the trapped-modes frequencies. In each chapter a variational technique was used to prove the existence of trapped modes in the lowest frequency band for a sufficiently long plate.

In chapter 5 a different type of trapped mode was sought. We considered of an array of parallel plates of equal distance apart each containing an identical finite length gap. For this problem the trapped modes travel through the gaps and decay down the plates and are known as Rayleigh-Bloch waves. The problem was described by two parameters and trapped modes were found using the modified residue calculus method in three frequency bands.

In chapter 6 we sought trapped modes in a pair of concentric circular cylindrical waveguides coupled laterally by a finite length gap. A modified residue calculus method was used to compute trapped-mode frequencies below the first cut-off and the modes

found each had a particular angular variation.

The problem of a pair of planar layers coupled by a circular hole was considered in chapter 7. When the planar layers were of equal width the problem reduced to a circular disc on the centreline of a planar waveguide. Using a method based on the truncation of an eigenfunction expansion we were able to find trapped modes below the first cut-off for one and two discs on the centreline and one off-centre hole. It is fairly simple to extend the work to consider the case of a pair of planar layers coupled by a number of circular holes.

In chapter 8 we considered the problem of a circular cylindrical waveguide of annular cross-section containing a number of thin radial fins of finite length. Using a method based on the truncation of an eigenfunction expansion we were able to find trapped modes below the first cut-off. We also provided an accurate estimate to the frequencies when the number of blades became large.

Appendix A

Integral of product of Bessel functions

We consider the integral

$$I_{m\mu}^{n\nu} = \int_b^d \psi_{mn}(\rho) \psi_{\mu\nu}(\rho) \rho \, d\rho. \quad (\text{A.1})$$

With $(\sigma(\mu), \nu) \neq (0, 1)$, we have from (8.2.24),

$$I_{m\mu}^{n\nu} = \int_b^d \left(Y'_{\sigma(m)}(\eta_{\sigma(m)n}) J_{\sigma(m)}(\eta_{\sigma(m)n}\rho/b) - J'_{\sigma(m)}(\eta_{\sigma(m)n}) Y_{\sigma(m)}(\eta_{\sigma(m)n}\rho/b) \right) \\ \left(Y'_{\sigma(\mu)}(\eta_{\sigma(\mu)\nu}) J_{\sigma(\mu)}(\eta_{\sigma(\mu)\nu}\rho/b) - J'_{\sigma(\mu)}(\eta_{\sigma(\mu)\nu}) Y_{\sigma(\mu)}(\eta_{\sigma(\mu)\nu}\rho/b) \right) \rho \, d\rho, \quad (\text{A.2})$$

and when $m = \mu$ we have

$$I_{\mu\mu}^{n\nu} = \int_b^d \left(Y'_{\sigma(\mu)}(\eta_{\sigma(\mu)n}) Y'_{\sigma(\mu)}(\eta_{\sigma(\mu)\nu}) J_{\sigma(\mu)}(\eta_{\sigma(\mu)n}\rho/b) J_{\sigma(\mu)}(\eta_{\sigma(\mu)\nu}\rho/b) \right. \\ \left. - Y'_{\sigma(\mu)}(\eta_{\sigma(\mu)n}) J'_{\sigma(\mu)}(\eta_{\sigma(\mu)\nu}) J_{\sigma(\mu)}(\eta_{\sigma(\mu)n}\rho/b) Y_{\sigma(\mu)}(\eta_{\sigma(\mu)\nu}\rho/b) \right. \\ \left. - J'_{\sigma(\mu)}(\eta_{\sigma(\mu)n}) Y'_{\sigma(\mu)}(\eta_{\sigma(\mu)\nu}) Y_{\sigma(\mu)}(\eta_{\sigma(\mu)n}\rho/b) J_{\sigma(\mu)}(\eta_{\sigma(\mu)\nu}\rho/b) \right. \\ \left. + J'_{\sigma(\mu)}(\eta_{\sigma(\mu)n}) J'_{\sigma(\mu)}(\eta_{\sigma(\mu)\nu}) Y_{\sigma(\mu)}(\eta_{\sigma(\mu)n}\rho/b) Y_{\sigma(\mu)}(\eta_{\sigma(\mu)\nu}\rho/b) \right) \rho \, d\rho. \quad (\text{A.3})$$

From Jones (1986), p675 we find

$$\int^z t \mathcal{Z}_\nu^{(m)}(kt) \mathcal{Z}_\nu^{(n)}(lt) \, dt = z \left\{ k \mathcal{Z}_{\nu+1}^{(m)}(kz) \mathcal{Z}_\nu^{(n)}(lz) \right. \\ \left. - l \mathcal{Z}_\nu^{(m)}(kz) \mathcal{Z}_{\nu+1}^{(n)}(lz) \right\} / (k^2 - l^2) \quad (k \neq l) \quad (\text{A.4})$$

$$= \frac{z^2}{2} \left\{ \mathcal{Z}_\nu^{(m)'}(kz) \mathcal{Z}_\nu^{(n)'}(kz) \right. \\ \left. + \mathcal{Z}_\nu^{(m)}(kz) \mathcal{Z}_\nu^{(n)}(kz) \left(1 - \frac{\nu^2}{k^2 z^2} \right) \right\} \quad (k = l), \quad (\text{A.5})$$

where $\mathcal{Z}_\nu^{(1)}$, and $\mathcal{Z}_\nu^{(2)}$ are J_ν and Y_ν respectively. We now define

$$I_1 = Y'_{\sigma(\mu)}(\eta_{\sigma(\mu)n}) Y'_{\sigma(\mu)}(\eta_{\sigma(\mu)\nu}) \int^z J_{\sigma(\mu)}(\eta_{\sigma(\mu)n}\rho/b) J_{\sigma(\mu)}(\eta_{\sigma(\mu)\nu}\rho/b) \rho \, d\rho, \quad (\text{A.6})$$

$$I_2 = -Y'_{\sigma(\mu)}(\eta_{\sigma(\mu)n}) J'_{\sigma(\mu)}(\eta_{\sigma(\mu)\nu}) \int^z J_{\sigma(\mu)}(\eta_{\sigma(\mu)n}\rho/b) Y_{\sigma(\mu)}(\eta_{\sigma(\mu)\nu}\rho/b) \rho \, d\rho, \quad (\text{A.7})$$

$$I_3 = -J'_{\sigma(\mu)}(\eta_{\sigma(\mu)n}) Y'_{\sigma(\mu)}(\eta_{\sigma(\mu)\nu}) \int^z Y_{\sigma(\mu)}(\eta_{\sigma(\mu)n}\rho/b) J_{\sigma(\mu)}(\eta_{\sigma(\mu)\nu}\rho/b) \rho \, d\rho, \quad (\text{A.8})$$

$$I_4 = J'_{\sigma(\mu)}(\eta_{\sigma(\mu)n}) J'_{\sigma(\mu)}(\eta_{\sigma(\mu)\nu}) \int^z Y_{\sigma(\mu)}(\eta_{\sigma(\mu)\nu}\rho/b) Y_{\sigma(\mu)}(\eta_{\sigma(\mu)\nu}\rho/b) \rho \, d\rho. \quad (\text{A.9})$$

If $n \neq \nu$ we can evaluate (A.6)–(A.9) as

$$I_1 = \left(\frac{Y'_{\sigma(\mu)}(\eta_{\sigma(\mu)n}) Y'_{\sigma(\mu)}(\eta_{\sigma(\mu)\nu}) z b^2}{(\eta_{\sigma(\mu)n}^2 - \eta_{\sigma(\mu)\nu}^2)} \right) \left\{ \frac{\eta_{\sigma(\mu)n}}{b} J_{\sigma(\mu)+1}(\eta_{\sigma(\mu)n}z/b) J_{\sigma(\mu)}(\eta_{\sigma(\mu)\nu}z/b) \right. \\ \left. - \frac{\eta_{\sigma(\mu)\nu}}{b} J_{\sigma(\mu)}(\eta_{\sigma(\mu)n}z/b) J_{\sigma(\mu)+1}(\eta_{\sigma(\mu)\nu}z/b) \right\}, \quad (\text{A.10})$$

$$I_2 = - \left(\frac{Y'_{\sigma(\mu)}(\eta_{\sigma(\mu)n}) J'_{\sigma(\mu)}(\eta_{\sigma(\mu)\nu}) z b^2}{(\eta_{\sigma(\mu)n}^2 - \eta_{\sigma(\mu)\nu}^2)} \right) \left\{ \frac{\eta_{\sigma(\mu)n}}{b} J_{\sigma(\mu)+1}(\eta_{\sigma(\mu)n}z/b) Y_{\sigma(\mu)}(\eta_{\sigma(\mu)\nu}z/b) \right. \\ \left. - \frac{\eta_{\sigma(\mu)\nu}}{b} J_{\sigma(\mu)}(\eta_{\sigma(\mu)n}z/b) Y_{\sigma(\mu)+1}(\eta_{\sigma(\mu)\nu}z/b) \right\}, \quad (\text{A.11})$$

$$I_3 = - \left(\frac{J'_{\sigma(\mu)}(\eta_{\sigma(\mu)n}) Y'_{\sigma(\mu)}(\eta_{\sigma(\mu)\nu}) z b^2}{(\eta_{\sigma(\mu)n}^2 - \eta_{\sigma(\mu)\nu}^2)} \right) \left\{ \frac{\eta_{\sigma(\mu)n}}{b} Y_{\sigma(\mu)+1}(\eta_{\sigma(\mu)n}z/b) J_{\sigma(\mu)}(\eta_{\sigma(\mu)\nu}z/b) \right. \\ \left. - \frac{\eta_{\sigma(\mu)\nu}}{b} Y_{\sigma(\mu)}(\eta_{\sigma(\mu)n}z/b) J_{\sigma(\mu)+1}(\eta_{\sigma(\mu)\nu}z/b) \right\}, \quad (\text{A.12})$$

$$I_4 = \left(\frac{J'_{\sigma(\mu)}(\eta_{\sigma(\mu)n}) J'_{\sigma(\mu)}(\eta_{\sigma(\mu)\nu}) z b^2}{(\eta_{\sigma(\mu)n}^2 - \eta_{\sigma(\mu)\nu}^2)} \right) \left\{ \frac{\eta_{\sigma(\mu)n}}{b} Y_{\sigma(\mu)+1}(\eta_{\sigma(\mu)n}z/b) Y_{\sigma(\mu)}(\eta_{\sigma(\mu)\nu}z/b) \right. \\ \left. - \frac{\eta_{\sigma(\mu)\nu}}{b} Y_{\sigma(\mu)}(\eta_{\sigma(\mu)n}z/b) Y_{\sigma(\mu)+1}(\eta_{\sigma(\mu)\nu}z/b) \right\}. \quad (\text{A.13})$$

We now use the result

$$\mathcal{Z}_{\nu+1}^{(m)}(z) = \frac{\nu}{z} \mathcal{Z}_\nu^{(m)}(z) - \mathcal{Z}_\nu^{(m)'}(z), \quad m = 1, 2, \quad (\text{A.14})$$

with (A.10)–(A.13) to produce

$$I_1 = \left(\frac{Y'_{\sigma(\mu)}(\eta_{\sigma(\mu)n}) Y'_{\sigma(\mu)}(\eta_{\sigma(\mu)\nu}) z b}{(\eta_{\sigma(\mu)n}^2 - \eta_{\sigma(\mu)\nu}^2)} \right) \left\{ \eta_{\sigma(\mu)\nu} J_{\sigma(\mu)}(\eta_{\sigma(\mu)n} z/b) J'_{\sigma(\mu)}(\eta_{\sigma(\mu)\nu} z/b) \right. \\ \left. - \eta_{\sigma(\mu)n} J'_{\sigma(\mu)}(\eta_{\sigma(\mu)n} z/b) J_{\sigma(\mu)}(\eta_{\sigma(\mu)\nu} z/b) \right\}, \quad (\text{A.15})$$

$$I_2 = \left(\frac{Y'_{\sigma(\mu)}(\eta_{\sigma(\mu)n}) J'_{\sigma(\mu)}(\eta_{\sigma(\mu)\nu}) z b}{(\eta_{\sigma(\mu)n}^2 - \eta_{\sigma(\mu)\nu}^2)} \right) \left\{ \eta_{\sigma(\mu)\nu} J_{\sigma(\mu)}(\eta_{\sigma(\mu)n} z/b) Y'_{\sigma(\mu)}(\eta_{\sigma(\mu)\nu} z/b) \right. \\ \left. - \eta_{\sigma(\mu)n} J'_{\sigma(\mu)}(\eta_{\sigma(\mu)n} z/b) Y_{\sigma(\mu)}(\eta_{\sigma(\mu)\nu} z/b) \right\}, \quad (\text{A.16})$$

$$I_3 = \left(\frac{J'_{\sigma(\mu)}(\eta_{\sigma(\mu)n}) Y'_{\sigma(\mu)}(\eta_{\sigma(\mu)\nu}) z b}{(\eta_{\sigma(\mu)n}^2 - \eta_{\sigma(\mu)\nu}^2)} \right) \left\{ \eta_{\sigma(\mu)\nu} Y_{\sigma(\mu)}(\eta_{\sigma(\mu)n} z/b) J'_{\sigma(\mu)}(\eta_{\sigma(\mu)\nu} z/b) \right. \\ \left. - \eta_{\sigma(\mu)n} Y'_{\sigma(\mu)}(\eta_{\sigma(\mu)n} z/b) J_{\sigma(\mu)}(\eta_{\sigma(\mu)\nu} z/b) \right\}, \quad (\text{A.17})$$

$$I_4 = \left(\frac{J'_{\sigma(\mu)}(\eta_{\sigma(\mu)n}) J'_{\sigma(\mu)}(\eta_{\sigma(\mu)\nu}) z b}{(\eta_{\sigma(\mu)n}^2 - \eta_{\sigma(\mu)\nu}^2)} \right) \left\{ \eta_{\sigma(\mu)\nu} Y_{\sigma(\mu)}(\eta_{\sigma(\mu)n} z/b) Y'_{\sigma(\mu)}(\eta_{\sigma(\mu)\nu} z/b) \right. \\ \left. - \eta_{\sigma(\mu)n} Y'_{\sigma(\mu)}(\eta_{\sigma(\mu)n} z/b) Y_{\sigma(\mu)}(\eta_{\sigma(\mu)\nu} z/b) \right\}. \quad (\text{A.18})$$

If we let

$$\gamma = \frac{\eta_{\sigma(\mu)n}}{\eta_{\sigma(\mu)\nu}}, \quad (\text{A.19})$$

then we can rewrite (A.3) using (A.15)–(A.19) as

$$\begin{aligned}
I_{\mu\mu}^{n\nu} = & \left(\frac{Y'_{\sigma(\mu)}(\eta_{\sigma(\mu)n}) Y'_{\sigma(\mu)}(\eta_{\sigma(\mu)\nu}) \eta_{\sigma(\mu)\nu}}{(\eta_{\sigma(\mu)n}^2 - \eta_{\sigma(\mu)\nu}^2)} \right) \left\{ db J_{\sigma(\mu)}(\eta_{\sigma(\mu)n}\delta) J'_{\sigma(\mu)}(\eta_{\sigma(\mu)\nu}\delta) \right. \\
& - db \gamma J'_{\sigma(\mu)}(\eta_{\sigma(\mu)n}\delta) J_{\sigma(\mu)}(\eta_{\sigma(\mu)\nu}\delta) - b^2 J_{\sigma(\mu)}(\eta_{\sigma(\mu)n}) J'_{\sigma(\mu)}(\eta_{\sigma(\mu)\nu}) \\
& \left. - b^2 \gamma J'_{\sigma(\mu)}(\eta_{\sigma(\mu)n}) J_{\sigma(\mu)}(\eta_{\sigma(\mu)\nu}) \right\} \\
& - \left(\frac{Y'_{\sigma(\mu)}(\eta_{\sigma(\mu)n}) J'_{\sigma(\mu)}(\eta_{\sigma(\mu)\nu}) \eta_{\sigma(\mu)\nu}}{(\eta_{\sigma(\mu)n}^2 - \eta_{\sigma(\mu)\nu}^2)} \right) \left\{ db J_{\sigma(\mu)}(\eta_{\sigma(\mu)n}\delta) Y'_{\sigma(\mu)}(\eta_{\sigma(\mu)\nu}\delta) \right. \\
& - db \gamma J'_{\sigma(\mu)}(\eta_{\sigma(\mu)n}\delta) Y_{\sigma(\mu)}(\eta_{\sigma(\mu)\nu}\delta) - b^2 J_{\sigma(\mu)}(\eta_{\sigma(\mu)n}) Y'_{\sigma(\mu)}(\eta_{\sigma(\mu)\nu}) \\
& \left. - b^2 \gamma J'_{\sigma(\mu)}(\eta_{\sigma(\mu)n}) Y_{\sigma(\mu)}(\eta_{\sigma(\mu)\nu}) \right\} \\
& - \left(\frac{J'_{\sigma(\mu)}(\eta_{\sigma(\mu)n}) Y'_{\sigma(\mu)}(\eta_{\sigma(\mu)\nu}) \eta_{\sigma(\mu)\nu}}{(\eta_{\sigma(\mu)n}^2 - \eta_{\sigma(\mu)\nu}^2)} \right) \left\{ db Y_{\sigma(\mu)}(\eta_{\sigma(\mu)n}\delta) J'_{\sigma(\mu)}(\eta_{\sigma(\mu)\nu}\delta) \right. \\
& - db \gamma Y'_{\sigma(\mu)}(\eta_{\sigma(\mu)n}\delta) J_{\sigma(\mu)}(\eta_{\sigma(\mu)\nu}\delta) - b^2 Y_{\sigma(\mu)}(\eta_{\sigma(\mu)n}) J'_{\sigma(\mu)}(\eta_{\sigma(\mu)\nu}) \\
& \left. - b^2 \gamma Y'_{\sigma(\mu)}(\eta_{\sigma(\mu)n}) J_{\sigma(\mu)}(\eta_{\sigma(\mu)\nu}) \right\} \\
& + \left(\frac{J'_{\sigma(\mu)}(\eta_{\sigma(\mu)n}) J'_{\sigma(\mu)}(\eta_{\sigma(\mu)\nu}) \eta_{\sigma(\mu)\nu}}{(\eta_{\sigma(\mu)n}^2 - \eta_{\sigma(\mu)\nu}^2)} \right) \left\{ db Y_{\sigma(\mu)}(\eta_{\sigma(\mu)n}\delta) Y'_{\sigma(\mu)}(\eta_{\sigma(\mu)\nu}\delta) \right. \\
& - db \gamma Y'_{\sigma(\mu)}(\eta_{\sigma(\mu)n}\delta) Y_{\sigma(\mu)}(\eta_{\sigma(\mu)\nu}\delta) - b^2 Y_{\sigma(\mu)}(\eta_{\sigma(\mu)n}) Y'_{\sigma(\mu)}(\eta_{\sigma(\mu)\nu}) \\
& \left. - b^2 \gamma Y'_{\sigma(\mu)}(\eta_{\sigma(\mu)n}) Y_{\sigma(\mu)}(\eta_{\sigma(\mu)\nu}) \right\}. \tag{A.20}
\end{aligned}$$

Expanding (A.20) we find

$$\begin{aligned}
I_{\mu\mu}^{n\nu} = & \left(\frac{b^2 \eta_{\sigma(\mu)\nu}}{(\eta_{\sigma(\mu)n}^2 - \eta_{\sigma(\mu)\nu}^2)} \right) \left\{ \delta Y'_{\sigma(\mu)}(\eta_{\sigma(\mu)n}) Y'_{\sigma(\mu)}(\eta_{\sigma(\mu)\nu}) J_{\sigma(\mu)}(\eta_{\sigma(\mu)n}\delta) J'_{\sigma(\mu)}(\eta_{\sigma(\mu)\nu}\delta) \right. \\
& - \delta \gamma Y'_{\sigma(\mu)}(\eta_{\sigma(\mu)n}) Y'_{\sigma(\mu)}(\eta_{\sigma(\mu)\nu}) J'_{\sigma(\mu)}(\eta_{\sigma(\mu)n}\delta) J_{\sigma(\mu)}(\eta_{\sigma(\mu)\nu}\delta) \\
& - Y'_{\sigma(\mu)}(\eta_{\sigma(\mu)n}) Y'_{\sigma(\mu)}(\eta_{\sigma(\mu)\nu}) J_{\sigma(\mu)}(\eta_{\sigma(\mu)n}) J'_{\sigma(\mu)}(\eta_{\sigma(\mu)\nu}) \\
& + \gamma Y'_{\sigma(\mu)}(\eta_{\sigma(\mu)n}) Y'_{\sigma(\mu)}(\eta_{\sigma(\mu)\nu}) J'_{\sigma(\mu)}(\eta_{\sigma(\mu)n}) J_{\sigma(\mu)}(\eta_{\sigma(\mu)\nu}) \\
& - \delta Y'_{\sigma(\mu)}(\eta_{\sigma(\mu)n}) J'_{\sigma(\mu)}(\eta_{\sigma(\mu)\nu}) J_{\sigma(\mu)}(\eta_{\sigma(\mu)n}\delta) Y'_{\sigma(\mu)}(\eta_{\sigma(\mu)\nu}\delta) \\
& + \delta \gamma Y'_{\sigma(\mu)}(\eta_{\sigma(\mu)n}) J'_{\sigma(\mu)}(\eta_{\sigma(\mu)\nu}) J'_{\sigma(\mu)}(\eta_{\sigma(\mu)n}\delta) Y_{\sigma(\mu)}(\eta_{\sigma(\mu)\nu}\delta) \\
& + Y'_{\sigma(\mu)}(\eta_{\sigma(\mu)n}) J'_{\sigma(\mu)}(\eta_{\sigma(\mu)\nu}) J_{\sigma(\mu)}(\eta_{\sigma(\mu)n}) Y'_{\sigma(\mu)}(\eta_{\sigma(\mu)\nu}) \\
& - \gamma Y'_{\sigma(\mu)}(\eta_{\sigma(\mu)n}) J'_{\sigma(\mu)}(\eta_{\sigma(\mu)\nu}) J'_{\sigma(\mu)}(\eta_{\sigma(\mu)n}) Y_{\sigma(\mu)}(\eta_{\sigma(\mu)\nu}) \\
& - \delta J'_{\sigma(\mu)}(\eta_{\sigma(\mu)n}) Y'_{\sigma(\mu)}(\eta_{\sigma(\mu)\nu}) Y_{\sigma(\mu)}(\eta_{\sigma(\mu)n}\delta) J'_{\sigma(\mu)}(\eta_{\sigma(\mu)\nu}\delta) \\
& + \delta \gamma J'_{\sigma(\mu)}(\eta_{\sigma(\mu)n}) Y'_{\sigma(\mu)}(\eta_{\sigma(\mu)\nu}) Y'_{\sigma(\mu)}(\eta_{\sigma(\mu)n}\delta) J_{\sigma(\mu)}(\eta_{\sigma(\mu)\nu}\delta) \\
& + J'_{\sigma(\mu)}(\eta_{\sigma(\mu)n}) Y'_{\sigma(\mu)}(\eta_{\sigma(\mu)\nu}) Y_{\sigma(\mu)}(\eta_{\sigma(\mu)n}) J'_{\sigma(\mu)}(\eta_{\sigma(\mu)\nu}) \\
& - \gamma J'_{\sigma(\mu)}(\eta_{\sigma(\mu)n}) Y'_{\sigma(\mu)}(\eta_{\sigma(\mu)\nu}) Y'_{\sigma(\mu)}(\eta_{\sigma(\mu)n}) J_{\sigma(\mu)}(\eta_{\sigma(\mu)\nu}) \\
& + \delta J'_{\sigma(\mu)}(\eta_{\sigma(\mu)n}) J'_{\sigma(\mu)}(\eta_{\sigma(\mu)\nu}) Y_{\sigma(\mu)}(\eta_{\sigma(\mu)n}\delta) Y'_{\sigma(\mu)}(\eta_{\sigma(\mu)\nu}\delta) \\
& - \delta \gamma J'_{\sigma(\mu)}(\eta_{\sigma(\mu)n}) J'_{\sigma(\mu)}(\eta_{\sigma(\mu)\nu}) Y'_{\sigma(\mu)}(\eta_{\sigma(\mu)n}\delta) Y_{\sigma(\mu)}(\eta_{\sigma(\mu)\nu}\delta) \\
& - J'_{\sigma(\mu)}(\eta_{\sigma(\mu)n}) J'_{\sigma(\mu)}(\eta_{\sigma(\mu)\nu}) Y_{\sigma(\mu)}(\eta_{\sigma(\mu)n}) Y'_{\sigma(\mu)}(\eta_{\sigma(\mu)\nu}) \\
& \left. + \gamma J'_{\sigma(\mu)}(\eta_{\sigma(\mu)n}) J'_{\sigma(\mu)}(\eta_{\sigma(\mu)\nu}) Y'_{\sigma(\mu)}(\eta_{\sigma(\mu)n}) Y_{\sigma(\mu)}(\eta_{\sigma(\mu)\nu}) \right\}. \tag{A.21}
\end{aligned}$$

Collecting constant terms and terms involving δ , $\delta \gamma$, γ from (A.21) and using (8.2.23) we see that when $n \neq \nu$

$$I_{\mu\mu}^{n\nu} = 0. \tag{A.22}$$

When $n = \nu$ (A.6)–(A.9) become:

$$I_1 = \left(1/2 Y_{\sigma(\mu)}'^2(\eta_{\sigma(\mu)\nu}) z^2\right) \left\{ J_{\sigma(\mu)}'^2(\eta_{\sigma(\mu)\nu} z/b) + J_{\sigma(\mu)}^2(\eta_{\sigma(\mu)\nu} z/b) \left[1 - \frac{\sigma^2(\mu) b^2}{\eta_{\sigma(\mu)\nu}^2 z^2}\right] \right\}, \quad (\text{A.23})$$

$$I_2 = - \left(1/2 Y_{\sigma(\mu)}'(\eta_{\sigma(\mu)\nu}) J_{\sigma(\mu)}'(\eta_{\sigma(\mu)\nu}) z^2\right) \left\{ J_{\sigma(\mu)}'(\eta_{\sigma(\mu)\nu} z/b) Y_{\sigma(\mu)}'(\eta_{\sigma(\mu)\nu} z/b) \right. \\ \left. + J_{\sigma(\mu)}(\eta_{\sigma(\mu)\nu} z/b) Y_{\sigma(\mu)}(\eta_{\sigma(\mu)\nu} z/b) \left[1 - \frac{\sigma^2(\mu) b^2}{\eta_{\sigma(\mu)\nu}^2 z^2}\right] \right\}, \quad (\text{A.24})$$

$$I_3 = - \left(1/2 Y_{\sigma(\mu)}'(\eta_{\sigma(\mu)\nu}) J_{\sigma(\mu)}'(\eta_{\sigma(\mu)\nu}) z^2\right) \left\{ J_{\sigma(\mu)}'(\eta_{\sigma(\mu)\nu} z/b) Y_{\sigma(\mu)}'(\eta_{\sigma(\mu)\nu} z/b) \right. \\ \left. + J_{\sigma(\mu)}(\eta_{\sigma(\mu)\nu} z/b) Y_{\sigma(\mu)}(\eta_{\sigma(\mu)\nu} z/b) \left[1 - \frac{\sigma^2(\mu) b^2}{\eta_{\sigma(\mu)\nu}^2 z^2}\right] \right\}, \quad (\text{A.25})$$

$$I_4 = \left(1/2 J_{\sigma(\mu)}'^2(\eta_{\sigma(\mu)\nu}) z^2\right) \left\{ Y_{\sigma(\mu)}'^2(\eta_{\sigma(\mu)\nu} z/b) + Y_{\sigma(\mu)}^2(\eta_{\sigma(\mu)\nu} z/b) \left[1 - \frac{\sigma^2(\mu) b^2}{\eta_{\sigma(\mu)\nu}^2 z^2}\right] \right\}. \quad (\text{A.26})$$

Using (A.23)–(A.26), we have from (A.1)

$$\begin{aligned}
2 d^{-2} I_{\mu\mu}^{\nu\nu} &= \left\{ Y_{\sigma(\mu)}^{\prime 2}(\eta_{\sigma(\mu)\nu}) J_{\sigma(\mu)}^{\prime 2}(\eta_{\sigma(\mu)\nu}\delta) + Y_{\sigma(\mu)}^{\prime 2}(\eta_{\sigma(\mu)\nu}) J_{\sigma(\mu)}^2(\eta_{\sigma(\mu)\nu}\delta) \left[1 - \frac{\sigma^2(\mu)}{\eta_{\sigma(\mu)\nu}^2 \delta^2} \right] \right. \\
&\quad - 2Y_{\sigma(\mu)}'(\eta_{\sigma(\mu)\nu}) J_{\sigma(\mu)}'(\eta_{\sigma(\mu)\nu}) J_{\sigma(\mu)}'(\eta_{\sigma(\mu)\nu}\delta) Y_{\sigma(\mu)}'(\eta_{\sigma(\mu)\nu}\delta) \\
&\quad - 2Y_{\sigma(\mu)}'(\eta_{\sigma(\mu)\nu}) J_{\sigma(\mu)}'(\eta_{\sigma(\mu)\nu}) J_{\sigma(\mu)}(\eta_{\sigma(\mu)\nu}\delta) Y_{\sigma(\mu)}(\eta_{\sigma(\mu)\nu}\delta) \left[1 - \frac{\sigma^2(\mu)}{\eta_{\sigma(\mu)\nu}^2 \delta^2} \right] \\
&\quad + J_{\sigma(\mu)}^{\prime 2}(\eta_{\sigma(\mu)\nu}) Y_{\sigma(\mu)}^{\prime 2}(\eta_{\sigma(\mu)\nu}\delta) + J_{\sigma(\mu)}^{\prime 2}(\eta_{\sigma(\mu)\nu}) Y_{\sigma(\mu)}^2(\eta_{\sigma(\mu)\nu}\delta) \left[1 - \frac{\sigma^2(\mu)}{\eta_{\sigma(\mu)\nu}^2 \delta^2} \right] \left. \right\} \\
&\quad - \frac{1}{\delta^2} \left\{ Y_{\sigma(\mu)}^{\prime 2}(\eta_{\sigma(\mu)\nu}) J_{\sigma(\mu)}^{\prime 2}(\eta_{\sigma(\mu)\nu}) + Y_{\sigma(\mu)}^{\prime 2}(\eta_{\sigma(\mu)\nu}) J_{\sigma(\mu)}^2(\eta_{\sigma(\mu)\nu}) \left[1 - \frac{\sigma^2(\mu)}{\eta_{\sigma(\mu)\nu}^2} \right] \right. \\
&\quad - 2Y_{\sigma(\mu)}^{\prime 2}(\eta_{\sigma(\mu)\nu}) J_{\sigma(\mu)}^{\prime 2}(\eta_{\sigma(\mu)\nu}) \\
&\quad - 2Y_{\sigma(\mu)}'(\eta_{\sigma(\mu)\nu}) J_{\sigma(\mu)}'(\eta_{\sigma(\mu)\nu}) J_{\sigma(\mu)}(\eta_{\sigma(\mu)\nu}) Y_{\sigma(\mu)}(\eta_{\sigma(\mu)\nu}) \left[1 - \frac{\sigma^2(\mu)}{\eta_{\sigma(\mu)\nu}^2} \right] \\
&\quad \left. + J_{\sigma(\mu)}^{\prime 2}(\eta_{\sigma(\mu)\nu}) Y_{\sigma(\mu)}^{\prime 2}(\eta_{\sigma(\mu)\nu}) + J_{\sigma(\mu)}^{\prime 2}(\eta_{\sigma(\mu)\nu}) Y_{\sigma(\mu)}^2(\eta_{\sigma(\mu)\nu}) \left[1 - \frac{\sigma^2(\mu)}{\eta_{\sigma(\mu)\nu}^2} \right] \right\} \\
&= \left\{ \left(Y_{\sigma(\mu)}'(\eta_{\sigma(\mu)\nu}) J_{\sigma(\mu)}'(\eta_{\sigma(\mu)\nu}\delta) - J_{\sigma(\mu)}'(\eta_{\sigma(\mu)\nu}) Y_{\sigma(\mu)}'(\eta_{\sigma(\mu)\nu}\delta) \right)^2 \right. \\
&\quad + \left(Y_{\sigma(\mu)}'(\eta_{\sigma(\mu)\nu}) J_{\sigma(\mu)}(\eta_{\sigma(\mu)\nu}\delta) - J_{\sigma(\mu)}'(\eta_{\sigma(\mu)\nu}) Y_{\sigma(\mu)}(\eta_{\sigma(\mu)\nu}\delta) \right)^2 \left[1 - \left(\frac{\sigma(\mu)}{\eta_{\sigma(\mu)\nu} \delta} \right)^2 \right] \left. \right\} \\
&\quad - \frac{1}{\delta^2} \left\{ \left(Y_{\sigma(\mu)}'(\eta_{\sigma(\mu)\nu}) J_{\sigma(\mu)}(\eta_{\sigma(\mu)\nu}) - J_{\sigma(\mu)}'(\eta_{\sigma(\mu)\nu}) Y_{\sigma(\mu)}(\eta_{\sigma(\mu)\nu}) \right)^2 \left[1 - \left(\frac{\sigma(\mu)}{\eta_{\sigma(\mu)\nu}} \right)^2 \right] \right\}.
\end{aligned} \tag{A.27}$$

When $\mu = 0$ and $\nu = 1$ from (A.1) we have,

$$I_{11}^{00} = \int_b^d \rho \, d\rho = \frac{1}{2}(d^2 - b^2), \tag{A.28}$$

and so

$$2 d^{-2} I_{11}^{00} = (1 - 1/\delta^2). \tag{A.29}$$

Combining (A.22), (A.27) and (A.29) we can define

$$I_{\mu\mu}^{\nu\nu} = \delta_{\nu\nu} q_{\mu\nu}, \tag{A.30}$$

where

$$2d^{-2}q_{\mu\nu} = \left\{ \begin{array}{l} \left(\left\{ \left(Y'_{\sigma(\mu)}(\eta_{\sigma(\mu)\nu}) J'_{\sigma(\mu)}(\eta_{\sigma(\mu)\nu}\delta) - \right. \right. \right. \\ \qquad \qquad \qquad \left. \left. \left. J'_{\sigma(\mu)}(\eta_{\sigma(\mu)\nu}) Y'_{\sigma(\mu)}(\eta_{\sigma(\mu)\nu}\delta) \right)^2 \right. \right. \\ + \left(Y'_{\sigma(\mu)}(\eta_{\sigma(\mu)\nu}) J_{\sigma(\mu)}(\eta_{\sigma(\mu)\nu}\delta) - \right. \\ \qquad \qquad \qquad \left. \left. J'_{\sigma(\mu)}(\eta_{\sigma(\mu)\nu}) Y_{\sigma(\mu)}(\eta_{\sigma(\mu)\nu}\delta) \right)^2 \right. \\ \qquad \qquad \qquad \left. \left. \left[1 - \left(\frac{\sigma(\mu)}{\eta_{\sigma(\mu)\nu} \delta} \right)^2 \right] \right\} \\ - \frac{1}{\delta^2} \left\{ \left(Y'_{\sigma(\mu)}(\eta_{\sigma(\mu)\nu}) J_{\sigma(\mu)}(\eta_{\sigma(\mu)\nu}) - \right. \right. \\ \qquad \qquad \qquad \left. \left. J'_{\sigma(\mu)}(\eta_{\sigma(\mu)\nu}) Y_{\sigma(\mu)}(\eta_{\sigma(\mu)\nu}) \right)^2 \right. \\ \qquad \qquad \qquad \left. \left. \left[1 - \left(\frac{\sigma(\mu)}{\eta_{\sigma(\mu)\nu}} \right)^2 \right] \right\}, \quad (\sigma(\mu), \nu) \neq (0, 1), \\ (1 - 1/\delta^2), \quad (\sigma(\mu), \nu) = (0, 1). \end{array} \right. \quad (\text{A.31})$$

Appendix B

Zeros of cross-products of Bessel functions

Below we prove that if we write η_{mn} as the n th non-negative zero of the cross-product

$$f_m(x) = J'_m(x) Y'_m(\delta x) - Y'_m(x) J'_m(\delta x), \quad \delta > 1, \quad (\text{B.1})$$

then for $m \in \mathbb{N}$,

$$\eta_{m1} < m < \delta \eta_{m1}, \quad (\text{B.2})$$

and therefore as $\delta \rightarrow 1$,

$$\eta_{m1} \rightarrow m. \quad (\text{B.3})$$

We begin by noting that, for any m ,

$$\frac{d}{dx} \left[\frac{Y'_m(x)}{J'_m(x)} \right] = -\frac{(m^2 - x^2)}{J_m'^2(x) x^2} \left[\frac{2}{\pi x} \right]. \quad (\text{B.4})$$

Integrating (B.4) with respect to x we have,

$$\frac{Y'_m(b)}{J'_m(b)} - \frac{Y'_m(a)}{J'_m(a)} = -\frac{2}{\pi} \int_a^b \frac{(m^2 - x^2)}{x^3 J_m'^2(x)} dx, \quad (\text{B.5})$$

provided $0 < a \leq b$ and $J'_m(x) \neq 0$, $a \leq x \leq b$. Putting $a = x$, $b = \delta x$, and $\delta > 1$, into (B.5) we find

$$f_m(x) = -\frac{2}{\pi} J'_{\sigma(m)}(x) J'_{\sigma(m)}(x\delta) \int_x^{x\delta} \frac{(\sigma(m)^2 - s^2)}{s^3 J_{\sigma(m)}'^2(s)} ds, \quad (\text{B.6})$$

provided $J'_{\sigma(m)}(s) \neq 0$ for $s \in [x, x\delta]$.

For any $m \in \mathbb{N}$ we have $j'_{m,1} > m$ (see Watson (1944), §15.3) and therefore from (B.6) we see that $f_m(x) < 0$ provided $0 < x\delta \leq m$. It therefore follows that

$$\delta\eta_{m1} > m, \quad m \in \mathbb{N}. \quad (\text{B.7})$$

Putting $x = \eta_{m1}$ in (B.6) we obtain

$$f_m(\eta_{m1}) = -\frac{2}{\pi} J'_{\sigma(m)}(\eta_{m1}) J'_{\sigma(m)}(\delta\eta_{m1}) \int_{\eta_{m1}}^{\delta\eta_{m1}} \frac{(\sigma(m)^2 - s^2)}{s^3 J'^2_{\sigma(m)}(s)} ds = 0, \quad (\text{B.8})$$

but from (B.7) $J'_m(\eta_{m1}) > 0$ and $J'_m(\delta\eta_{m1}) > 0$ and so

$$0 < \eta_{m1} < m, \quad m \in \mathbb{N}. \quad (\text{B.9})$$

Combining (B.7) and (B.9) we have the required inequality (B.2).

Bibliography

- Abramowitz, M. and I. A. Stegun (1972). *Handbook of Mathematical Functions with Formulas, Graphs and Mathematical Tables*. New York: Wiley-Interscience.
- Aslanyan, A., L. Parnovski, and D. Vassiliev (2000). Complex resonances in acoustic waveguides. *Quarterly Journal of Mechanics and Applied Mathematics* 53(3), 429–447.
- Behnke, H., U. Mertins, M. Plum, and C. Wieners (2000). Eigenvalue inclusions via domain decomposition. *Proceedings of the Royal Society of London A* 456, 2717–2730.
- Berry, M. V. and M. Wilkinson (1984). Diabolical points in the spectra of triangles. *Proceedings of the Royal Society of London A* 392, 15.
- Berz, F. (1951). Reflection and refraction of microwaves at a set of parallel plates. *Proceedings of the IEE* 98(3), 47–55.
- Bonnet-Bendhia, A.-S. and F. Starling (1994). Guided waves by electromagnetic gratings and non-uniqueness examples for the diffraction problem. *Mathematical Methods in the Applied Sciences* 17, 305–338.
- Bulla, W., F. Gesztesy, W. Renger, and B. Simon (1997). Weakly coupled bound states in quantum waveguides. *Proceedings of the American Mathematical Society* 125(5), 1487–1495.
- Callan, M., C. M. Linton, and D. V. Evans (1991). Trapped modes in two-dimensional waveguides. *Journal of Fluid Mechanics* 229, 51–64.
- Carini, J. P., J. T. Londergan, K. Mullen, and D. P. Murdock (1992). Bound states and resonances in waveguides and quantum wires. *Physical Review B* 46(23), 15538–15541.

- Courant, R. and D. Hilbert (1989). *Methods of Mathematical Physics I*. New York: Wiley-Interscience.
- Davies, E. B. and L. Parnowski (1998). Trapped modes in acoustic waveguides. *Quarterly Journal of Mechanics and Applied Mathematics* 51(3), 477–492.
- Duclos, P. and P. Exner (1995). Curvature-induced bound states in quantum waveguides in two and three dimensions. *Reviews in Mathematical Physics* 7(1), 73–102.
- Evans, D. V. (1990). The wide-spacing approximation to multiple scattering and sloshing problems. *Journal of Fluid Mechanics* 210, 647–658.
- Evans, D. V. (1992). Trapped acoustic modes. *IMA Journal of Applied Mathematics* 49, 45–60.
- Evans, D. V. and M. Fernyhough (1995). Edge waves along periodic coastlines. Part 2. *Journal of Fluid Mechanics* 297, 307–325.
- Evans, D. V. and N. Kuznetsov (1997). Trapped modes. In J. N. Hunt (Ed.), *Gravity Waves in Water of Finite Depth*, International Series on Advances in Fluid Mechanics. Computational Mechanics Publications, Southampton.
- Evans, D. V., M. Levitin, and D. Vassiliev (1994). Existence theorems for trapped modes. *Journal of Fluid Mechanics* 261, 21–31.
- Evans, D. V. and C. M. Linton (1991). Trapped modes in open channels. *Journal of Fluid Mechanics* 225, 153–175.
- Evans, D. V. and C. M. Linton (1993). Edge waves along periodic coastlines. *Quarterly Journal of Mechanics and Applied Mathematics* 46, 643–656.
- Evans, D. V. and C. M. Linton (1994). Acoustic resonance in ducts. *Journal of Sound and Vibration* 173(1), 85–94.
- Evans, D. V., C. M. Linton, and F. Ursell (1993). Trapped mode frequencies embedded in the continuous spectrum. *Quarterly Journal of Mechanics and Applied Mathematics* 46(2), 253–274.
- Evans, D. V. and P. McIver (1991). Trapped waves over symmetric thin bodies. *Journal of Fluid Mechanics* 223, 509–519.
- Evans, D. V. and R. Porter (1997). Trapped modes about multiple cylinders in a channel. *Journal of Fluid Mechanics* 339, 331–356.

- Evans, D. V. and R. Porter (1998). Trapped modes embedded in the continuous spectrum. *Quarterly Journal of Mechanics and Applied Mathematics* 52, 263–274.
- Evans, D. V. and R. Porter (1999). Trapping and near-trapping by arrays of cylinders in waves. *Journal of Engineering Mathematics* 35, 149–179.
- Evans, D. V. and R. Porter (2002). On the existence of embedded surface waves along arrays of parallel plates. To appear in *Quarterly Journal of Mechanics and Applied Mathematics*.
- Exner, P., P. Šeba, M. Tater, and D. Vaněk (1996). Bound states and scattering in quantum waveguides coupled laterally through a boundary window. *Journal of Mathematical Physics* 37, 4867–4887.
- Exner, P. and S. A. Vugalter (1996). Asymptotic estimates for bound states in quantum waveguides coupled laterally through a narrow window. *Annales de L'Institut Henri Poincaré - Physique Théorique* 65(1), 109–123.
- Exner, P. and S. A. Vugalter (1997). Bound-state asymptotic estimates for window-coupled Dirichlet strips and layers. *Journal of Physics A: Mathematics and General* 30, 7863–7878.
- Farina, L. and P. A. Martin (1998). Scattering of water waves by a submerged disc using a hypersingular integral equation. *Applied Ocean Research* 20, 121–134.
- Franklin, R. E. (1972). Acoustic resonance in cascades. *Journal of Sound and Vibration* 25(4), 587–595.
- Gradshteyn, I. S. and I. M. Ryzhik (1980). *Table of Integrals, Series, and Products*. Corrected and Enlarged Edition. New York: Academic Press.
- Groves, M. D. (1998). Examples of embedded eigenvalues for problems in acoustic waveguides. *Mathematical Methods in the Applied Sciences* 21(6), 479–488.
- Hirayama, Y., Y. Tokura, A. D. Wieck, S. Koch, R. J. Haug, K. von Klitzing, and K. Ploog (1993). Transport characteristics of a window-coupled in-plane-gated wire system. *Physical Review B* 48(11), 7991–7998.
- Hirayama, Y., A. D. Wieck, T. Bever, K. von Klitzing, and K. Ploog (1992). Parallel in-plane-gated wires coupled by a ballistic window. *Physical Review B* 46(7), 4035–4040.

- Hobson, E. W. (1926). *The theory of functions of a real variable and the theory of Fourier's series*, Volume II. New York: Dover.
- Hurd, R. A. (1954). The propagation of an electromagnetic wave along an infinite corrugated surface. *Canadian Journal of Physics* 32(12), 727–734.
- Hutson, V. and J. S. Pym (1980). *Applications of Functional Analysis and Operator Theory*. London: Academic Press.
- Itoh, T. and R. Mittra (1969). An analytical study of the echelette grating with application to open resonators. *IEEE Transactions on Microwave Theory and Techniques* 17(6), 319–327.
- Jones, D. S. (1953). The eigenvalues of $\nabla^2 u + \lambda u = 0$ when the boundary conditions are given on semi-infinite domains. *Proceedings of the Cambridge Philosophical Society* 49, 668–684.
- Jones, D. S. (1979). *Methods in Electromagnetic Wave Propagation*. Oxford: Clarendon Press.
- Jones, D. S. (1986). *Acoustic and Electromagnetic Waves*. Oxford: Clarendon Press.
- Karim-Panahi, K. (1983). Antiplane strain harmonic wave in infinite, elastic, periodically triple-layered media. *Journal of the Acoustic Society of America* 74(1), 314–319.
- Khallaf, N. S. A., L. Parnovski, and D. Vassiliev (2000). Trapped modes in a waveguide with a long obstacle. *Journal of Fluid Mechanics* 403, 251–261.
- Koch, W. (1983). Resonant acoustic frequencies of flat plat cascades. *Journal of Sound Vibration* 88(2), 233.
- Kunze, C. (1993). Leaky and mutually coupled wires. *Physical Review B* 48(19), 14338–14346.
- Liboff, R. L. (1999). The many faces of the Helmholtz equation. *Physics Essays* 12(3), 492–497.
- Linton, C. M. and D. V. Evans (1991). Trapped modes above a submerged horizontal plate. *Quarterly Journal of Mechanics and Applied Mathematics* 44(3), 487–506.
- Linton, C. M. and D. V. Evans (1992). Integral equations for a class of problems concerning obstacles in waveguides. *Journal of Fluid Mechanics* 245, 349–365.

- Linton, C. M. and D. V. Evans (1993). Acoustic scattering by an array of parallel plates. *Wave Motion* 18, 51–65.
- Linton, C. M. and M. McIver (1998a). Trapped modes in cylindrical waveguides. *Quarterly Journal of Mechanics and Applied Mathematics* 51(3), 389–412.
- Linton, C. M. and M. McIver (2002). Periodic structures in waveguides. Submitted.
- Linton, C. M., M. McIver, P. McIver, K. Ratcliffe, and J. Zhang (2002). Trapped modes for off-centre structures in guides. To appear in *Wave Motion*.
- Linton, C. M. and P. McIver (1998b). Acoustic resonances in the presence of radial fins in circular cylindrical waveguides. *Wave Motion* 28, 99–117.
- Linton, C. M. and P. McIver (2001). *Handbook of Mathematical Techniques for Wave/Structure Interactions*. Chapman and Hall/CRC.
- Maniar, H. D. and J. N. Newman (1997). Wave diffraction by a long array of cylinders. *Journal of Fluid Mechanics* 339, 309–330.
- Martin, P. A. (1995). Asymptotic approximations for functions defined by a series, with some applications to the theory of guided waves. *IMA Journal of Applied Mathematics* 54, 139–157.
- Martin, P. A. and L. Farina (1997). Radiation of water waves by a heaving submerged horizontal disc. *Journal of Fluid Mechanics* 337, 365–379.
- McIver, M. and C. M. Linton (1995). On the non-existence of trapped modes in acoustic waveguides. *Quarterly Journal of Mechanics and Applied Mathematics* 48(4), 543–555.
- McIver, M., C. M. Linton, P. McIver, J. Zhang, and R. Porter (2001). Embedded trapped modes for obstacles in two-dimensional waveguides. *Quarterly Journal of Mechanics and Applied Mathematics* 54(2), 273–293.
- McIver, M., C. M. Linton, and J. Zhang (2002). The branch structure of embedded trapped modes in two-dimensional waveguides. To appear in *Quarterly Journal of Mechanics and Applied Mathematics*.
- Mitra, R. and S. W. Lee (1971). *Analytical Techniques in the Theory of Guided waves*. Oxford: Macmillan.

- Parker, R. (1966). Resonance effects in wake shedding from parallel plates: Some experimental observations. *Journal of Sound Vibration* 4, 62.
- Parker, R. (1967). Resonance effects in wake shedding from parallel plates: Calculation of resonance frequencies. *Journal of Sound Vibration* 5, 330.
- Parker, R. and S. A. T. Stoneman (1989). The excitation and consequences of acoustic resonances in enclosed fluid flow around solid bodies. *Proceedings of the Institute of Mechanical Engineers* 203, 9–19.
- Petit, R. (1980). *Electromagnetic Theory of Gratings*. Topics in Current Physics. Springer.
- Porter, R. and D. V. Evans (2002). Embedded Rayleigh-Bloch surface waves along periodic rectangular arrays. To appear in *Wave Motion*.
- Roitberg, I., D. Vassiliev, and T. Weidl (1998). Edge resonance in an elastic strip. *Quarterly Journal of Mechanics and Applied Mathematics* 51(1), 1–13.
- Stakgold, I. (1970). *Boundary Value Problems of Mathematical Physics*, Volume I. London: Macmillan.
- Stokes, G. G. (1846). Report on recent researches in hydrodynamics. British Association report.
- Takagaki, Y. and K. Ploog (1994). Ballistic electron transmission in coupled parallel waveguides. *Physical Review B* 49(3), 1782–1788.
- Ursell, F. (1951). Trapping modes in the theory of surface waves. *Proceedings of the Cambridge Philosophical Society* 47, 347–358.
- Ursell, F. (1991). Trapped modes in a circular cylindrical acoustic waveguide. *Proceedings of the Royal Society of London A* 435, 575–589.
- VanBlaricum Jr, G. F. and R. Mittra (1969). A modified residue-calculus technique for solving a class of boundary value problems—Part I: Waveguide discontinuities. *IEEE Transactions on Microwave Theory and Techniques* 17(6), 302–309.
- Watson, G. N. (1944). *A Treatise on the Theory of Bessel Functions*. Second Edition. Cambridge University Press.
- Whitehead, E. A. N. (1951). The theory of parallel-plate media for microwave lenses. *Proceedings of the IEE* 98(3), 133–140.

- Wilcox, C. H. (1984). *Scattering Theory for Diffraction Gratings*. Berlin: Springer.
- Witsch, K. J. (1990). Examples of embedded eigenvalues for the Dirichlet-Laplacian in domains with infinite boundaries. *Mathematical Methods in the Applied Sciences* 12, 177–182.

